DOCTOR OF PHILOSOPHY

# Application of model based predictive control to a pumped storage hydroelectric plant

Munoz - Hernandez, German

*Award date:*
2005

*Awarding institution:*
Bangor University

# Application of Model Based Predictive Control to a Pumped Storage Hydroelectric Plant

Thesis submitted to the University of Wales
in candidature for the degree of Doctor of Philosophy

March 2005

By

German Ardul Munoz Hernandez




**University of Wales, Bangor**

**School of Informatics**

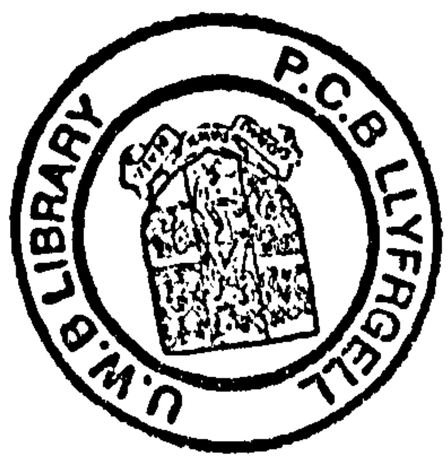

Third party material to be excluded from digitised thesis:

Appendix 1 pp123-132

Readers may consult the original thesis if they wish to see this material

# Summary

This thesis describes the development of a Predictive Control to SISO and multivariable linear and nonlinear models of Dinorwig pumped storage hydroelectric power station. The results show that Generalised Predictive Control (GPC) offers significantly better performance across the plant's operating range when compared with classic PI controllers. The GPC controller produces a faster response when the station is operating with a single unit while preserving stability as the operating conditions change when multiple units are on-line.

Inclusion of constraints in the GPC controller yields a fast, well-damped response in the common case when only a single Unit is in operation, without compromising stability when multiple Units are on-line. Simulation has also shown that improved power delivery is obtained when the plant is operated in frequency control mode.

In the final part of the work a Mixed Logical Dynamical (MLD) predictive control was developed and applied to a MIMO nonlinear elastic model of Dinorwig. The results show that MLD predictive control is faster and less sensitive than the constrained GPC. The MLD predictive control can also be integrated with high-level plant functions.

# Acknowledgements

I am grateful for the professional support offered by my supervisor Dr. Dewi I. Jones, throughout the course of this study. It has been a privilege to work for and with him.

Thanks to Dr. Sa'ad P. Mansoor, for his help and advice since I arrived at Bangor. Also I wish to thank F.C Aris and G.R. Jones of the First Hydro Company, for their assistance.

I am grateful to "*ANUIES-SUPERA*" and the "*Instituto Tecnológico de Puebla*" who have partially economically supported me in my studies. Thanks to my ITP's co-workers, the staff and students of the School of Informatics of the UWB, the Mexican "flota" in Bangor and Tres Valles.

During all my life I have been blessed with a lot of friends, in these lines I want to mention, in a *strange alphabetic* order, some of them that have been a truly support throughout my studies in Bangor. Angeles and Oscar, Edgar and his family, Edwin, Emlyn, Enrique, Evelyn and Armando, Fede, Franck, Fred, Guille and Pedro, Ian, Jon Paul, Jose Gregorio, Juan Manuel and his family, Judith, MACD, Maru, Melanie and James, Nikos, Pablo, Paty and Juan Antonio, Penny, Seong and Min, Sharmila and her family, and Sotero. They have helped us to have a good time in Bangor, even when some of them were not here.

I want to thank my parents Elpidia and Ardul for their support during all my life; I am lucky to have them. I hope that my daughters can feel the same love that I have for my Parents. Also, thanks to all my family and my wife's family for all the effort made to maintain contact with us during this time.

Finally, I must thank my girls:

Rita Melisa Melanie

who have been by my side throughout the development of this project and for all the love over the years. I am very glad that they love me despite of my "darkside". Without my girls my life would be empty, they are my light, my force and the reason to believe.

# Contents

# Chapter 1

# Introduction

## 1.1 Background

In all industrial sectors, highly competitive markets oblige companies to have reliable and optimal processes. In the electricity supply sector, the market is a constantly changing power network, which is formed by producers and consumers. Good real time balance between consumption and production is necessary to secure the quality of the electricity supply. Although for business purposes a slot of half an hour is considered, the demand varies second-by-second. As a result, the stations which feed power to the national grid must work under diverse operational conditions in order to keep the grid in balance. Further, the power generation industry faces an increasing demand to supply cheap and high quality electricity, due to financial and regulatory changes. That means improving the accuracy and speed of response to grid load perturbations in order to maintain financial profitability. To assure the quality of the electricity supply, both voltage and frequency have to be maintained at their required values within specified bounds with negligible harmonics, no voltage dips or spikes and no power cuts/outages. For the British national grid the specified bounds are 230 volts +10%-6% (household) and 50 hertz ± 0.5Hz, respectively.

Dinorwig power station is a large pumped storage hydroelectric scheme located in North Wales. The station feeds power into the national grid from six 300 MW rated turbines, driving synchronous generators. Water flows from an upper reservoir (lake Marchlyn) through the main tunnel. Each turbine receives the water flow from a penstock, using a guide vane to regulate the flow; all the penstocks are connected to the main tunnel by a manifold. Individual classic controllers on each unit control the electrical power generated. The water is pumped back into the upper reservoir, during off-peak periods, using the turbo/generators as a motorised pump.

The outstanding feature of Dinorwig is that it can produce large and very rapid changes in the power it delivers to (or extracts from) the grid. How well it achieves this is crucially dependent on the turbine/generator's control system, usually referred to as its 'Governor'. The Governor at Dinorwig has two control modes, power and frequency control, in each unit. The power control loop adjusts the turbine guide vane position depending on the power deviation, which is multiplied by a speed regulation factor. A Proportional and Integral configuration is used for this control. The frequency control loop adjusts the power demand, depending on the frequency deviation from 50 Hz. This control has a PID configuration.

In practice, it is possible to separate the control of voltage and frequency, the former being done by changing the excitation of the synchronous generator, and thereby the reactive power, whereas system frequency depends on the real power component of generation. Dinorwig power station assists in frequency control by delivering power to the grid as demanded by the co-ordinator, National Grid Transco (NGT). The business process for this provision is known as 'ancillary services'.

The classic PID Governor at Dinorwig is not able to maintain an optimal performance in all operational conditions, therefore a better control should be considered. The central theme of this thesis is an investigation of whether improved power delivery can be achieved by replacing the Governor's current PID algorithm with a more advanced method, specifically Model Based Predictive Control (MBPC).

## 1.2 Thesis outline

### 1.2.1 Motivation

Dinorwig is a complex plant. It has non-minimum-phase dynamics, nonlinear relationship between flow and power, poorly damped poles and significant hydraulic coupling between the turbines because of the common supply, *i.e.* it is a multivariable nonlinear system.

The current Governor is a classic PID, every penstock having an independent controller, so the cross-coupling interaction is not properly treated. Also, the controllers are tuned conservatively to deal with the worst case (six units operational), producing a slow response when only one unit is active. It is hoped that an advanced multivariable controller that introduces more information into the loop can maintain stable performance over all operational conditions, reduce the cross-coupling interaction and provide more rapid and accurate tracking of the demanded power target.

Model Based Predictive Control (MBPC) seems to be a good candidate because it provides an integrated approach to station control and deals with multivariable systems. It also offers to deal with nonlinearities and the possibility of including constraints in the controller.

### 1.2.2 Aims

The aim of this work is to evaluate the application of Model Based Predictive Control to Dinorwig, in order to assess whether it can improve the performance of the station. The main benefits sought are as follows:

- To improve the speed of response of the power station when tracking the demanded power.

- To maintain plant stability over all operational conditions.

- To reduce cross-coupling interaction.

- To include constraints in order to maintain the system within its operational and safety limits.

Besides the main topics, this study has explored other subjects that could help the effective installation of MBPC in Dinorwig, including:

- Provision of guidelines for tuning the Model Based Predictive Control when it is applied to Dinorwig.

- Development of a software tool that facilitates the design and test of different control approaches.

- Development of a strategy that can integrate different levels of control.

### 1.2.3 Structure

Chapter 2 describes linear and nonlinear models of the Power Plant. The dynamic responses of the hydraulic, guide vane and electric subsystems are illustrated. Simulink models of the subsystems are also presented. Finally, the accuracy and validity of different types of models are discussed.

Chapter 3 discusses advances in primary speed/load control of hydroelectric plant and the development of the turbine-generator control is briefly reviewed. The current Dinorwig Governor configuration is presented and its step and ramp specifications are evaluated. Finally a closed loop analysis that shows the fundamental dynamic constraints of the Power Plant is presented.

Chapter 4 presents the basic theory of Model Based Predictive Controls (MBPC), with special emphasis on Generalised Predictive Control (GPC). Some MBPC approaches and their applications in electric power generation are briefly discussed. Guidelines to tuning the GPC controller are also presented. Finally, the software tool developed in

Simulink as an efficient instrument to investigate and evaluate classic and predictive controllers is discussed.

The behaviour of the plant under Generalised Predictive Control and classic PI is analysed in Chapter 5, where the Power Plant is modelled as a SISO linear system. The procedure followed in this study to tune both the classic and Predictive Control is presented. The limitations of the hydroelectric Power Plant linear model are also discussed. Finally, the performances of the PI and GPC controllers are compared.

Chapter 6 analyses the behaviour of the plant under GPC and PI control where the Power Plant is modelled as a MIMO linear system. This is later extended to include nonlinearities and elastic water column effects in the model. Finally, the performances of the PI and GPC controllers are evaluated.

Chapter 7 begins with a brief introduction to Mixed Logical Dynamical (MLD) systems and then presents a MLD model of the hydroelectric station. The MLD model and the MIMO nonlinear nonelastic model of the hydroelectric plant are compared. The behaviour of the plant under Generalised Predictive Control with constraints (CGPC) and MLD-GPC is analysed and shows the improved response provided by MLD-GPC. The potential application of MLD to represent high-level rules in the optimisation of power plant is briefly considered.

Finally, Chapter 8 draws general conclusions on this study and suggests the possible direction and nature of future work.

## 1.3 Contributions to published literature

**Accepted**

- G. A. Munoz-Hernandez and D. I. Jones, "Applying Generalized Predictive Control to a pumped-storage hydroelectric power station", IASTED MIC, pp. 380-385, Grindelwald, Switzerland. February 2004.

- G. A. Munoz-Hernandez and D. I. Jones, "Modelling, simulation and control of a hydroelectric pumped storage power station", UKAC Control, Art. 214. Bath, U.K. September 2004

- G. A. Munoz-Hernandez, D. I. Jones and S. I. Fuentes-Goiz, "Modelling and Simulation of a hydroelectric power station using MLD", CONIELECOMP, Puebla Mexico. February-March 2005.

- G. A. Munoz-Hernandez, D. I. Jones and S. P. Mansoor, "Evaluation of a MLD predictive control in a nonlinear model of a power station". IASTED MS, Cancun, Mexico. May 2005.

- G. A. Munoz-Hernandez and D. I. Jones, "MIMO generalized predictive control for a hydroelectric power station", IEEE Transactions on Energy Conversion.

**In preparation**

- G. A. Munoz-Hernandez and D. I. Jones, "Simulation studies of a GPC controller for a hydroelectric plant".

# Chapter 2

# Hydroelectric System Model

## 2.1 Introduction

This chapter describes the various mathematical models used to represent the dynamic characteristics of the Dinorwig Hydroelectric Pumped Storage Plant. The models were developed systematically with increasing complexity, each model suitable for a particular system dynamic study. For instance, linear models can be applied to represent the effects of low frequency and guidance in speed control and nonlinear models are required when large changes of speed and power are considered, such as in islanding, load rejection and systems restoration studies [1, 2]. As Dinorwig has six units, the approaches considered both Single Input Single Output (SISO) and multivariable (Multiple Inputs Multiple Outputs, MIMO) models.

Figure 2.1 shows this arrangement for 2 of the 6 penstocks. Each penstock feeds a Francis turbine to generate power using a guide vane to regulate the flow. The synchronous generator converts the mechanical power from the Francis turbine to electrical power at a specific voltage and frequency. The electrical power generated is controlled by individual feedback loops on each unit. The turbine and generator are briefly discussed in the following paragraphs.

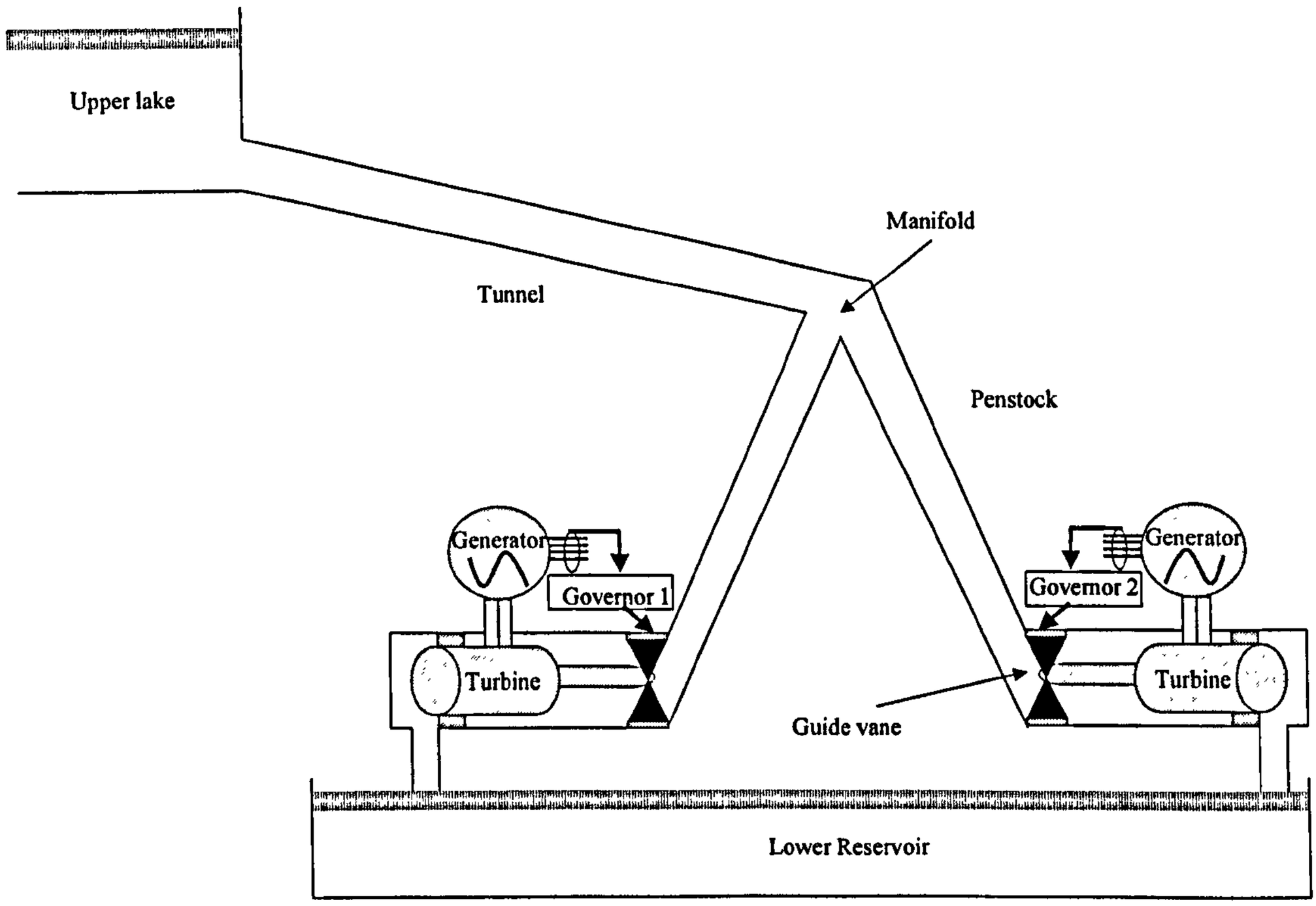


*Figure 2.1: Schematic of pumped storage plant.*

Figures 2.2 and 2.3 show simplified diagrams of a radial inflow Francis turbine [3-5]. The water flows from the penstock and it is distributed consistently onto a spiral casing (volute). The cross sectional area of the volute decreases along the water path maintaining the water velocity constant in magnitude. The guide vanes, which are mounted all around the periphery of the runner (Figure 2.2), direct the water from the volute to the runner. The guide vanes can synchronously alter the flow rate throughout the turbine by pivots on each vane.

The torque applied on the runner depends on the rate of change of momentum of the water, whose velocity is changed in magnitude and direction by the turbine blades (Figure 2.3). The water is turned into the axial direction, from the centre of the runner, and flows to the tailrace via the draft tube. The lower end of the draft tube is always submerged below the water level in the tailrace in order to ensure that the hydraulic turbine is full of water [3-5].

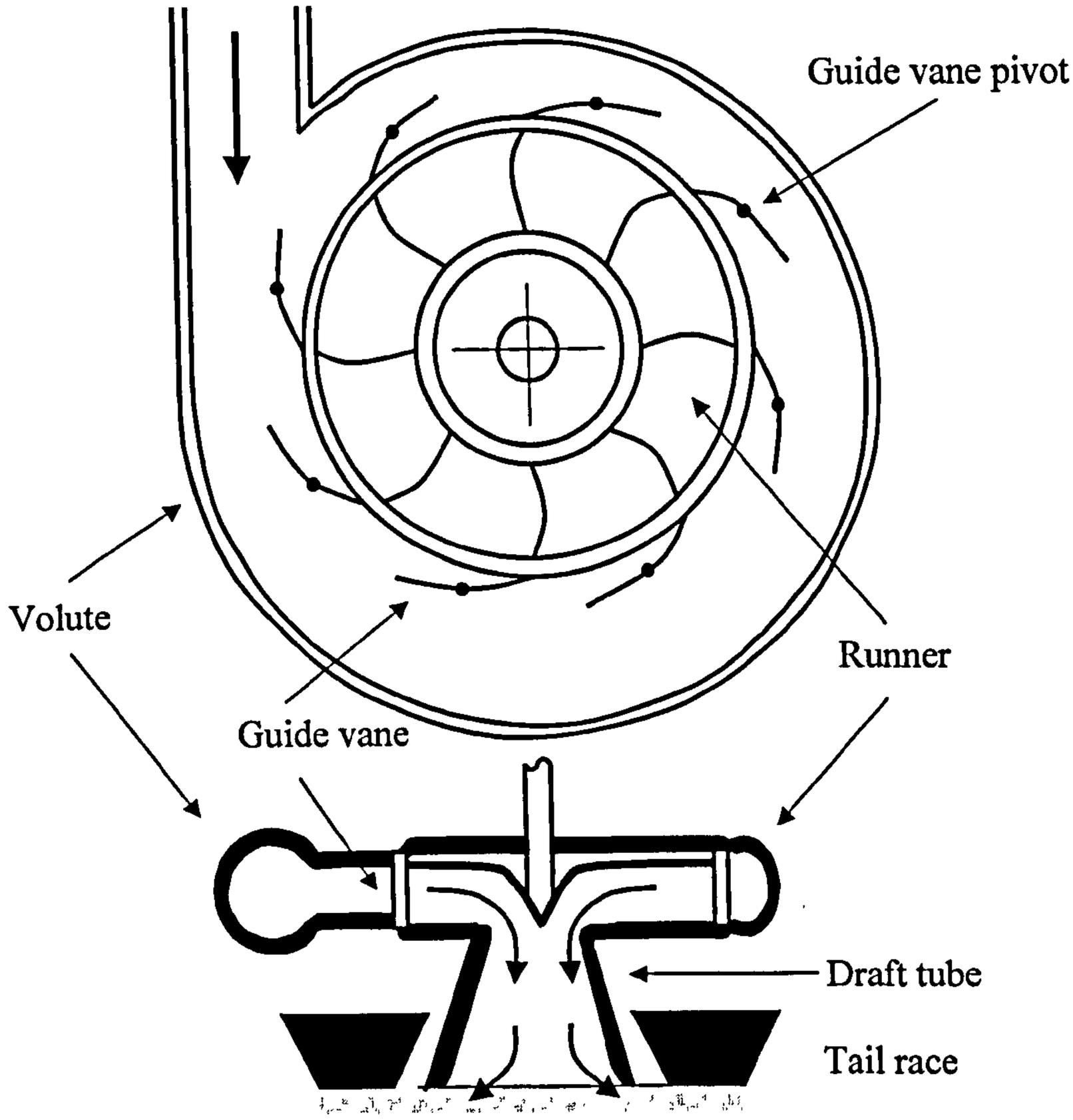


*Figure 2.2: Simplified diagram of a Francis Turbine.*

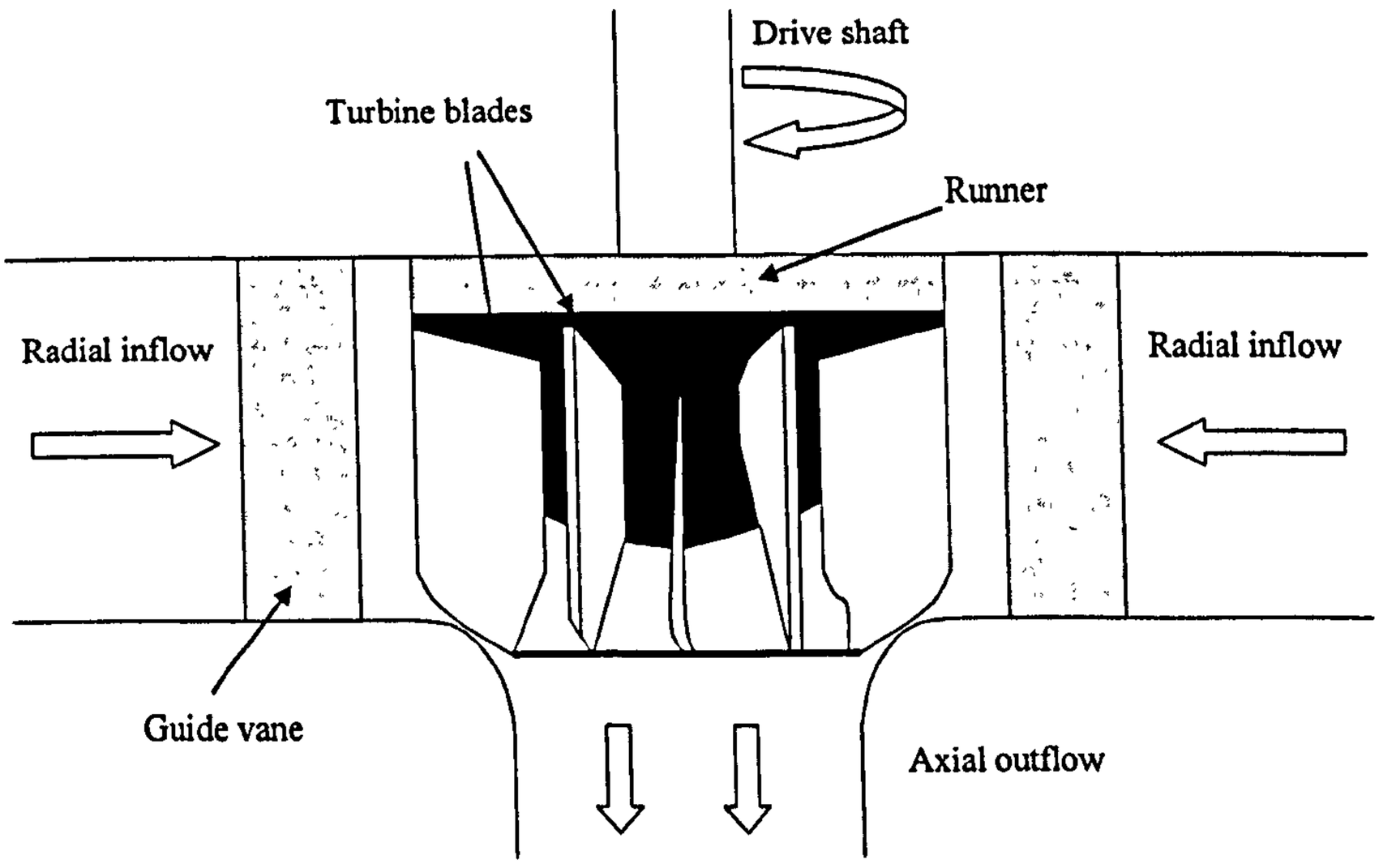


*Figure 2.3: Simplified diagram of a Francis Turbine, cross-sectional view.*

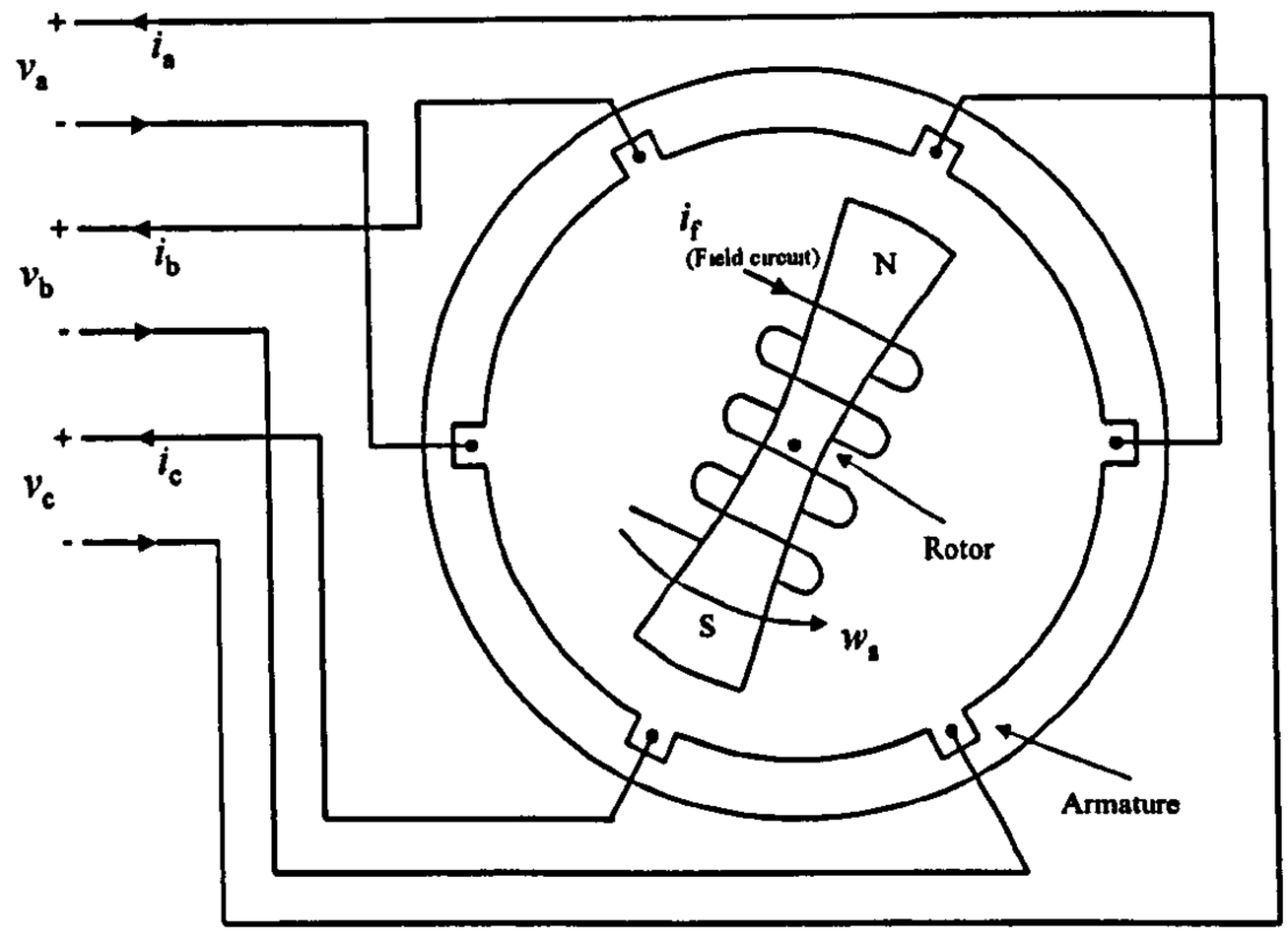


*Figure 2.4: Elementary Two-Pole Three-Phase synchronous generator.*

Figure 2.4 illustrates an elementary two-pole three-phase generator. The rotor holds the field circuit, which is excited by direct current. The Francis turbine at a constant speed drives the rotor and its magnetic field induces sinusoidal voltages in the windings of the armature ($v_a$, $v_b$ and $v_c$). These windings are located on the stator of the generator. The parameters that determine the frequency of the induced armature voltages are the speed at which the rotor turns and the number of poles [6, 7].

The model of the system can be separated into three main subsystems (Figure 2.5). Mansoor *et al* [8] have derived a multivariable nonlinear simulation of this plant, which has provided an improved understanding of its characteristics. Its main features are non-minimum-phase dynamics, poorly damped poles (associated with water-hammer in the supply tunnel and electrical synchronisation) and a nonlinear relationship between flow and power. It is also known [1, 2] that there is significant hydraulic coupling between the turbines because of the common supply.

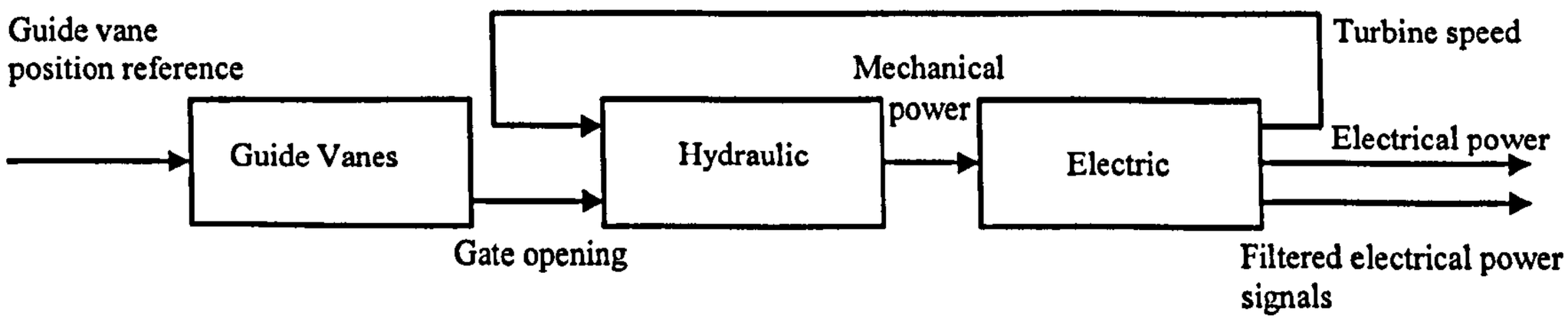


*Figure 2.5: The subsystems of the hydroelectric plant.*

Models of the guide vane subsystem, hydraulic subsystem and electric subsystem are presented in this chapter. Section 2.2 describes the hydraulic subsystem; section 2.3 explains the dynamic response of the guide vane subsystem, while 2.4 describes the electric subsystem. The models developed in Simulink are presented in section 2.5. The accuracy and validity of these models are discussed in section 2.6. Finally some conclusions are drawn in section 2.7.

## 2.2 Hydraulic subsystem

The layout of the Dinorwig pumped storage station is shown in Figure 2.6. This scheme consists of the upper reservoir, a low-pressure tunnel and a high-pressure tunnel. Six individual penstocks are connected to the high-pressure tunnel by a manifold. The flow in the common tunnel is the sum of the individual flows in each penstock; this generates a significant hydraulic coupling. The dimensions given in Figure 2.4 were used by Mansoor [3] to calculate the dynamic parameters for Dinorwig; these parameters are used later in the thesis for simulation studies. The surge tank controls hydraulic transients and pressure changes; it causes poorly damped slow oscillations between the tank and the reservoir. Nonetheless, as they have a slow cycle (few minutes), their effect can be neglected in this investigation. This study is concentrated on the analysis of governor characteristics and load frequency control, where the transient response over a few seconds is of interest. The water column that feeds the hydraulic subsystem has a strong influence on the performance of the turbines. The main effects of the water column are water inertia, water compressibility and pipe wall elasticity. The water inertia causes changes in turbine flow that generate changes in the guide vane opening. Pipe wall elasticity produces travelling waves of pressure, they are produced when water is decelerated or accelerated; this phenomenon is called water hammer [1-3], and is one of the factors that produces poorly damped poles.

The mechanical power ($P_{mech}$) available from a hydraulic turbine is related to the head ($h$) and flow by the following equation:

$$P_{mech} = A_t h(q-q_{nl})-D_n G\Delta n. \tag{2.1}$$

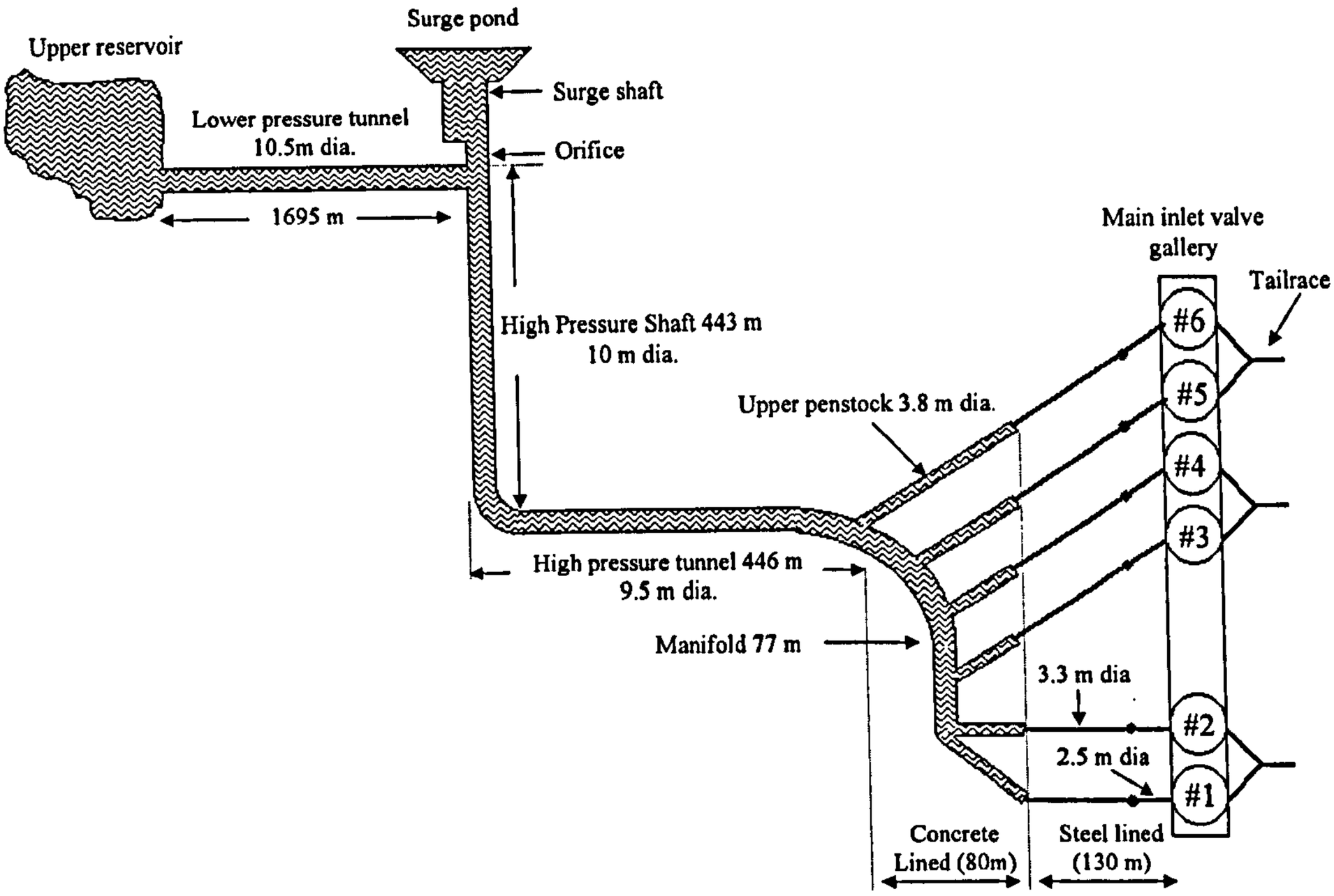


*Figure 2.6: Dinorwig hydraulic subsystem (not a scale).*

In (2.1) $q_{nl}$, the no-load flow, is subtracted from the net flow ($q$) in order to represent the fact that the turbine is not 100% efficient. $A_t$ is the turbine gain; its value depends directly on the turbine MW rating and inversely on the Generator MVA rating. A turbine damping effect is also included; this effect is a function of the guide vane opening ($G$), the speed variation ($\Delta n$) and the turbine-damping coefficient ($D_n$). The models are expressed in the per-unit system, normalised to 300 MW and 50 Hz.

The net flow through the turbine depends on the guide vane opening and the pressure, or head ($h$), according to

$$q = G\sqrt{h}\,. \tag{2.2}$$

The nonlinear relationships (2.1) and (2.2) cause the effective gain of the plant (i.e. change in generated power with guide vane opening) to vary significantly with flow and head. They also show that reducing steady state power output requires the guide vanes to be closed. Doing so causes a transient increase in the turbine inlet pressure whose amplitude depends on the rate of closure. However, as a consequence of the inertia of the moving water column, there is no change in the instantaneous flow and there is consequently a transient increase in the power output, which is the opposite of the

desired effect. This is termed a non-minimum phase (NMP) response and is an important limiting factor on the dynamic performance of fast-response hydroelectric plant.

### 2.2.1 Linearised model

#### *2.2.1.1 SISO linearised model*

For small variations around an operating point the hydraulic model can be linearised, considering the main dynamic characteristics of the hydraulic subsystem [1-3], by the equation 2.3. In this approximation, the hydraulic coupling is not considered. This SISO linear model is appropriate to represent the operation of Dinorwig with a single unit active or when multiple units active are working synchronously. It is also suitable for studies for control tuning using linear analysis tools.

$$\frac{P_{mech}(s)}{G(s)} = \frac{A_t(1 - G_0 T_{wti} s)}{\left(1 + \frac{G_0 T_{wti}}{2} s\right)} \tag{2.3}$$

In the transfer function (2.3), $P_{mech}$ is the mechanical power produced by a single turbine and $G_o$ is the operating point. $T_{mt}$ is the *water starting time* of the main tunnel, $T_{wi}$ is the water starting time of any single penstock and $T_{wti}$ is the water starting time of the main tunnel and a single penstock, that is $T_{wti}=T_{mt}+T_{wi}$. Kundur defines the *water starting time* as the time required for a given head to accelerate the water in the penstock from standstill to a specific velocity [2]. The values of $T_{mt}$, $T_{wi}$ and $T_{wti}$ depend directly on the constructional dimensions of the main tunnel and penstocks.

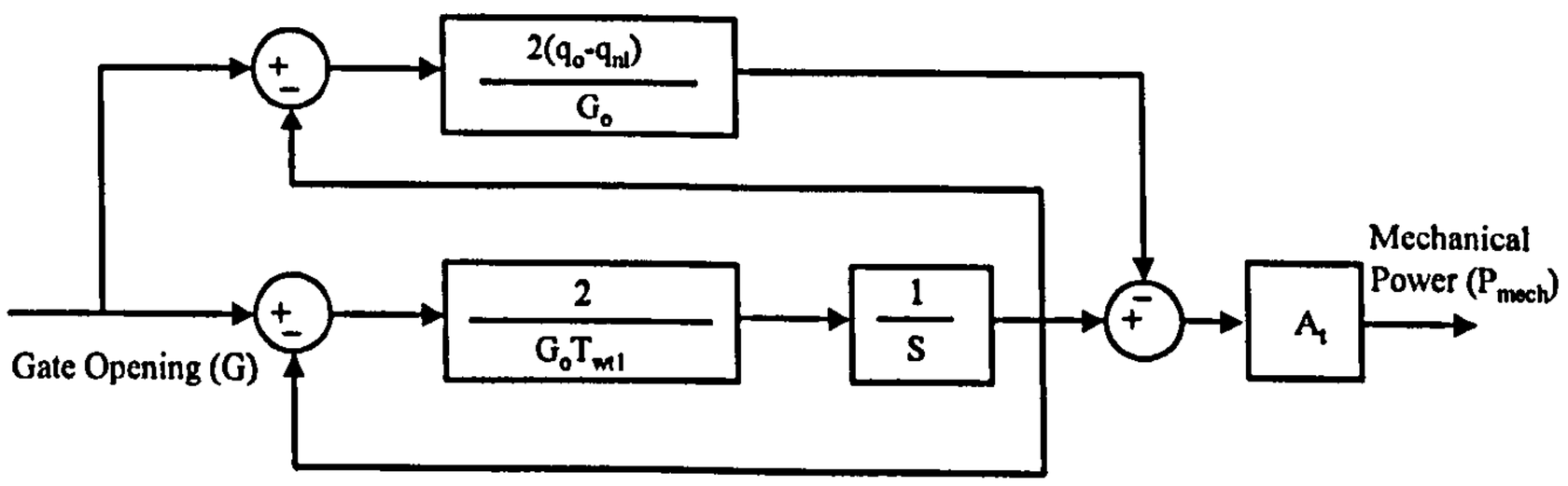


*Figure 2.7: Linear model of the hydraulic subsystem.*

Figure 2.7 is the block diagram for the equation (2.3). Friction losses are neglected but the effects of flow variation are considered [1, 2]. $q_o$ is the steady state flow rate at the operating point and $q_{nl}$ is the no-load flow, note that $G_o=q_o$. The values are in the per unit system. The per unit (p.u.) system used in this work is normalized to 300 MW and 50 Hz.

### *2.2.1.2 MIMO linearised model*

Like many other stations, the hydraulic subsystem at Dinorwig is inherently multivariable, because the common supply conduit produces significant dynamic coupling between the turbines [1]. This is known to have an adverse effect on the stability margin in closed loop. Units that are on-line react, via their governors, to pressure and flow (and therefore power) perturbations caused by other Units whereas those that are off-line have their guide vanes closed and do not interact. The structure of the plant therefore varies with time, depending on the number of active Units. For this MIMO linearised model an inelastic water column and negligible losses are assumed and all 6 Units are taken to be identical (although minor differences due to manufacturing tolerances do occur in practice).

The rate of change of the flow in the penstock can be determined as:

$$\frac{dq}{dt} = (h_o - h - h_i)\frac{gA}{l} \tag{2.4}$$

where: $A$ – cross-section area of tunnel.

$h_o$ – the static head of water column in per unit notation.

$h$ – the head at the turbine admission in per unit notation.

$h_i$ – the head loss due to friction.

$l$ – length of tunnel.

$g$ – acceleration due to gravity.

The momentum of the water in an individual penstock is:

$$h - h_i = \frac{l_i}{A_i g}\left(q_{i0}\frac{dq_i}{dt}\right) \tag{2.5}$$

The sum of the flows in the individual penstocks must be equal to the total flow in the common tunnel, then using (2.4) the momentum equation for the water at the common tunnel is:

$$h_o - h = \frac{l}{Ag}\left(\frac{dq_1}{dt} + \frac{dq_2}{dt} + \cdots + \frac{dq_n}{dt}\right) \tag{2.6}$$

Eliminating $h$ in equation (2.6) using equation (2.5), the hydraulic MIMO model can be described using a matrix of relations (2.7); this matrix changes its value depending on the number of units active [9].

$$\begin{bmatrix} q_1 \\ q_2 \\ \vdots \\ q_n \end{bmatrix} = \begin{bmatrix} T_{wtn} & T_{mt} & \cdots & T_{mt} \\ T_{mt} & T_{wtn} & \cdots & T_{mt} \\ \vdots & \vdots & \ddots & \vdots \\ T_{mt} & T_{mt} & \cdots & T_{wtn} \end{bmatrix}^{-1} \begin{bmatrix} h'_1 \\ h'_2 \\ \vdots \\ h'_n \end{bmatrix} \tag{2.7}$$

The effect of hydraulic coupling can be expressed as an effective increase of the water starting time as the number of Units on-line increases [3, 9]. The total water starting time, $T_{wtn}$, is given by:

$$T_{wtn} = T_w + T_{mt}. \tag{2.8}$$

In this model the variation of the hydraulic coupling will be considered as a discrete function, therefore the contribution of any active unit, in the starting time, is always considered at its maximum value even if its guide vane is not open at 100%.

Considering the case of two units active:

$$\begin{bmatrix} T_{wt} & T_{mt} \\ T_{mt} & T_{wt} \end{bmatrix}^{-1} = \begin{bmatrix} \dfrac{2T_{wt}}{G_o\left(T_{wt}^2 - T_{mt}^2\right)} & \dfrac{-2T_{mt}}{G_o\left(T_{wt}^2 - T_{mt}^2\right)} \\ \dfrac{-2T_{mt}}{G_o\left(T_{wt}^2 - T_{mt}^2\right)} & \dfrac{2T_{wt}}{G_o\left(T_{wt}^2 - T_{mt}^2\right)} \end{bmatrix} \tag{2.9}$$

In equation 2.9 the two penstocks are considered equal, that is $T_{wt}=T_{wt1}=T_{wt2}$. Figure 2.8 shows this case. An extended MIMO model, Figure 2.9, which includes all six machines is used later in simulations.

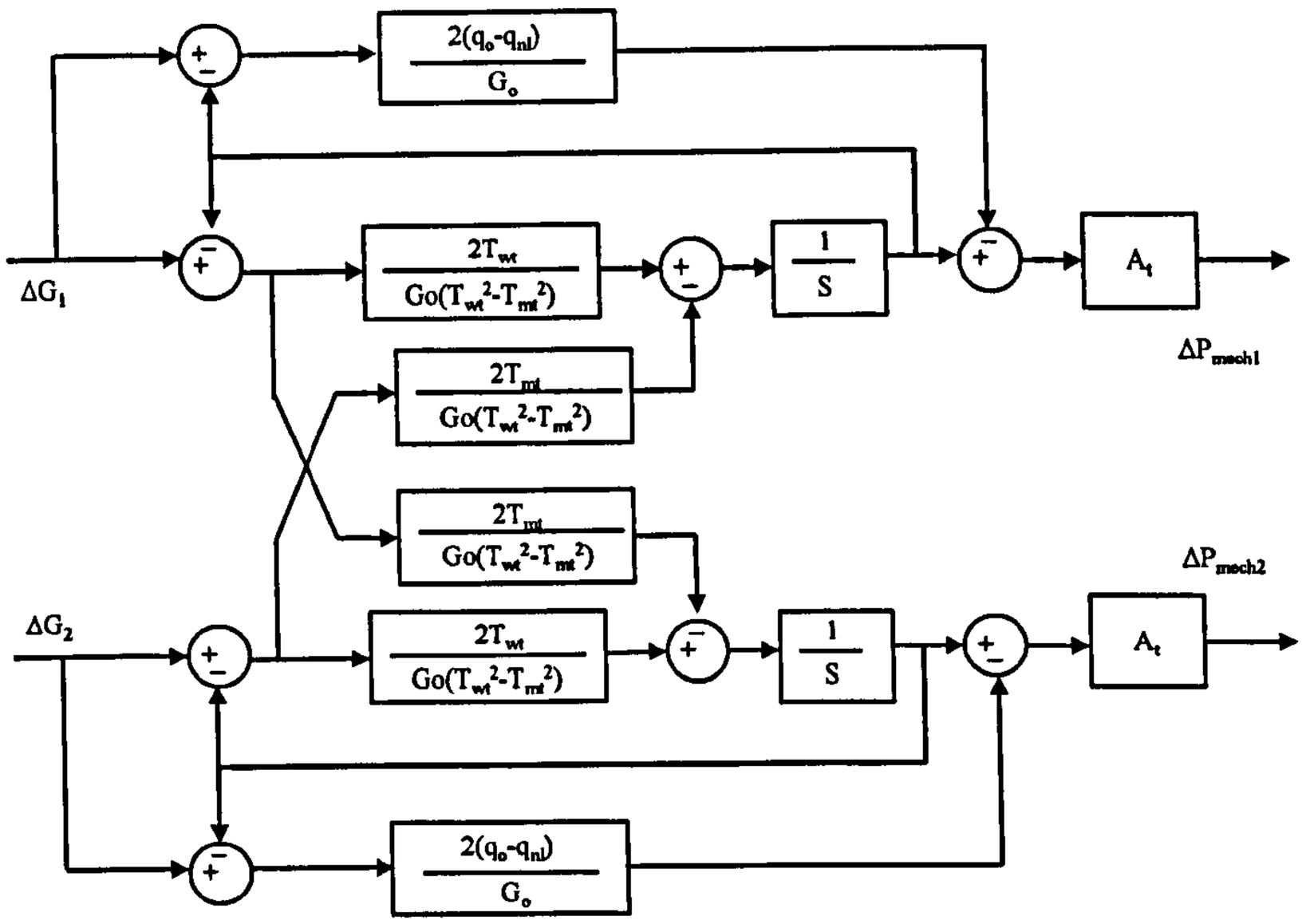


*Figure 2.8: MIMO linear model of the hydraulic subsystem.*

In Figure 2.9, $\Delta G$ is the guide vane opening, $\Delta P_{mech}$ is the turbine's mechanical power and $\Delta P_e$ is the electrical power. The current governor comprises an individual classic PI controller on each turbine.

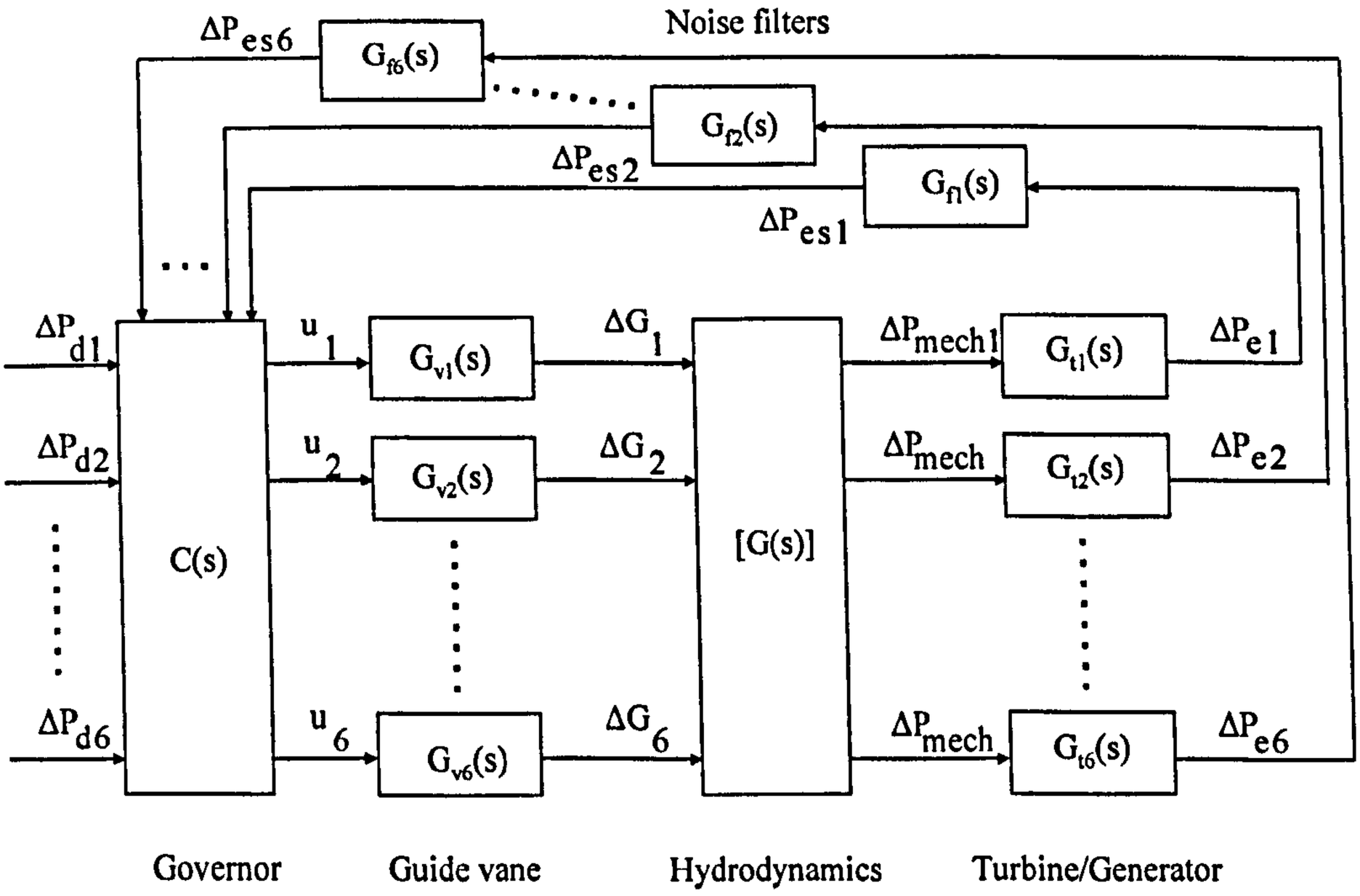


*Figure 2.9: Extended MIMO model of the hydroelectric plant.*

The hydrodynamics block of the extended MIMO model has the ability to change the matrix transfer function, that relate Mechanical Power with Gate opening, depending on the number of units active. The elements of the matrix transfer function (*G(s)*) are the direct transfer function (diagonal) $G_i(s)$ and cross-coupling transfer function (symmetric) $X_i(s)$. The rules to determine whether a unit is on- or off-line are:

- Unit *n* comes on-line when $P_{di} > 0$
- Unit *n* goes off-line when $[(\Delta P_{di} = 0)$ and $(\Delta P_{mechi}) = 0]$.

Table 2.1 summarises the elements of the matrix transfer function *G(s)* of the extended MIMO model. The values are expressed in the per-unit system, normalized to 300MW and 50Hz, and assume a Grid system with infinite busbars. The analysis used to obtain them is discussed in Appendix I.

*Table 2.1*

*Variation of transfer function matrix with number of active units (0.95 operating point)*

| $U_o$ | $G_i(s)$ | $X_i(s)$ |
|---|---|---|
| 1 | $\frac{-2.358s + 3.395}{0.076s^3 + 0.8204s^2 + 2.788s + 3.031}$ | 0 |
| 2 | $\frac{-2.358s^2 - 5.454s + 14.96}{0.076s^4 + 1.26s^3 + 7.213s^2 + 16.69s + 13.35}$ | $\frac{-8.559s}{0.076s^4 + 1.26s^3 + 7.213s^2 + 16.69s + 13.35}$ |
| 3 | $\frac{-2.358s^2 - 1.986s + 11.01}{0.076s^4 + 1.221s^3 + 6.643s^2 + 14.1s + 9.83}$ | $\frac{-6.301s}{0.076s^4 + 1.221s^3 + 6.643s^2 + 14.1s + 9.83}$ |
| 4 | $\frac{-2.358s^2 + 0.03428s + 8.711}{0.076s^4 + 1.198s^3 + 6.311s^2 + 12.59s + 7.778}$ | $\frac{-4.985s}{0.076s^4 + 1.198s^3 + 6.311s^2 + 12.59s + 7.778}$ |
| 5 | $\frac{-2.358s^2 + 1.357s + 7.207}{0.076s^4 + 1.183s^3 + 6.093s^2 + 11.6s + 6.435}$ | $\frac{-4.124s}{0.076s^4 + 1.183s^3 + 6.093s^2 + 11.6s + 6.435}$ |
| 6 | $\frac{-2.358s^2 + 2.289s + 6.145}{0.076s^4 + 1.173s^3 + 5.94s^2 + 10.9s + 5.487}$ | $\frac{-3.517s}{0.076s^4 + 1.173s^3 + 5.94s^2 + 10.9s + 5.487}$ |

## 2.2.2 Nonlinear nonelastic model

The parameters of a linearised model vary with the operating point, $G_0$ and $q_0$, and then the results from simulation can only be accurate near the point selected during the design process. In order to allow the simulation of large changes of speed and power, a nonlinear model, that assumes an incompressible fluid, a rigid conduit and an unrestricted head, was considered [1]. Figure 2.10 shows this multivariable nonlinear nonelastic model, $\Delta w$ is the variation of the generator's speed, $D_n$ is the turbine-

damping coefficient and $f_{pj}$ is the head loss coefficient for the $j_{th}$ unit. The matrix of relations utilised in this figure is the equation (2.7).

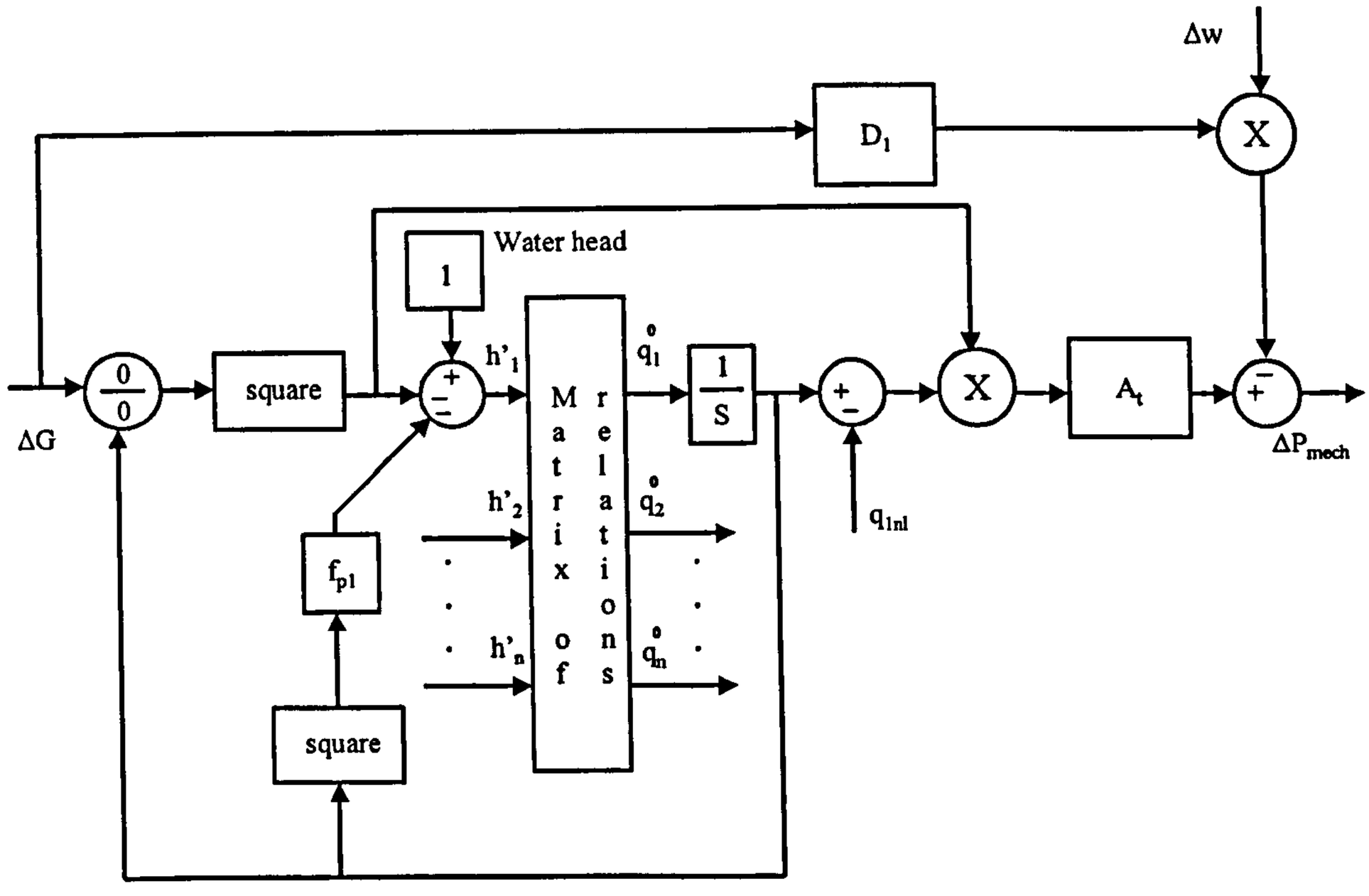


*Figure 2.10: Nonlinear nonelastic hydraulic model for multiple penstocks.*

### 2.2.3 Nonlinear elastic model

Modelling of water columns assuming elastic behaviour is important when the hydraulic subsystem has large penstocks [1]. In this section a nonlinear model that takes into account the effects of the water column, including water compressibility and pipe wall elasticity, is discussed. The coupling effect is represented with the inclusion of the main tunnel, which is modelled with the same form of transfer function as a penstock. Figure 2.11 shows the nonlinear elastic model of a single penstock. $Z_0$ is the surge impedance of the conduit (2.10). $T_e$ is the wave travel time (2.11), which is defined as the time taken for the pressure wave to travel the length of the penstock ($l$) to the open surface.

$$Z_0 = \frac{T_W}{T_e} \tag{2.10}$$

$$T_e = \frac{l}{v} \tag{2.11}$$

where $v$ is the velocity of sound in water.

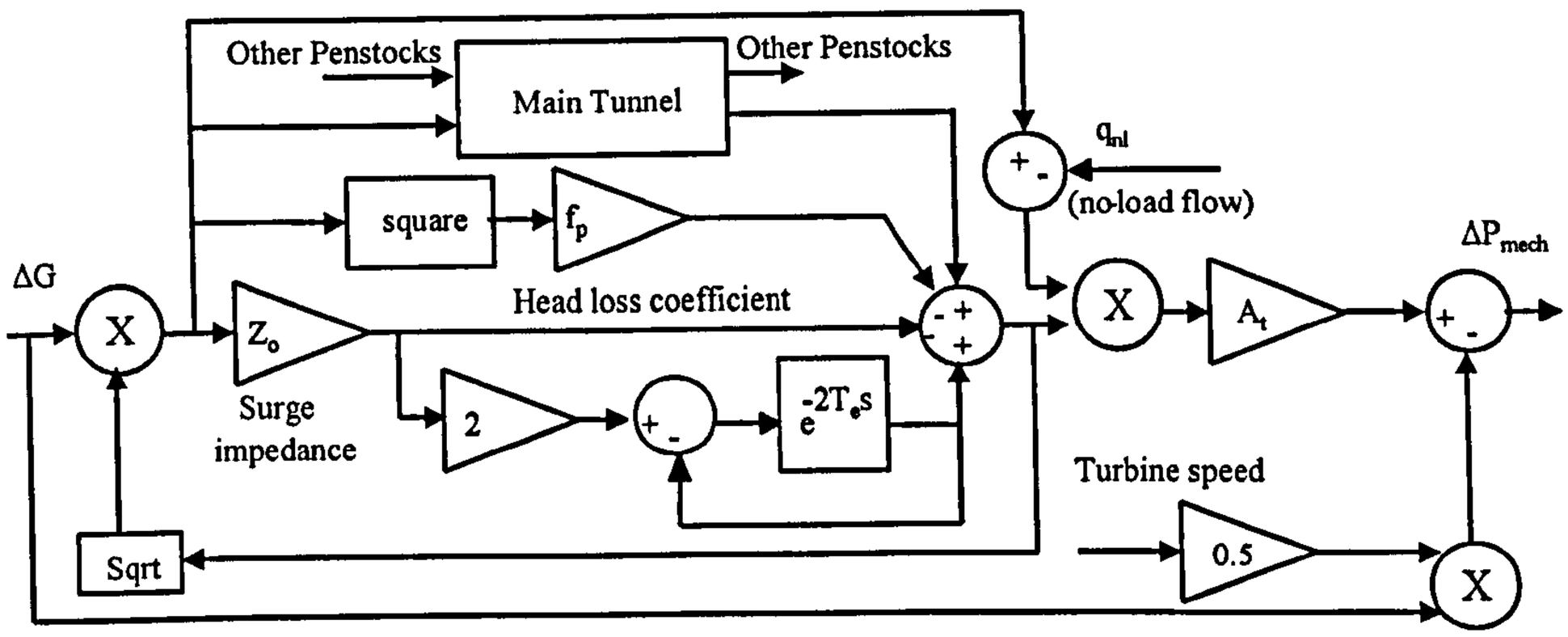


*Figure 2.11: Nonlinear elastic model of a single penstock.*

## 2.3 Guide vanes

The flow in the penstocks is regulated by the guide vane subsystem. The position of the guide vane depends on the control signal from the governor. The guide vane dynamics can be seen as a two-stage system with an internal feedback loop where the input signal is the desired position and the output signal is the actual position of the guide vane [2, 3]. The electrical signals from the governor act as the reference to the guide vane subsystem; these signals are converted to hydraulic force and drive the servomotors that adjust the guide vane's positions. The guide vane subsystem dynamics are represented by the transfer function:

$$\frac{G(s)}{U(s)} = \frac{1}{(0.19s+1)(0.4s+1)} \tag{2.12}$$

where $G(s)$ is the guide vane position

and $U(s)$ is the control signal.

As shown in Figure 2.12, a *saturation constraint* limits the maximum guide vane opening to about 95% of the physical aperture to prevent it from hitting its end-stop. A fixed *rate-limit* at which the guide vane can open or close prevents excessive variation in tunnel pressure (for safety reasons and to minimise fatigue stresses on the wall

material). This plays a vital role in alleviating the non-minimum phase (NMP) response, which occurs during the initial part of rapid power transients.

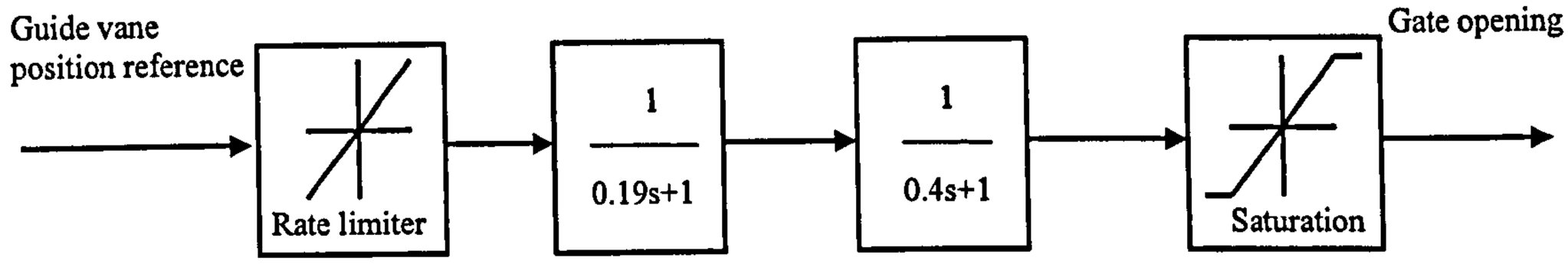


*Figure 2.12: The guide vane subsystem.*

## 2.4 Electric subsystem

The quality of the power supply is strongly dependent on the dynamic behaviour of the generators. Dinorwig has six synchronous generators that are fed with mechanical power from the hydraulic subsystem to produce electrical power at a specific voltage and frequency. The generator model is based on its response to frequency changes because the system frequency depends on the active power balance.

### 2.4.1 Dinorwig electric subsystem

In Figure 2.13 can be seen how the turbine's mechanical power output $\Delta P_{mech}$ drives the electrical subsystem. Figure 2.13 represents the well-known 'swing' equations [2]. The power is measured, and fed back to the governor.

$$\frac{\Delta P_e(s)}{\Delta P_{mech}(s)} = \frac{K_s\omega_0/2H}{s^2 + \left(K_D/2H\right)s + K_s\omega_0/2H} \quad . \tag{2.13}$$

In (2.13) $H$ is the turbine/generator inertia constant, $K_s$ is the synchronising torque coefficient, $K_D$ is the damping coefficient and $\omega_0$ is the base rotor electrical speed. A first order filter for noise reduction is included in each power feedback loop, which has the transfer function:

$$\frac{\Delta P_e(s)}{\Delta P_e(s)} = \frac{1}{s+1} \quad . \tag{2.14}$$

The electrical coupling between generators connected in parallel, as in Dinorwig, is considerable [3]. This coupling produces an action reaction effect, for example if a generator has a disturbance at its output, this changes the balance of the system and all the generators react, as is illustrated by the feedback of the frequency variation from the power system. This variation appears when the power system load changes, its frequency varies and the power supplied will be increased or decreased from the controlled units to attempt to return the system frequency to its base value.

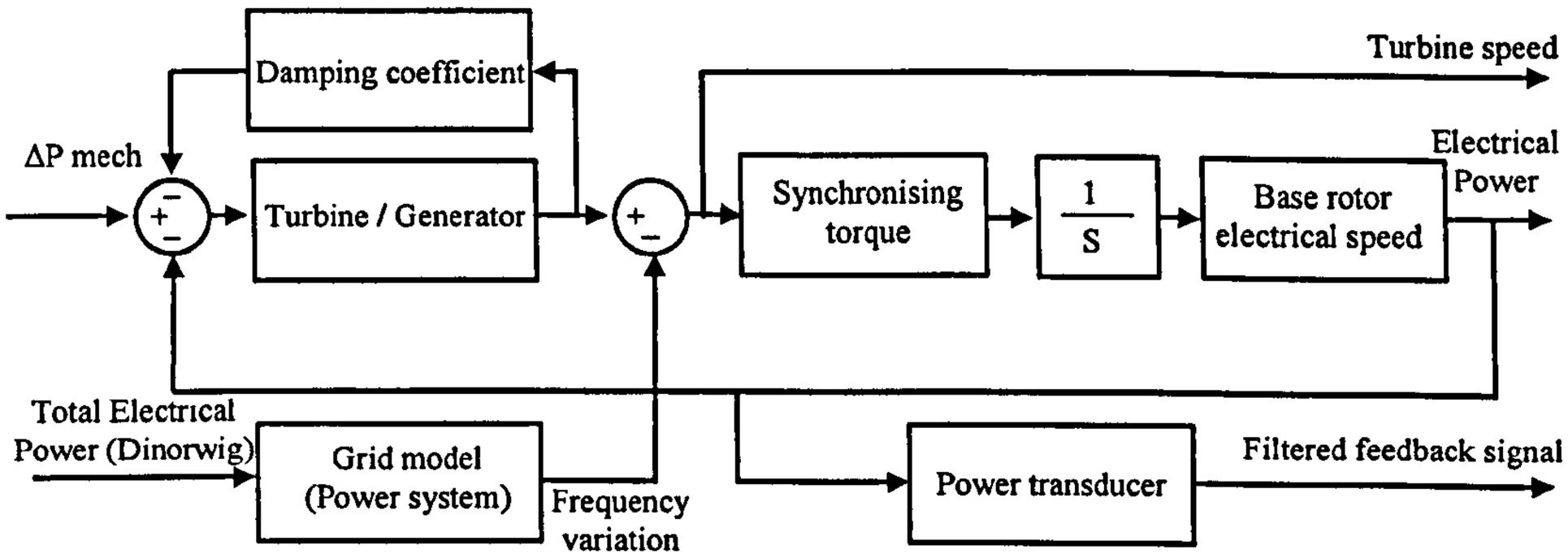


*Figure 2.13: The Dinorwig electric subsystem.*

### 2.4.2 Load model

The load model can be seen as a second order transfer function (2.15) [10], where the response is dominated by two time constants, one that is the summative of all inertias of rotating machines associated with the system and another with the collective effect of all regulatory mechanisms ($T_R$).

$$\Delta f(s) = \frac{\omega_n^2 T_R}{\beta}\left(\frac{s+\frac{1}{T_R}}{s^2+2\zeta\omega_n s+\omega_n^2}\right)(\Delta P_e(s)-\Delta P_L(s)) \tag{2.15}$$

In (2.15) the frequency ($\Delta f$) is related to the difference between the power input by Dinorwig ($\Delta P_e$) and the load imbalance power ($\Delta P_L$), $\omega_n$ is the natural frequency, $\zeta$ is the damping factor and $\beta$ is the grid stiffness. $\omega_n$, $\zeta$ and $\beta$ depend on the droop settings, regulatory time constants and inertia of all the plant connected to the power system. They are time variant.

This study uses an Auto Regressive Moving Average and exogenous input (ARMAX) approximation to the load model that was proposed by Jones [11]. The main advantage of this representation is that it can calculate the parameters online using operational data and taking into account the input. Then (2.15) can be written in polynomial form as:

$$\Delta f(k) = -a_1 f(k-1) - a_2 f(k-2) - a_3 f(k-3) + b_0 \Delta P_e(k) + b_1 \Delta P_e(k-1) + c_0 e(k) + c_1 e(k-1) + c_2 e(k-2) + c_3 e(k-3) \tag{2.16}$$

or in a general input-output discrete third order form, considering the noise equal to zero, as:

$$\frac{\Delta f(z)}{\Delta P_e(z)} = \frac{z^2(b_0 z + b_1)}{z^3 + a_1 z^2 + a_2 z + a_3} \quad . \tag{2.17}$$

Figure 2.14 shows the complete grid model used in this study to simulate the frequency variation of the power system. The Band-limited white noise is used as a "driver" for the disturbance component of the ARMAX model. A deterministic power disturbance is used to simulate changes in the power reference target produced by deviations in the national grid frequency.

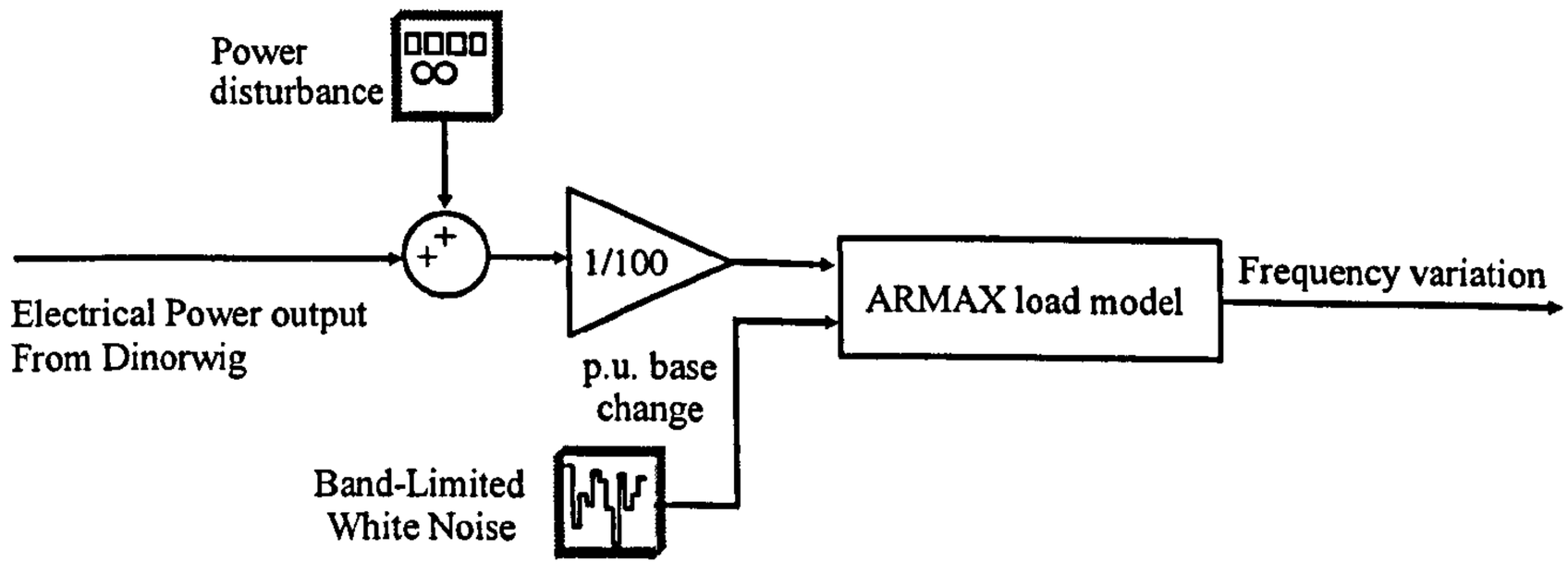


*Figure2.14: Grid model.*

## 2.5 Models for simulation

A software tool for Simulink was developed to facilitate studies of the power plant under different governors. The tool has libraries of special functions (blocks) and the power plant models were constructed by connecting these functions to the standard Simulink functions [12]. Using a dialog box, the parameters of a specific block can be adjusted. For example, the operating point of linear models may be changed. These models can represent the power plant as SISO or MIMO system and linear or nonlinear behaviour may be selected. Figure 2.15 shows a schematic of the Simulink power plant

model. The values of constants and parameters of Dinorwig were obtained from the work of Mansoor [3], as given in Table 2.2.

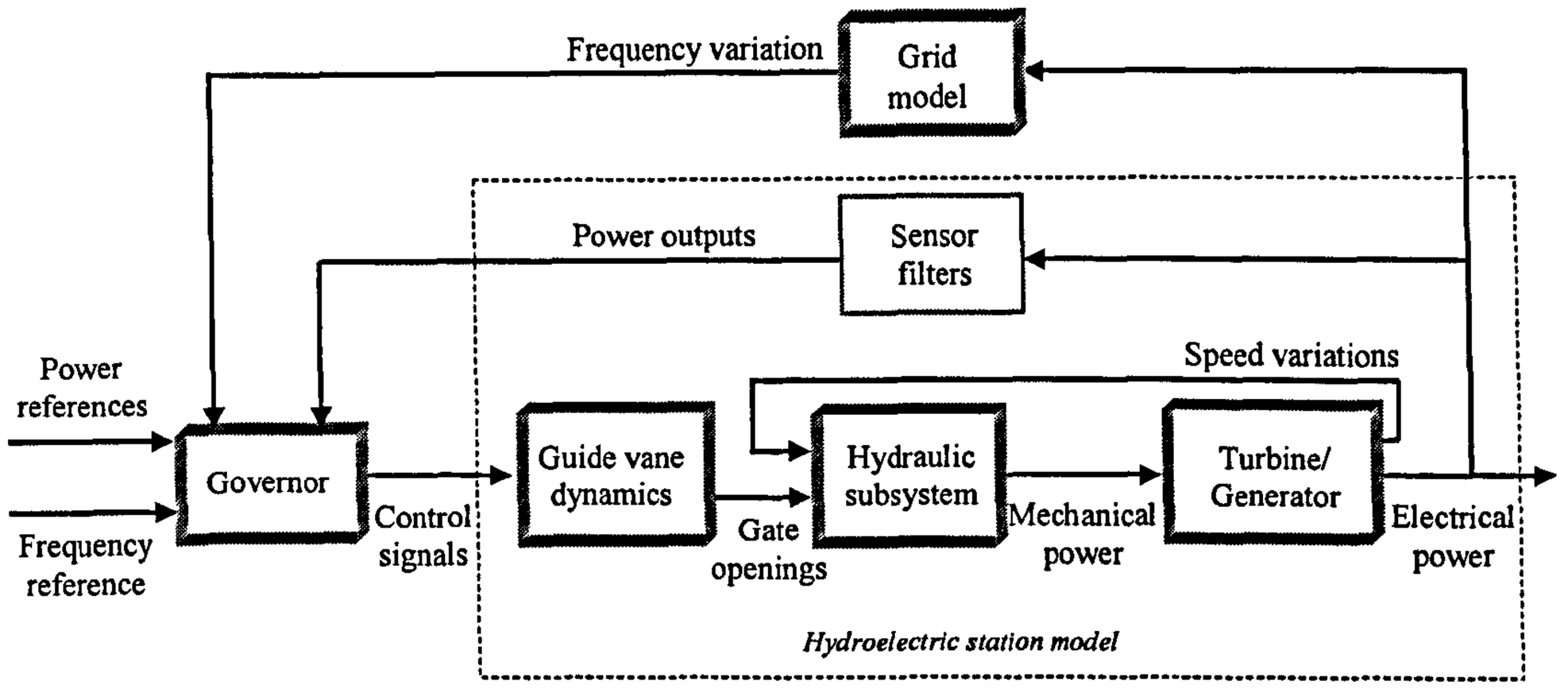


*Figure2.15: Schematic of the Simulink model developed.*

*Table 2.2*

*Dinorwig parameter used in simulations.*

| Symbol | Name | Subsystem | Value |
|---|---|---|---|
| $T_{mt}$ | Water starting time of the main tunnel. | Hydraulic | 0.388 s |
| $T_w$ | Water starting time of a single penstock | Hydraulic | 0.3066 s |
| $T_{em}$ | Wave travel (propagation) time in the main tunnel. | Hydraulic | 0.642 s |
| $T_e$ | Wave travel (propagation) time in one penstock | Hydraulic | 0.148 s |
| $A_t$ | Turbine gain | Hydraulic | Max 1.18<br>Avr. 1.12<br>Min 1.05 |
| $f_{pt}$ | Head loss coefficient in main tunnel | Hydraulic | 0.00002873 $m/(m^3/s)^2$ |
| $f_{pn}$ | Head loss coefficient in penstock | Hydraulic | 0.00052 $m/(m^3/s)^2$ |
| $Z_{0T}$ | Surge impedance main tunnel | Hydraulic | 0.6044 |
| $Z_0$ | Surge impedance single penstock | Hydraulic | 2.1 |
| $D_n$ | Turbine-damping coefficient | Hydraulic-Electric | 0.5 |
| $T_m$ | Machine starting time | Hydraulic-Electric | 7.99 s |
| $K_D$ | Turbine-damping coefficient | Electric | 8.38 |
| H | Turbine/generator inertia constant | Electric | 3.995 $Jn_m^2$/MVA |
| $K_s$ | Synchronising torque coefficient | Electric | 0.7071 |
| $\omega_0$ | Base rotor electrical speed | Electric | 314.1592 rad/s |

The full hydroelectric station model is constructed combining the four sub-systems: Guide vane dynamics, hydraulic subsystem, turbine/generator and sensor filters. Each block is part of the Simulink library developed for this study; they can be selected to represent a diversity of modes of operation. For example there are three models available to simulate the hydraulic subsystem: Linear, nonlinear nonelastic and nonlinear elastic.

The guide vane dynamics can be selected with or without rate limitation and saturation. The sensor filters block is a fixed block. The grid model can be adjusted to represent different conditions of the national grid. Through the governor block classic and advanced controls can be selected, as will be discussed in Chapter 4.

## 2.6 Evaluation of the models

Several simulations were carried out in order to establish consistency between different models, over the operational envelope. The evaluation was concentrated mostly on the hydraulic subsystem. The nonlinear elastic model was taken as a basis for comparison [3, 8]. The hydraulic models evaluated were the linear model, which was discussed in section 2.2.1, and the nonlinear nonelastic model (section 2.2.2).

Figure 2.16 shows the open loop step response of the linear and nonlinear hydraulic models when only one unit is in operation. A step of 0.76 (p.u.) was applied to all models to fix the operating point, and then a 0.04 step was applied at 100 seconds of simulation. The nonlinear nonelastic and linear models have a very similar response, although the linear model produces a more pronounced NMP response. The response of the nonlinear elastic model has a marked oscillation, which is not present in the other models; it is attributable to the elastic characteristics of the fluid included in this model.

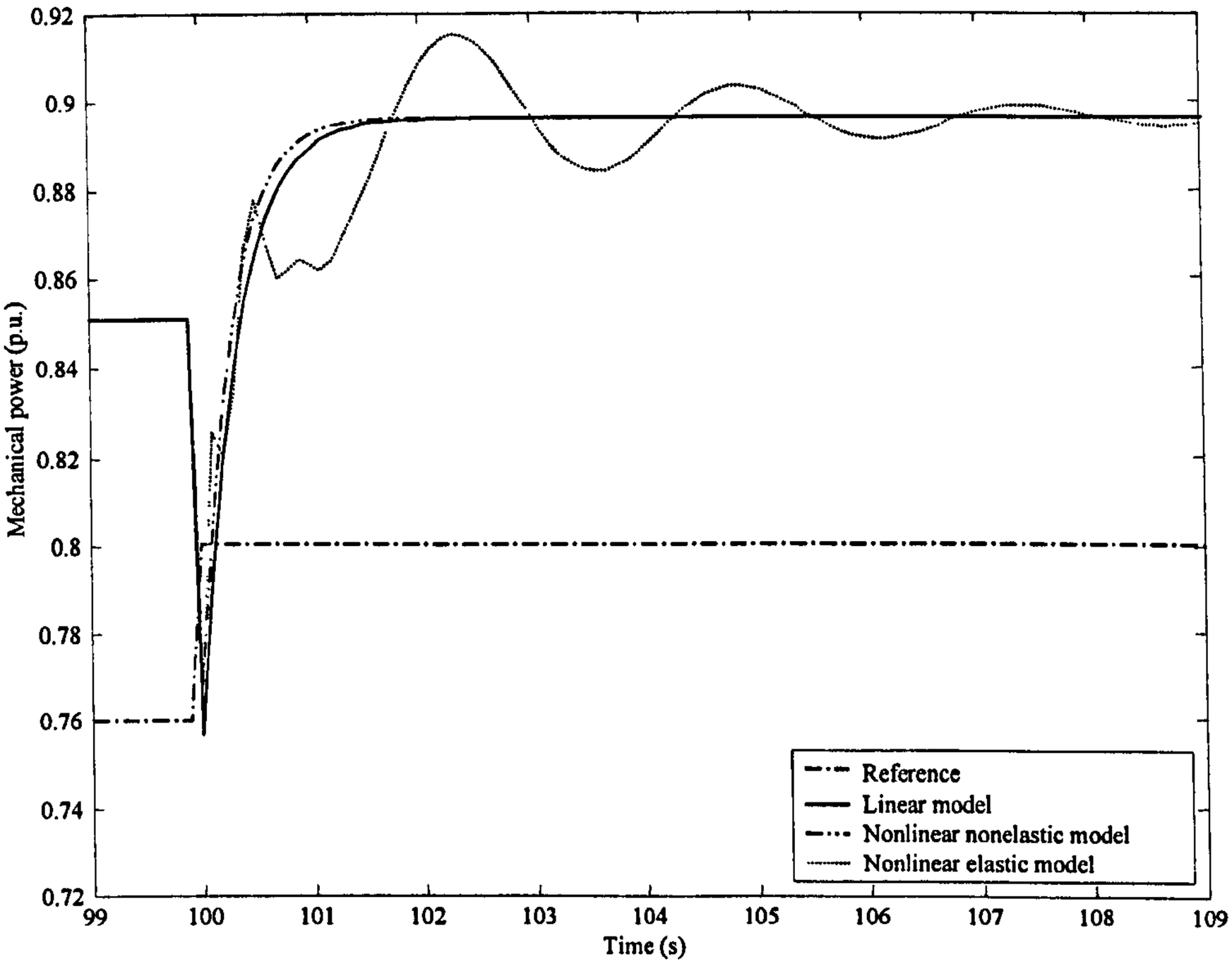


*Figure2.16: Step response of the hydraulic models with one unit active.*

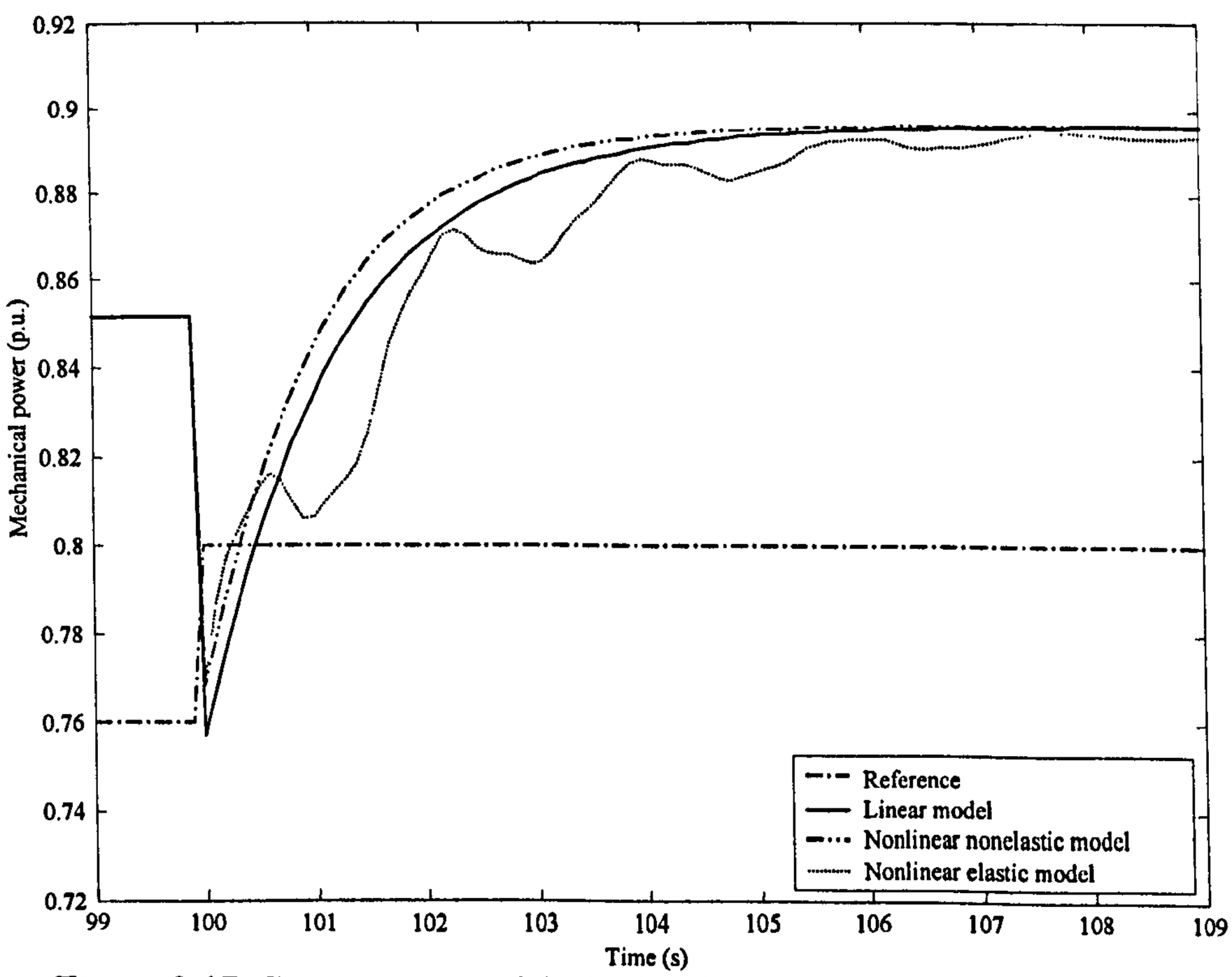


*Figure 2.17: Step response of the hydraulic models with six units active.*

As can be seen from Figure 2.17, when six units are active the open loop responses of the nonlinear nonelastic and linear model have some differences. The nonlinear model also has oscillation but it is less significant that in the one unit operational case.

Figure 2.18 shows again the open loop case with six units operational but at a different operating point (0.6). The nonlinear nonelastic and linear models now have marked differences. The nonlinear models react to this change however the linear model depends on this parameter. The Simulink linear model has the option to change it, but in order to show the limitation of this fixed model, the operating point was left at 0.8.

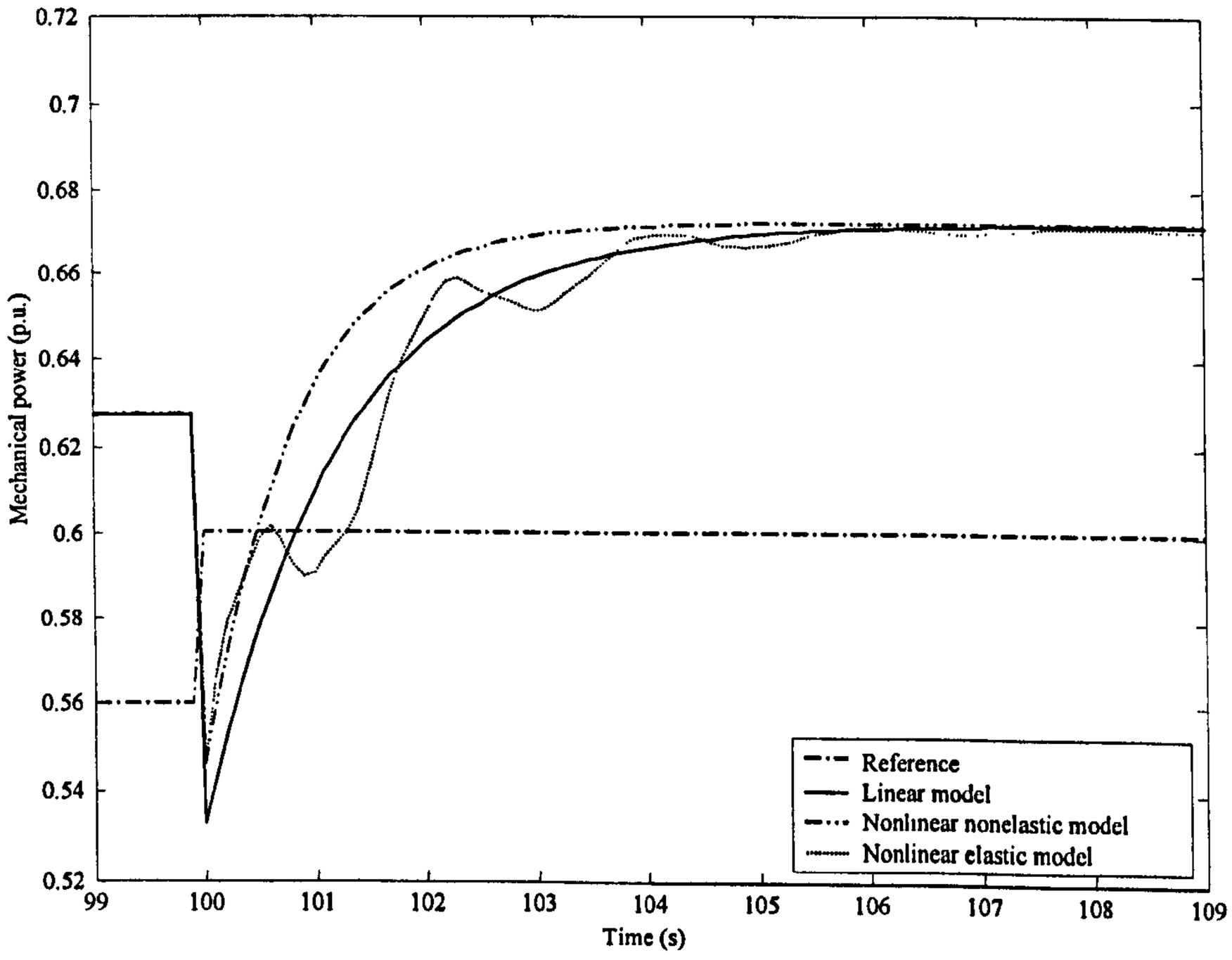


*Figure 2.18: Step response of the hydraulic models with six units active, operating point at 0.6.*

Figure 2.19 shows the direct and cross-coupling open loop step responses of the hydraulics plus guide vane models. In the upper graphic is shown the response of the unit one and in the lower graphic is shown the response of the units 2-6 in synchrony. In this simulation an operating point of 0.76 p.u. was first established in all units. Then a step of 0.04 was applied to unit one at 100 seconds of simulation, followed by a step of the same amplitude applied to units 2-6 at 110 seconds.

As can be seen from Figure 2.19 the responses of the models are comparable. In both graphics the response of the nonlinear elastic and linear models have a good approximation to the response of the nonlinear nonelastic model. The guide vane dynamics acts as a filter for the oscillation of the elastic nonlinear model; other effects are the reduction of the NMP response and an increase in the time constant of all models. The linear model seems to be a good approximation to both nonlinear models and is less computationally demanding.

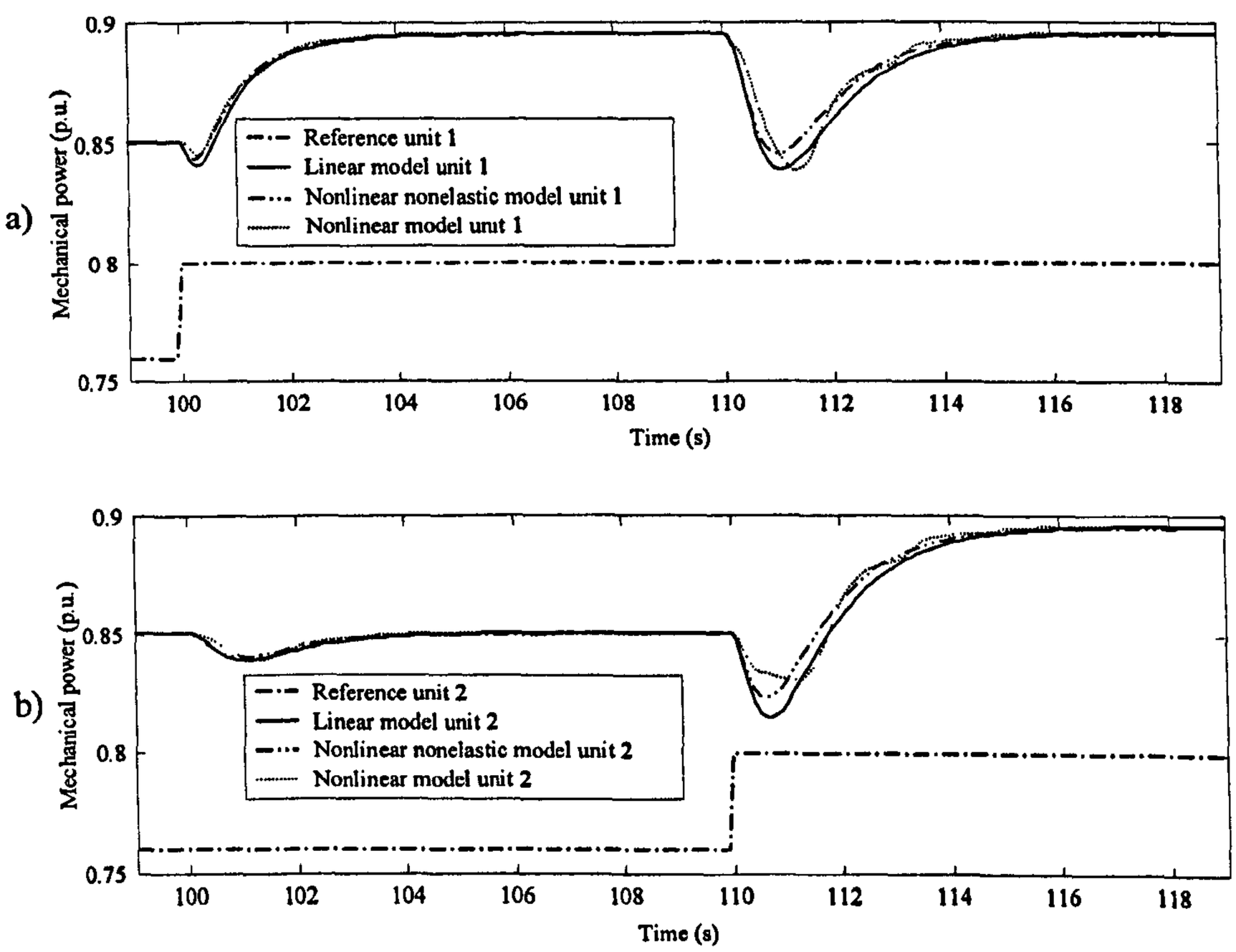


*Figure 2.19: Responses of integrated models to 0.04 p.u. step power demand, (a) Unit 1, (b) Units 2-6.*

## 2.7 Conclusions

In this chapter, linear and nonlinear models of pumped storage stations have been discussed. These models were applied to the Dinorwig power plant. The models included representation of the guide vane, hydraulic and electrical subsystems and contain the principal features of the plant's dynamics. The discussion of the Governor will be addressed in Chapter 3.

The models will be used in Chapters 5 and 6 to compare the performance of the hydroelectric station under different controls. The Linear model will be used in time domain simulation when small perturbations are analysed, while the nonlinear elastic model will be employed in simulations when small and large amplitude signals are fed to the Power plant.

# Chapter 3

# Characteristics of the Speed Governor

## 3.1 Introduction

Having described the characteristics of the guide vane, hydraulic and electric subsystems in Chapter 2, this Chapter describes advances in primary speed/load control, commonly named the Speed Governor. As was shown previously, the governor calculates the control signal that drives the guide vanes. It measures the system frequency and power demand in order to regulate the flow of water through the penstock and to help restore grid frequency to nominal.

Advances in generic primary speed/load control as well as the specific governor in Dinorwig are discussed in this Chapter. Section 3.2 is a brief review of Turbine-generator control developments and then the Dinorwig Governor Configuration is presented in section 3.3, followed by discussion of the step and ramp specifications in section 3.4. Section 3.5 deals with a closed loop analysis that shows some of the dynamic and control limitations of the Power Plant. Finally, some conclusions are drawn in section 3.6.

## 3.2 Turbine-generator control developments

Old civilizations used hydropower. In ancient Greece and Rome the waterwheel was common machinery, while in China the use of hydropower goes back at least 2000 years. In the Middle Ages the variety and applications of waterwheels increased greatly, though it was not until the 18th Century that the first comprehensive theoretical studies of waterwheels were developed. The first turbines appeared in the 19th Century and during the final years of that Century centrifugal regulators controlled the turbines' speed. The most successful regulator used for these first turbines was the Flyball governor. This device was the main component of the earliest mechanical governors [13].

Figure 3.1 shows a simple schematic of the Flyball. The rotation of the fly balls is proportional to turbine speed. The spring force opposes the centrifugal force of the fly balls and when both forces are in equilibrium the valve maintains its position [14]. The mechanical Governors employed power amplification to move the valve or the gates of the turbine. The latest mechanical Governors were highly sensitive and precise devices with fixed control structures, usually PI and PID. However, the control parameters were very hard to change and it was almost impossible to adjust them on-line [13].

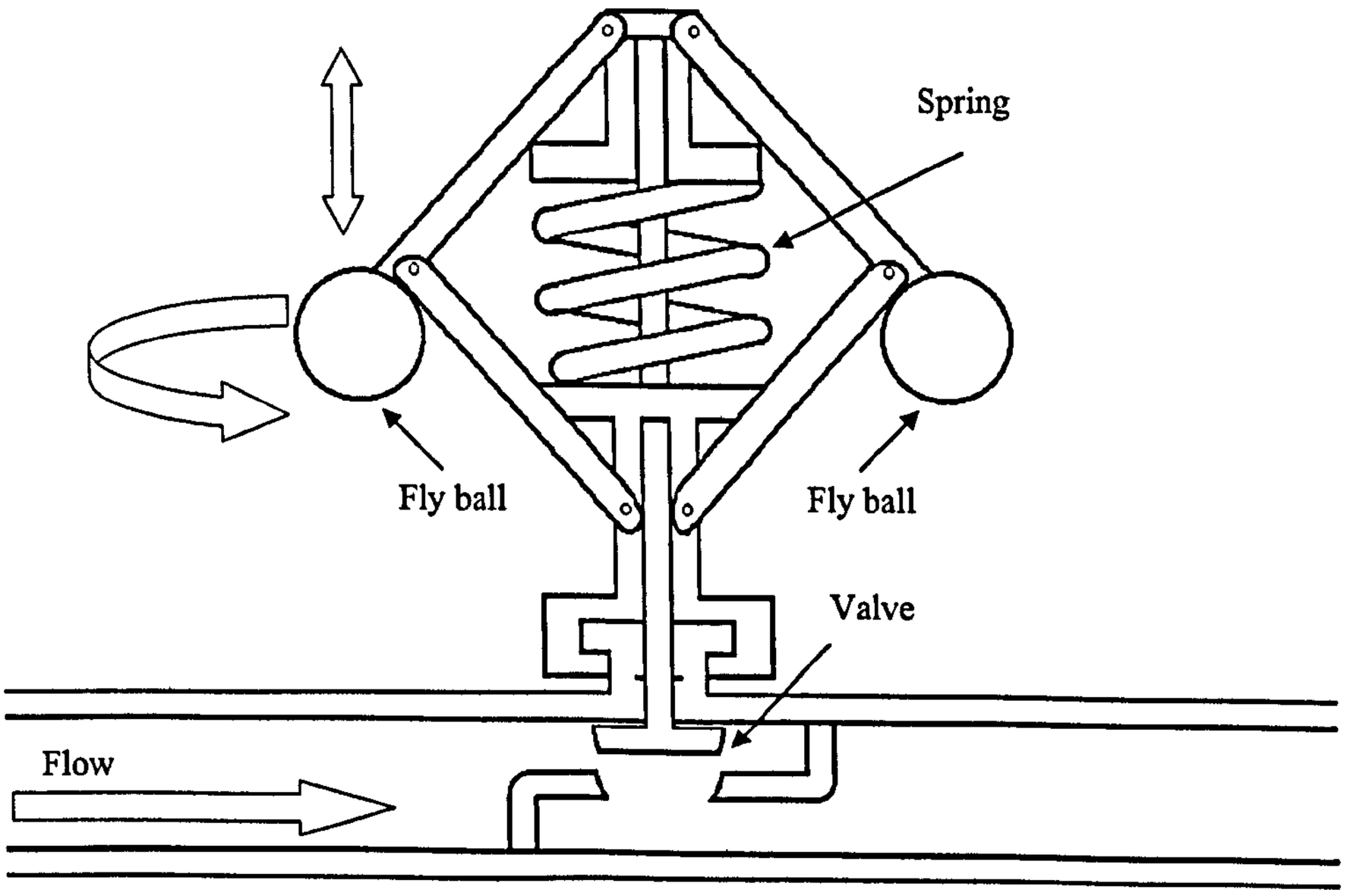


*Figure 3.1: Flyball governor.*

A big step in the development of Governors was replacement of the Flyball by electrical or magneto-electrical devices to measure the rotation speed. The main advantages of these analog electric Governors were the improvement in transient response, flexibility of physical layout and the possibility of combining single controls into one overall power plant regulator [15]. The analog Governors had rigid PI or PID structures, even if they offered the possibility of easily changing the control parameters. The arrival of digital governors solved this limitation [13, 16].

Digital Governors have the capability to take into account the differences between all operational conditions. For example, bringing the generator up to the same frequency as the power system and achieving a phase match for synchronization are the goals when a machine is starting up. On the other hand the goal of on-line governing is to provide smooth and fast load speed regulation during frequency disturbances.

Advanced control design methods have been applied to Power Plants although, until recently, all control system design for hydroelectric plants was done on the basis of SISO linearised models. Simulations, however, are usually done on a nonlinear model. As was noted in Chapter 2, the parameters of a linearised model vary with the water flow and hydraulic head. A fixed parameter PI controller can therefore only be optimum at the operating point selected during design. The behaviour of hydraulic power station controlled by classic PID governor has been studied by several authors. Thorne and Hills studied the stability region of a hydraulic turbine generating unit having a PID governor [17]. Dhaliwal and Wichert studied the effect of derivative gain on the stability of a SISO system supplying an isolated load, their work also being extended to cover the case of two machines [18]. Hagihara applied the Root Locus method to investigate the effect of the PID parameters on the stability boundaries of a hydraulic turbine generating unit supplying an isolated load [19]. Mansoor reported a comprehensive study where the behaviour and operation of Dinorwig is investigated [3]. In this latter study, Routh-Hurwitz and Root Locus methods were utilised in order to determine the optimal set of PID parameters for Dinorwig.

Methods for improving performance across the operating envelope have been developed which adapt the controller according to the operating condition. For instance, Orelind *et al* [20] demonstrated the use of a gain-scheduled controller which selects the parameters

of a PID compensator as a function of the guide vane angle. Ye *et al* [21] also describe a controller whose parameters vary over the plant's operating envelope as a function of the static head, guide vane angle and turbine speed. The parameter values (e.g. PI gains) are pre-determined from linearised analyses at various points across the operating envelope and stored for on-line access. They also note that the dynamics are affected by the guide vane rate limit and propose a nonlinear gain term to compensate for its effect. Finally, they propose that the structure of the controller should change in order to accommodate various operational modes, e.g. frequency-control or speed-regulation.

Adaptive controllers have also been considered. Mansoor *et al* [22] have shown that open loop gain scheduling according to the number of Units on-line is a simple but reasonably effective measure. Lansberry and Wozniak [23] suggest using a genetic algorithm to perform the adaptive function so that the gains of a PI governor are made to continuously track changes in either the water starting time or the grid stiffness (i.e. the sensitivity of grid frequency to load). In a recent paper, Eker and Tumay [24] use the method of $H_\infty$ optimisation to design a robust controller which is insensitive to uncertainties in plant parameters, including the water starting time and the wave travel time for an inelastic water column. Simulation results indicate that the $H_\infty$ controller, although linear and fixed, gives better rejection of both electrical load disturbances and 'water' disturbances (such as may occur if the guide vane on another Unit is opened or closed rapidly), than does a PID controller. Designing on the basis of a SISO model, with every governor tuned for the worst-case interaction (all Units on-line), leads to conservative tuning [9]. The need for caution is understandable because exceeding the stability boundary can cause highly undesirable frequency oscillation to occur on the grid [25]. It is common, however, for hydroelectric plant to spend considerable periods with only one or two Units active, when the conservative tuning leads to sub-optimal performance. This is less tolerable in the new economic climate of privatised utilities. It is preferable to address the effect of coupling directly by multivariable methods. Jones [4] has shown that a 2-input, 2-output model gives a more accurate representation of the dynamics and demonstrates the loss of stability margin due to hydraulic cross-coupling. It is also shown how a decoupling controller can be designed, using the Direct Nyquist Array (DNA) technique, to counter this effect.

## 3.3 Dinorwig Governor Configuration

Dinorwig has a digital Governor whose general configuration is shown in Figure 3.2. There are two control loops, for power and frequency [3].

- In the power control loop the turbine's guide vane is adjusted depending on the power deviation multiplied by the speed regulation droop. A PI configuration is used for this control.
- The frequency control loop provides a reference to the power control loop, which is proportional to the frequency error. There is also a derivative feed-forward loop so that the system responds to rapidly-changing grid frequency.

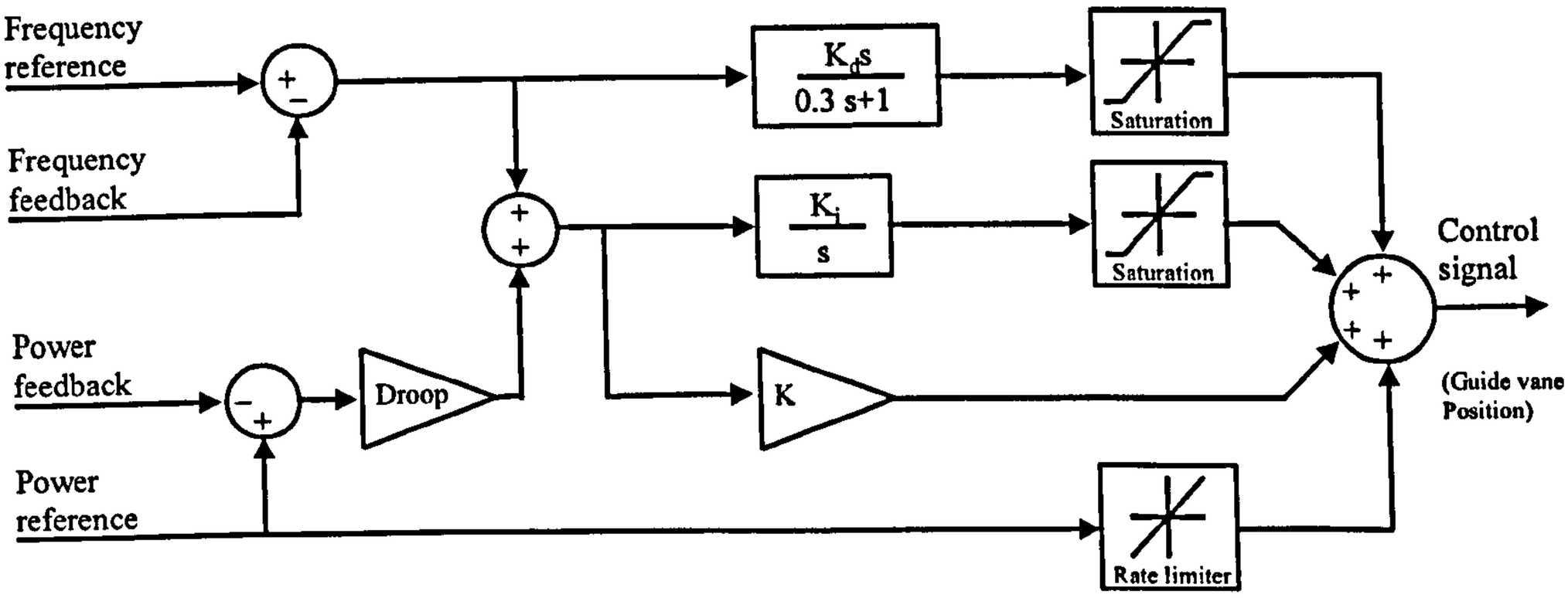


*Figure 3.2: Scheme of the Dinorwig Governor.*

The generators must maintain the speed within an operational band because the utility grid has them working synchronously. The Droop gain is used to change the speed reference of the governor. When the reference is raised the governor valve will open, thus increasing load. On the other hand when the output signal is lowered the reference signal to the governor valve will close, decreasing load [14]. At Dinorwig the governor operates with two droop settings; 1% for high regulation and 4% for low regulation [3].

The power reference signal sets the reference position for guide vane opening and defines the operating point for the unit when it is working in frequency regulation mode (part load response). Changing the power reference, which also acts as a feed-forward signal, directly sets the guide vane position, in order to produce a rapid reaction when

big changes in the power reference appear. The guide vane position reference signal (control signal) is produced by adding the output signals from the P, I and D parts to the feed-forward signal. The power feedback loop compensates the system for the non-linear relationship between guide vane opening and power.

## 3.4 Specification

The role of a hydroelectric station in frequency control mode is to provide timely and accurate supply of its target power contribution to the power system. The actual form of the power demand is related to Grid frequency variation but, for testing, it can be specified in terms of step, ramp and random input signals [26, 27]. In this section, the step and ramp response specifications for single unit operation, which were proposed by Jones *et al* [26], are presented.

The intention here is to introduce, for research purposes, a more challenging set of specifications than are currently in use for commercial purposes. The specifications in this section represent a balance between a significant improvement in speed and accuracy of response but not so demanding that they result in unrealistic control activity and tunnel pressures. The specifications themselves are for single unit operation but it is implicit that any controller that achieves them also maintains an acceptable response over the remainder of the operating envelope.

### 3.4.1 Step response

The step response specification for single unit operation is expressed in Figure 3.3 and Table 3.1 (these are not valid for commercial purposes). The most important criterion is usually Test P1 for the *primary response,* which requires that the station, under defined conditions, achieves at least 90% of the demanded step power change within 10s of initiation. Table 3.1 also shows that the over-shoot $P_2$ must not exceed 5% and the initial negative excursion $P_6$ (undershoot), associated with the non-minimum phase response, must not exceed 2%.

*Table 3.1*

*Specification of step response for advanced control design at Dinorwig.*

| Test | Specification for single unit operation. | Single unit response with current governor. |
|---|---|---|
| P1 | $P_1 \geq 90\%$ at $t_{p1} = 10s$ | 81% at 10s, 90% at 13.7s |
| P2 | $P_2 \leq 5\%$ and $t_{p2} \leq 20s$ | No overshoot |
| P3 | $t_{p3} = 25s$ for $P_3 \leq 1\%$ | 25.9s |
| P4 | $t_{p4} = 60s$ for $P_4 \leq 0.5\%$ | 29.2s |
| P5 | $t_{p5} = 8s$ | 12.1s |
| P6 | $P_6 = 2\%$ | 1.75% |
| P7 | $t_{p7} = 1.5s$ | 0.88s |

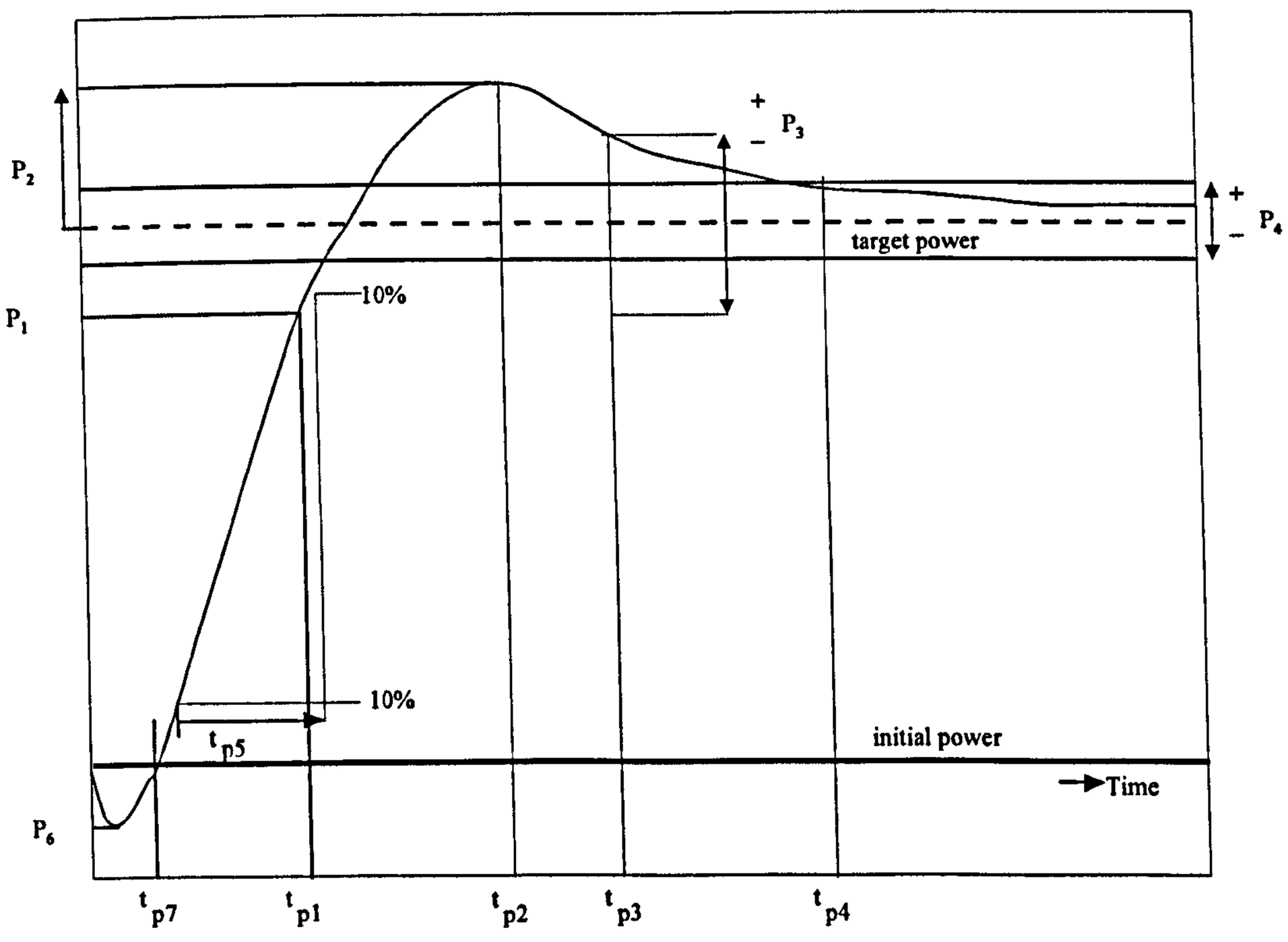


*Figure 3.3: Specifications for a response to a step change in demanded power.*

The small-step response of the nonlinear elastic model of Dinorwig is shown in Figure 3.4. In order to illustrate the operational envelope at Dinorwig, one and six units operational, with all units in synchrony, are included. Also an artificial response that complies with all step response specifications is shown. It can be seen that the response in the case of one unit operational is slower than the specification, although it has a

shorter undershoot. The six units operational response is faster than the specification, but has a larger undershoot. If the control parameters are tuned to increase the speed response in the one unit operational case, the response of the six units operational case will be faster but its undershoot and overshoot will fail to comply with the specification.

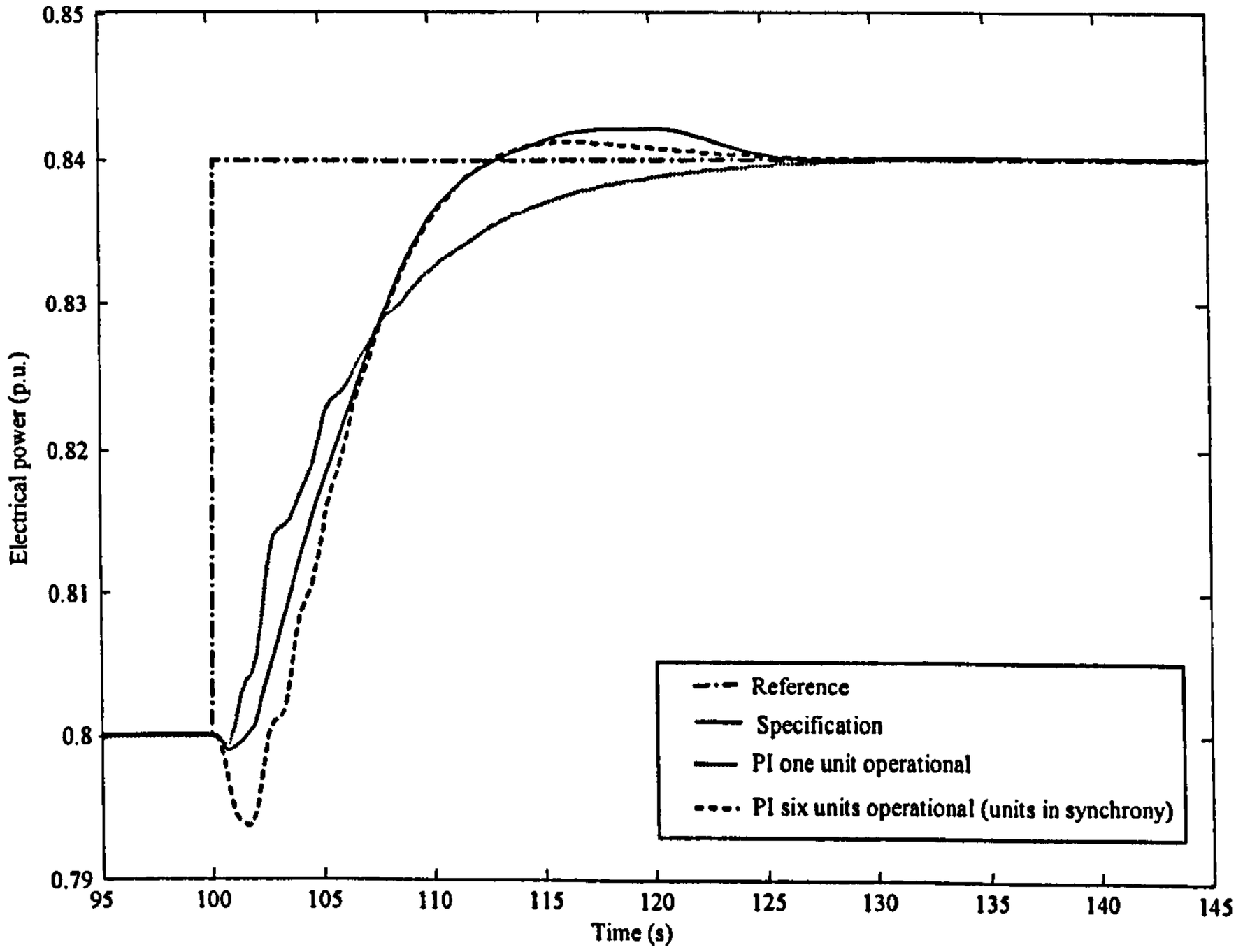


*Figure 3.4: Step response of the hydroelectric plant under a PI controller.*

### 3.4.2 Ramp response

The ramp response specification for single unit operation is expressed in Figure 3.5 and Table 3.2. Again, the most important criterion is usually Test Q1 for the *primary response ($t_{q1}$)*, which requires that the station, under defined conditions, achieves at least 90% of the demanded power change, ramp amplitude ($A_r$), within 15s of initiation. Table 3.2 also shows that the maximum rate $Q_2$ must not be less than 90% of the ramp rate and the steady-state accuracy $Q_3$ must not be longer than 30s. Test $Q_4$ shows the effective under-delivery of power over the period of the ramp [26]. The ramp response of the nonlinear elastic model of Dinorwig is shown in Figure 3.6.

*Table 3.2*

*Specification of ramp response for advanced control design at Dinorwig.*

| Test | Specification for a single unit operation | Single unit response with current PI control |
|---|---|---|
| $Q_1$ | $Q_1 \geq 90\%$ at $t_{q1}=15s$ | 14.7 |
| $Q_2$ | $Q_2=90\%$ of 6 $MWs^{-1}$ | 1.8 $MWs^{-1}$ |
| $Q_3$ | $t_{q3}=30s$ for $Q_3 \leq 1\%$ | 27 |
| $Q_4$ | None specified | E(RMS)=3.09 MW for $t_{q4}=50s$ |

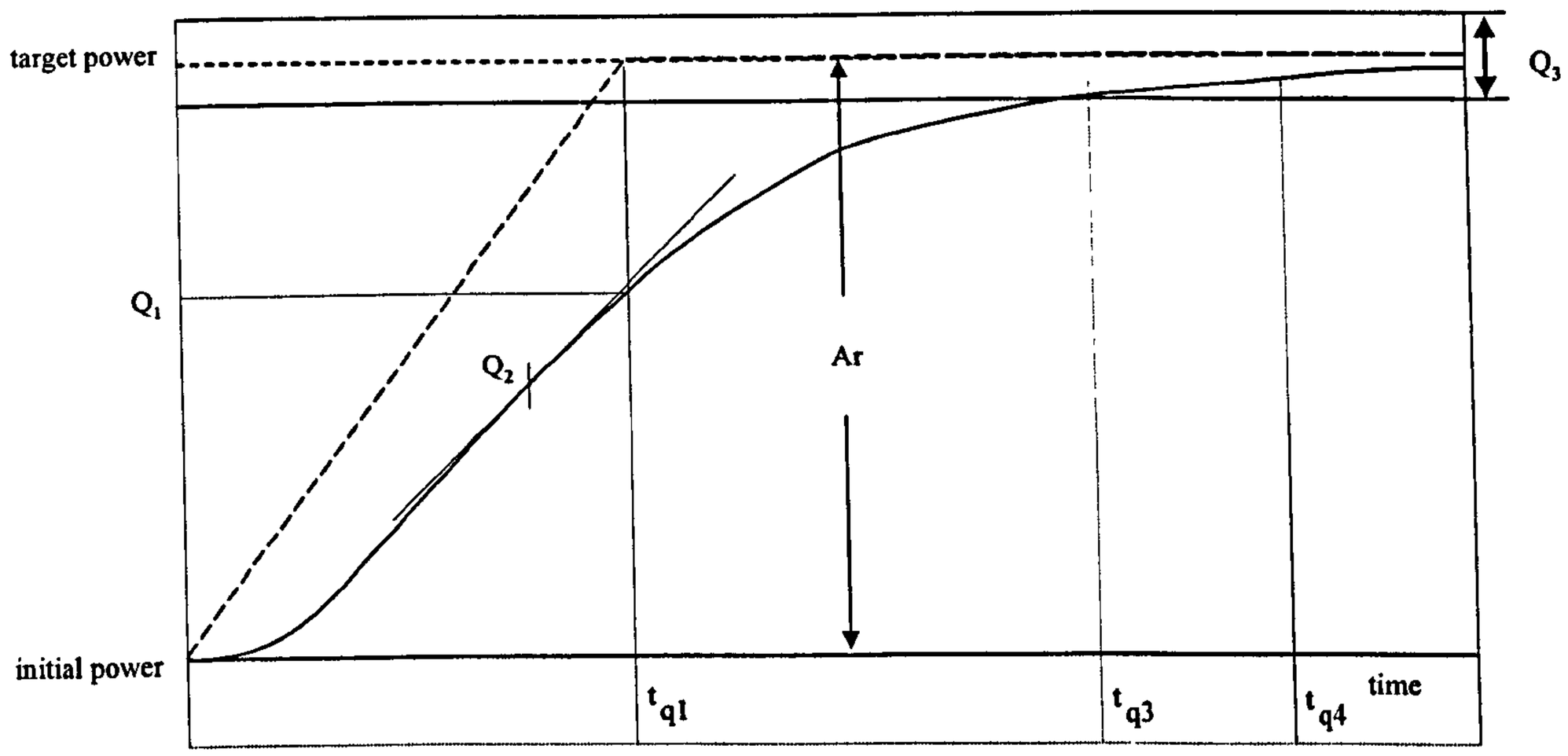


*Figure 3.5: Specification for a ramp input power target.*

Figure 3.6 shows the ramp response of the nonlinear elastic model of Dinorwig. Again the one and six units operational cases, with all units in synchrony, are presented, plus an artificial response that complies with all ramp response specifications. As can be seen, in the case of one unit operational, the response is slower than the specification and has no undershoot. The six units operational response is as fast as the specification, and it has a lower undershoot. As for the small-step response, if the response of the one unit operational case is accelerated, the response of the six units operational case will be faster but its undershoot and overshoot will exceed the specification.

The comparison of the model's response with a PI controller with the specification has shown that several criteria are not satisfied. The application of a small-step demand in the six units operational results in overshoot because the hydraulic coupling has increased the effective water starting time. The standard PI controller setting is a

compromise between one and six units operational, it has its parameters fixed to a constant value. Increasing the loop gain would improve the one-unit response but make the six-unit response even worse. The aim of the improved controller considered in this thesis should therefore be to satisfy the single-unit specification and also achieve fast, well-damped and low-interaction responses during multi-unit operation. This is not possible with a fixed-parameter PI controller [28].

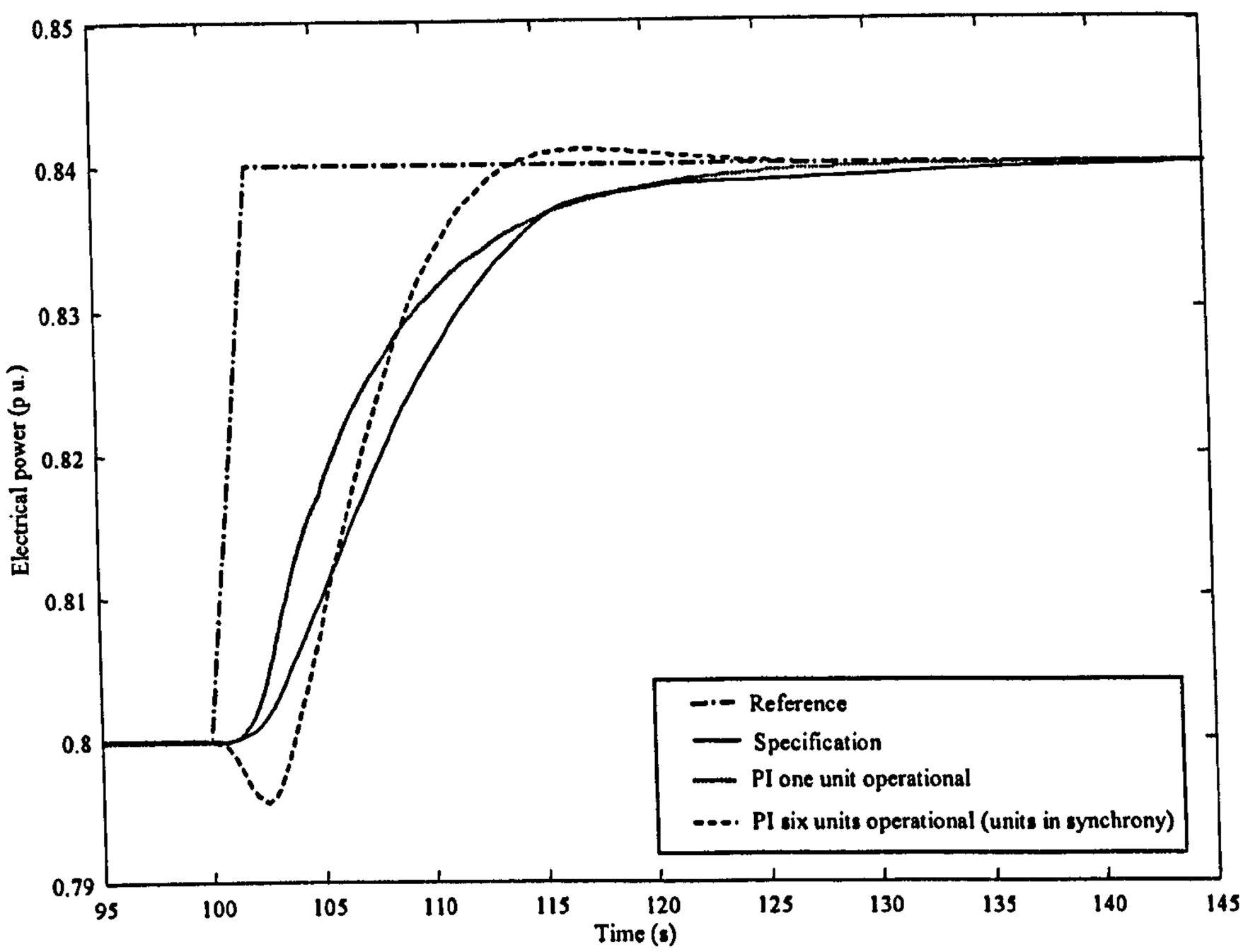


*Figure 3.6: Ramp response of the hydroelectric plant under a PI controller.*

## 3.5 Closed loop analysis

In order to increase the understanding of the relationship between parameters of the hydraulic system response and the parameters of the P and PI controllers, using an unit step as an input signal, several simulations were carried out, using Matlab Simulink [12] combined with theoretical analysis. The study can be seen as a visualisation approach to control tuning [29]. These methods are designed to visualise the system's dynamic behaviour across variations in system and control parameters. Heuristic rules, based on *a priori* knowledge, are employed to select the tests required to evaluate the system performance. It is necessary to generate several performance tables and graphics to

visualise a system adequately. This method was selected not only with the intention of not repeating the classic analysis developed by Mansoor [3], but also to offer another perspective which could provide a better understanding of the tuning problem in Dinorwig.

Figure 3.7 shows the most basic system model in closed loop control. The parameters under study were primary response, undershoot and zero crossover time. As is shown in Figure 3.8, the initial amplitude (undershoot) is the output signal value when the time is zero. The zero crossover time is the time when the output signal reaches zero after the non-minimum phase behaviour.

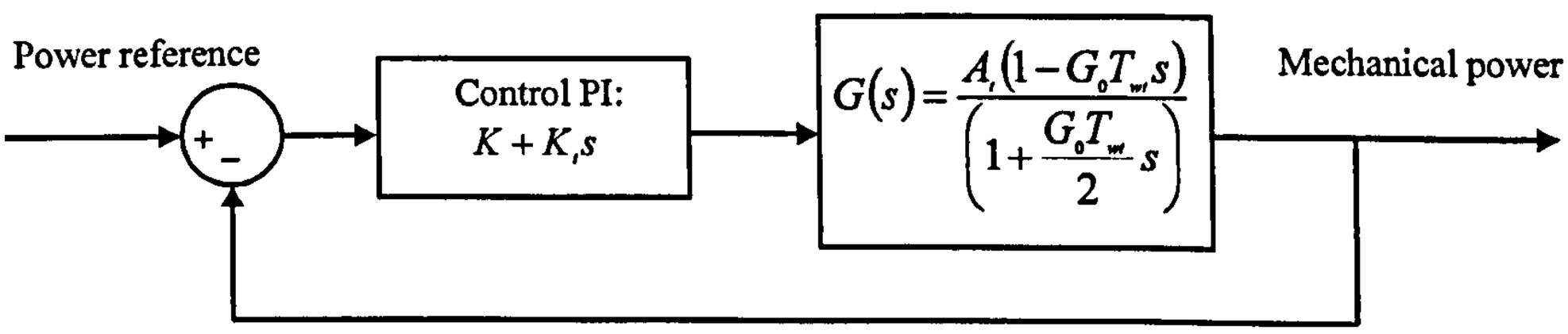


*Figure 3.7: Closed loop hydraulic system.*

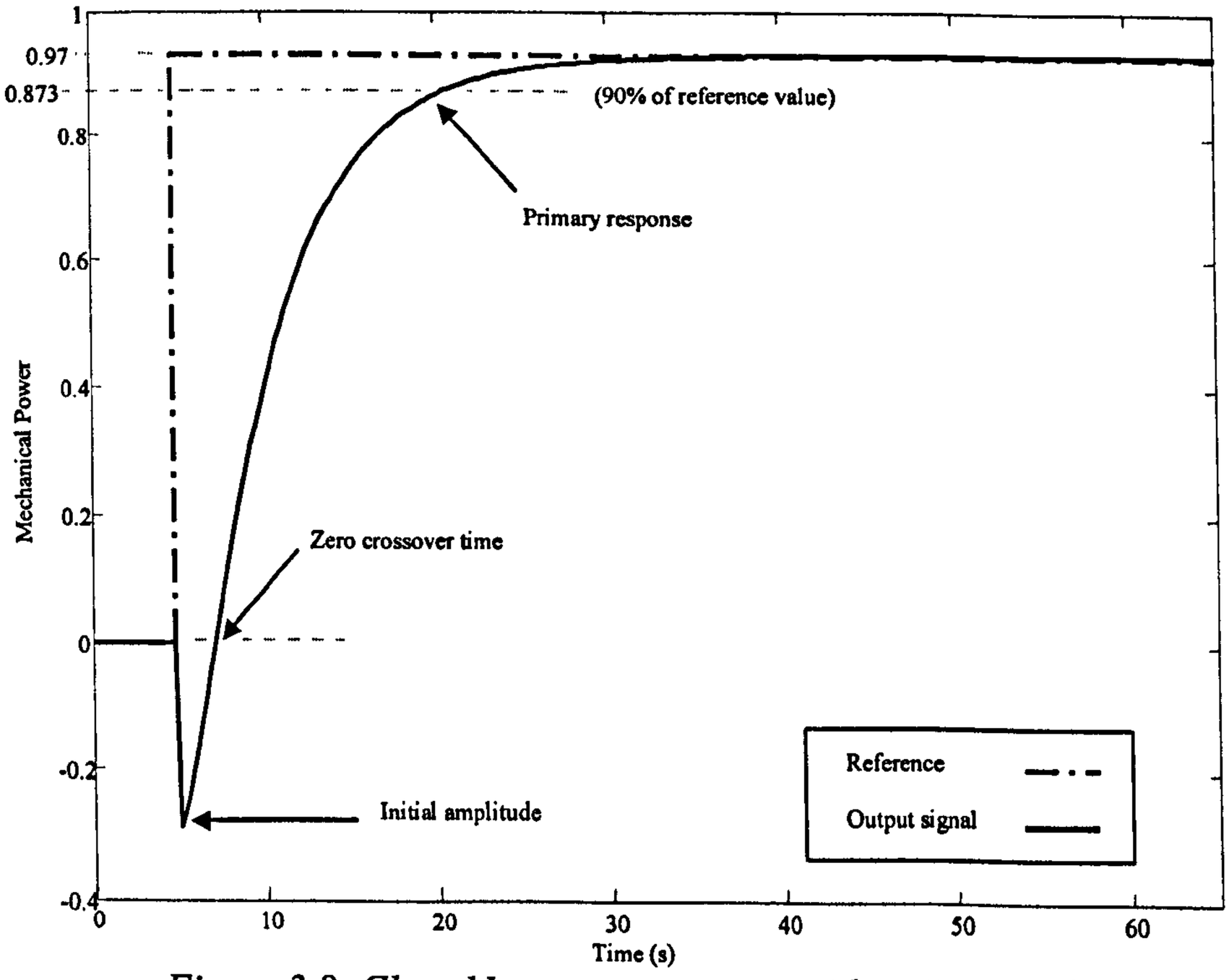


*Figure 3.8: Closed loop step response with a PI control.*

The effects of the control parameters on zero crossover time and the relationships between it and other parameters were investigated. Table 3.3 shows that $T_{wt}$ depends on the number of units under operation and that there is a linear relation between zero crossover time and $T_{wt}$, the zero crossover time increasing by 0.14 seconds per unit in operation. As is shown in Figure 3.9, variations in the operating point, $G_o$, produce a steady increase in the zero crossover time, while the slope of this relationship depends inversely on K.

*Table 3.3.*

*Variations of Zero crossover time and $T_{wt}$.*

| Units under operation | $T_{wt}$ | Zero Crossover time |
|---|---|---|
| 1 | 0.70 | 0.31 |
| 2 | 1.00 | 0.45 |
| 3 | 1.31 | 0.59 |
| 4 | 1.62 | 0.73 |
| 5 | 1.93 | 0.86 |
| 6 | 2.23 | 1.00 |

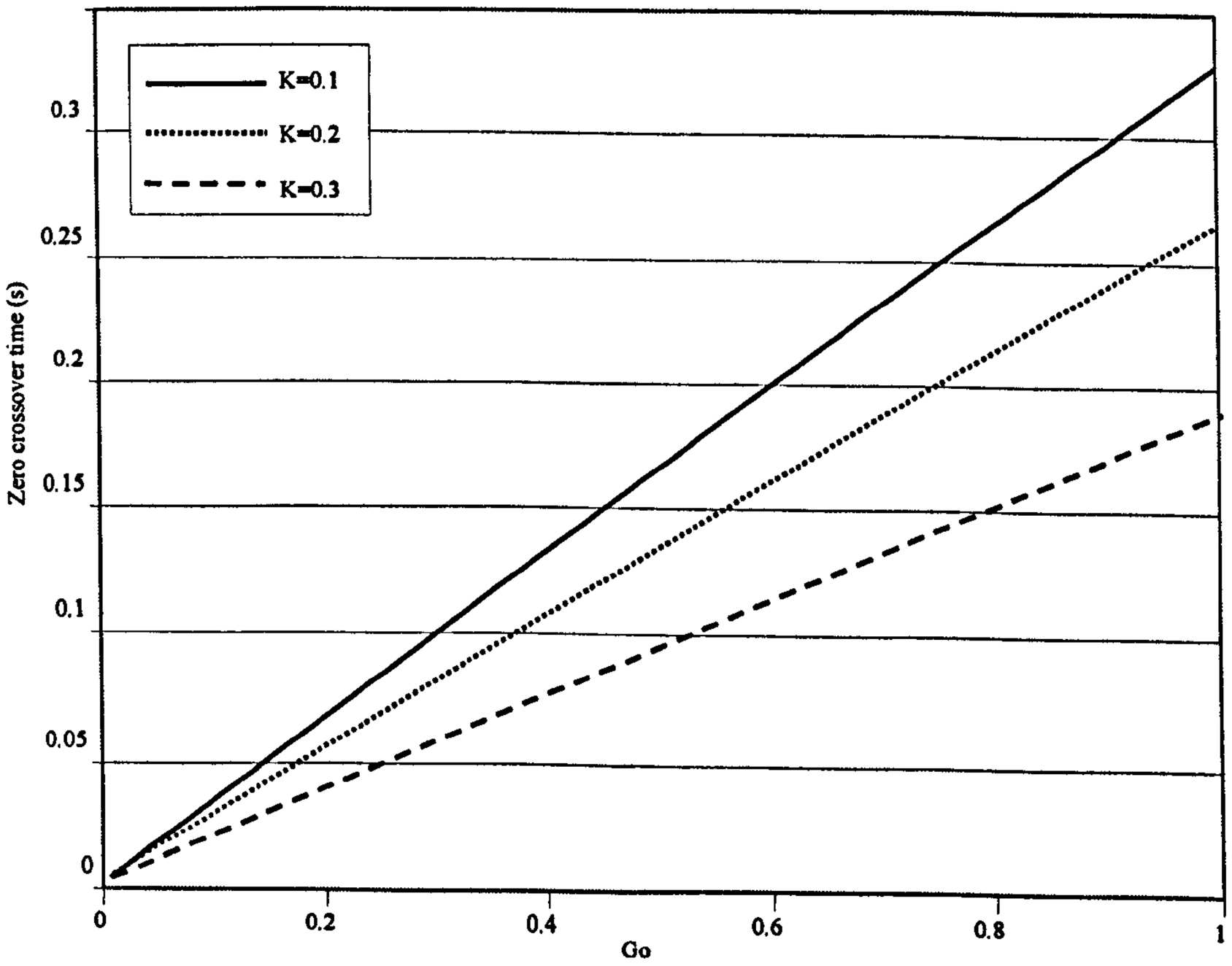


*Figure 3.9: Zero crossover time under P control with different values of K and $G_o$.*

When the plant parameters are fixed at $T_{wt}$=0.7 and $G_o$=0.95, the zero crossover time decreases as $K$ increases (see Figure 3.10). On the other hand, its value grows as $K_l$

increases for a fixed $K$ (see Figure 3.11). Its value has an inverse dependence on $K$ and a direct dependence on $K_i$.

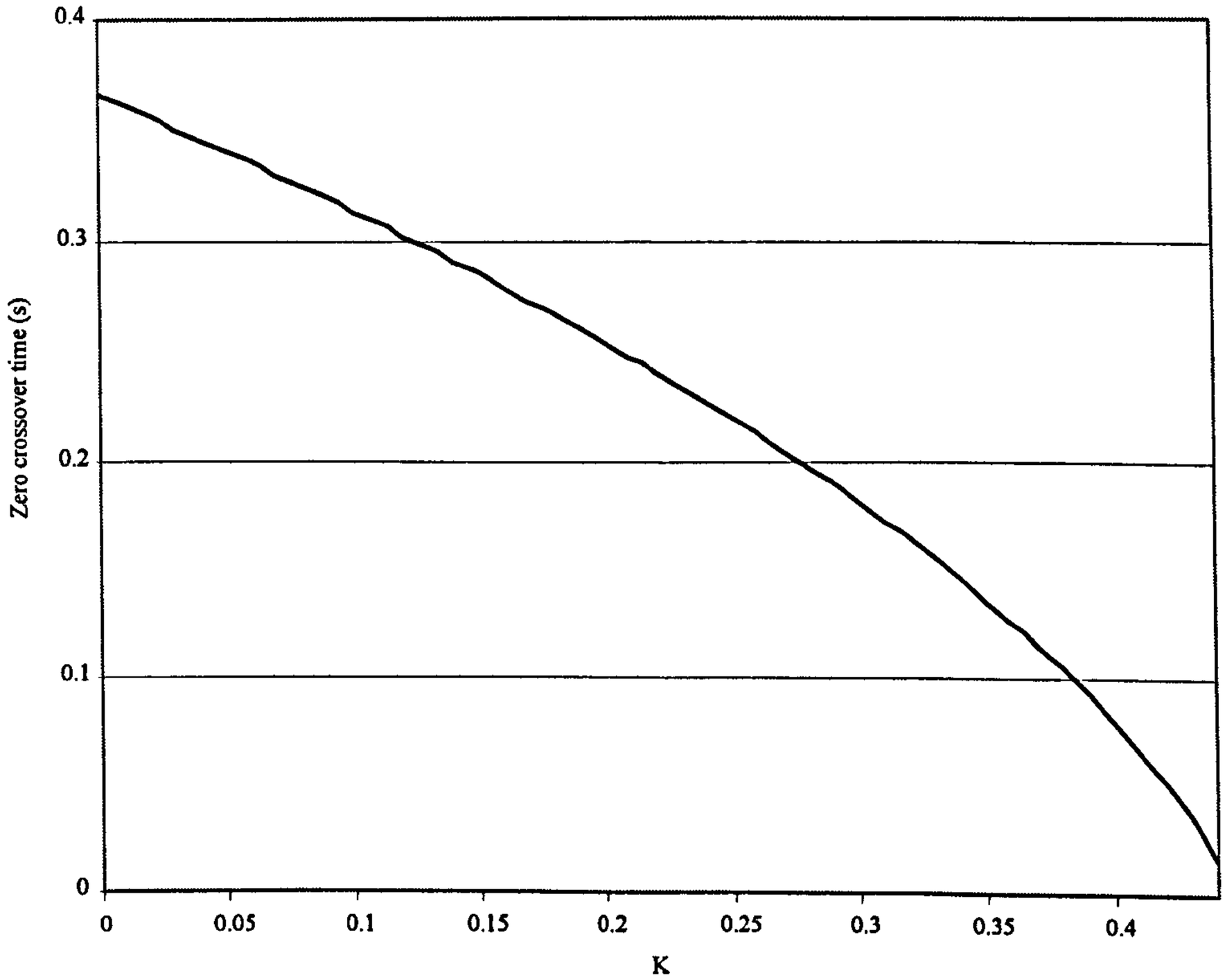


*Figure 3.10: Zero crossover time under P control.*

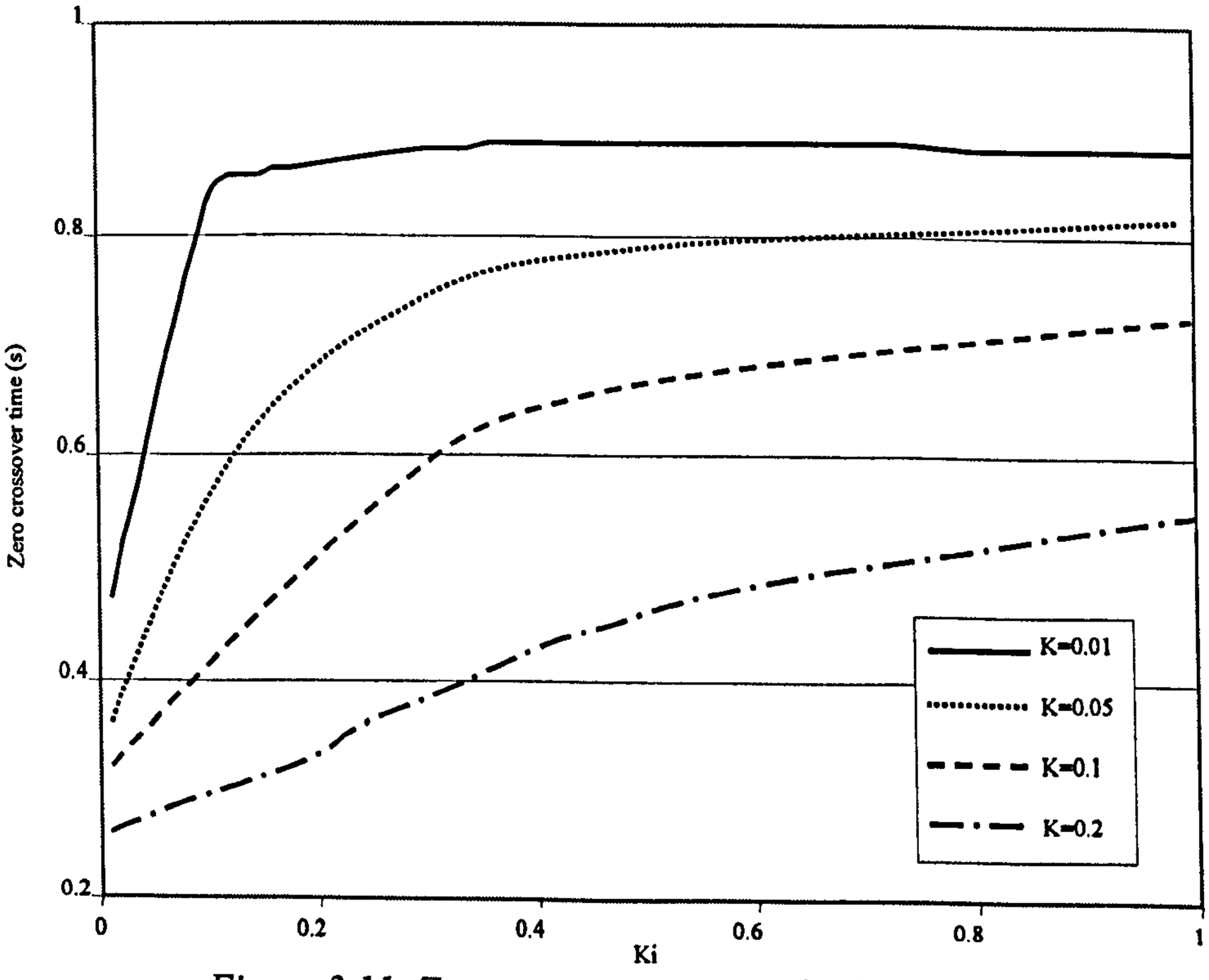


*Figure 3.11: Zero crossover time under PI control.*

The relationship between the initial amplitude and the control parameters was examined. It was found that the initial amplitude (undershoot) depends only on $K$, even when PI control is used. According to Figure 3.12 its value decreases rapidly as $K$ increases. With values of $K > 0.23$, this parameter is outside the saturation value.

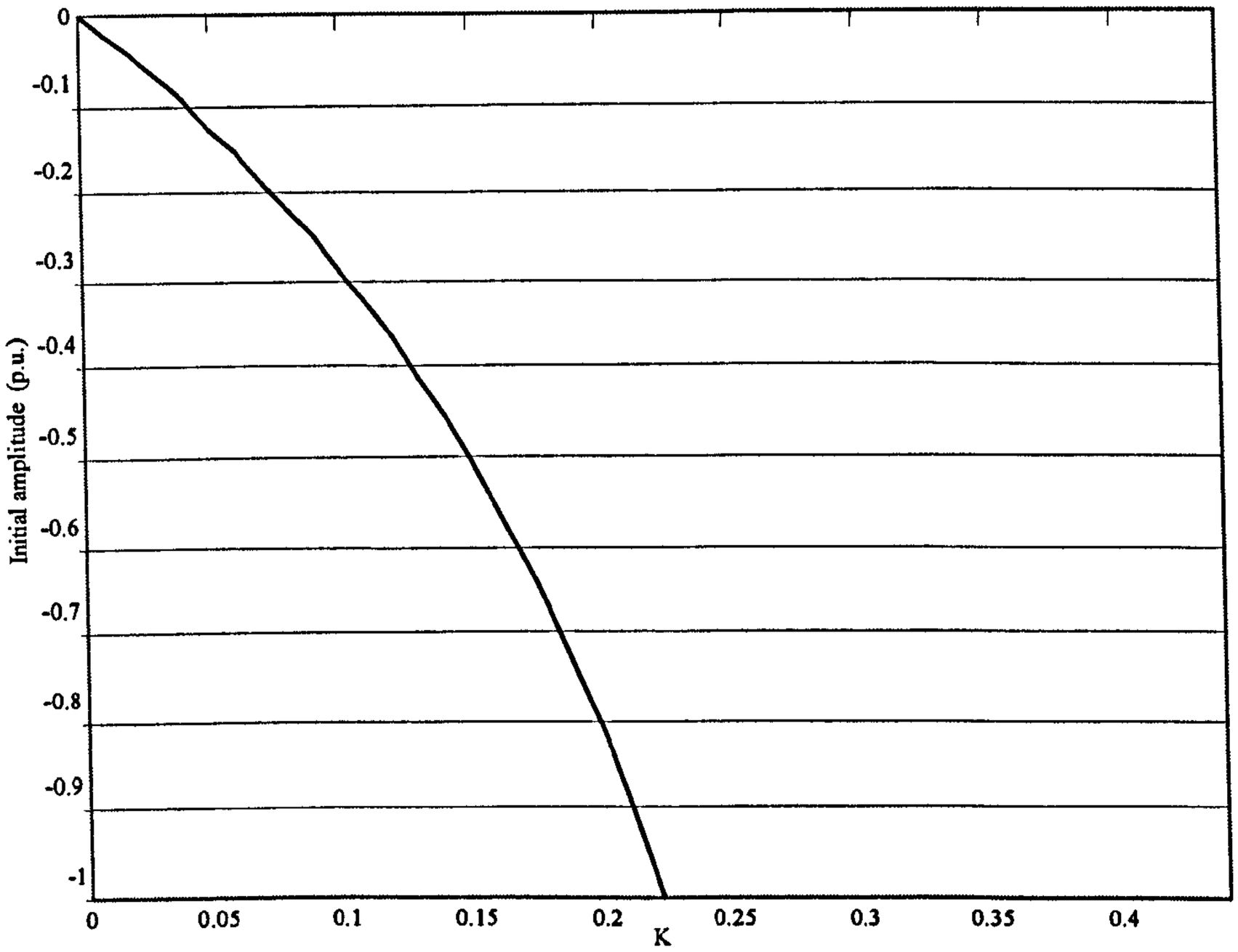


*Figure 3.12: Initial amplitude under P and PI controls.*

The effect of variation of the control parameters over the Primary response was studied. As is shown in Figure 3.13, variations in lower values of $K_i$ ($K_i \leq 0.4$) decrease dramatically the primary response; variations of $K_i$ over 0.4 show a gradual drop in primary response.

Finally the connection between primary response and zero crossover time was investigated. As shown in Figure 3.14 there is an inverse relationship between these parameters: it is not possible to decrease one of them without increasing the other. Variations of $K_i$ from 0.3 to 0.7, when $K$ is fixed to 0.1 and 0.2, are shown in Figure 3.14. These values were selected because lower values of $K$ produce a long zero crossover time and very long primary response, Figures 3.11 and 3.14.

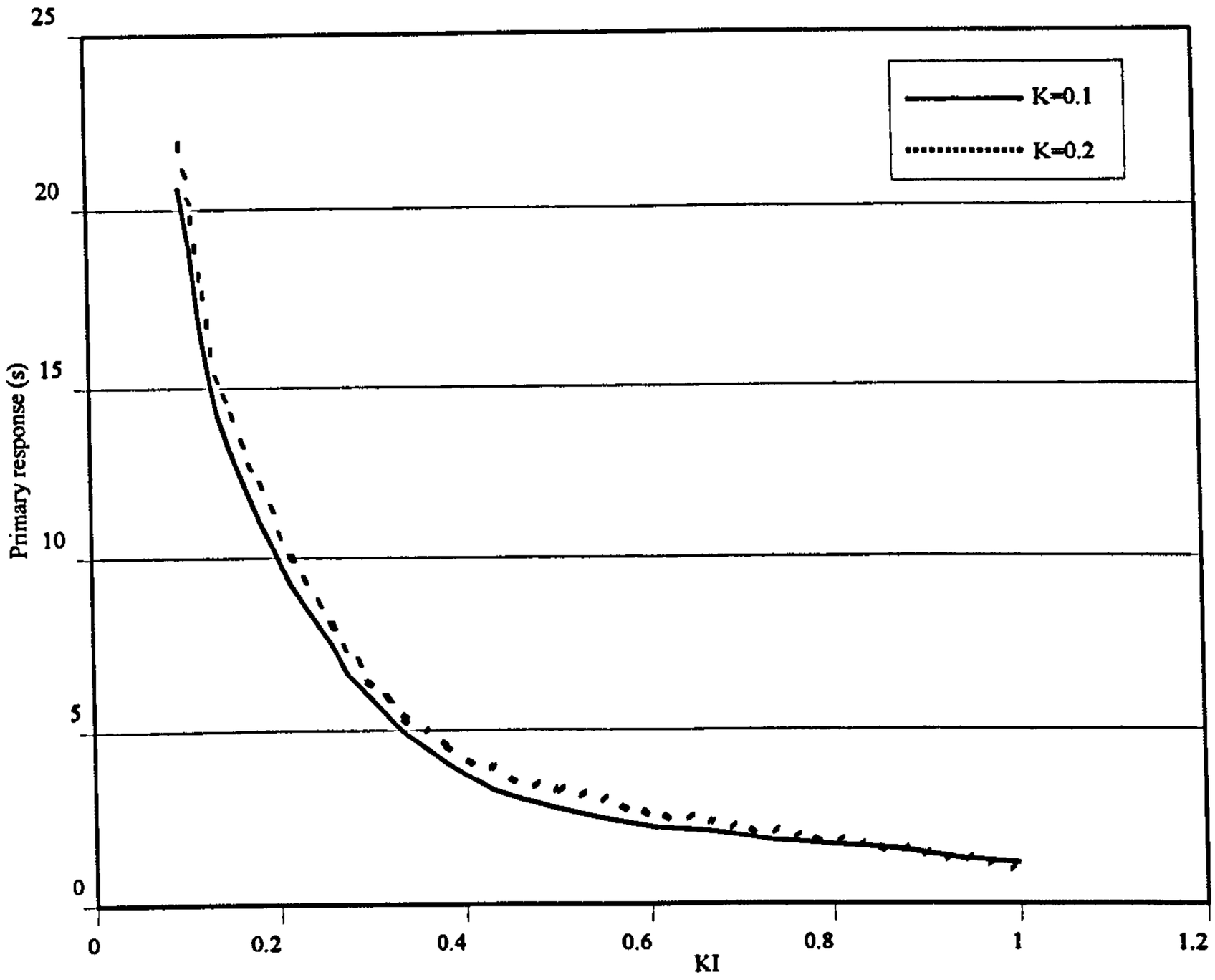


*Figure3.13: Primary response under PI control.*

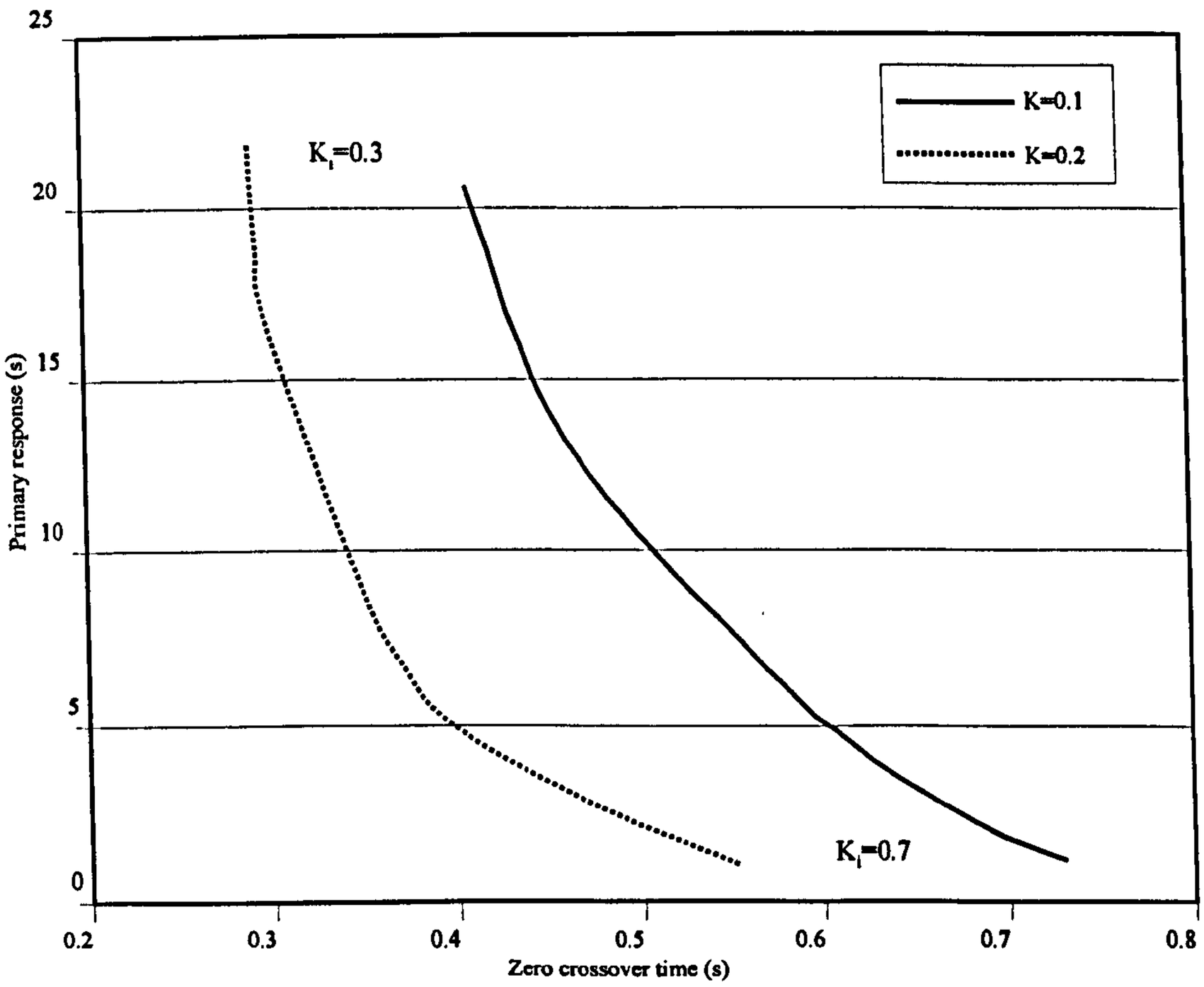


*Figure 3.14: Zero crossover time and primary response with K fixed and $K_I$ variable.*

Considering the points discussed in this section, a suitable range for the parameters of a PI controller can be selected for $K$ and $K_I$ as follows: $0.23 \geq K \geq 0.1$ and $0.5 > K_I > 0.1$.

Similar analyses have been conducted with classical control techniques [1, 3] and the results are congruent with those stated here. The conclusion that there is a close relationship between zero crossover and primary response is valid despite the structure of control applied to the system. However this and other effects can be attenuated if features such as multivariable behaviour and nonlinear dynamics are considered in the controller.

## 3.6. Conclusions

In the first part of the Chapter the general features of speed governors were discussed and the configuration of the Dinorwig speed governor was presented. The closed loop analysis offers guidance for selecting the parameters for classic PI control. It has been shown that, because of the relationship between the dynamical parameters of the system, it is not possible to improve one of them without deterioration in another parameter.

Model Based Predictive Control (MBPC), [30, 31], seems to offer a solution for the following reasons:

- It is widely acknowledged as being straightforward to extend to multivariable systems.
- Perhaps its greatest advantage (which has stimulated its widespread acceptance in industrial process control) is that it deals naturally with hard constraints on the control and state variables, whereas linear methods (like the Direct Nyquist Array) do not.
- It offers an integrated treatment that connects control at governor level to the supervisory layer, allowing its effect on factors such as plant aging, revenue from power sales and asset depreciation to be optimised [32].

In summary, the abilities to manage multivariable and nonlinear systems and to cope with constraints make MBPC a good candidate to be evaluated for application at Dinorwig. Therefore, this control method will be described in Chapter 4 and its application to the models of Dinorwig will be discussed in Chapters 5 and 6.

# Chapter 4

# Model Based Predictive Control

## 4.1 Introduction

In Chapter 3 the Governor currently implemented at Dinorwig was examined. It was concluded that a fixed-parameter PI controller is not able to deliver satisfactory performance in all the operational conditions of the hydroelectric plant. A better control method should therefore be considered. As was also pointed out, Model Based Predictive Control (MBPC) seems to be a good candidate to improve performance of the Dinorwig plant since it provides an integrated approach to station control and also because it has the following characteristics:

- Deals with multivariable processes.
- Takes actuator limitations into account.
- Allows the process to run near constraints.
- Has a short updating time.

Model Based Predictive Controls (MBPC) methods, with special emphasis on Generalised Predictive Control (GPC), are discussed in this Chapter. Section 4.2 presents the general theory behind MBPC and also discusses briefly some MBPC approaches and their applications in electric power generation. The theory of GPC is

analysed in detail in section 4.3, and is followed by some tuning guidelines in section 4.4. The software platform developed in Simulink to investigate and evaluate both classic and predictive controllers is discussed in section 4.5. Finally, some conclusions are drawn in section 4.6.

## 4.2 Model Based Predictive Control in electric power generation

### 4.2.1 Model Based Predictive Control elements

Model Based Predictive Control (MBPC) or Model Predictive Control (MPC) are the general names for those methods that find the future control signals by looking for the minimum of a cost function over one horizon of prediction, Figure 4.1. The receding horizon for Predictive Control is like the real horizon for a person who is walking; the horizon moves as he walks. The principle of the method is to calculate, using a mathematical model of the plant, the predicted output signal over some horizon into the future [30, 31, 33]. The control is calculated to minimise a defined performance index. Predictive control can also calculate the future reference trajectory that the output of the system must follow, Figure 4.1.

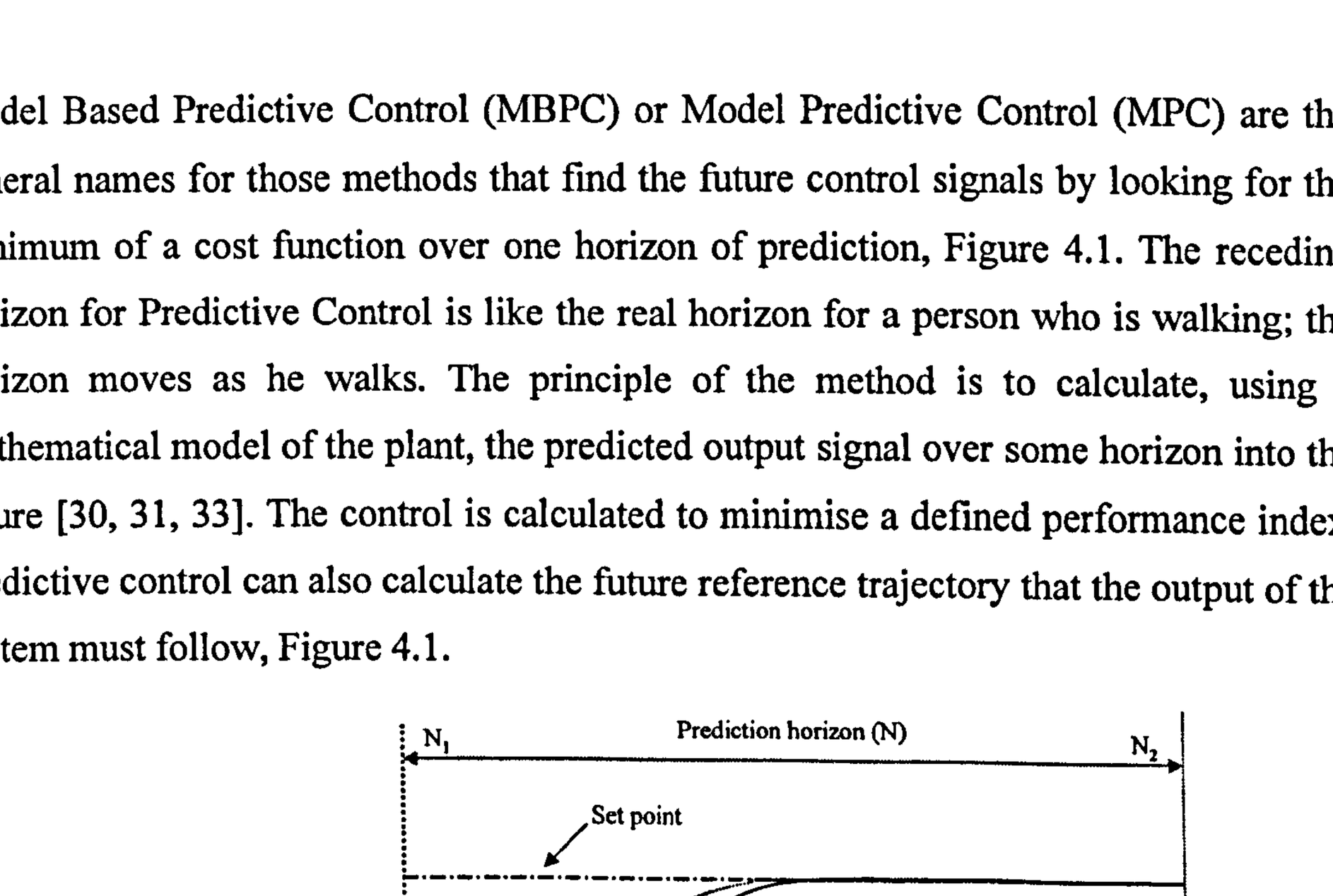


*Figure 4.1: Model Predictive Control strategy.*

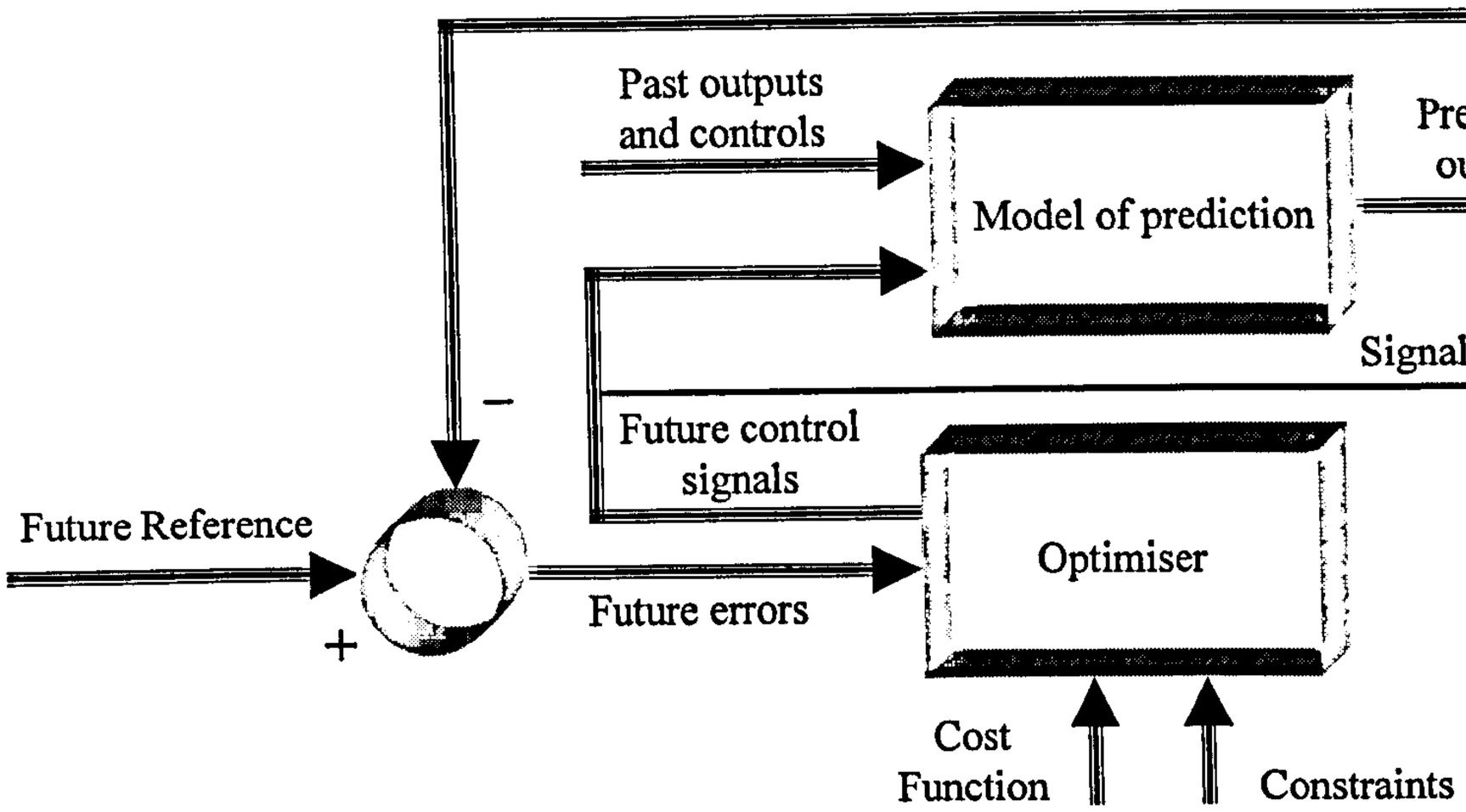


*Figure 4.2: General schema of a Model Predictive Control.*

A criterion of optimisation is used to calculate the control signal. This criterion is normally a quadratic function of the deviation of the predicted output signal from a future reference trajectory. The effort of control is usually included in the criterion of optimisation. The optimiser, Figure 4.2, produces the control actions.

The number of variables and the size of the horizon and control predictions are some of the factors that determine the complexity of the optimisation problem. The introduction of constraints also increases significantly the difficulty of finding the optimal solution. Typically, only the first control signal is sent to the process while the remaining control signals that have been calculated are rejected because, at the next sampling instant, a new output $y(t+1)$ is already known.

As can be seen in Figure 4.2, the model of prediction is used to calculate the predicted outputs based on past inputs and outputs and future inputs (control signals), from the Optimiser. Different Predictive Control approaches use different models of prediction but, in all cases, the process model must be able to represent the dynamics of the process in order to accurately predict the future outputs without consuming too much computational time.

### 4.2.2 Brief review of some MBPC approaches

There are many variants of predictive control, for example:

- Generalised Predictive Control (GPC)
- Dynamic Matrix Control (DMC)
- Extended Prediction Self-Adaptive Control (EPSAC)
- Model Algorithmic Control (MAC)
- Predictive Functional Control (PFC)
- Quadratic Dynamic Matrix Control (QDMC)
- Sequential Open Loop Optimisation (SOLO)

The first applications of Predictive Control were made by industrial practitioners, which were implemented several years before the first publications appeared [31]. Several people made the first advances in predictive control almost simultaneously.

Richalet *et al* in 1978 proposed Model Predictive Heuristic Control [34], and called it a new method of digital process control. In Model Predictive Heuristic Control the MIMO system is represented by its impulse responses; a long-range prediction by the digital control uses these responses on-line. The behaviour of the closed-loop system is set by means of reference trajectories that are initiated at each sample time. A heuristic method is used to compute the control variables.

Peterka in 1984 introduced Predictor–based Self-tuning Control [35], which was defined as a time-domain method of quadratic-optimum control. In that method the control strategy is designed to minimise the expected value using a quadratic criterion over a control horizon. The system is modelled using two representations named positional and incremental. The positional model uses past output and input signals plus a noise signal. The incremental model uses incremental past and input signals plus an incremental noise signal. Peterka called it "a new numerical method for LQ-optimum control synthesis", suggesting that the incremental model rather than the positional be used, because this has an integral action.

Cutler and Ramaker proposed Dynamic Matrix Control (DMC), first named Cutler's Method [30, 36], which uses the step response to model the process. It is assumed that the process is open-loop stable and has no integrators. This method only takes into account the first N step response terms to model the system. The objective is to drive the output close to the setpoint by minimising a quadratic function that includes a penalty term on the input moves. Only the first element of the output is sent to the plant and the calculation is made every sample time.

The Generalised Predictive Control (GPC) method, first proposed by Clarke *et al* [37], finds the future control signals by looking for the minimum of a cost function over a horizon of prediction. The function to be optimised is a quadratic function of some sequence of reference and predicted outputs, both signals being calculated over a defined horizon of prediction. In the next section this method is discussed in detail.

### 4.2.3 Applications of MBPC in Power Plants

Several examples of MPC applied to conventional power plant have appeared over the last few years. Recently, Prasad *et al* [38] describe controlling a thermal (boiler-turbine) power plant using a hierarchical MPC approach. Here, two of the plant's loops (one of which is open loop unstable and the other fast-response) are controlled by local PIDs whereas the relatively slow interaction and optimisation of the overall plant is dealt with by MPC. The authors report excellent disturbance-rejection properties and alleviation of plant-wide interactions for simulations performed on a 200MW power plant. Rossiter *et al* [39] also consider control of a fossil-fired power station where they are faced with a design constraint due to limitations of the hardware available for implementation. They proceed to derive a slightly sub-optimal algorithm called efficient constrained GPC (ECGPC) with the interesting conclusion that a marginal improvement in the output of the plant is achieved, compared to using a PID, but with much reduced control activity.

To date, there seems to have been little interest in applying MPC to power and frequency control of hydroelectric plants (which have very different characteristics and time-scales to thermal generation plant). Ramond *et al* [40] proposed MPC for controlling the level of the lake which supplies a hydroelectric plant. Sansevero and Bottura [41] considered a small-perturbation SISO model relating turbine speed to input

power. Their results indicate that, provided the prediction horizon has adequate length (compared with $T_W$), the MPC controller can be tuned less conservatively than PI while retaining closed loop stability. They concluded that even linear MPC is competitive with the standard PI controllers installed at two stations currently in operation.

## 4.3 Generalised Predictive Control

Generalised Predictive Control (GPC) was selected for this application due to its success in similar applications, [30, 39, 42-46], and also because there is enough information available in the literature to program the algorithm [30, 31, 33, 37, 47, 48]. The objective of GPC is to drive future plant outputs close to a reference trajectory taking into account the control activity required to achieve this goal.

### 4.3.1. Unconstrained GPC

The GPC method finds the future control signals by looking for the minimum of a quadratic cost function, equation (4.1), over one horizon of prediction.

$$J(N_1, N_2, N_u) = \sum_{j=N_1}^{N_2} \left[\hat{y}(t+j|t) - w(t+j)\right]^2 \overline{Q} + \sum_{j=1}^{N_u} \left[\Delta u(t+j-1)\right]^2 \overline{R} \qquad (4.1)$$

where: $\hat{y}(t+j|t)$ – Optimum system predicted output j steps ahead calculated at time t.

$\Delta$ – $(1-q^{-1})$ operator

$N_1, N_2$ – Minimum and maximum of the prediction horizon

$N_u$ – Control horizon

$\overline{Q}$ and $\overline{R}$ – Positive definite weighting matrices.

$w(t+j)$ – Future reference trajectory, for constant references:

$w(t+k) = \alpha w(t+k-1) + (1-\alpha) r(t+k)$, with $1 > \alpha \geq 0$ and $r(t+k)$ fixed reference.

To model the plant GPC uses a Model Controller Auto-Regressive Moving-Average with integrator (CARIMA) form, equation (4.2).

$$A(q^{-1})y(t) = q^{-d}B(q^{-1})u(t-1) + C(q^{-1})\frac{e(t)}{1-q^{-1}} \qquad (4.2)$$

where $A(q^{-1})$ and $C(q^{-1})$ are monic polynomial matrices of order n x n, and $B(q^{-1})$ is a polynomial matrix of order n x m, defined as:

$$A(q^{-1}) = I_{nxn} + A_1 q^{-1} + A_2 q^{-2} + \ldots + A_{na} q^{-na}$$

$$B(q^{-1}) = B_0 + B_1 q^{-1} + B_2 q^{-2} + \ldots + B_{nb} q^{-nb}$$

$$C(q^{-1}) = I_{nxn} + C_1 q^{-1} + C_2 q^{-2} + \ldots + C_{nc} q^{-nc} \ .$$

To derive a j-step ahead predictor of $y(t+j)$ let us multiply (4.2) by $\Delta E_j(q^{-1})q^j$ and consider $C(q^{-1})$=1, then

$$\Delta E_j(q^{-1})q^j A(q^{-1})y(t) = \Delta E_j(q^{-1})q^j q^{-d} B(q^{-1})u(t-1) + \Delta E_j(q^{-1})q^j \frac{e(t)}{1-q^{-1}} .$$

Defining $\tilde{A}(q^{-1}) = \Delta A(q^{-1})$

$$E_j(q^{-1})\tilde{A}(q^{-1})y(t+j) = E_j(q^{-1})B(q^{-1})\Delta u(t+j-d-1) + E_j(q^{-1})e(t+j) \ . \qquad (4.3)$$

Considering the following Diophantine equation:

$$I_{nxn} = E_j(q^{-1})\tilde{A}(q^{-1}) + q^{-j}F_j(q^{-1}) \qquad (4.4)$$

the equation (4.3) can be written as:

$$y(t+j) = F_j(q^{-1})y(t) + E_j(q^{-1})B(q^{-1})\Delta u(t+j-d-1) + E_j(q^{-1})e(t+j) . \qquad (4.5)$$

The noise terms, $e(t+j)$, in equation (4.5) are all in the future because the degree of polynomial $E_j(q^{-1})$ is j-1. The best prediction of y(t+j) is therefore:

$$\hat{y}(t+j|t) = G_j(q^{-1})\Delta u(t+j-d-1) + F_j(q^{-1})y(t)$$

where $G_j(q^{-1}) = E_j(q^{-1})B(q^{-1}) = \sum_{i=0}^{j-1} G_i q^{-i}$ then

$$\begin{bmatrix} \hat{y}(t+1|t) \\ \hat{y}(t+2|t) \\ \hat{y}(t+j|t) \\ \hat{y}(t+N|t) \end{bmatrix} = \left[\begin{array}{cc:c:c} G_0 & 0 & 0 & 0 \\ G_1 & G_0 & 0 & 0 \\ \hdashline G_{j-1} & G_{j-2} & G_0 & 0 \\ \hdashline G_{N-1} & G_{N-2} & \cdots & G_0 \end{array}\right] \begin{bmatrix} \Delta u(t) \\ \Delta u(t+1) \\ \hdashline \Delta u(t+j-1) \\ \hdashline \Delta u(t+N-1) \end{bmatrix} + \begin{bmatrix} f_1 \\ f_2 \\ \hdashline f_j \\ \hdashline f_N \end{bmatrix}$$

or in condensed form: $y = Gu + f$ . (4.6)

$f$ is the free response term and can be calculated recursively by:

$$f_{j+1} = q\left(I - \tilde{A}(q^{-1})\right)f_j + B(q^{-1})\Delta u(t+j) \qquad (4.7)$$

with $f_0 = y(t)$ and $\Delta u(t+j)=0$ for $j \geq 0$.

If the control signal is considered a constant after $N_u$ steps of control, the predictions' set

$$y_{N12} = \left[\hat{y}(t+N_1|t)^T, \hat{y}(t+N_1+1|t)^T, \cdots, \hat{y}(t+N_2|t)^T\right]$$

affecting the cost function, equation (4.1), can be expressed as:

$$y_{N12} = G_{N12} u_{N_u} + f_{N12} \tag{4.8}$$

where $u_{N_u} = \left[\Delta u(t)^T, \cdots, \Delta u(t+N_u-1)^T\right]^T$, $f_{N12} = \left[f_{N_1}{}^T, f_{N_1+1}{}^T, \cdots, f_{N_2}{}^T\right]^T$

and $G_{N12}$ is the following submatrix of G, with $G_i=0$ for $i<0$.

$$G_{N12} = \begin{bmatrix} G_{N_1-1} & G_{N_1-2} & \cdots & G_{N_1-N_u} \\ G_{N_1} & G_{N_1-1} & \cdots & G_{N_1+1-N_u} \\ \vdots & \vdots & \ddots & \vdots \\ G_{N_2-1} & G_{N2-2} & \cdots & G_{N_1-N_u} \end{bmatrix}.$$

The equation (4.1) can be rewritten as:

$$J = \left(G_{N12} u_{N_u} + f_{N12} - w\right)^T \overline{Q}\left(G_{N12} u_{N_u} + f_{N12} - w\right) + u_{N_u}^T \overline{R} u_{N_u} \tag{4.9}$$

where

$$\overline{Q} = diag(Q, \cdots, Q) \text{ and } \overline{R} = diag(\lambda, \cdots, \lambda).$$

Typically Q=1 and λ is constant.

If constraints are not considered, the optimum control signal can be calculated by:

$$u = \left(G_{N12}^T \overline{R} G_{N12} + \overline{Q}\right)^{-1} G_{N12}^T \overline{R}\left(w - f_{N12}\right). \tag{4.10}$$

### 4.3.2. Constrained GPC

It is common to formulate an equation of control assuming that all signals possess an unlimited range. However, this is not realistic because, in the real world, all plants are subject to constraints. There are constructional and safety reasons for these constraints. Limited range of actuators and limited slew rate are some examples of constructional

constraints. Levels in tanks and pressures in vessels are examples of safety constraints [49-51].

In Predictive control, normally three kinds of constraints are considered: limits on control signals (saturation), rate limits on control signals and limits on output signals. These constraints can be represented by the following equations:

$$\underline{u} \le u(t) \le \overline{u} \quad \forall t$$

$$\underline{\Delta u} \le u(t) - u(t-1) \le \overline{\Delta u} \quad \forall t$$

$$\underline{y} \le y(t) \le \overline{y} \quad \forall t \,.$$

If equation (4.1) is expressed in the following form:

$$J(u) = \frac{1}{2} u^T H u + b^T u + f_0 \tag{4.11}$$

where

$$f_0 = (f_{N12} - w)^T (f_{N12} - w), \qquad b^T = 2(f_{N12} - w)^T G_{N12}$$

and $\quad H = 2(G_{N12}^T G_{N12} + \lambda I),$

the predictive control formulation can be expressed as a Quadratic Programming problem, with $J(u) = \frac{1}{2} u^T H u + b^T u$ (4.12)

as the function to optimise under the following constraints: $A_{qp} u \le b_c$ .

In this treatment $f_0$ is not used because, at every stage of the optimisation, it is a constant whose value does not depend on $u$, and every value of $J(u)$ and $u$ are non-negative. $A_{qp}$ and $b_c$ are the following matrix and vector of order $6N_u$ x m and $6N_u$ respectively:

$$A_{qp} = \begin{bmatrix} I \\ -I \\ I \\ -I \\ G_{N12} \\ -G_{N12} \end{bmatrix}, \qquad b_c = \begin{bmatrix} 1(\overline{u} - u) \\ -1(\underline{u} + u) \\ 1\Delta u \max \\ -1\Delta u \max \\ 1\overline{y} - f \\ -1\underline{y} + f \end{bmatrix}, \qquad \text{where} \quad 1 = \begin{bmatrix} 1 \\ 1 \\ \vdots \\ 1 \end{bmatrix}.$$

## 4.4 Tuning guidelines

Controllers are normally designed to satisfy a wide range of specifications and their performances have a strong dependence on the value of their parameters. The objective is generally to achieve a balance between good sensitivity, input activity and speed of response [33]. The cost function to be optimised determines the performance of the system; in GPC a quadratic function (4.1) is utilised. The parameters to be tuned in the GPC controller are:

$N_1, N_2$ – Minimum and maximum of the prediction horizon

$N_u$ – Control horizon

$\alpha$ – Future reference trajectory weight factor.

$\lambda$ – Cost function control signal weight factor.

$N_1$ is normally fixed as 1 plus the dead time of the system. $N_2$ is set to approximate the rise-time of the plant. $N_u$ can be set to 1 to obtain a reasonable performance; however increasing its value makes the control signal and the response of the system more active. Nonetheless, there is a point after which any further increase in $N_u$ makes little difference to the response of the system [37, 52].

There are many equations that can be used to calculate the future reference trajectory [30, 37]; in this study the equation discussed in section 4.3 was employed. Values of $\alpha$ near zero produce fast responses and values of $\alpha$ near to 1 produce slow responses. In this study a value of $\alpha$=0 is normally selected.

$\lambda$ has a strong effect on the effort of control, low values of this parameter producing an "active" control while high values produce a "passive" control [33, 37, 52]. There is a relationship between the lowest feasible values of $\lambda$ and the accuracy of the model of prediction; only accurate models of prediction support low values of $\lambda$ and therefore an active control.

The model of prediction plays a central role in all MBPC approaches. Linear stable systems could be modelled with a first order plus dead time transfer function. On the

other hand, nonlinear systems with complex dynamics must have an accurate model of prediction in order to achieve a precise prediction [30, 33, 37].

The process of selecting the parameters of the GPC controller utilised in this study begins with the selection of an appropriate model of prediction. Then, with a high value of $\lambda$, the horizon of prediction is determined. It is desirable to maintain this parameter as low as possible in order to reduce computing time. The horizon of control is normally fixed to the same value as $N_2$ but it can be fixed to a lower value or even $N_u$=1 if an active control is not important. Finally $\lambda$ is reduced to the lowest value possible; its exact value depends on the characteristics of the system and the desirable response.

## 4.5 The Software development platform

A flexible software tool to investigate and evaluate classic and predictive controllers was developed; Matlab functions that can interact with Simulink were designed, see Figure 4.3. Using Simulink blocks, different input signals can be selected and the output signals can be visualised in either numeric or graphic form. The model of the Power Plant, including Power System representations, can be selected from a library that also contains classic and predictive controllers.

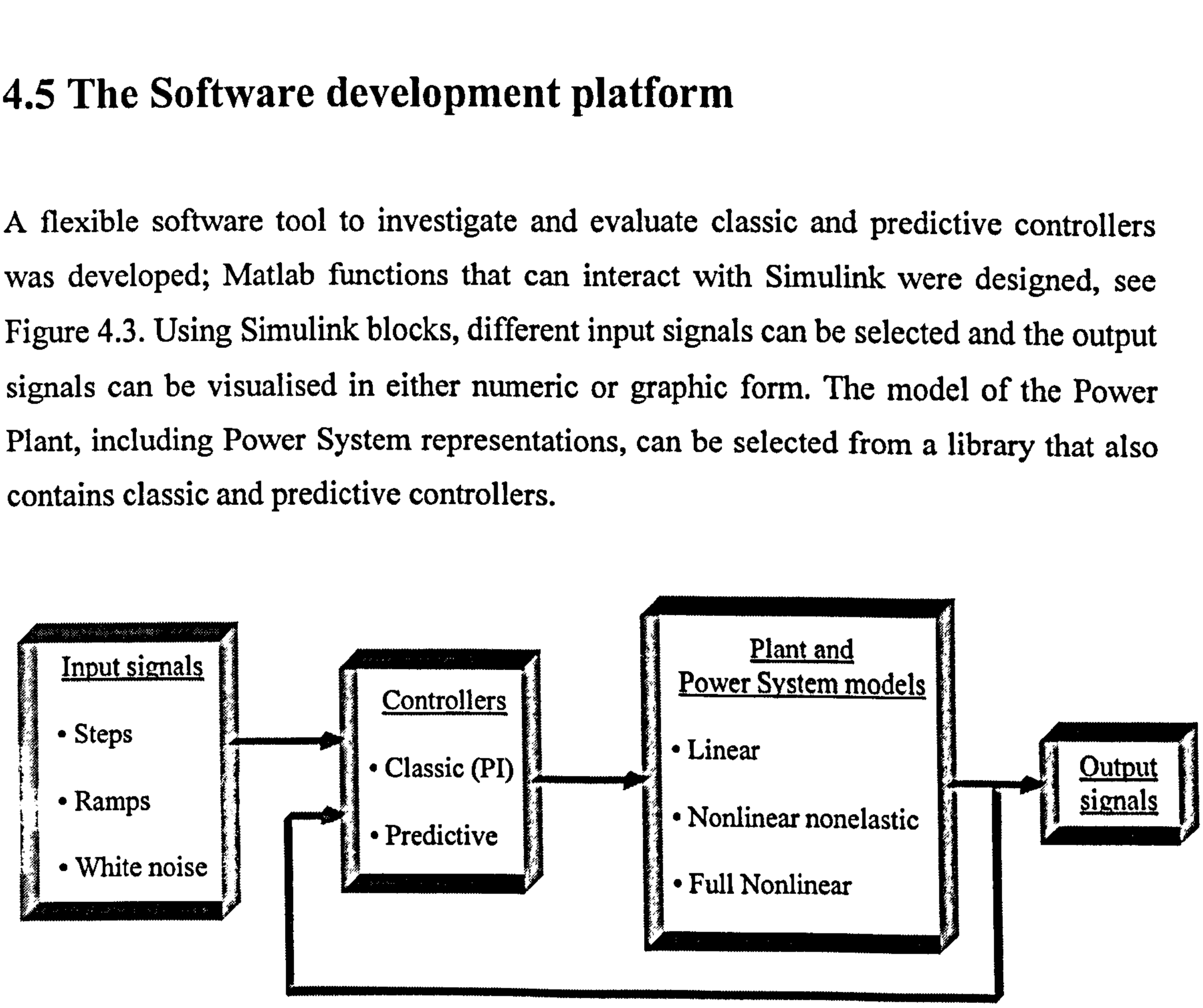


*Figure 4.3: Flow diagram of the General schema of the software platform for investigating controllers and plant models.*

The models of the power plant contain all the features discussed in Chapter 2. A variety of modes of operation can be chosen, such as: only the hydraulic linear model, guide

vane-hydraulic linear model or guide vane-hydraulic-electric nonlinear model. The power plant can be simulated as a SISO system or a MIMO system. The models require some external information, such as the hydraulic head. Linear models also require the value of the operating point.

Classic and predictive controllers can be selected from a library. The classic controllers that can be selected are P, PI, PID and anti-windup PI. For comparison purposes the Dinorwig Governor configuration was also developed. The parameters of these controllers are supplied by Simulink user interfaces.

The predictive controls that can be selected are GPC based algorithms. The S-Function PC_main.m, which constitutes a Simulink block, is the main procedure (Figure 4.4). It makes the connection with the plant and the input signals; it also accepts information from a dialog box. $N_u$, $N$, $\lambda$, $\alpha$, number of inputs, number of outputs, matrix A and B, and the values of constraints are its input data.

Figure 4.4 shows a simple flow chart of the main procedure PC_main.m. The first part of this program accepts user data, and with these the values of matrix G, and the free response are calculated. Then a simulation is made for the number of samples fixed for the user (iterative loop). The free response of the system is calculated at every step of the simulation, using equation (4.7). The predictive output signals are found with equation (4.6) and the vector of control signals is calculated by equation (4.10).

The control signals are sent to the plant. The subroutine GPC_c.m is called from the main procedure to obtain the parameters of the control law as required; the Diophantine equation (4.4) is solved recursively. This procedure is continued until the time of simulation is finished.

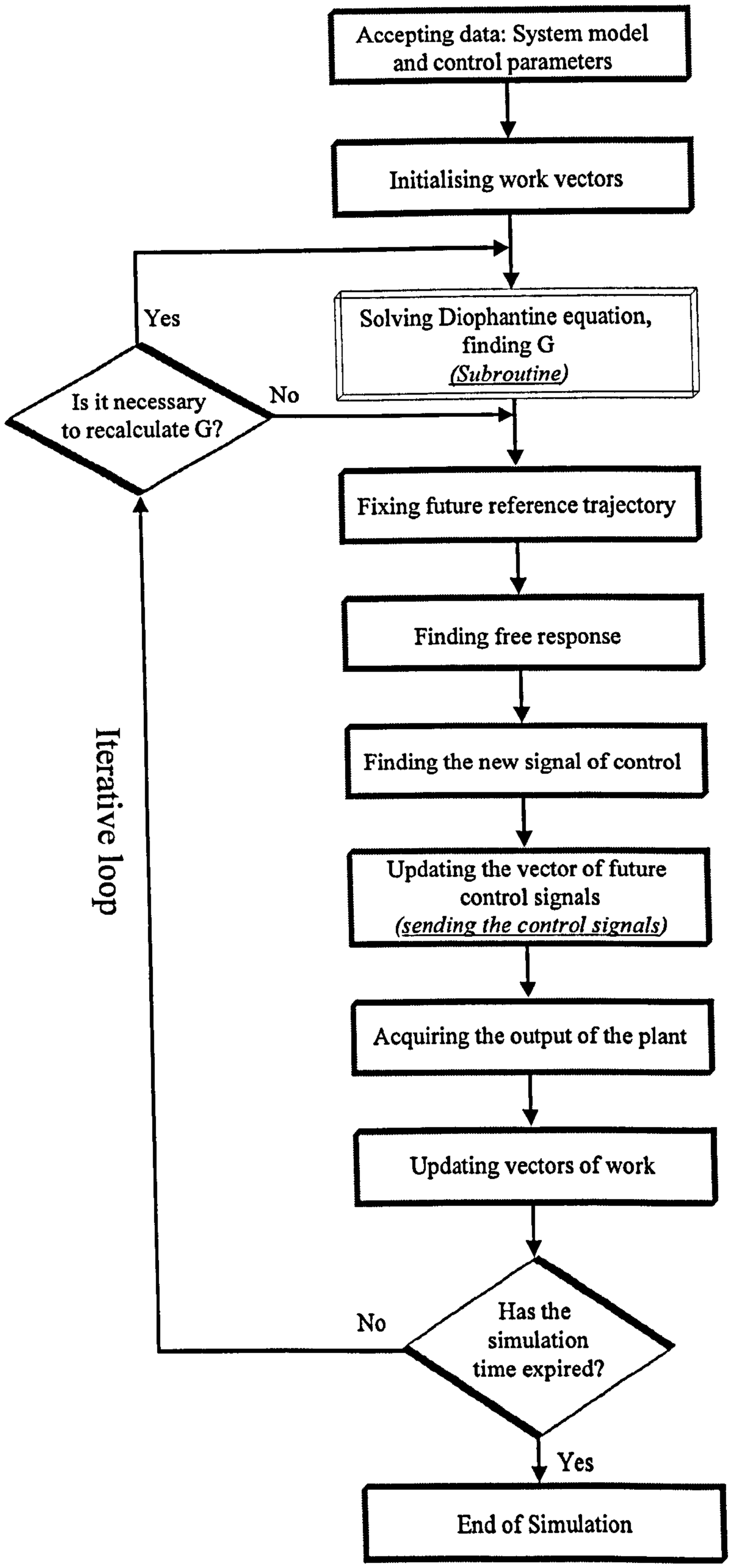


*Figure 4.4: Flow diagram of the main procedure PC_main.m of the GPC controller.*

## 4.6 Conclusions

In the first part of the Chapter, the general features of Model Based Predictive Control were presented. Then the basic theory of GPC was described. The method has been easily implemented on a computer. The GPC algorithms have been programmed using Matlab. Simulations of simple systems have confirmed that the results are consistent with others presented in papers from the literature [30, 37]. The unconstrained and constrained cases of GPC were reviewed.

The software tool developed to analyse the models of the hydroelectric station and control methods has been described. The modular characteristic of this platform has been important to gradually increasing the complexity of the simulations. The open architecture makes possible the rapid inclusion of other control methods and also the incremental improvement of the control approaches and models already included.

The GPC method will be applied in Chapters 5 and 6 to the linear and nonlinear models of the hydroelectric station, comparing its performance with classic PI controllers. Chapter 7 deals with MLD-GPC, and here the scalability and open features of the software tool were especially valuable during its development.

# Chapter 5

# PI and GPC controllers for a SISO linear model

## 5.1 Introduction

Having described the characteristics of the hydroelectric Power Station and its Speed Governor in earlier chapters, the application of Generalised Predictive Control (GPC) to a SISO linear model of Dinorwig is discussed here. Figure 5.1 summarises the principal features of the classic Governor as implemented currently and also presents, in the highlighted block, the main characteristics of the evaluation accomplished in this chapter.

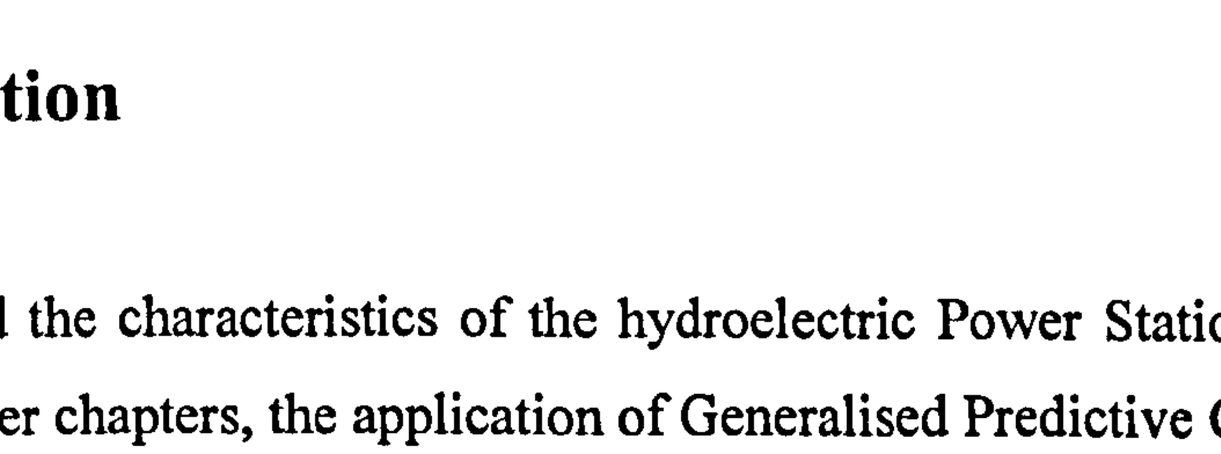


*Figure 5.1: Evolution of the control proposal for Dinorwig.*

As has been stated in earlier chapters the PI/PID Governor cannot maintain its performance in all operational conditions of the Power Plant. In this chapter, it will be shown that the inclusion of more information about the system characteristics, via the model of prediction in the GPC, yields less sensitive performance of the system. Therefore, the aims of this chapter are to evaluate the performance of a GPC controller, when it is used as a governor for Dinorwig, and to present the method used to tune this controller. The initial goal is to establish the principle of using GPC in this application so a simple SISO linear model was chosen. This linear model is based on the theory discussed in Chapter 2 and the specific values of the parameters are taken from the work developed by Mansoor [3]. In subsequent chapters a nonlinear elastic model will be used to represent the plant and these studies will be extended.

As shown in Chapter 2, hydroelectric power plants have complex dynamics and many different models have been proposed to represent them [1, 2, 9, 53, 54]. Full nonlinear models take into account the majority of the dynamical characteristics of these systems. However, as was shown by Kundur [2] and a Working group of the IEEE [1], assuming incompressible fluid flow and neglecting factors such as friction losses in the penstock, small perturbation analysis allow linearised models to be obtained. Control systems can be studied with linearised models when small-signal responses are evaluated. In this chapter a SISO linear model of Dinorwig is considered for different operational conditions. Special attention is given to the different performance of the system as the number of active units varies. Therefore, the number of active units is established at the beginning of the simulation, and then responses from different operational conditions are evaluated. The comparison is concentrated on the two extreme cases, one and six units operational, for small step inputs. In the case of six units operational, all units work in synchrony.

This chapter begins presenting the procedure followed to tune the classic and Predictive controllers evaluated in this study, section 5.2. The behaviour of the plant under Generalised Predictive Control and classic PI is analysed in section 5.3 where the Power Plant is modelled as a SISO linear system and constraints are not considered. Section 5.4 evaluates the controllers when constraints are activated. Finally, section 5.5 draws some conclusions.

## 5.2 Tuning the controllers

Classic and advanced controllers can satisfy a wide range of specifications, but their performance depends strongly on the value of their internal parameters. A good balance between sensitivity, control effort and speed of response is generally the main objective of tuning [33].

### 5.2.1 Proportional and Integral

The Proportional (P), Integral (I) and Derivative (D) actions are standard modes of control for industrial applications. The controllers that contain these actions are robust and simple and these features make them suitable for manual adjustment. The current Speed Governor at Dinorwig uses a PI control in the power control loop with derivative feed-forward from the frequency control loop. In this section the process followed to tune a PI controller for the hydraulic station is discussed.

#### *5.2.1.1 Classic PI*

Tuning a Proportional and Integral controller (PI) requires selection of the correct values of $K$ and $K_i$ that allow the control to achieve a desired plant performance. Mansoor has studied the selection of the control parameters for the speed governor at Dinorwig [3]. The values that are currently implemented in the Hydroelectric Plant are $K$=0.1 and $K_i$=0.12, and will be used as a basis of comparison. The PI controller with these parameters has a performance which is a compromise between one and six unit operation. Therefore, to optimise the performance of the plant different sets of parameters were selected for the extreme cases, one and six units operational. The evaluation accomplished in Chapter 3 shows that suitable ranges for the parameters of the PI are $0.23 \geq K \geq 0.1$ and $0.5 > K_i > 0.1$.

Using classical Bode and Root Locus techniques plus a final manual adjustment, different sets of parameters were selected for the PI controller. The goal is to optimise the response of the plant in the one and six units operational modes, reducing the primary response of the system without producing large overshoot. Table 5.1 shows the set of values selected for each case.

*Table 5.1.*

*Parameters of the PI controller.*

| | Parameters currently in use | Optimised One unit | Optimised Six Units |
|---|---|---|---|
| $K$ | 0.10 | 0.175 | 0.165 |
| $K_i$ | 0.12 | 0.210 | 0.110 |

*5.2.1.2 PI anti-windup*

A PI carefully tuned can offer good performance but, as was stated in Chapter 4, all processes are subject to constraints. The plant alters its behaviour when constraints are activated, and the performance of a linear controller, such as PI, can deteriorate significantly [55]. When the plant has actuator saturation the integrator value becomes excessively large compared to a linear response (an actuator without saturation), it "winds up". In addition, a higher integrator output and a longer settling time are caused by the saturation effect [55-57].

The windup is produced when the control signal saturates the actuator, because an additional increase of the control signal will not accelerate the response of the plant. If this behaviour persists the integrator value becomes very large, without affecting the output of the plant. To bring back the system to its steady-state value, the control error has to be of the opposite sign for a long time, resulting, as was pointed out, in a large overshoot and a longer settling time [56].

Figure 5.2 shows a general scheme of a PI with tracking anti-windup structure [56]. This controller has an internal feedback path, which drives the integrator to a negative value and forces the output of the system to be in the linear range. The internal saturation is used to reduce the integrator input. As can be seen from Figure 5.2 the signal to be integrated is modified by the proportional gain ($K$), therefore the values of the integral gain ($K_i$) are adjusted in order to maintain equivalence with the classic PI. Table 5.2 shows these values. The saturation limit and the dead zone depend on the constraints fixed by the operator; a value of 0.95 p. u. is commonly used.

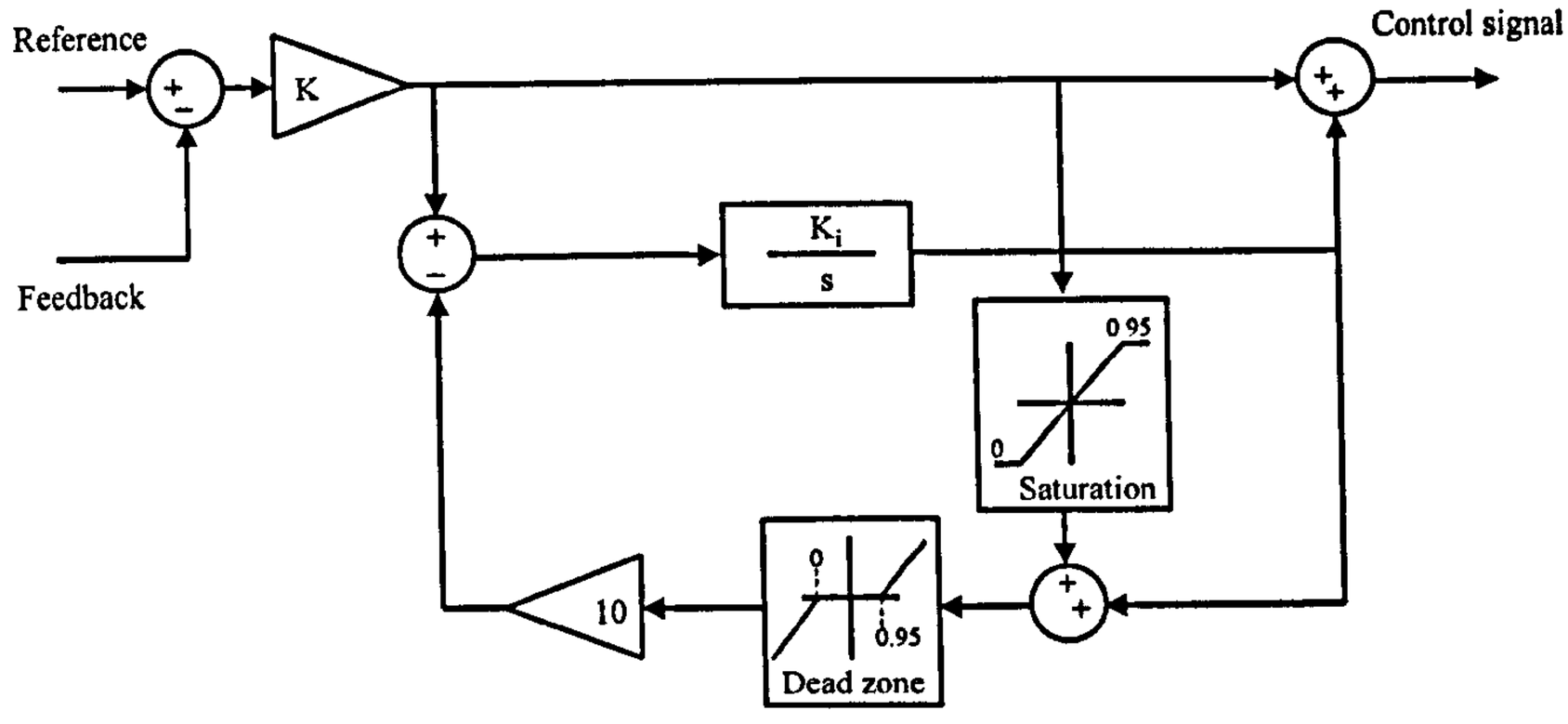


*Figure 5.2: General scheme of PI anti-windup.*

*Table 5.2.*

*Parameters of the PI controller with anti-windup.*

| | Parameters currently in use | Optimised One unit | Optimised Six Units |
|---|---|---|---|
| $K$ | 0.10 | 0.175 | 0.165 |
| $K_i$ | 1.2 | 1.2 | 0.66 |

## 5.2.2 GPC

As mentioned in Chapter 4, the performance of the GPC depends on the predictive model and control parameters selected. The process of selecting the parameters of the GPC controller utilised in this study begins with the selection of an appropriate model of prediction, from the reaction curve. Then with a high value of $\lambda$, the horizon of prediction is fixed. It is desirable to maintain the latter parameter as low as possible in order to reduce computational time. The horizon of control is normally fixed to the same value as the horizon of prediction, but it can be fixed to a lower value or even $N_u$=1 if the effort of control is not under consideration. Finally, $\lambda$ is reduced to the lowest value possible; its optimum value depends on the characteristics of the system and the desirable response.

### *5.2.2.1 Model of prediction*

The predictive model used by GPC in this Chapter is obtained by the reaction curve technique. This simple model is computationally economical but cannot reproduce the system's NMP behaviour accurately. Nevertheless, it will be shown that its short-term

predictive capability is adequate. Representing the plant's non-minimum phase response by a transport delay, the model obtained on the basis of a 10% - 50% increase in power output is given by (5.1) with one unit operational:

$$G(s)=\frac{1.12e^{-T_d s}}{1.2954s+1} \quad . \tag{5.1}$$

Converting to discrete time with a sample period $T_s$ = 0.25s and a transport delay of $T_d = 2.07$s gives (5.2):

$$G(z)=\frac{0.197}{z^8(z-0.8245)} \quad . \tag{5.2}$$

Figure 5.3 shows the open loop step response of the linear SISO model and the prediction control model for GPC (5.2). As the reaction curve model does not represent the NMP response, the first 3 seconds of simulation have a large error. On the other hand, the reaction curve model is close to the linear model after this delay.

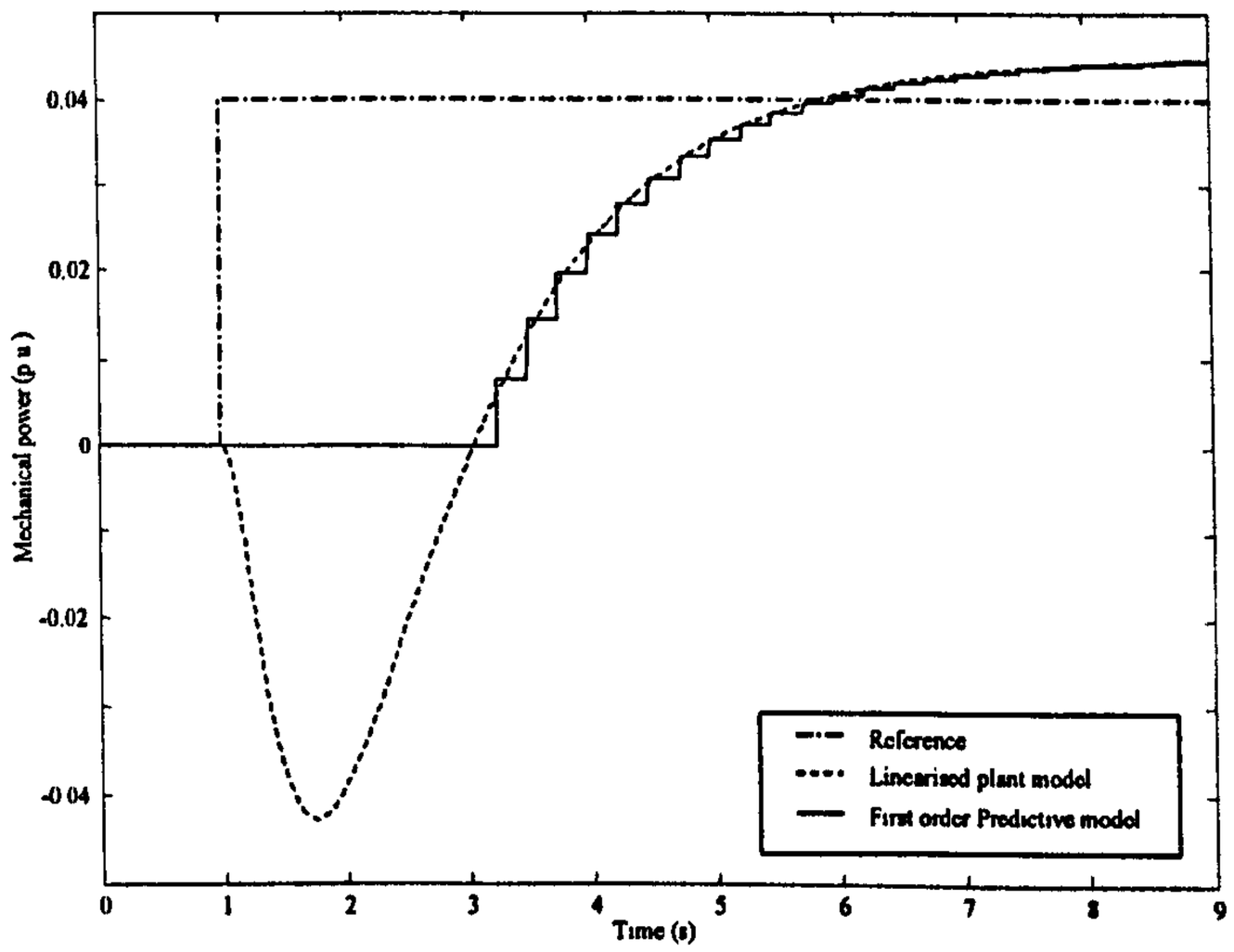


*Figure 5.3: Mechanical power output of the plant and prediction models to a 0.04 p.u. step in control u.*

### *5.2.2.2 Controller parameters*

Simulations were carried out to find the allowable range of parameters for the GPC algorithm when using (5.2) as the model of prediction and $T_s$=0.25. The hydroelectric plant was modelled as a linear system with six units operational. The effect of varying four parameters is studied below:

- $N$ – Horizon of prediction.
- $\lambda$ – Effort of control weighting factor.
- $N_u$ – Horizon of control.

- $\alpha$ – Future reference trajectory-tracking factor.

Varying the prediction horizon, $N$, leads to a variety of responses as shown in Figure 5.4. In this simulation the other parameters were fixed as follows: $N_u$=3, $\lambda$=200 and $\alpha$=0. $\alpha$ is fixed to this value in order to eliminate the tracking process that produces a slower response. Short horizons of prediction generate inaccurate estimation of the future output signals. It is desirable that the selected value of $N$ allows the future output to settle or at least to leave the NMP region, as in this case. A value of $N$=5 was selected because it produces a fast response with modest overshoot.

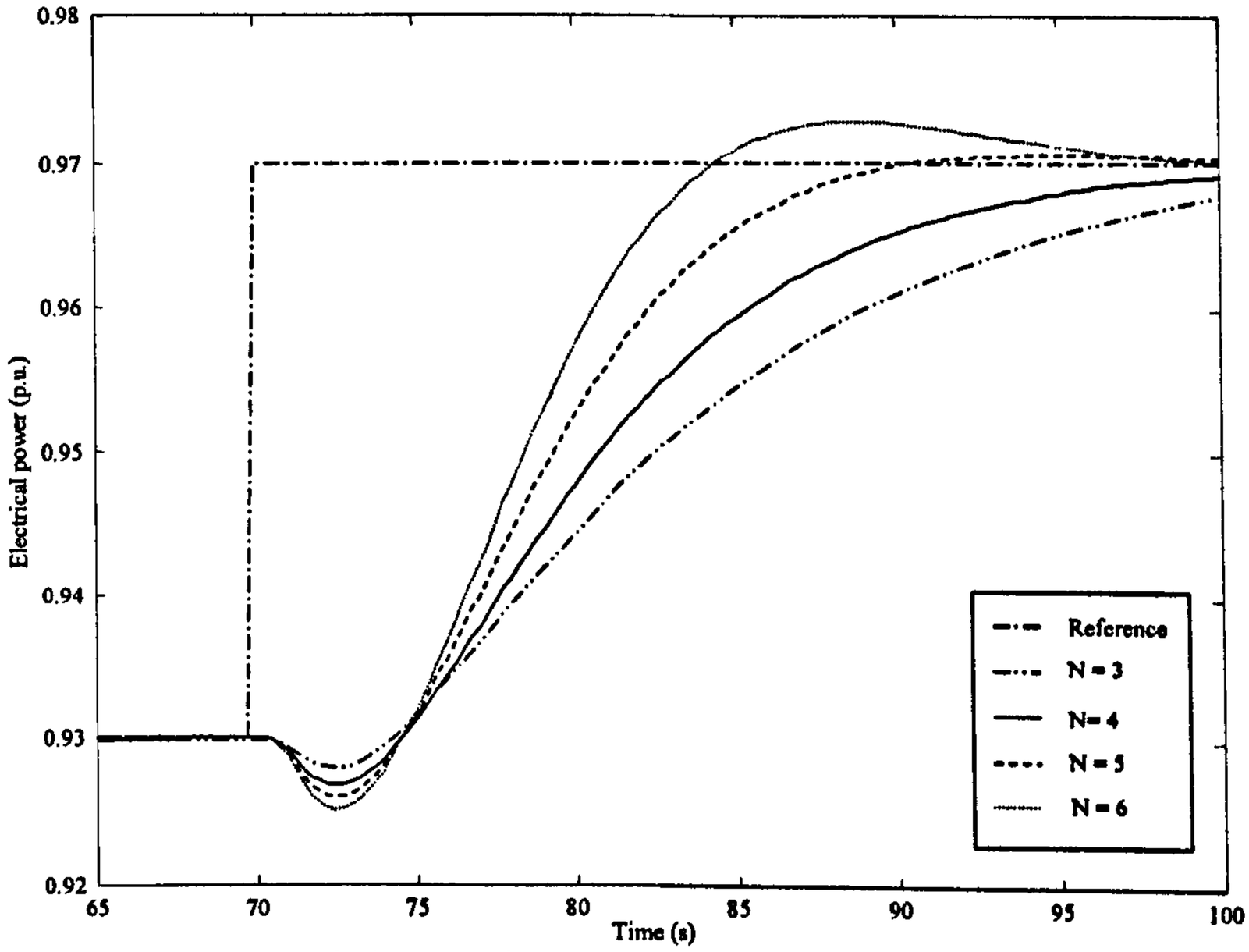


*Figure 5.4: Response of electrical power to a small step under GPC control with different values of prediction horizon N.*

With the prediction and control horizons fixed to $N$=$N_u$=5 and $\alpha$=0, simulations were conducted in order to determine the value of $\lambda$. Low values of $\lambda$ make the responses faster but both under- and over-shoot increase, Figure 5.5. To some extent it acts as the inverse of the loop gain in a conventional compensator because, as discussed in Chapter 4, this parameter directly affects the value of the control signal in the quadratic cost function of GPC.

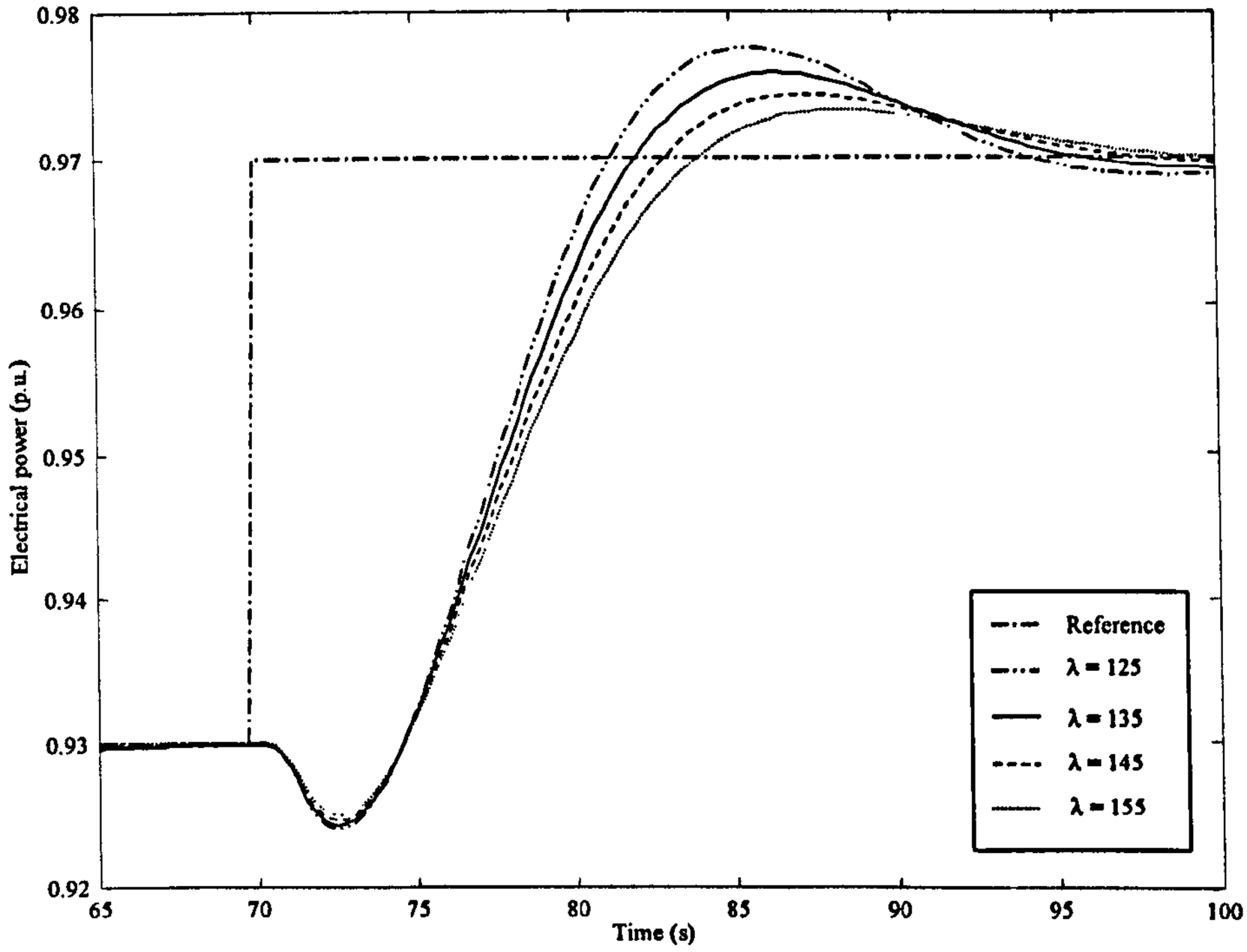


*Figure 5.5: Response of electrical power to a small step under GPC control with different values of effort of control weighting factor λ.*

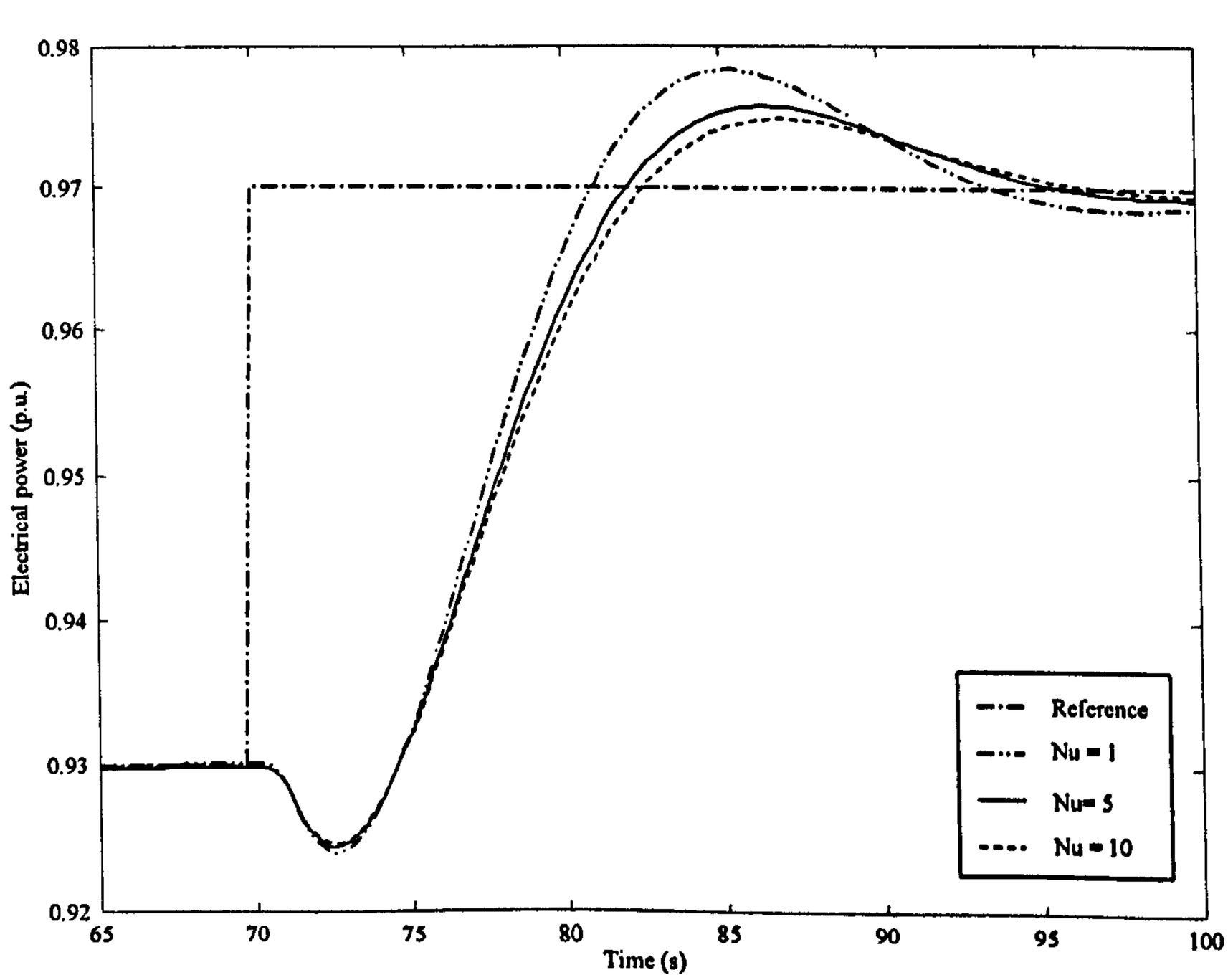


*Figure 5.6: Response of electrical power to a small step under GPC control with different values of horizon of control $N_u$.*

The horizon of control is normally fixed to the same value as the horizon of prediction. As is shown in Figure 5.6, when $N$=5, $\lambda$=135 and $\alpha$ = 0, higher values of $N_u$ yield a reduction of the overshoot without increasing the undershoot. It was found that values higher than 10 have no visible effect on the response, therefore $N_u$=10 was selected.

Figure 5.7 shows that the system allows values of $1 > \alpha \geq 0$, which is the normal range of values for this parameter. A value of $\alpha$=0 was selected because the tracking process, that reduces the speed of the future reference trajectory and the NMP response, was unnecessary due to the relatively small undershoot. Table 5.3 summarises the values of the parameters selected for the GPC.

*Table 5.3*

*Parameters of the GPC controller.*

| | Fixed parameters | Optimised One unit | Optimised Six Units | Constrained |
|---|---|---|---|---|
| $N$ | 5 | 20 | 20 | 20 |
| $N_u$ | 10 | 20 | 20 | 20 |
| $\lambda$ | 135 | 150 | 600 | 20 |
| $\alpha$ | 0 | 0 | 0 | 0 |

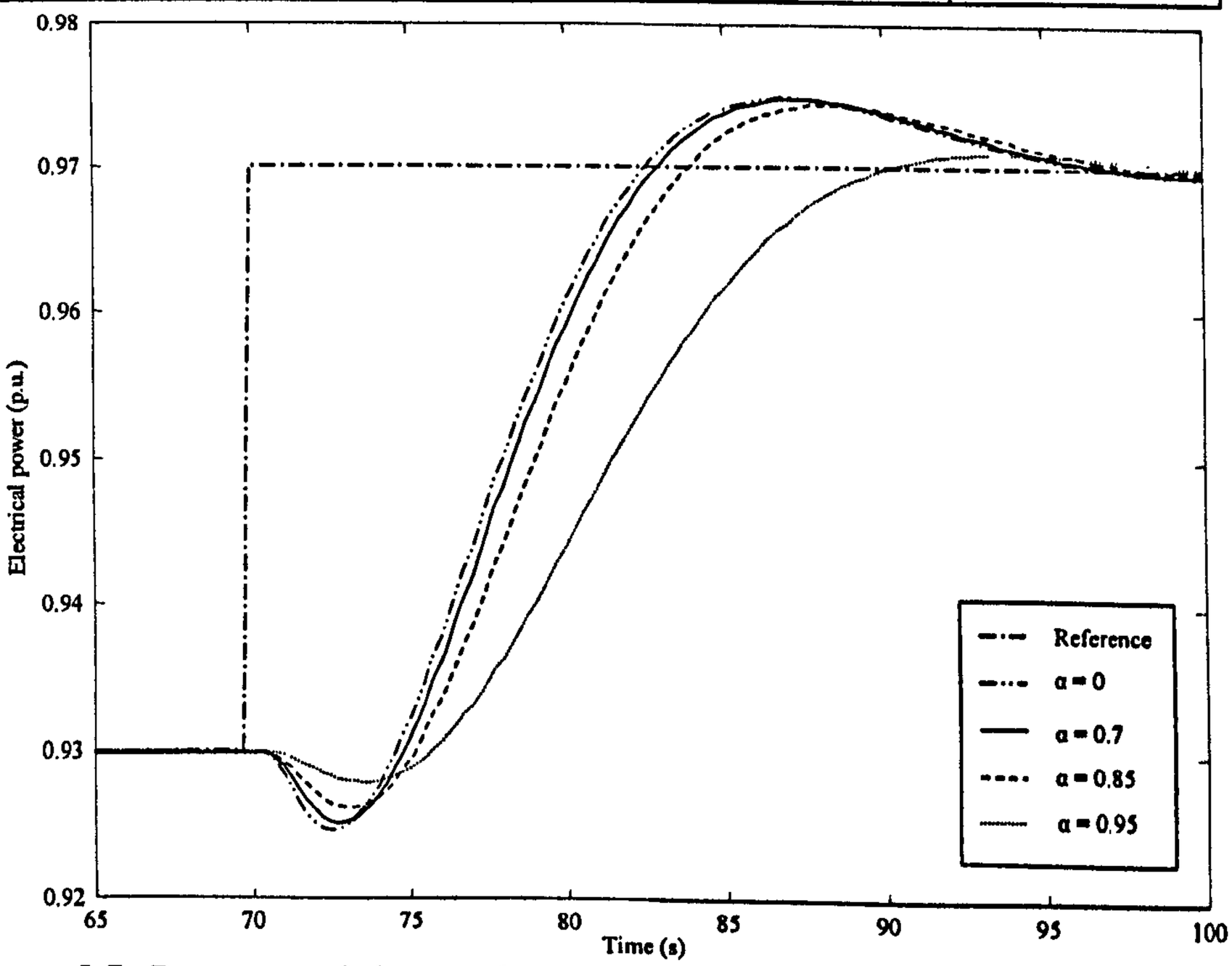


*Figure 5.7: Response of electrical power to a small step under GPC control with different values of future reference trajectory-tracking factor α.*

## 5.3 Comparison of the controllers, unconstrained case

As was discussed in earlier chapters the hydroelectric station has, as its principal objective, to provide timely and accurate supply of its target power contribution to the national Grid. The form of the power demand can be specified in terms of step, ramp and random input signals [26]. In this chapter, the step response specification for single unit operation is analysed. In order to cover the two extreme operational cases, the step response when all units are working in synchrony is also analysed. In this section, neither controller has any nonlinear constraints imposed.

In Figures 5.8 and 5.9, the electrical power outputs in response to a step demand are shown for GPC and PI controllers. The parameters of both controllers are fixed at values which give a compromise between the extremes of the $T_W$ variation. The PI parameters are fixed at $K$=0.1 and $K_i$=0.12 and the GPC parameters are fixed at $N_u$=10, $N$=5, $\lambda$=135 and $\alpha$=0 with (5.2) as the predictive model.

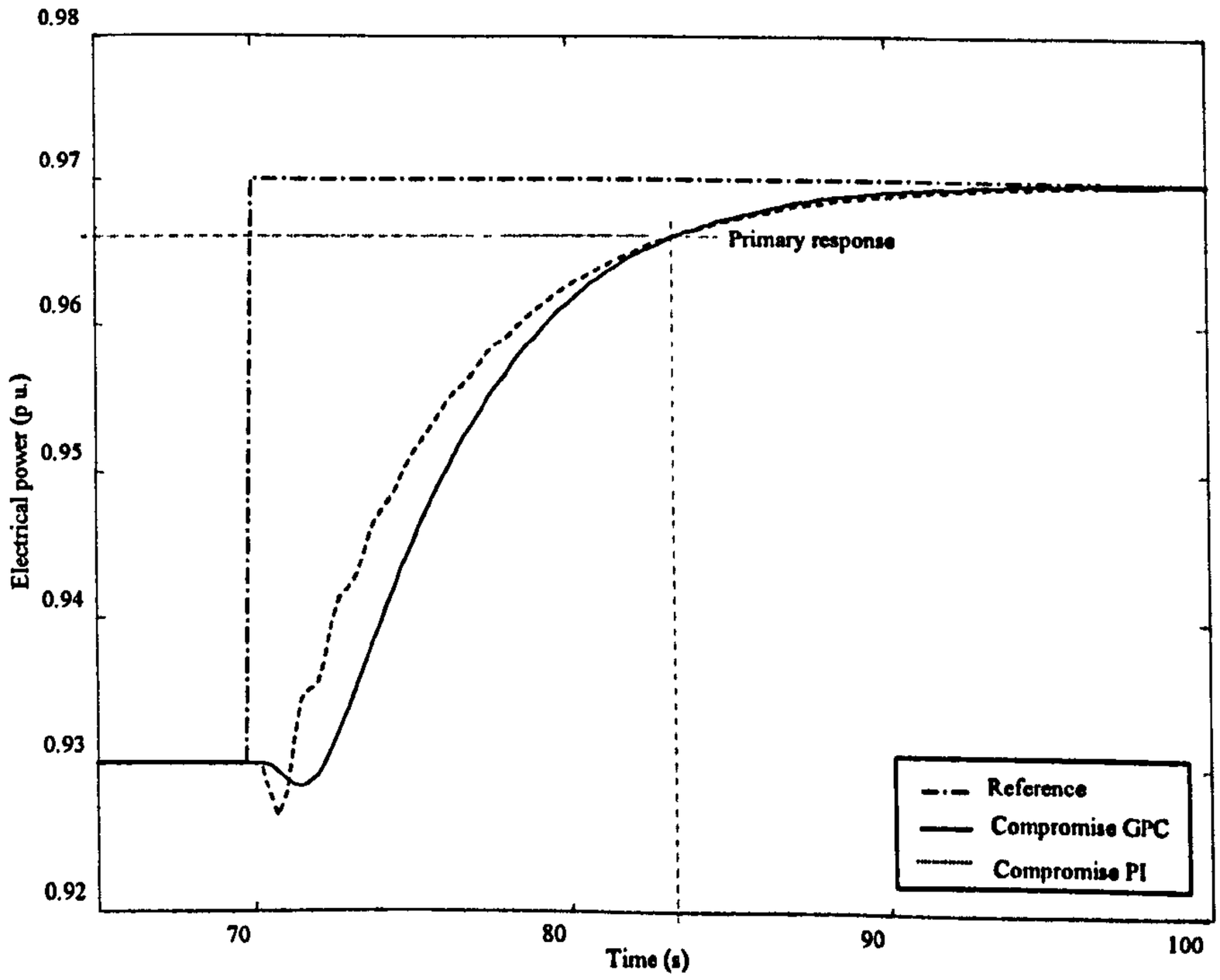


*Figure 5.8: Response of electrical power to a small step using fixed parameters PI and GPC controllers, one unit operational.*

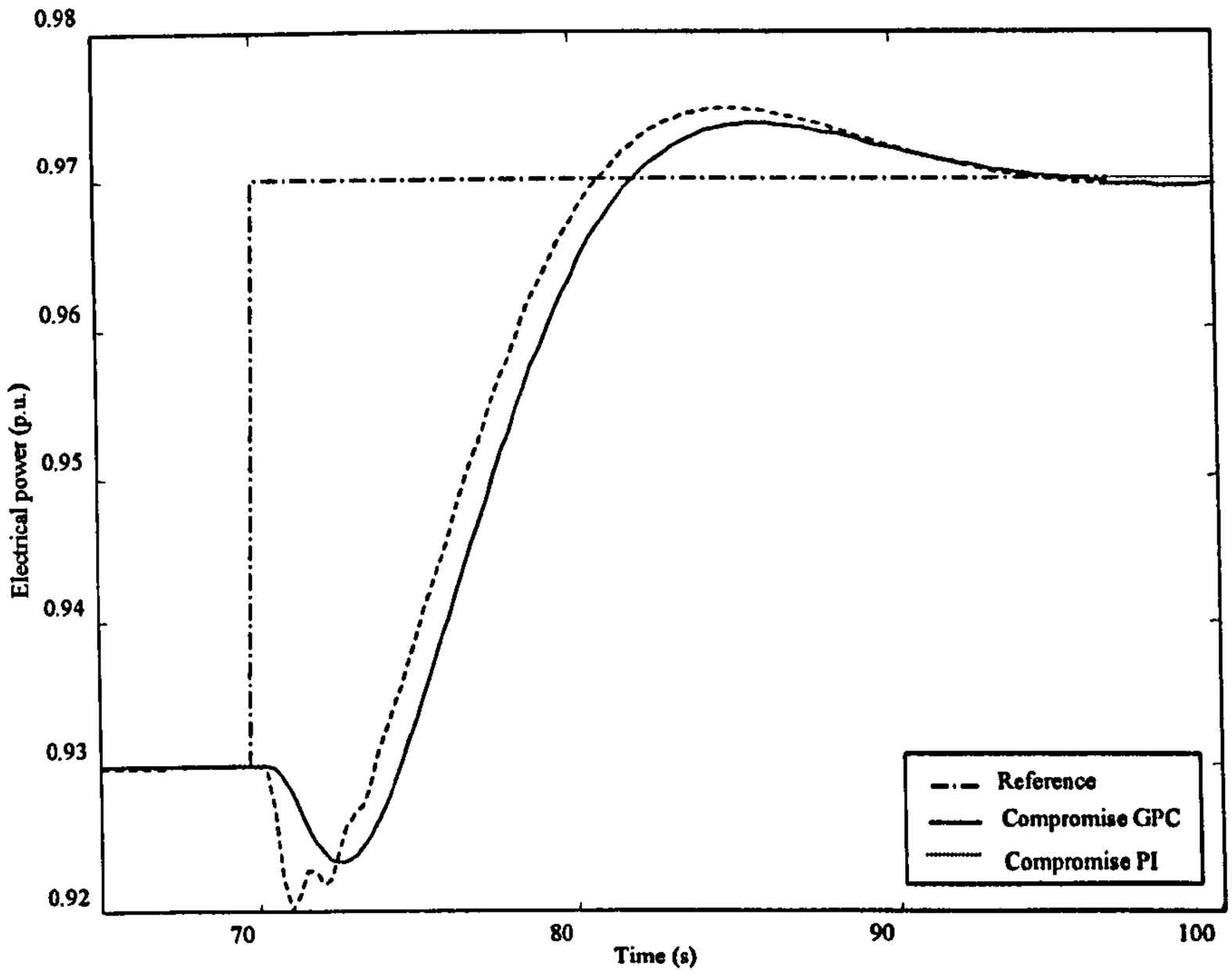


*Figure 5.9: Response of electrical power to a small step using fixed parameters PI and GPC controllers, six units operational.*

The responses are produced by the linearised model (see section 2.2), but are presented at the selected operating point. The step is therefore applied at $t = 70$s, which allows the simulation to settle to the correct initial conditions. Note how the one unit cases (Figure 5.8) both have rather sluggish responses whereas the six units cases (Figure 5.9) exhibit significant undershoot and overshoot.

As stated in Chapter 3, an important parameter for contractual purposes is the *primary response* of a generator. On this criterion, the performance of the GPC and PI controllers is comparable in the one unit case but the PI is superior in the six units case. The GPC controller produces less undershoot than the PI in both cases and less overshoot in the six units case. Note also that the relatively sharp control applied in the PI cases stimulates the small and fast oscillations seen during the first few seconds of responses, which are due to the generator synchronising to a new power angle. These are absent from the GPC responses. The comparison is summarised in Table 5.4.

*Table 5.4.*

*Comparison of undershoot, overshoot and primary response for the fixed parameters controllers.*

| | One Unit | | Six Units | |
|---|---|---|---|---|
| | PI | GPC | PI | GPC |
| Undershoot (%) | 8.8 | 3.8 | 25 | 16.3 |
| Overshoot (%) | - | - | 12 | 9.5 |
| Primary response (s) | 13.2 | 13.3 | 9.7 | 10.6 |

It is clear from Figures 5.8 and 5.9 that the fixed parameters controllers are not satisfactory at the extremes of the operational range, being rather slow and overdamped at one end and underdamped at the other end. As discussed in section 5.2.1, PI and GPC controllers were tuned to have an optimal performance depending on the number of Units in operation, see Table 5.1. Their responses are shown in Figures 5.10 and 5.11 and performance is summarised in Table 5.5. Comparing the graphs of Figures 5.8 and 5.10, it is seen that the optimised PI and GPC controllers now achieve a response near to critical damping in both the one and six units cases. Again, the GPC controller gives less undershoot than the PI. The overshoot for both controllers is comparable and almost critically damped but the primary response of the PI controller is better.

*Table 5.5.*

*Comparison of undershoot, overshoot and primary response for the optimised controllers.*

| | One Unit | | Six Units | |
|---|---|---|---|---|
| | PI | GPC | PI | GPC |
| Undershoot (%) | 15.5 | 6 | 34 | 19.8 |
| Overshoot (%) | 1 | 1.8 | 0.8 | 1.3 |
| Primary response (s) | 5.7 | 7.5 | 10.3 | 10.8 |

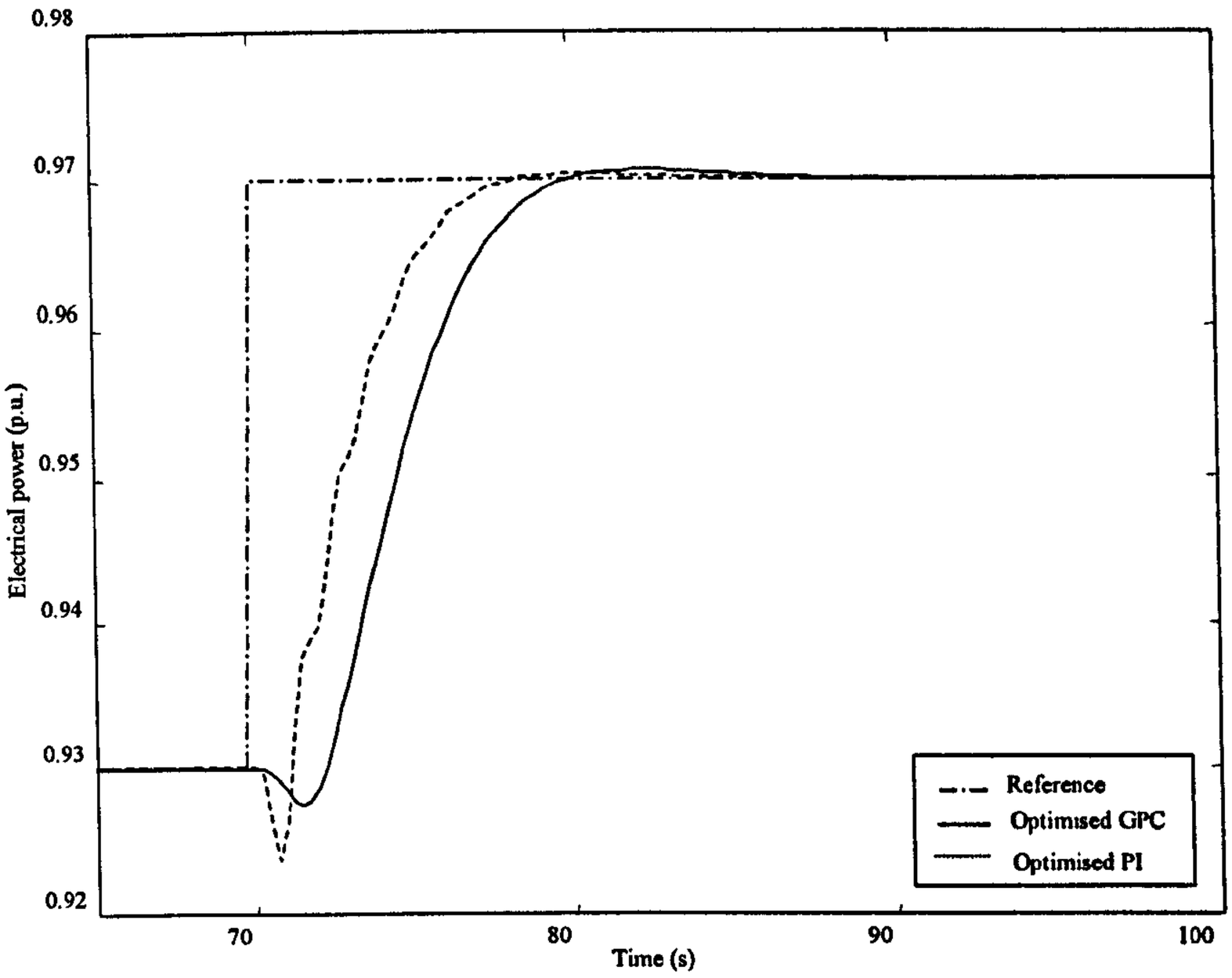


*Figure 5.10: Response of electrical power to a small step using the optimised PI and GPC controllers, one unit operational.*

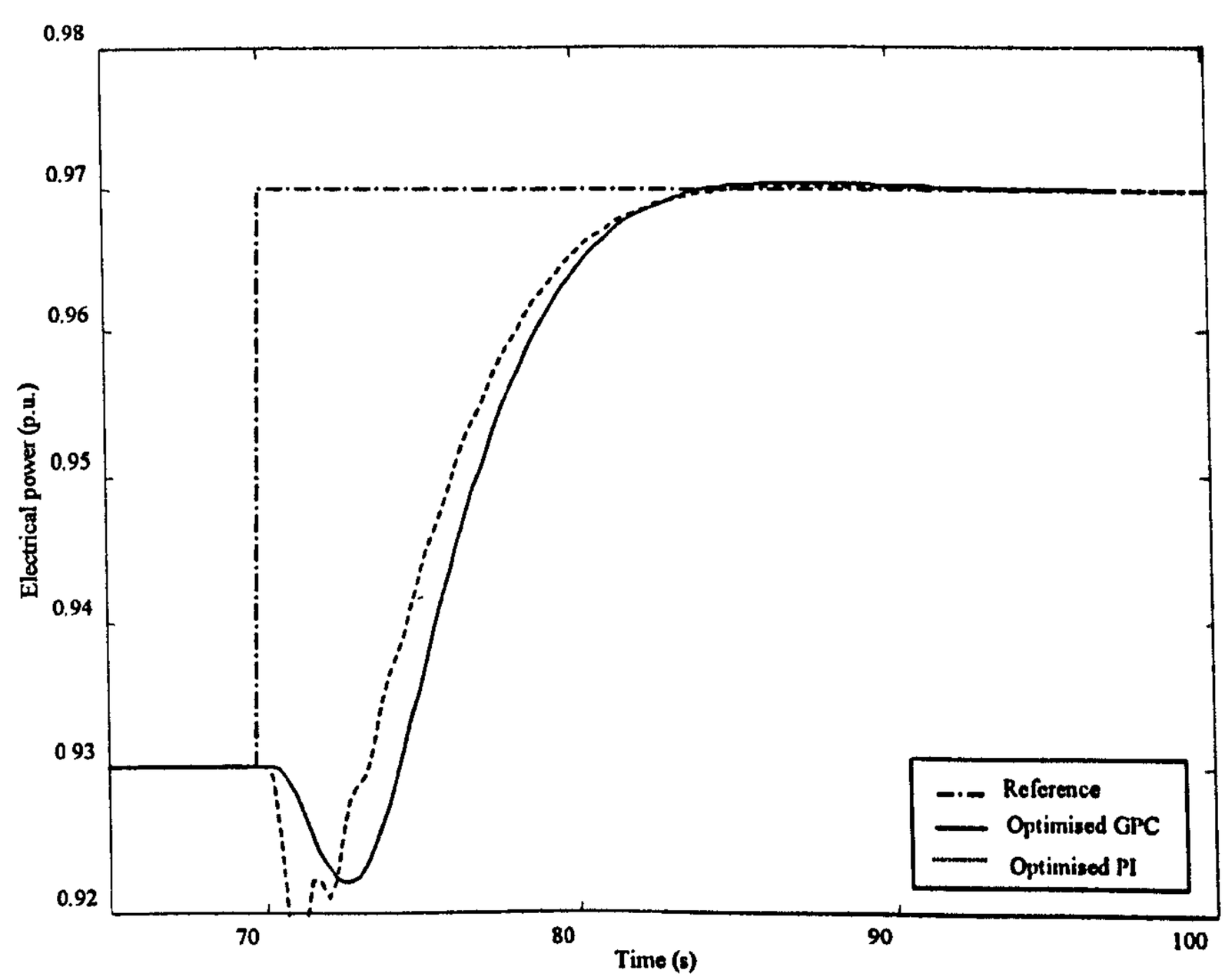


*Figure 5.11: Response of electrical power to a small step using the optimised PI and GPC controllers, six units operational.*

## 5.4 Comparison of the controllers, constrained case

The previous section has shown that the response using the GPC algorithm is comparable to the best PI controller, but neither seems capable of achieving a fast primary response while also minimising both under- and over-shoot. This bound on the performance achievable by linear controllers is due to the non-minimum phase zero implicit in the hydraulics subsystem [58]. Specifying the primary response to a fixed time leads to a trade-off between the under- and over-shoot [26]. The initial undershoot, in particular, is associated with undesirable variation of pressure in the penstock and it is common practice in hydroelectric control to minimise this effect by limiting the opening and closing rates of the guide vanes.

In an effort to improve on the responses of Figure 5.9, it was decided to experiment with nonlinear control. A rate limit of $-0.2 \leq \Delta u \leq 0.2$ p.u., approximately twice the current Governor value, was imposed on the control for both the PI anti windup and GPC methods. This rate limit allows the guide vanes to move more rapidly than is currently the case when necessary. An effective strategy for the control saturation limit is to cap its value according to:

$$\begin{aligned} 0 \leq u \leq P_d / A_t \quad & \dot{P}_d \geq 0 \\ P_d / A_t \leq u \leq 1 / A_t \quad & \dot{P}_d < 0 \end{aligned} \tag{5.3}$$

at each sample instant, i.e. the control is never allowed to exceed the steady-state value required by the demanded power. In the case of the PI method, a faster response was obtained simply by doubling the loop gain. The constrained version of the GPC algorithm [31], discussed in Chapter 4 (section 4.3.2), was used with the future control sequence determined by quadratic programming. The parameters were set to $N_u = N = 20$ and $\lambda = 20$. The introduction of the constraints, equation 5.3, allows the reduction of $\lambda$ thus increasing the speed of the response without producing overshoot.

The responses for the One Unit case are shown in Figure 5.12. Here, the constrained GPC is clearly superior because its primary response is now equal to that produced by the PI controller while retaining the advantages of smaller undershoot and smoother control. In Figure 5.12, the undershoot of the PI anti windup response is approximately 17% and is well in excess of the practical limit when large changes in power are demanded. Reducing the amplitude of the undershoot to that produced by the GPC

requires the PI anti windup rate limit to be reduced to 0.00625p.u., approximately 1/30 of its value in Figure 5.12. This has an adverse effect on the remainder of the response, as shown in Figure 5.13 where it is seen that the primary response for the PI anti windup is now much longer than that of the GPC. It is concluded that the low undershoot of the GPC controller cannot be reproduced simply by adjusting the fixed rate limit on the PI anti windup controller.

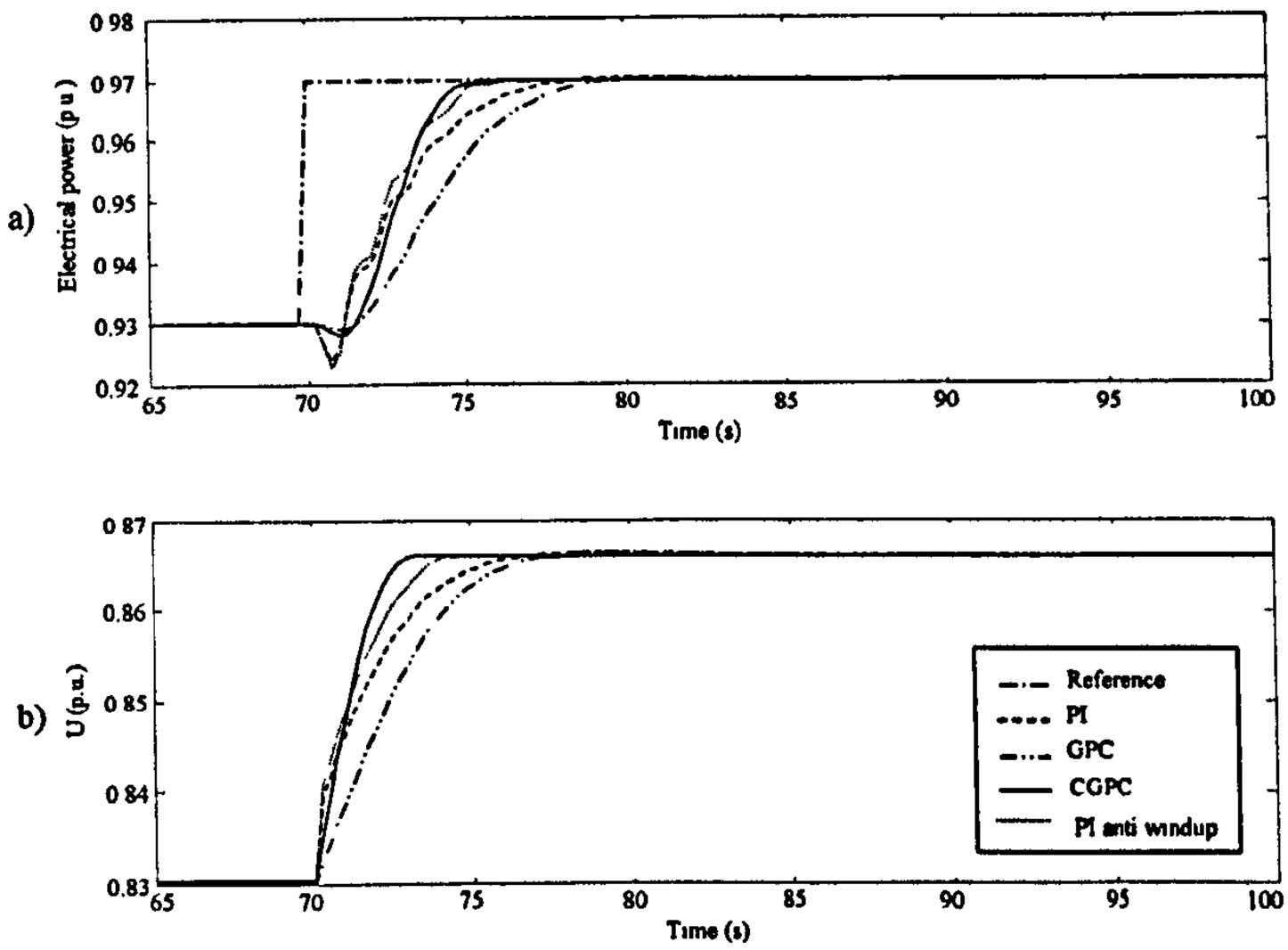


*Figure 5.12: Comparison of constrained and unconstrained control: (a) responses, (b) control signals, one unit operational.*

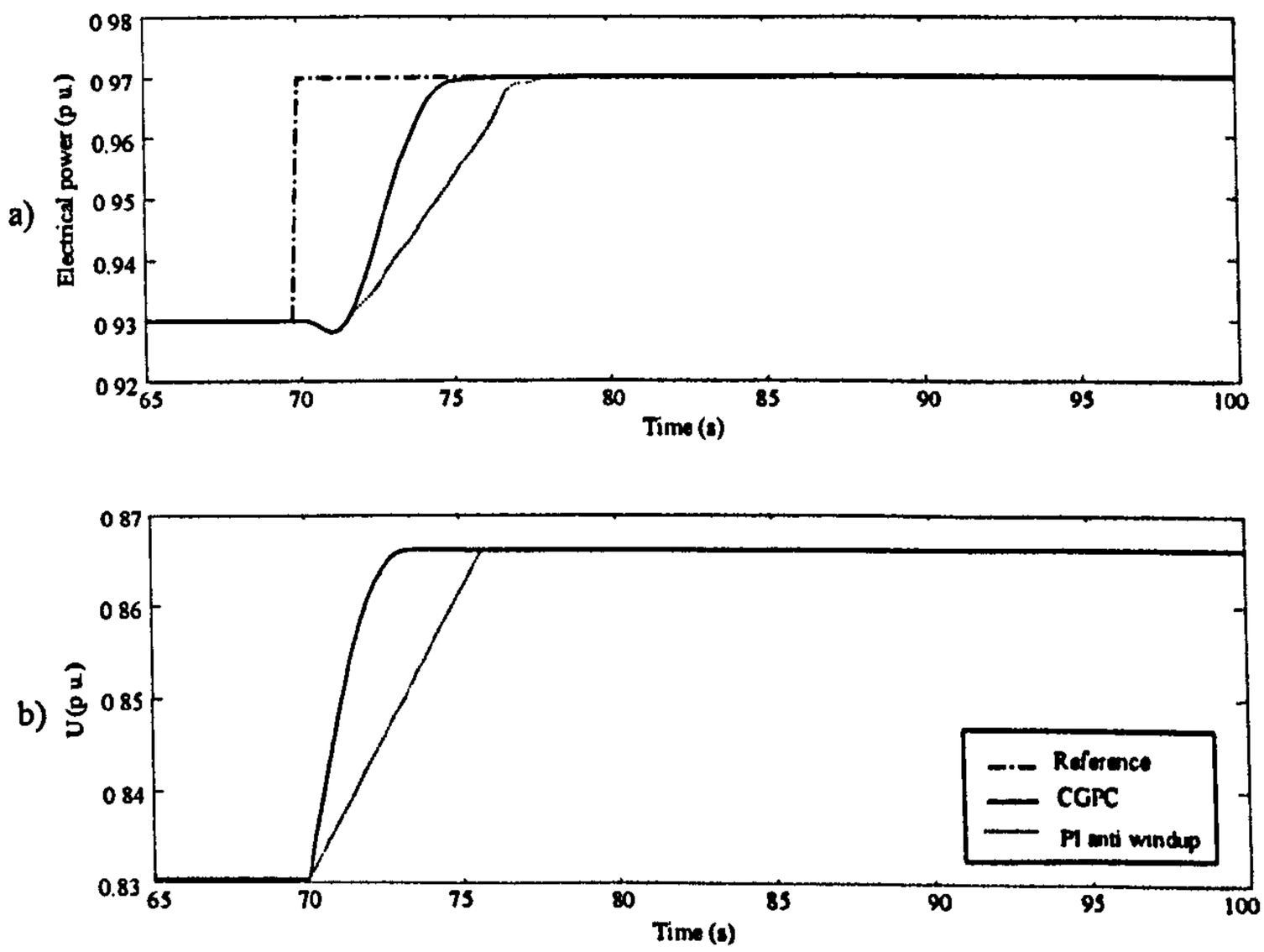


*Figure 5.13: Comparison of PI and CGPC with different rate limit: (a) responses, (b) control signals, one unit operational.*

## 5.5 Conclusions

This chapter has provided a general guide for optimum adjustment of the parameters of the GPC controller, where the selection of the appropriate values of these parameters yields an improved response of the linear SISO model of the hydroelectric plant.

The results from the unconstrained GPC controller were compared with the results from the classic PI Governor, currently implemented in Dinorwig. It has been shown that applying the GPC method to the hydroelectric pumped-storage station can improve its dynamic response. The primary advantage of GPC, relative to conventional PI control, is its smooth treatment of the non-minimum phase response, resulting in minimisation of the undershoot. In order to perform a comparable evaluation the PI controller was retuned, reducing the primary response of the system without allowing large overshoot.

When constraints on the control are introduced, their explicit inclusion within the GPC algorithm yields a response which is closer to the 'hydraulic limit' (i.e. using all the power available in the water column) than achieved by PI anti windup control, even when the latter has been designed carefully for maximum performance.

In summary, analysis assuming a SISO linearised plant model and unconstrained controllers shows that the PI and GPC controllers produce different response characteristics but neither has a clear superiority. On the other hand, when constraints are introduced, the improved performance of the GPC controller is evident and it is to be expected that the gap between the two will widen as the analysis is extended to MIMO models that include plant nonlinearities.

# Chapter 6

# PI and GPC controllers for MIMO models

## 6.1 Introduction

In Chapter 5 the application of Generalised Predictive Control (GPC) to a SISO linear model of Dinorwig was evaluated. It was concluded that constrained GPC in particular is superior to the classic PI currently implemented. In this chapter, the performance of GPC is evaluated when linear and nonlinear MIMO plant models are used. Figure 6.1 summarises the principal features of the controllers that have been evaluated already and also, in the highlighted block, the main characteristics of the evaluation performed in this chapter.

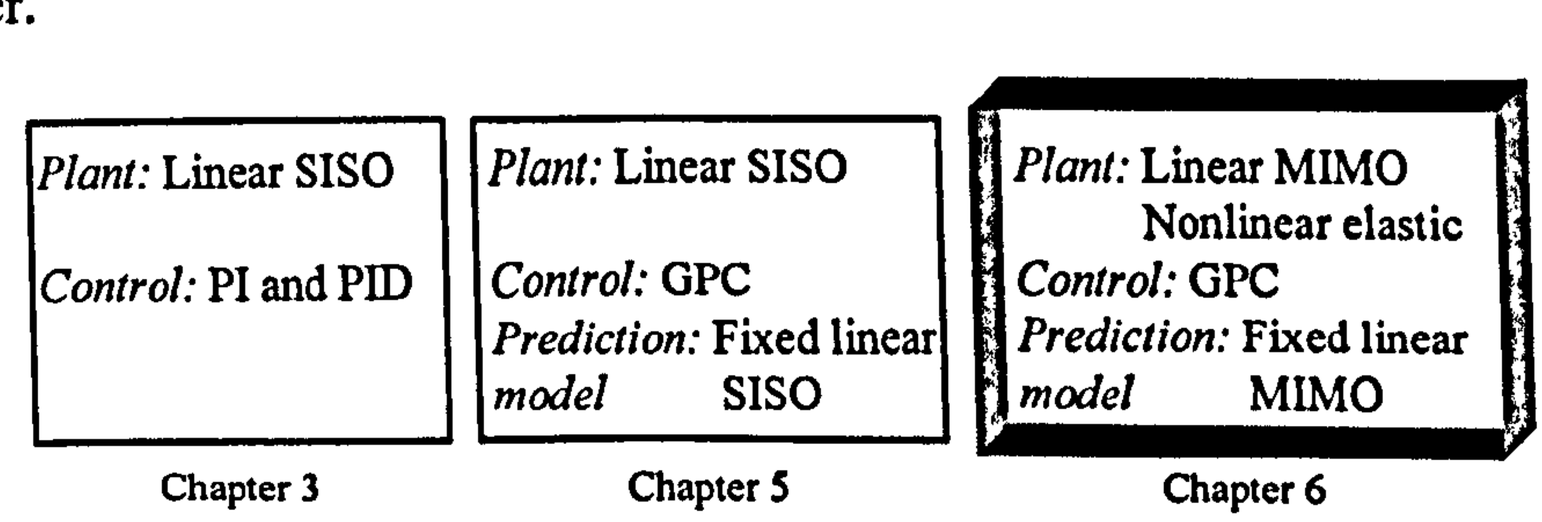


*Figure 6.1: Evolution of the control proposal for Dinorwig.*

The principle of GPC is that the predictive model provides more information on the system to the control algorithm resulting in better performance. Chapter 5 has shown how CGPC, using this extra information, can improve the response of the system under different operational conditions. However the scope of that chapter was limited to a SISO linear model and the multivariable effects of hydraulic cross-coupling were only taken into account as an effective change of the water starting time ($T_w$) with the number of units on-line (see section 5.4). Also, the study in that chapter was limited to small step responses. The aim of this chapter is to evaluate the performance of GPC when used with two MIMO models of Dinorwig described in Chapter 2:

- The MIMO linear model of section 2.2.1.2
- The nonlinear MIMO model of section 2.2.3 which includes the effect of an elastic water column.

The specific values of the parameters are taken from the work of Mansoor [3].

The MIMO linear model of Dinorwig can represent the multivariable hydraulic interactions that take place between the penstocks and main tunnel, and also the effects of the synchronisation of the generators. The water column is considered to be an inelastic fluid. This causes the effective water starting time to vary, depending on the number of units active. Therefore, the effects of the PI and GPC controllers in the reduction of cross-coupling interaction and their performance with different number of units active can be evaluated. An important difference between the two methods is that GPC is a single co-ordinated controller for all units on-line whereas the PI is a number of individual controllers.

The MIMO nonlinear elastic model of Dinorwig can be considered to be a "full nonlinear" model because it integrates all the nonlinearities and multivariable effects discussed in chapter 2. Again, the behaviour of the system with different operational conditions can be evaluated, where the 'operating point' now changes as the simulation proceeds. Also, both large and small signals can be used as inputs to the system. In summary, the scope of the simulation is greatly expanded and can be considered comparable to the "real" plant. Nevertheless, it must be remembered that even the MIMO nonlinear elastic model remains only a mathematical representation of the Hydroelectric Power Plant.

In section 6.2 the values of the control parameters for the classic PI and GPC controllers are selected. The behaviour of the plant with GPC and PI controllers is analysed in section 6.3, where the Power Plant is modelled as a MIMO linear system. Section 6.4 increases the model complexity further by evaluating the controllers with the MIMO nonlinear elastic model of Dinorwig. Finally, section 6.5 draws some conclusions.

## 6.2 Tuning the controllers

In Chapter 5 the procedures to select the control parameters for the classic PI and GPC controllers were discussed. The values of the parameters used in this section are the same for the PI controller but in the case of the GPC they have changed because another predictive model is used.

### 6.2.1 Proportional and Integral (PI)

In the first part of this chapter the evaluation is concentrated on the case of six units operational with the MIMO linear model of section 2.3.1.2 to represent the power plant. Therefore, the set of optimised parameter values for six units is chosen for the PI controller and the modified values (Tables 5.1 and 5.2) are used for the PI with anti windup, in the constrained case. The PI controller was set to its standard settings of $K$=0.1 and $K_i$=0.12 when the MIMO nonlinear elastic model is employed. Table 6.1 summarises the values of the parameters for the PI and PI anti windup controllers used in this chapter.

*Table 6.1*

*Parameters of the PI controller.*

| | Current values PI | Optimised Six units PI | Optimised Six Units PI anti windup |
|---|---|---|---|
| $K$ | 0.10 | 0.165 | 0.165 |
| $K_i$ | 0.12 | 0.110 | 0.660 |

### 6.2.2 GPC

In Chapter 5 a model derived from the reaction curve of the system, for a single active unit, was used as the model of prediction. In this chapter two types of predictive model are investigated. The first is a discrete-time analytical model, obtained using Zero-order hold on the inputs, based solely on the hydraulic and guide-vane subsystems models of sections 2.2.1.2 and 2.3 respectively. For instance, in the case of six units operating at $G_o$=0.95 and a sample period $T_s$ = 0.25s the direct and cross-coupling transfer functions of the analytical model are:

$$G_6(z)=\frac{-0.2312z^3+0.5145z^2-0.1481z-0.07865}{z^4-1.802z^3+1.093z^2-0.2616z+0.02113} \tag{6.1}$$

$$X_6(z)=\frac{-0.04757z^3-0.02751z^2+0.06817z+0.006913}{z^4-1.802z^3+1.093z^2-0.2616z+0.02113} \tag{6.2}$$

The second predictive model is obtained empirically from the reaction curve of the nonlinear nonelastic model using a small step (0.04 p.u.) when six unit are active. In this model of prediction the direct transfer function (6.1) is replaced by the simpler transfer function calculated from the reaction curve with six units operational but the cross-coupling transfer function (6.2) remains unchanged.

$$G_{6o}(z)=\frac{0.29044}{z^4-0.7422z^3} \tag{6.3}$$

The corresponding polynomials of a CARIMA model using (6.2) and (6.3) are (see Appendix 2):

$$A_6(z^{-1})=1-2.5442z^{-1}+2.4304z^{-2}-1.0728z^{-3}+0.2153z^{-4}-0.0157z^{-5} \tag{6.4}$$

$$B_6(z^{-1})=0.2904z^{-4}-0.5234z^{-5}+0.3175z^{-6}-0.076z^{-7}+0.0061z^{-8} \tag{6.5}$$

$$b_6(z^{-1})=-0.0476z^{-1}+0.0078z^{-2}+0.0886z^{-3}-0.0437z^{-4}-0.0051z^{-5} \tag{6.6}$$

where $A_6$, $B_6$ are diagonal elements and $b_6$ are the off-diagonal elements.

In fact, the predictions produced by both models are similar and agree well with the MIMO linear model output as shown in Figures 6.2 and 6.3, for the direct and cross-coupling responses, respectively. Both predictive models are derived for the case of 6 units in operation at 95% output, the extreme operational case. The predictive model is

fixed, regardless of how many units are actually in operation or their loading; this restriction will be relaxed in Chapter 7.

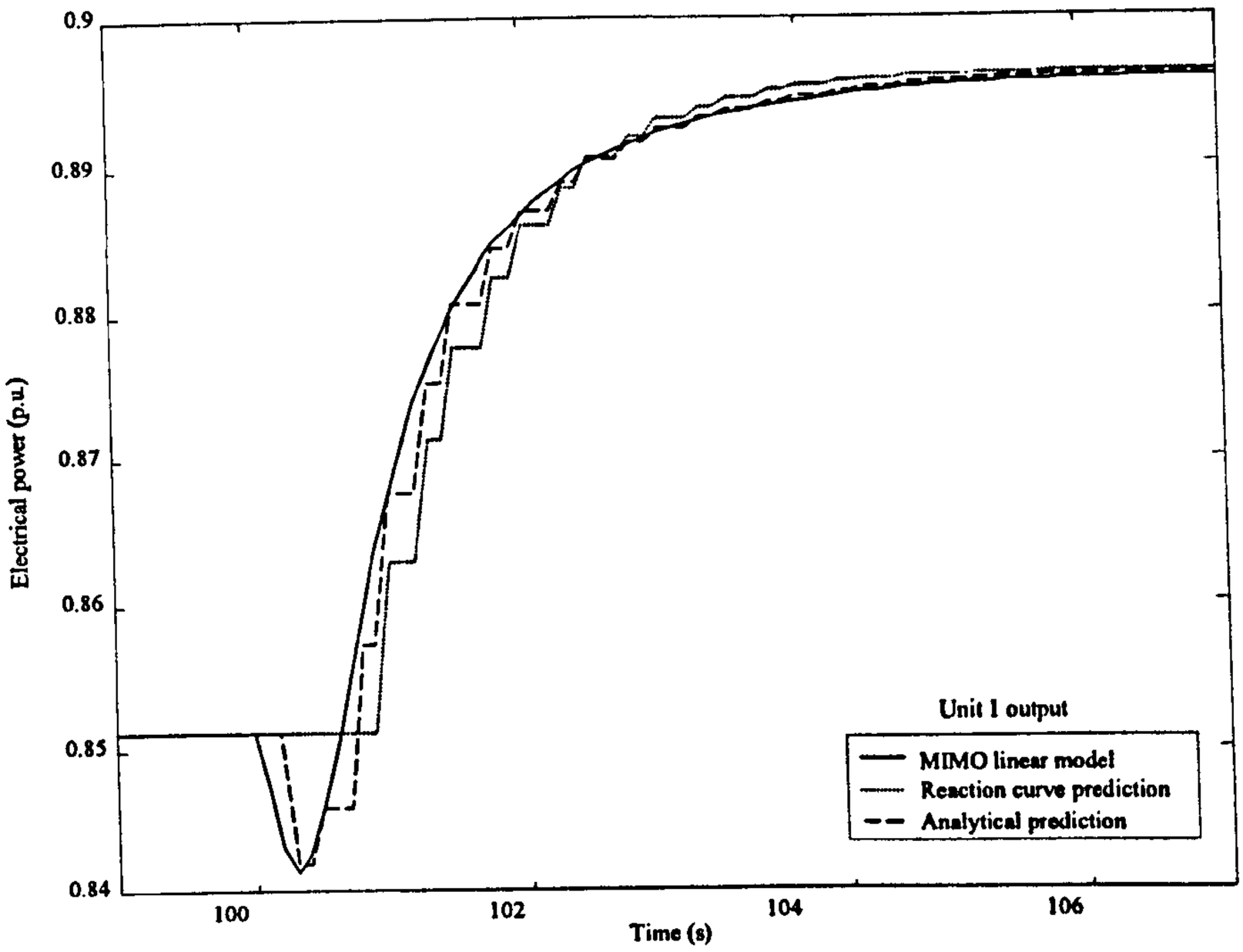


*Figure 6.2: Response of the Plant model and the predictive models to a step in control, applied to unit 1, with the controls for units 2-6 fixed at their initial values.*

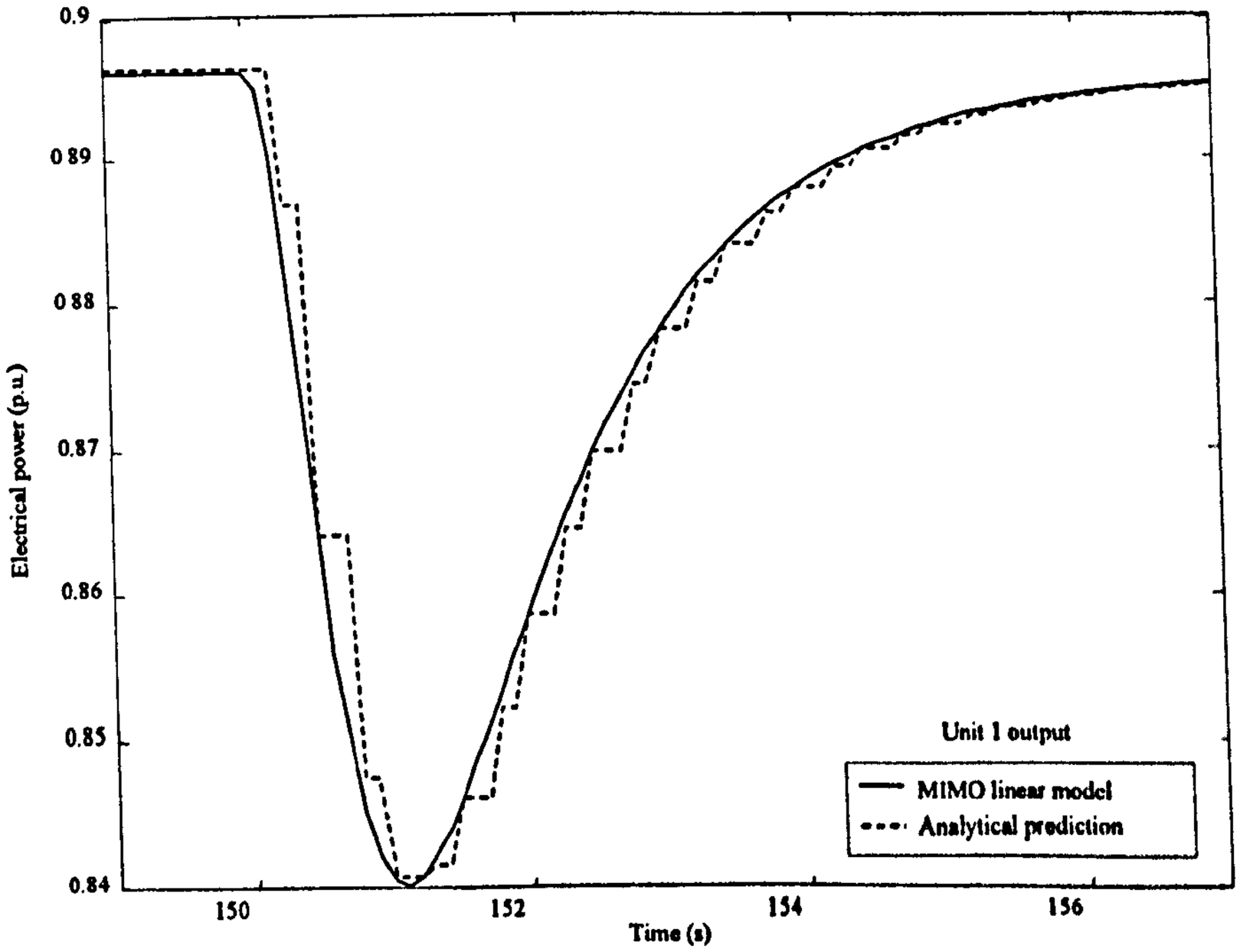


*Figure 6.3: Response of the Plant model and the predictive models to a step in control, applied simultaneously to units 2-6, with the control for unit 1 fixed at its initial value.*

GPC controllers were designed using both (6.1) and (6.3) as the direct transfer function in the predictive model. The results from both models were similar, omitting the initial error during the transport delay time, the maximum absolute error is 4.5% for the reaction curve model and 1% for the analytical model; so the more economical transfer function (6.3) was used for the remainder of the work. Reducing the complexity of the predictive model is very important in the Constrained GPC (CGPC) case, which involves Quadratic Programming iterations. In order to minimise the computational time, this method is usually tuned using low values of horizon of control and prediction. Using the guidelines mentioned in section 4.4 and the process discussed in section 5.2.2.2 the GPC controllers were tuned. Table 6.2 summarises the values of the parameters for the GPC and CGPC controllers used in this chapter.

*Table 6.2.*

*Parameters of the GPC controller.*

| | MIMO linear | | MIMO nonlinear | |
|---|---|---|---|---|
| | Unconstrained (GPC) | Constrained (CGPC) | Unconstrained (GPC) | Constrained (CGPC) |
| $N$ | 40 | 40 | 40 | 40 |
| $N_u$ | 20 | 10 | 40 | 10 |
| $\lambda$ | 425 | 350 | 300 | 250 |
| $\alpha$ | 0 | 0 | 0 | 0 |

## 6.3 MIMO linear model

In order to evaluate the performance of the GPC, several simulations were carried out. Step power demand signals are applied to the MIMO linear model of Dinorwig with both the PI and GPC controllers. The results are compared with the specifications stated in Chapter 3.

### 6.3.1 Comparison of the controllers, unconstrained case

To evaluate the step response, a small step of 0.04 p.u. is applied to the units after an operating point has been fixed. For the one unit case with the other units off-line, Table 6.3 and Figure 6.4 show that GPC produces a primary response (test $P_1$), which is 12% faster, settles 14% sooner and has only 30% of the NMP undershoot produced by the PI

controller (test $P_6$). GPC also produces a smoother control that inhibits the rapid, poorly-damped synchronous electrical mode which the relatively sharp PI control excites.

*Table 6.3.*

*Comparison of PI and GPC single-unit responses*

| Test | Specification for single unit operation | PI | GPC | CGPC |
|---|---|---|---|---|
| P1 | $P_1 \geq 90\%$ at $t_{p1} = 10s$ | 81% at 10s, 90% at 13.3s | 85% at 10s, 90% at 11.7s | 92% at 10s, 90% at 9.3s |
| P2 | $P_2 \leq 5\%$ and $t_{p2} \leq 20s$ | No overshoot | No overshoot | No overshoot |
| P3 | $t_{p3} = 25s$ for $P_3 \leq 1\%$ | 25s | 21.4s | 16.5s |
| P4 | $t_{p4} = 60s$ for $P_4 \leq 0.5\%$ | 29s | 24.3s | 19s |
| P5 | $t_{p5} = 8s$ | 11.8s | 9.4s | 7.1s |
| P6 | $P_6 = 2\%$ | 6.3% | 2% | 2.5% |
| P7 | $t_{p7} = 1.5s$ | 1.2s | 1.54s | 1.54s |

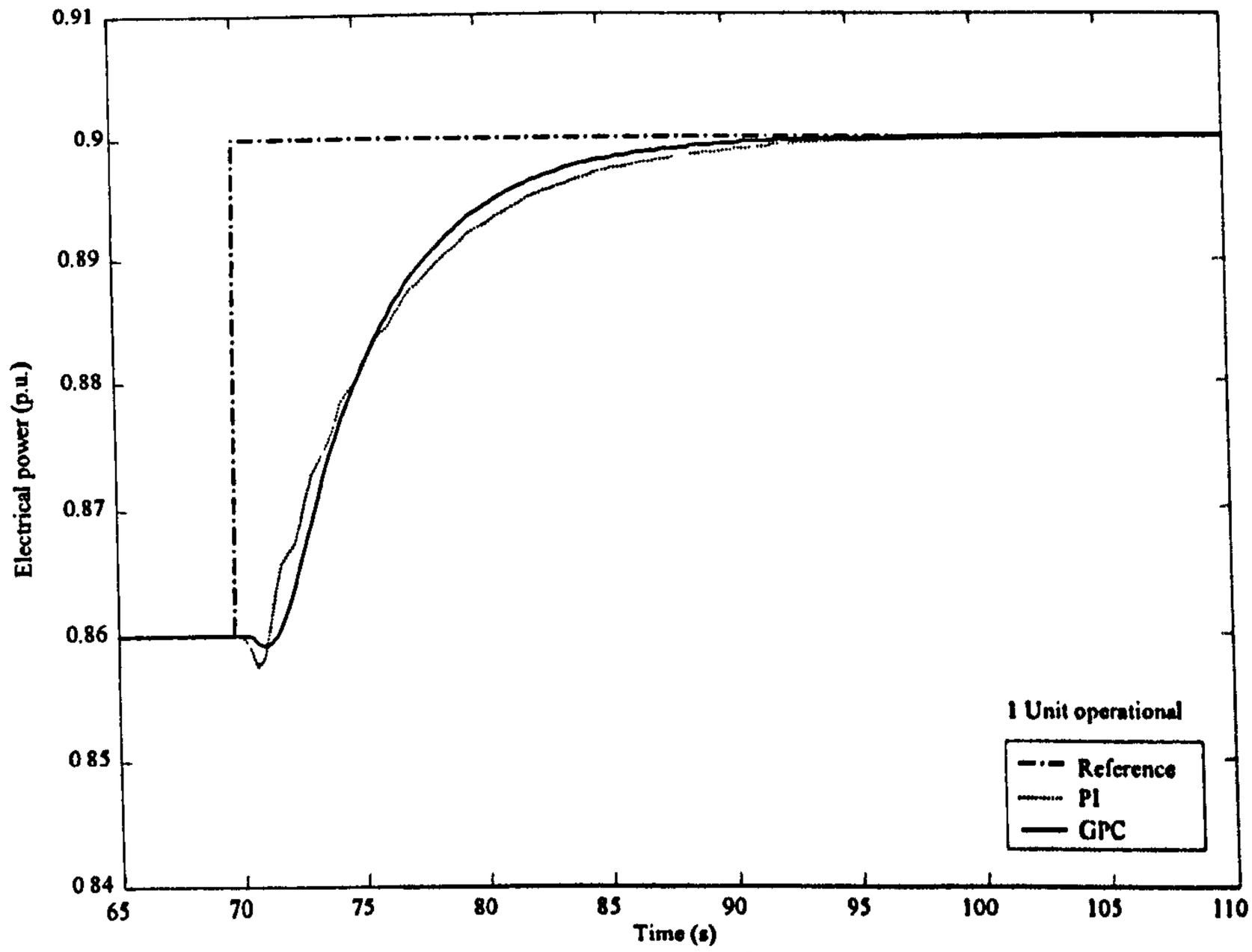


*Figure 6.4: Comparison of the step responses produced by GPC and PI controllers, one unit operational.*

In the six-Unit case, Figure 6.5, GPC almost eliminates the overshoot produced by the PI controller and also reduces the NMP undershoot, with no adverse effect on the

primary response. It is worth stressing here that neither controller (or any other controller of practical interest) can eliminate the NMP undershoot. As the guide vanes open, part of the mechanical power is diverted to accelerating the water column and is therefore denied to the output; this is a fundamental physical limitation. The controller may therefore distribute the power shortfall in time (by opening the guide vane slower) or by 'borrowing' from other turbines (decoupling control [4]), but it has no way to make up the power deficiency until the flow increases.

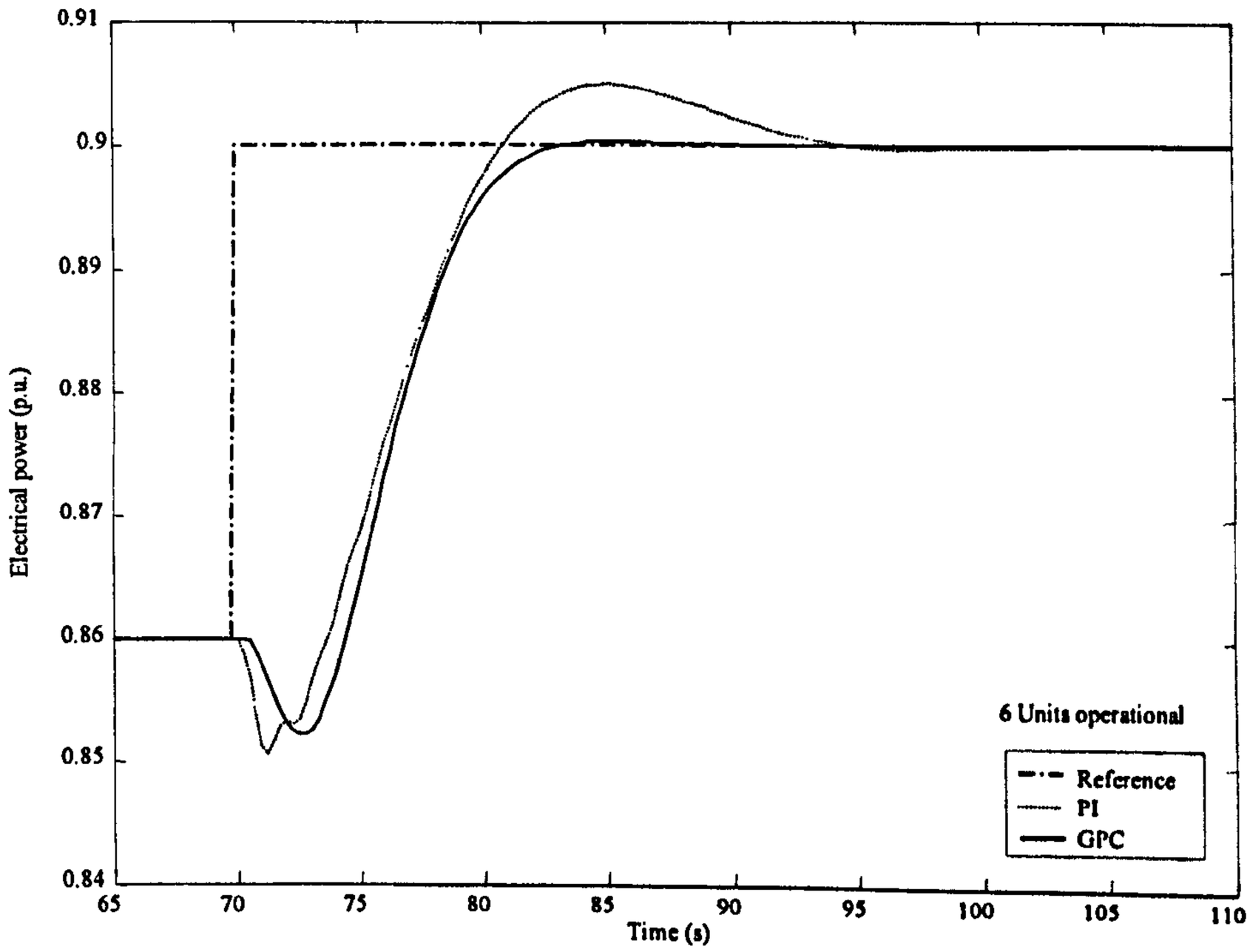


*Figure 6.5: Comparison of the step responses produced by GPC and PI controllers, 6 units operational.*

Figure 6.6 shows the cross-coupling responses of the two control systems. Initially, all six Units are operating at 0.86 p.u. At t = 100, a 0.04p.u. step demand is applied to Unit 1. Using GPC reduces the consequent perturbation on the outputs of the remaining five Units. At t = 140, a simultaneous step demand is applied to Units 2 – 6. Here, GPC eliminates the overshoot, reduces the initial undershoot and offers a small improvement in the cross-coupling onto Unit 1. Whilst the PI controller can be retuned to reduce the overshoot, it was found that this always slowed the response and caused a larger initial undershoot. It is concluded that GPC is superior to PI across the operating range of the plant.

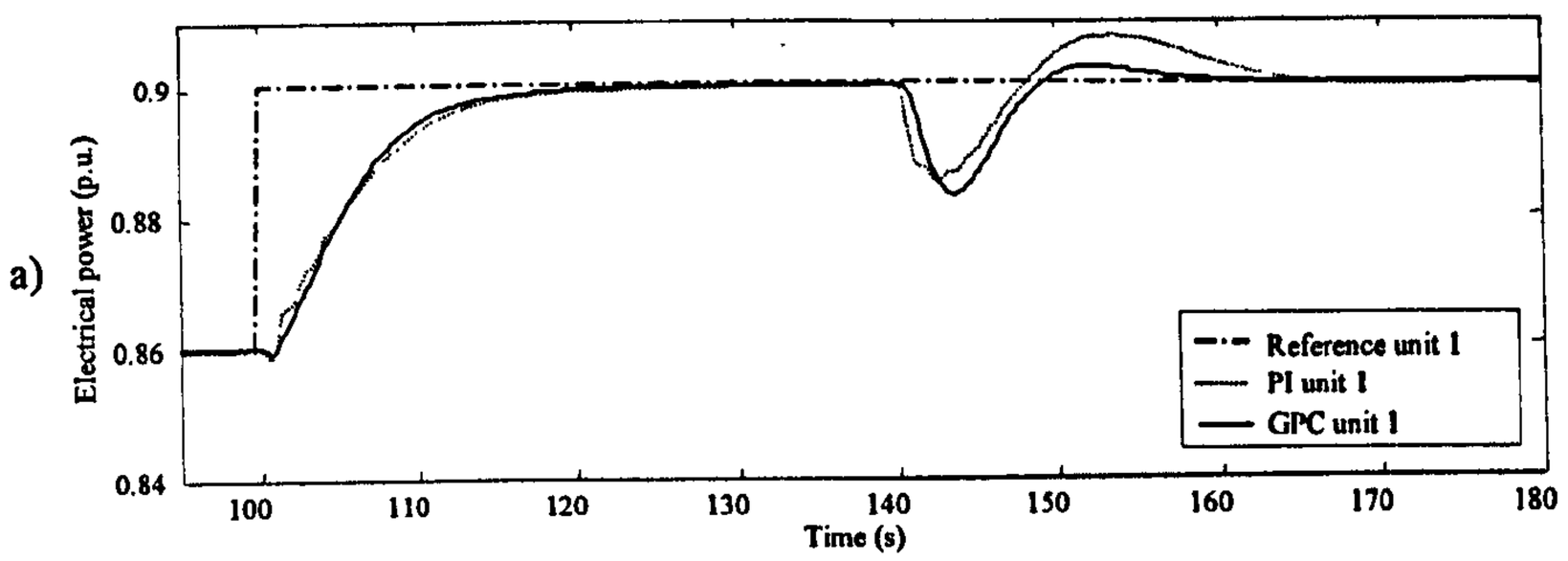


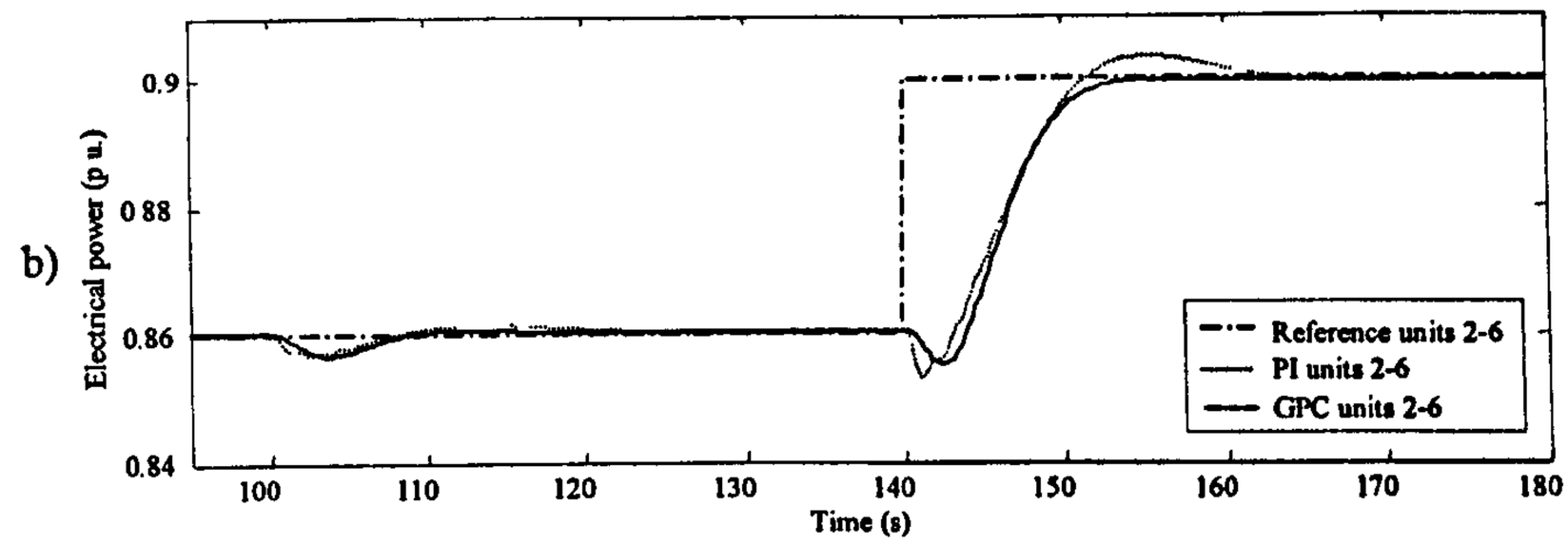


*Figure 6.6: Responses of unconstrained GPC and PI controllers to a step power demand, unit 1 (a) and units 2–6 (b).*

### 6.3.2 Comparison of the controllers, constrained case

Although unconstrained GPC is somewhat superior to PI, the performance indicators in Table 6.3 still fall short of the specification. Reducing the value of $\lambda$ yields a faster response but extensive simulations showed that it is always at the expense of other criteria. In this section, constraints on the guide vane rate and amplitude are incorporated within the theoretical framework of GPC. This allows the one-Unit specification to be satisfied while preserving stability during multiple unit operation. The control rate-limit is fixed at $-0.2 \leq \Delta u \leq 0.2$ p.u. and the strategy for saturation involving $P_d/A_t$ is followed, as explained in Chapter 5. Retuning the CGPC controller yielded the new parameters $N_u = 10$, $N = 40$, $\alpha = 0$ and $\lambda = 350$ (compared to $\lambda = 425$ for the unconstrained case, thus effectively increasing the 'loop gain'). To perform a fair comparison, the PI controller was also modified to include control constraints. The same rate limit of 0.2 p.u. was used and the saturation limit fixed to u = 1 p.u. in the anti-windup configuration. The PI parameter values were chosen as $K = 0.165$ and $K_I = 0.66$, to give the best response for the six-Unit case. The results are shown in Figures 6.7 and 6.8. Here, the CGPC response for the one-Unit case is faster than the unconstrained case but remains well damped and has a very small NMP undershoot. Its performance indicators (last column of Table 6.3) comply with the specification except for test P6. In

contrast, the response produced by the modified PI controller is barely faster than the unconstrained case and the electrical oscillation is prominent; in fact, this prevents any further increase in the loop gain.

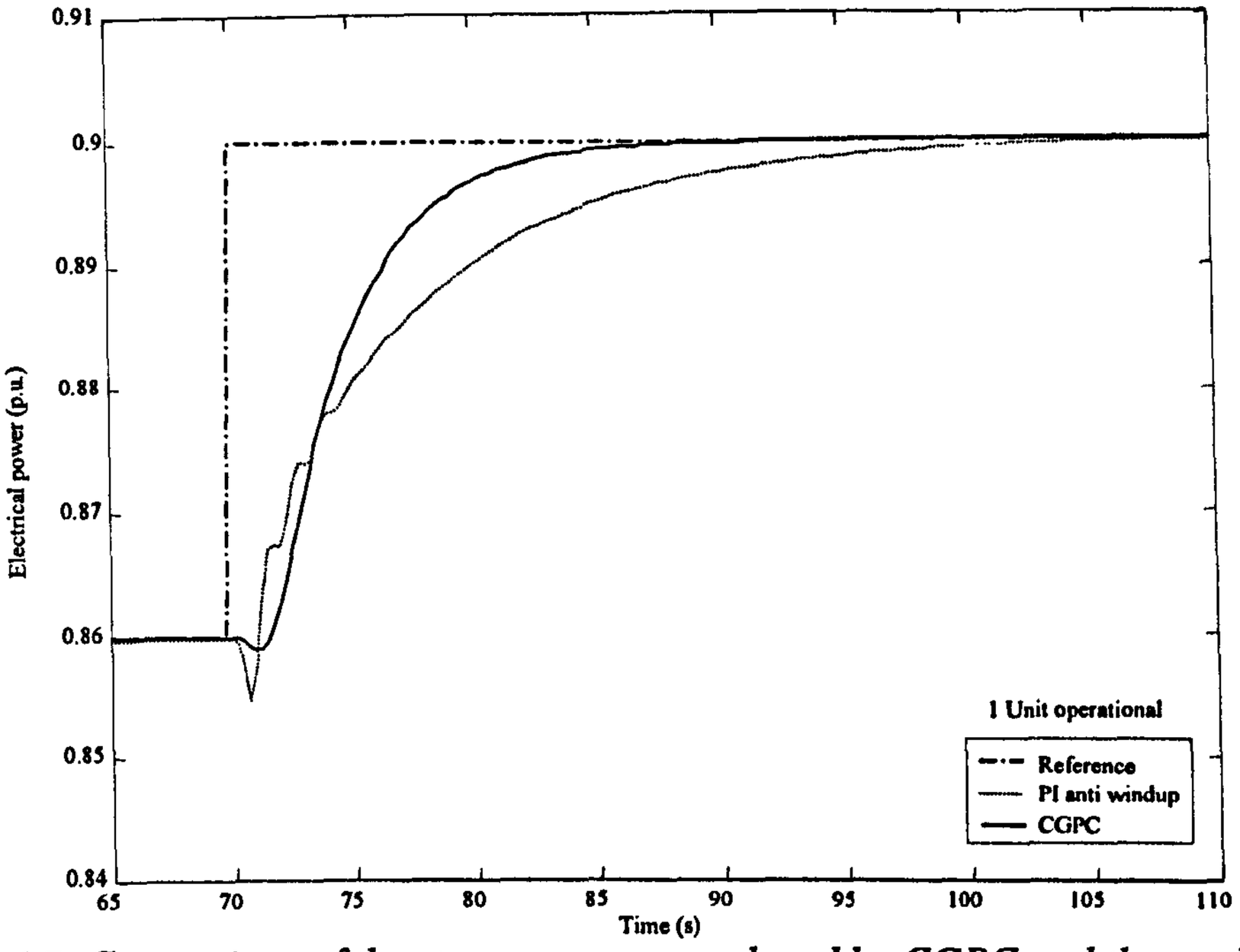


*Figure 6.7: Comparison of the step responses produced by CGPC and the modified PI controllers, 1 unit operational.*

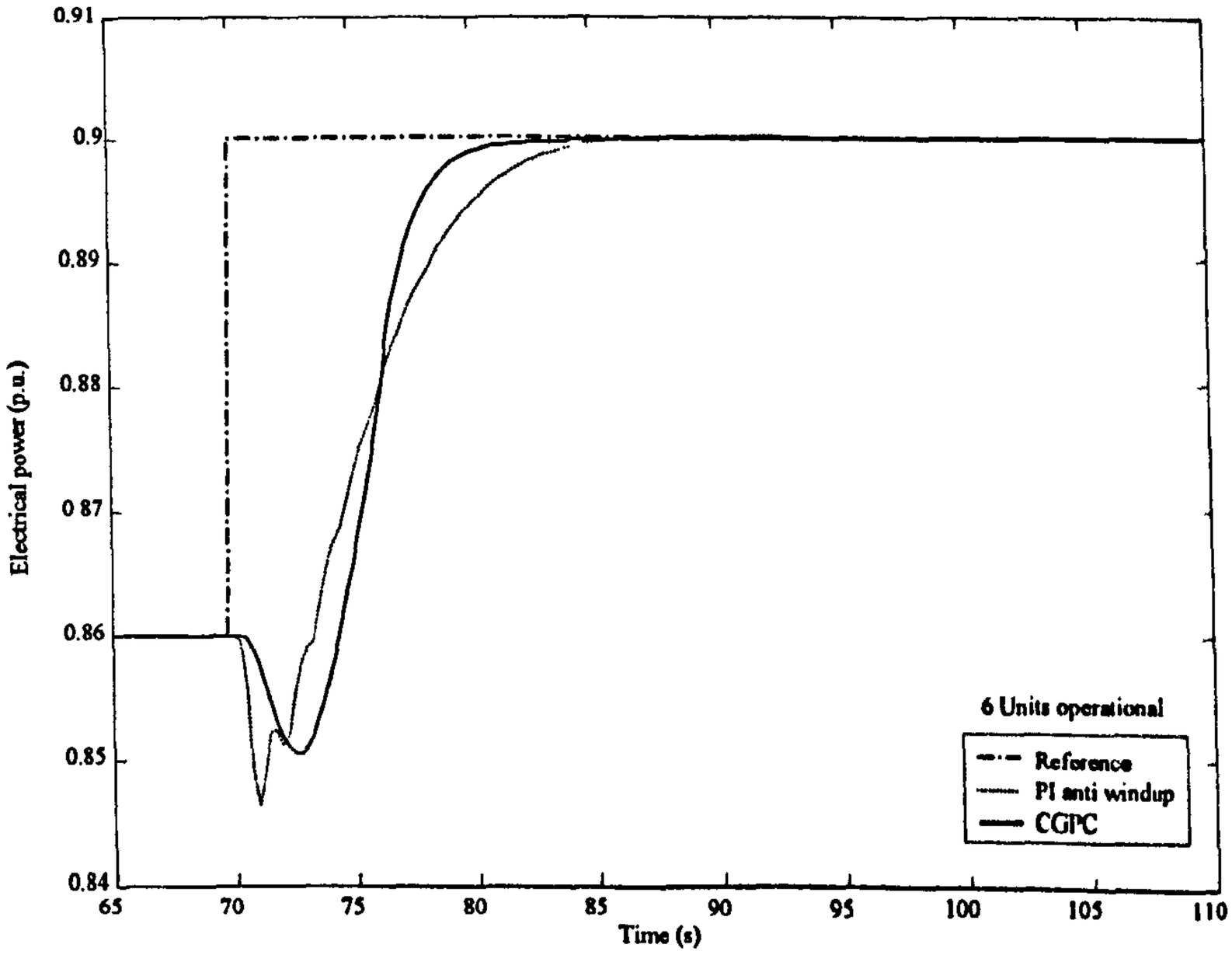


*Figure 6.8: Comparison of the step responses produced by CGPC and the modified PI controllers, 6 units operational.*

The advantage of the CGPC controller is retained in the six-Unit case of Figure 6.8, where it is seen to produce a smooth and fast response with no overshoot despite the change in operating conditions. Embedding knowledge of the constraints in the predictive model allows CGPC to make informed decisions about their effect and produce better controls.

The cross-coupling responses for CGPC and the modified PI are shown in Figure 6.9, where it is seen that the overshoot is improved in both the direct and coupled transients, with little effect on the speed response. However, as discussed previously, the NMP undershoot remains.

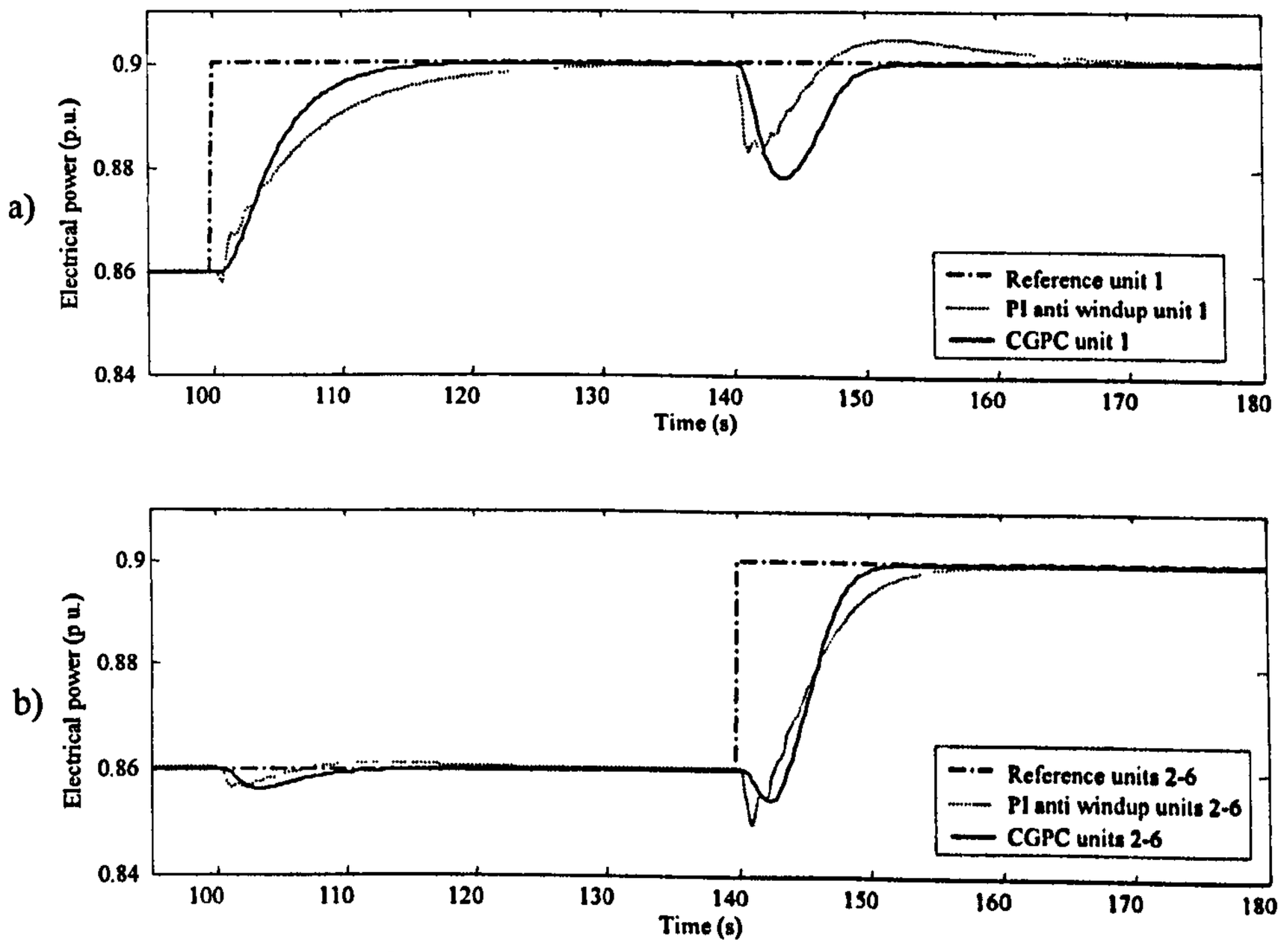


*Figure 6.9: Responses of CGPC and the modified PI controllers to a step power demand, unit 1 (a) and units 2–6 (b).*

## 6.4 MIMO nonlinear elastic model

In order to obtain a better assessment of GPC controllers, a MIMO nonlinear elastic model is used in this section to represent the Dinorwig power plant. In these simulations small step and large ramp input signals are applied to the model. As in the previous section the results are compared with the specifications stated in Chapter 3. The

response of the plant to variations in frequency is also assessed. Finally the robustness of the controllers with different operational conditions is investigated.

### 6.4.1. Small step responses, one unit operational

Here, the step responses produced by the GPC and CGPC controllers designed in section 6.2 are compared with those of the PI controller where the full MIMO nonlinear elastic model of Dinorwig is now in use. The GPC and CGPC controllers were tuned with the values given in Table 6.2 (section 6.2.2). The PI was tuned with its standard settings of $K$=0.1 and $K_i$=0.12.

The results for a 0.04 p.u. power demand are shown in Figure 6.10 and the corresponding control signals for these responses are shown in Figure 6.11. The test criteria are compared in table 6.4 and show that both GPC controllers produce primary responses that are 23% and 38% faster, settle 27% and 44% sooner and have 71% and 57% lower NMP responses, respectively, than the response produced by PI control. Again, GPC produces smoother controls that reduce the rapid, poorly-damped synchronous electrical mode which the relatively sharp PI control excites.

*Table 6.4*

*Comparison of PI and GPC single-unit step responses*

| Test | PI | GPC | CGPC |
|---|---|---|---|
| P1 | 81% at 10s, 90% at 13.68s | 88% at 10s, 90% at 10.58s | 90% at 8.45s |
| P2 | No overshoot | No overshoot | No overshoot |
| P3 | 25.93s | 18.87s | 14.65s |
| P4 | 29.20s | 21.06s | 16.30s |
| P5 | 12.05s | 8.33s | 6.26s |
| P6 | 1.75% | 0.50% | 0.75% |
| P7 | 0.88s | 1.15s | 1.28s |

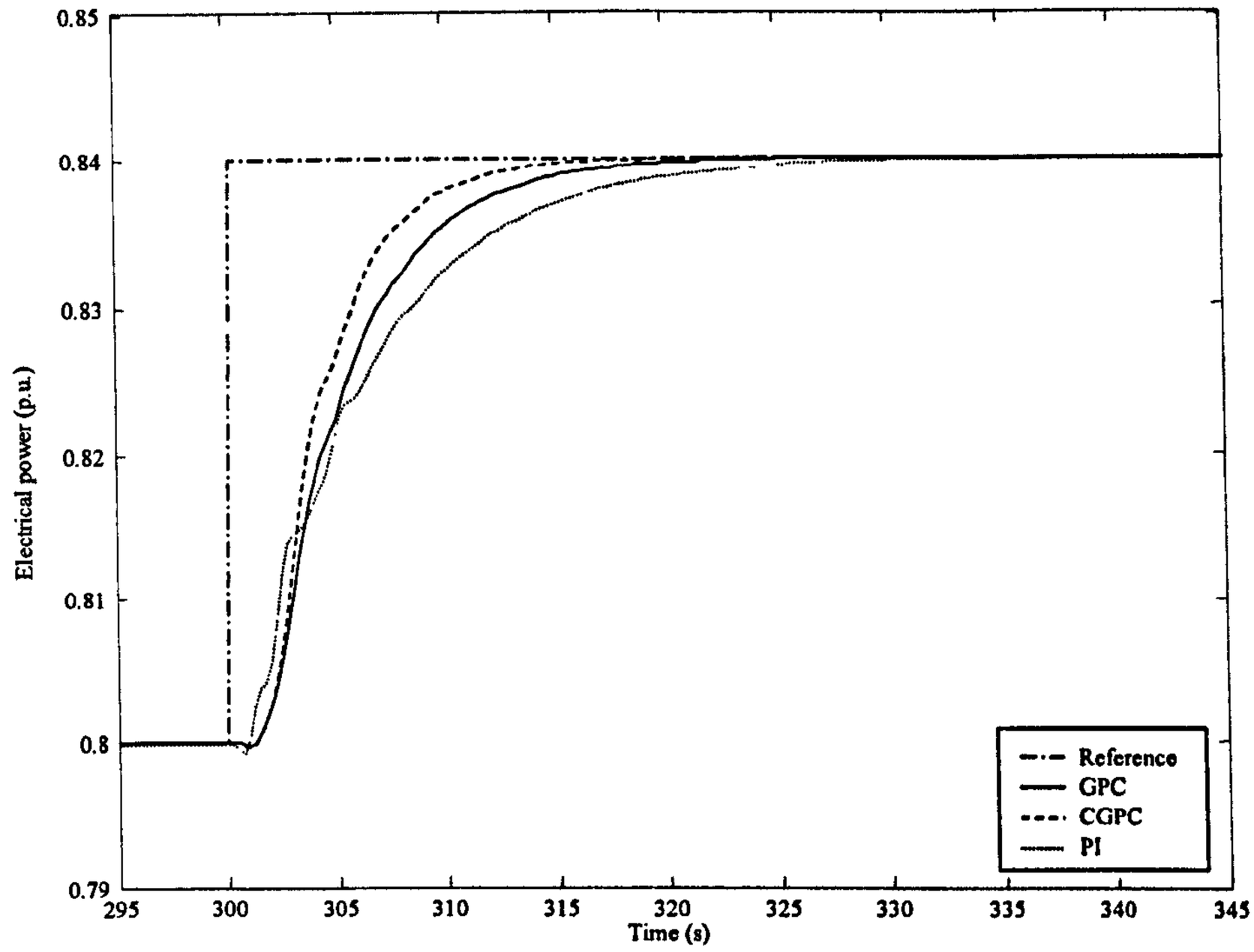


*Figure 6.10: Comparison of the step responses produced by GPC and PI controls, one unit operational.*

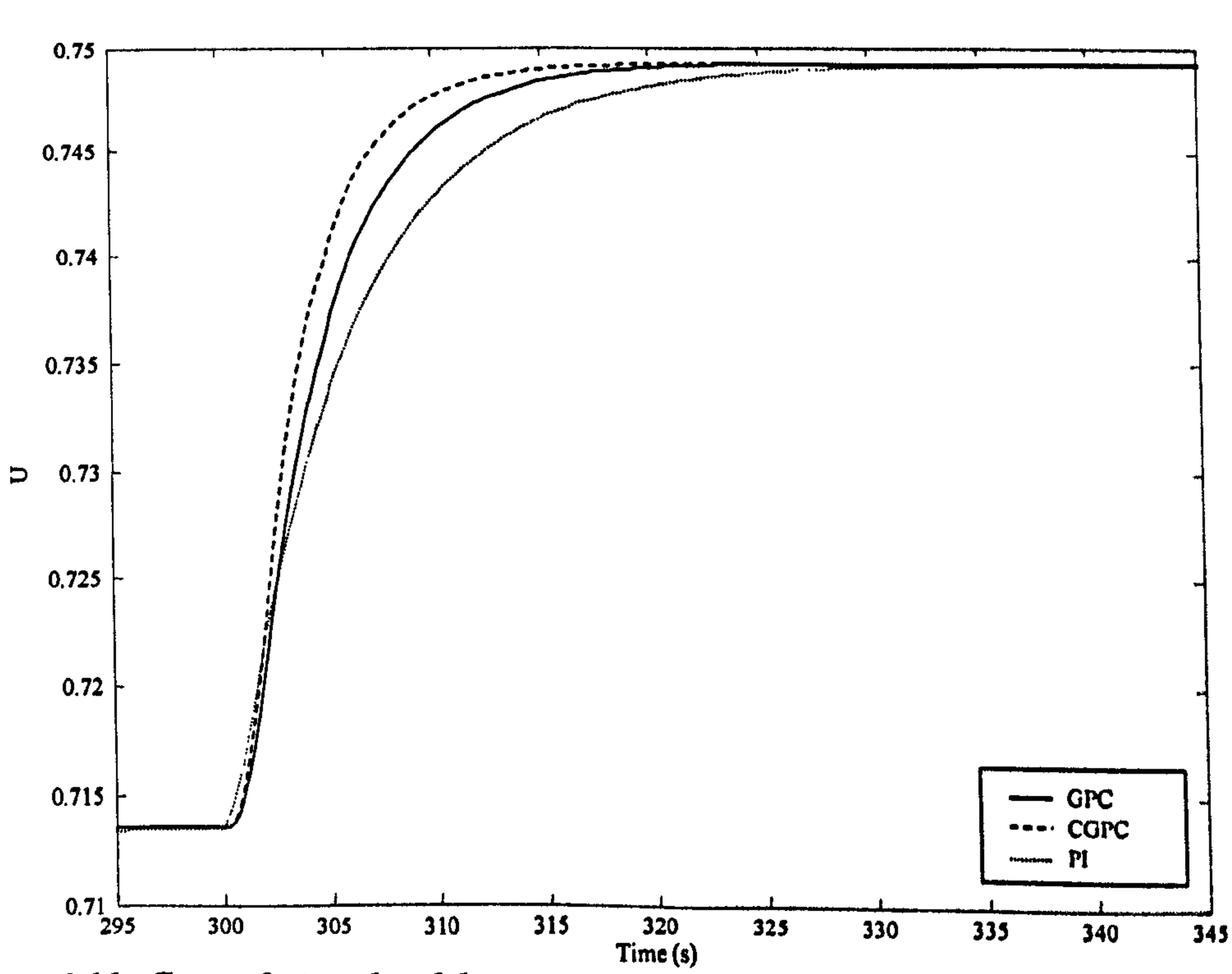


*Figure 6.11: Control signals of the step responses produced by GPC and PI controls, one unit operational.*

### 6.4.2 Small step responses, six units operational

As can be seen from Figure 6.12, all controllers have a different response when the number of active units varies. The figure shows the response of the system to a small step with the six units operating in synchrony. Under this operating condition the three controllers have a faster reaction than with one unit operational. The responses reach 90% of the new reference 14% (CGPC), 10% (GPC) and 23% (PI) sooner than for one unit operational. The NMP responses are more than ten times higher than in the one unit operational case. The PI controller produces the lowest undershoot but has significant overshoot. In general, the GPC controllers seem to be less sensitive to the variation in the number of units active.

The controllers now give a fast response. Actually, the primary response is better than with only one unit operational, because the system's stability margin is decreased by cross-coupling (*i.e* a longer $T_w$). However, the penalty is a very deep undershoot.

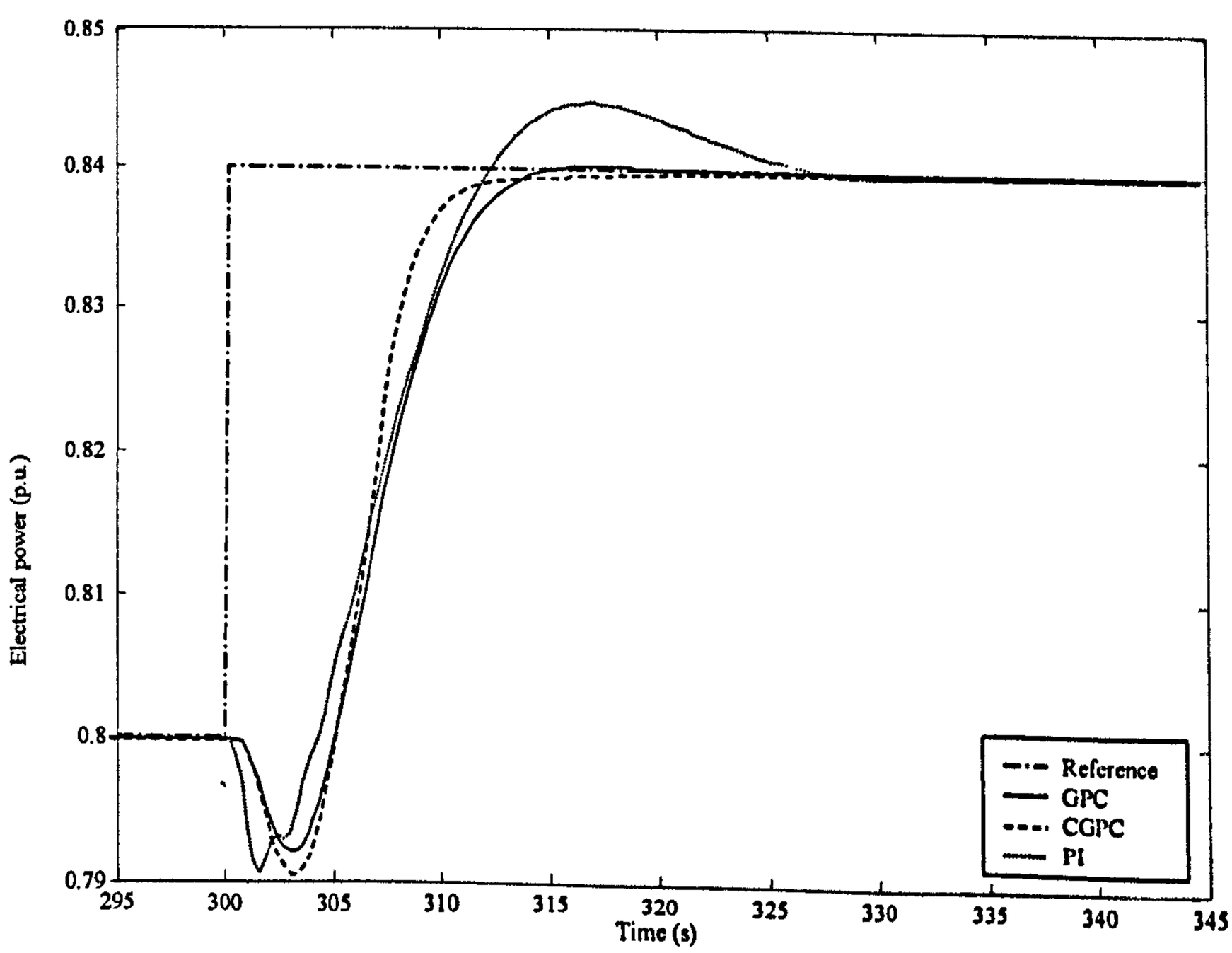


*Figure 6.12: Comparison of the step responses produced by the GPC six units operational.*

### 6.4.3. Large ramp responses

Dinorwig uses large ramp, instead of step, when large operating point changes are required; the main idea is to reduce the NMP response. In order to explore the behaviour of the plant under these operational conditions, large ramp responses produced by GPC controllers are compared with those by the PI controller, Figure 6.13 The GPC and PI controllers were tuned with the same values as the previous section. Figure 6.13 shows the response of the MIMO nonlinear elastic model to a large ramp. CGPC produces the faster response in the cases evaluated, one and six units operational, though the NMP response is bigger when the system is controlled by the GPC's.

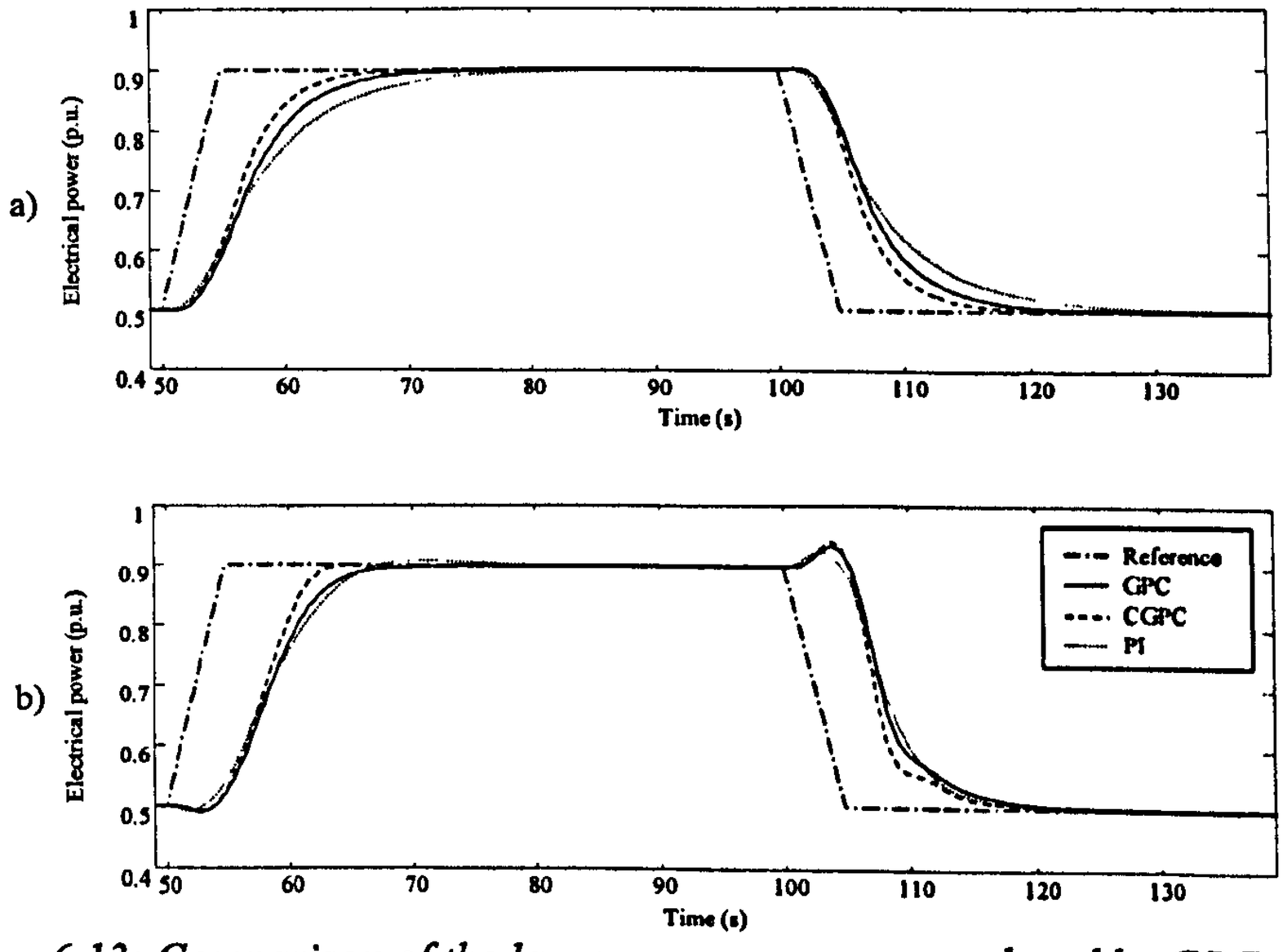


*Figure 6.13: Comparison of the large ramp responses produced by GPC and PI controls, a) one unit operational and b) six units operational.*

A method that has been employed at Dinorwig to accelerate the response, when large changes in reference are applied, is the introduction of a component of the reference signal directly into the control signal, see section 3.3 [3]. Figure 6.14 shows the response of the MIMO nonlinear elastic model to a large ramp, when the controllers have a component of feed forward in their control signal. All controllers produce a faster response as compared with Figure 6.13, where feed forward is not used. The PI controller has the fastest response in the one unit operational, but it produces a big overshoot in the six units operational case and also a slightly larger undershoot. CGPC

produces the faster response in the six units operational case without producing large overshoot.

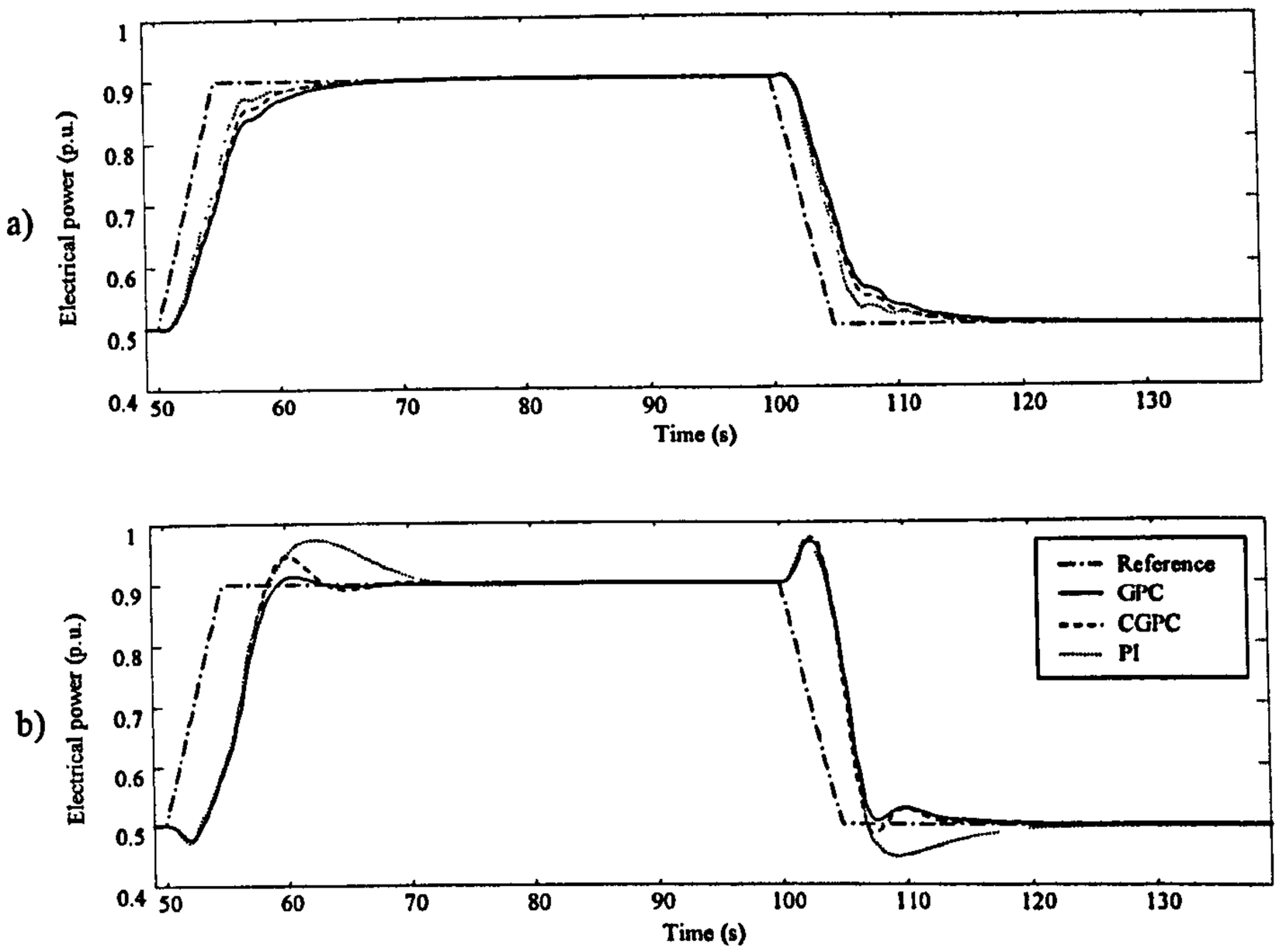


*Figure 6.14: Comparison of the large ramp responses produced by GPC and PI controls with feed-forward, a) one unit operational and b) six units operational.*

To evaluate the cross coupling interaction a 0.84 p.u. step was applied simultaneously at t=350 s. to units 2-6 and the perturbation of unit 1 was observed. As is shown in Figure 6.15 and Table 6.5, the PI control has a very high overshoot, 72% and 120% more than CGPC and GPC, respectively. Even though the PI has a lower undershoot, 34% and 44%, than the GPC controllers, the PI response has a longer settling time that is reflected in high values of the Integral Square Error (ISE) and the Integral Absolute Error (IAE).

*Table 6.5*

*Comparison of PI and GPC cross-coupling responses*

| | PI | GPC | CGPC |
|---|---|---|---|
| Undershoot | 0.76 | 0.73 | 0.72 |
| Overshoot | 0.90 | 0.85 | 0.86 |
| ISE | 0.23 | 0.19 | 0.19 |
| IAE | 4.06 | 3.31 | 3.18 |

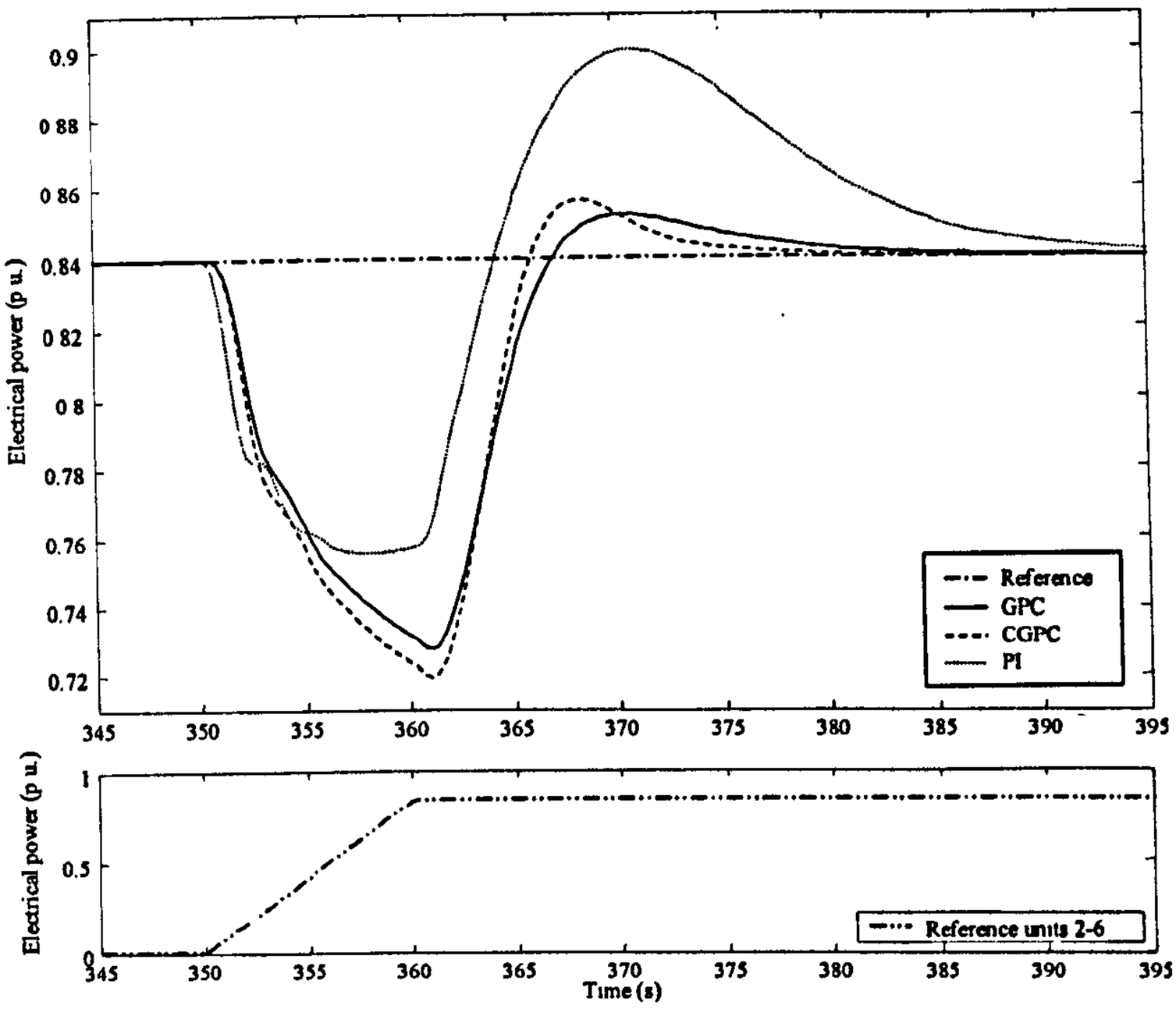


*Figure 6.15: Cross-coupling response of the plant using GPC and PI controls, six units operational.*

### 6.4.4. Different hydraulic head

As was discussed in section 2.2 the behaviour of the hydroelectric plant depends on the value of the hydraulic head. In order to determine the performance of the controllers when the plant is working under different conditions, simulations with different hydraulic heads were carried out.

Figure 6.16 shows the response of the system with GPC and PI controllers when a ramp is applied to the system with 90% of hydraulic head. Again, the one unit operational response region with 100% of hydraulic head is shown for comparison purposes. All the responses are slower with reduced head, the primary response, $t_{q1}$, being increased by 18% in the PI control case but by only 6% and 3% respectively for GPC and CGPC. The settling time, $t_{q3}$, is increased by 19% for the PI control, 10% for GPC and by only 7% for CGPC. Therefore, GPC controllers seem to be less sensitive to variation of hydraulic head.

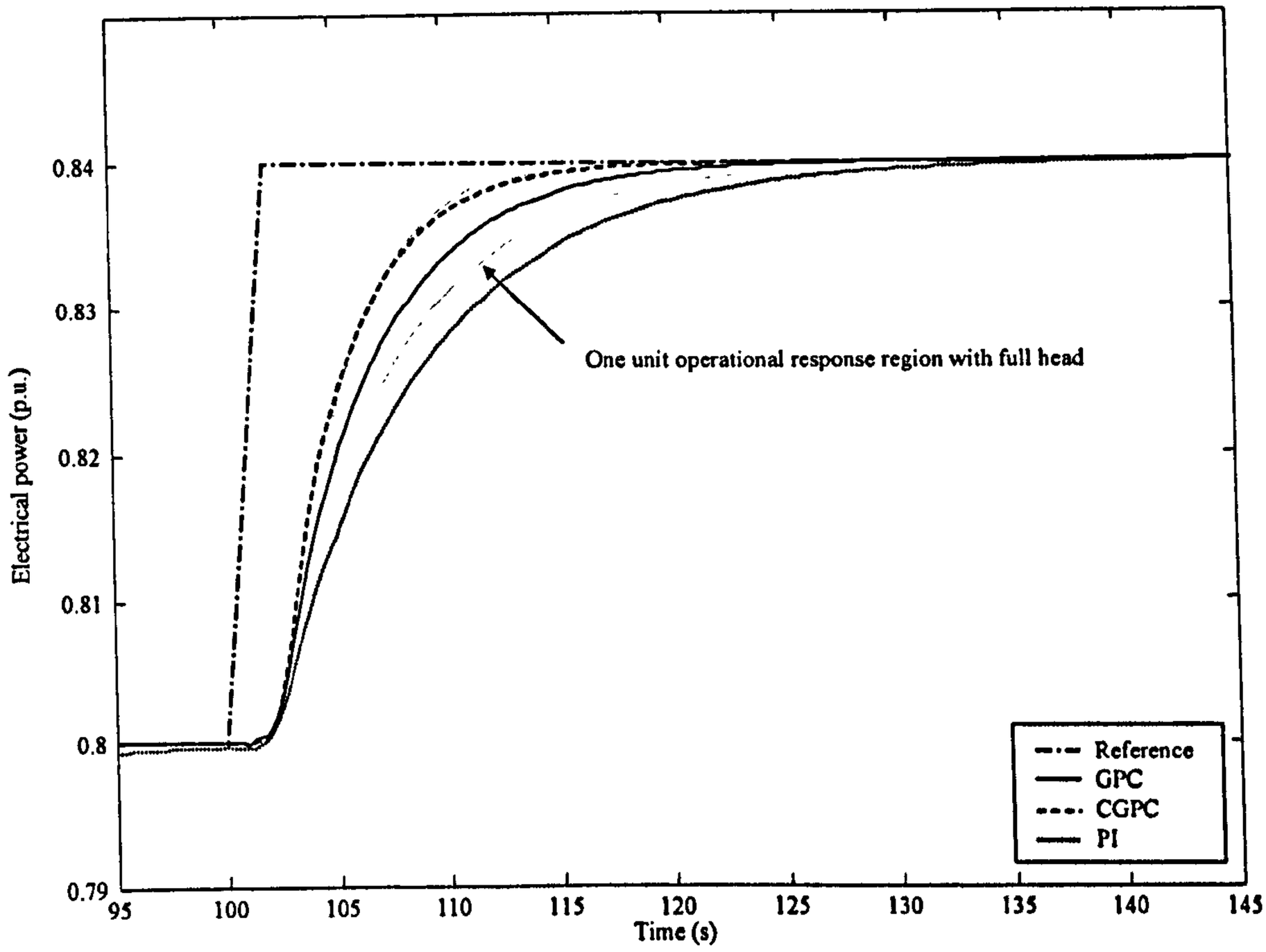


*Figure 6.16: Comparison of the ramp responses produced by the GPC (one unit operational) with 90% of hydraulic head.*

### 6.4.5. Effect of different rate limits

In order to determine if reducing the rate limit can reduce the NMP response when a CGPC controller is used, simulations with different rate limits were carried out.

Figure 6.17 shows the large ramp response of the plant with different rate limits. It can be seen that the lower the rate limit, the lower the NMP response. This reduction on the NMP response is more evident when the set point is being decreased (negative ramp). However, to significantly reduce the NMP response a very low rate limit is necessary. This low rate limit produces a very slow reaction increasing the primary response of the system. Therefore, a value of rate limit that produces a balance between low NMP and short primary response is normally selected.

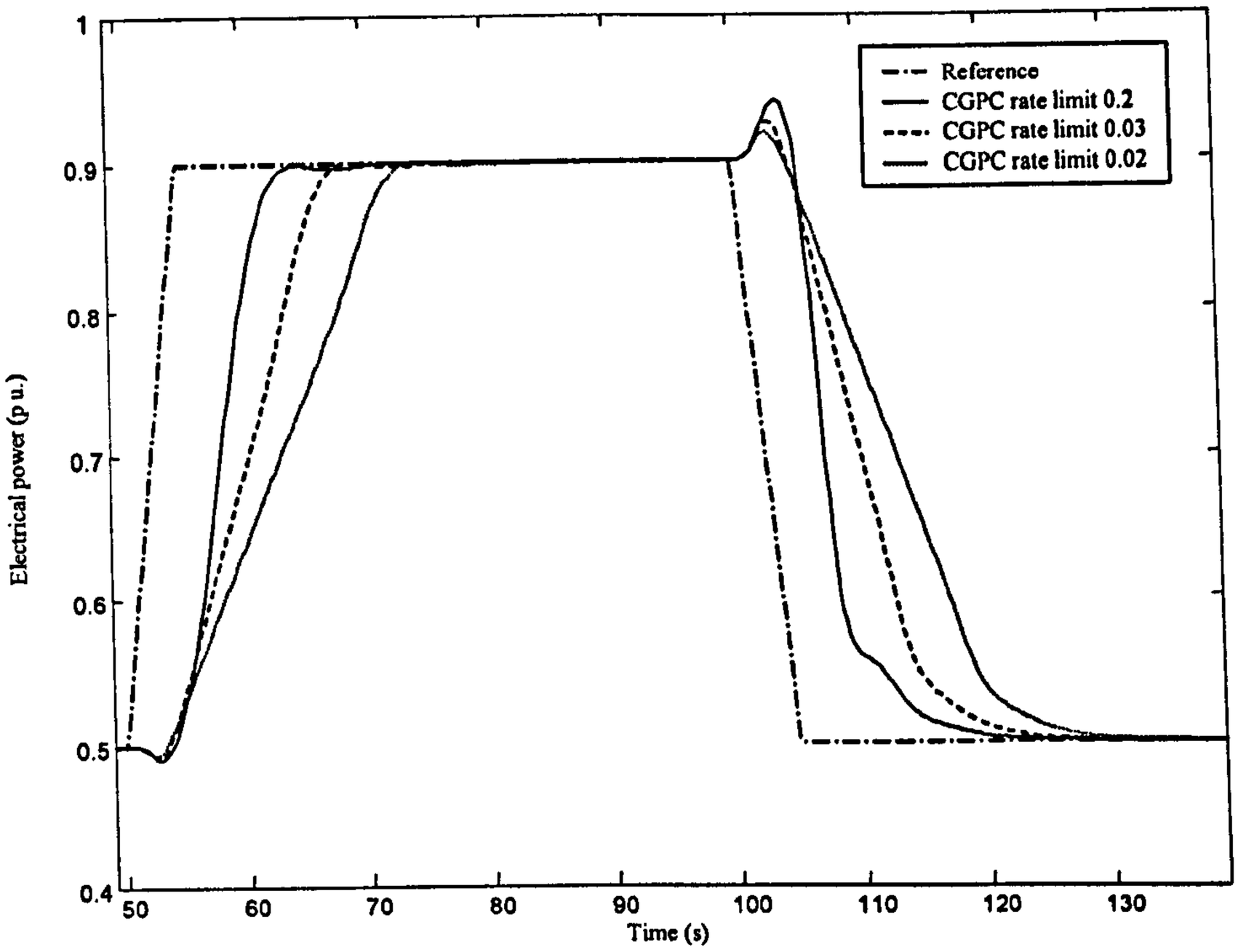


*Figure 6.17: Effects of different rate limits on large ramp response, six units operational.*

### 6.4.6. Response in automatic frequency control mode

Figure 6.18 shows the response of hydroelectric plant under PI and GPC controllers with six units operational and a power grid model based on the work of Jones and Mansoor [59]. As discussed in section 2.4.2, the grid model has a band-limited white noise input to simulate changes in the power reference target. As the power grid model has a sample period of 1/3s, the GPC controllers were retuned to fit this sample time. The parameters are chosen to match the step and ramp responses discussed in previous sections. For this simulation an ARMAX predictor [59], with prediction for 4 sample times ahead is used to produce a feed forward control, equation (6.7).

$$\Delta\hat{f}(k) = 2.19\Delta f(k-1) - 1.688\Delta f(k-2) + 0.5572\Delta f(k-3) - 0.07965\Delta f(k-4) \qquad (6.7)$$
$$+1.451e^{-7}\Delta P_e(k) + 4.362e^{-7}\Delta P_e(k-1) + 7.398e^{-7}\Delta P_e(k-2) + 9.697e^{-7}\Delta P_e(k-3) + e(k-1)$$

where:

$\Delta\hat{f}(k)$ is the predictive output, $\Delta f(k)$ is the output of the system, $\Delta P_e(k)$ is the input to the system (control signal) and $e(k)$ is the error between the predictive and output signals, all signals at the time $k$.

The hydroelectric plant has a better performance under GPC control; the responses follow the "noisy" reference closer than under PI control. As is shown in Table 6.6 the system under CGPC has lower values for ISE and IAE. The best performance is obtained when the predictor is used, 32% and 16% lower values in ISE and IAE, respectively, than PI.

*Table 6.6*

*Comparison of PI and GPC responses in automatic frequency control mode*

| | PI | CGPC | CGPC predictor |
|---|---|---|---|
| ISE | 0.0066 | 0.0057 | 0.0045 |
| IAE | 0.7858 | 0.7480 | 0.6639 |

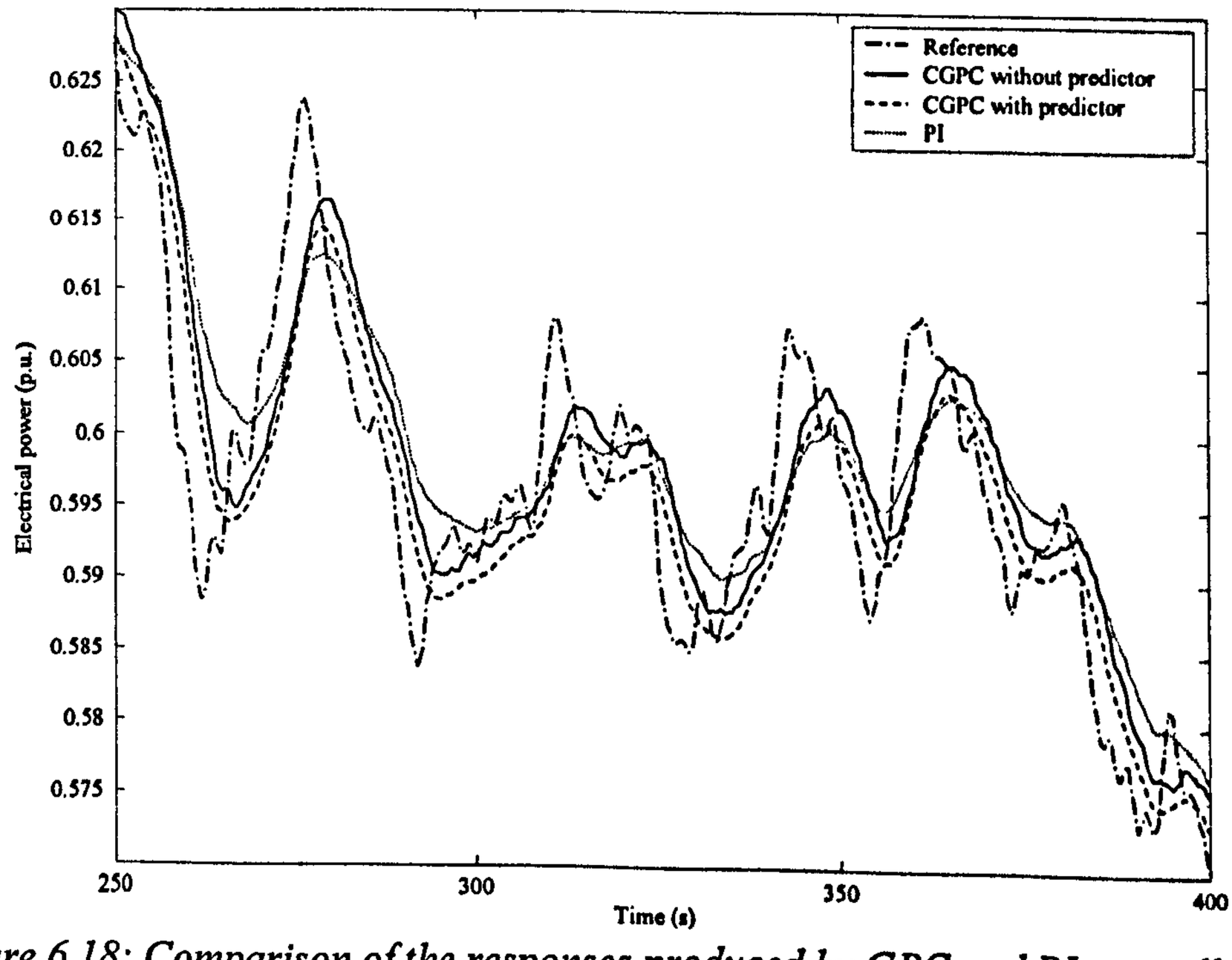


*Figure 6.18: Comparison of the responses produced by GPC and PI controllers in automatic frequency control mode with six units operational.*

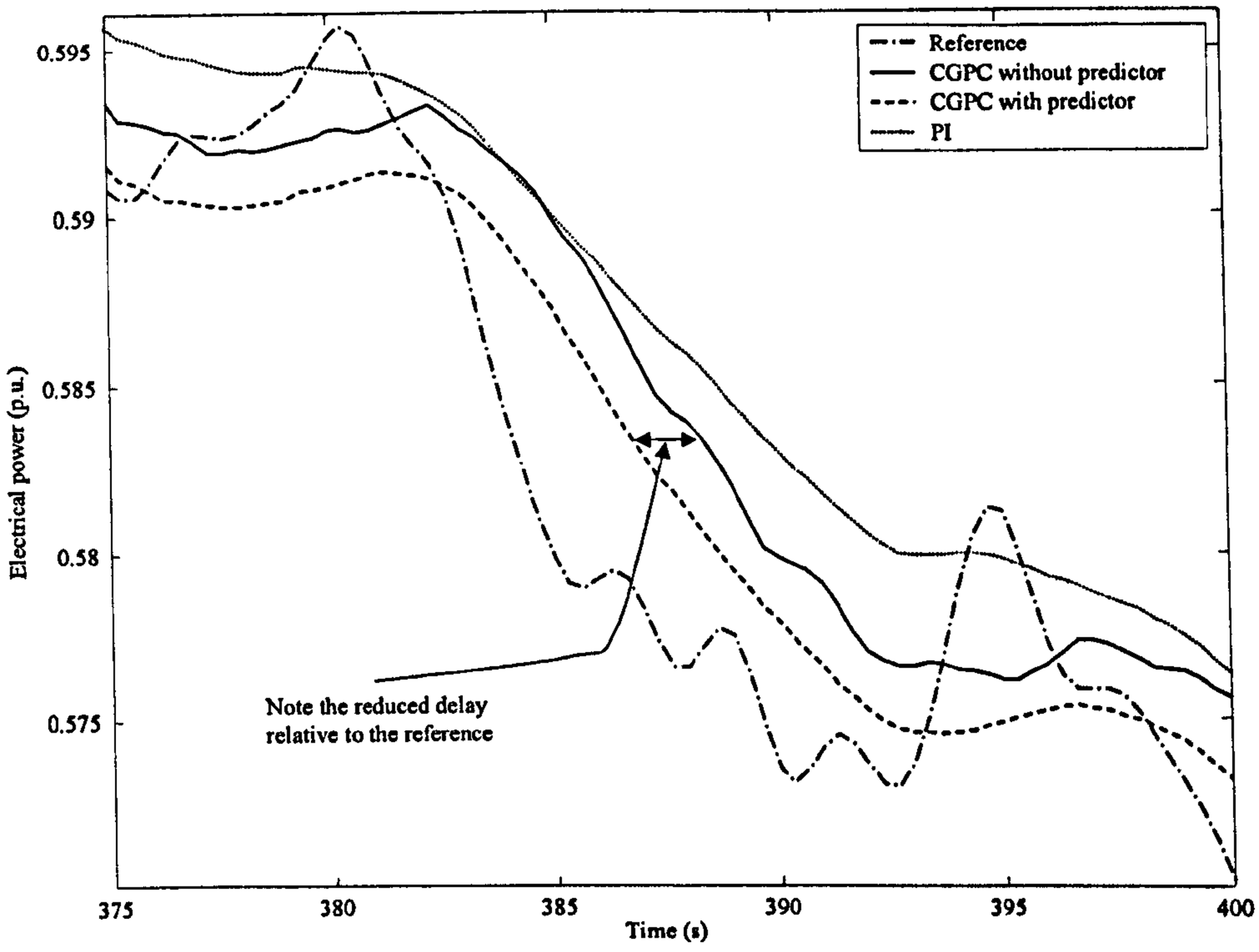


*Figure 6.19: Detail of the comparison of responses produced by GPC and PI controllers in automatic frequency control mode with six units operational.*

## 6.5 Conclusions

The basic question of whether GPC can improve the control of fast-response hydroelectric power stations has been answered positively in this chapter. Taking explicitly into account the multivariable nature of the plant improves both the direct and cross-coupled transient responses compared with PI control. Inclusion of a rate constraint in the GPC controller yields a fast and well-damped response in the common case when only a single Unit is in operation, without compromising stability when multiple Units are on-line.

Simulation has also shown that improved power delivery is obtained when the plant is operated in frequency control mode. The addition of reference feed-forward to the controller brings the response closer to the demanded target.

The sensitivity analysis has shown that both GPC and CGPC have better robustness to changes in the number of units active and variations in the hydraulic head than the

classic PI controller. This robustness feature is extremely important because of the varying conditions which occur during day-to-day operation. The hydraulic head, for instance, normally decreases during the day. Therefore, controllers that can cope with this diversity of operational conditions without losing their performance, such as GPC and CGPC, are very valuable. However, the fixed parameters GPC and CGPC have essentially the same limitations as the PI plus anti-windup. It can be said that a fixed parameter controller does not give optimum response across the operating envelope. In the following Chapter a variation of GPC that can use different models of prediction and different sets of tuning parameters, depending on the operation conditions, will be evaluated.

# Chapter 7

# MLD-GPC control for a nonlinear MIMO model

## 7.1. Introduction

In earlier chapters different control approaches for Dinorwig have been evaluated. Figure 7.1 summarises their principal features and also presents, in the highlighted block to the right, the main characteristics of the evaluation to be performed in this chapter. The principal addition is the ability of the controller, a form of open-loop adaptive controller, to change with the operational conditions, and to integrate logic rules.

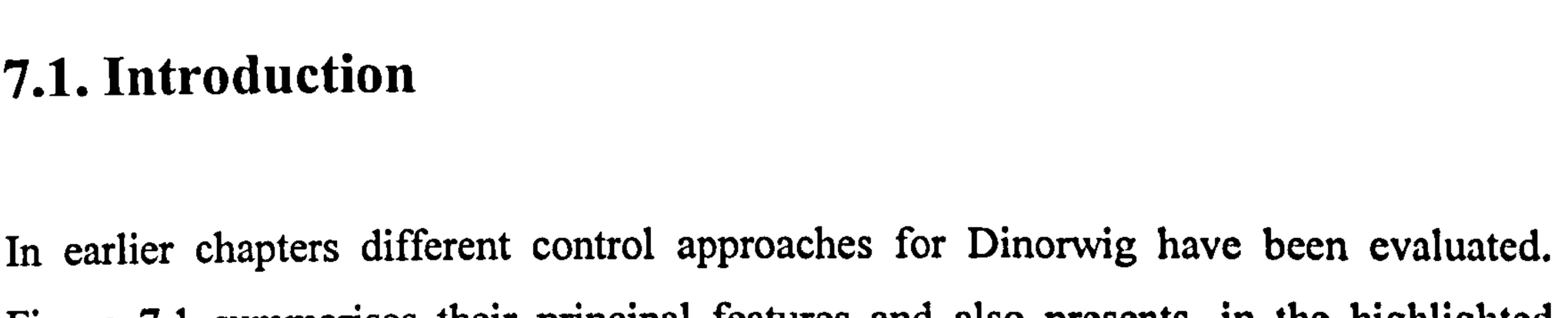


*Figure 7.1: Evolution of the control proposal for Dinorwig.*

Fixed linearised models have limited validity but are useful for control studies, design and tuning. Nonlinear models have the accuracy required for plant simulation but are computationally demanding, which poses a difficulty for real-time implementation. Mixed Logical Dynamical (MLD) provides an intermediate option that has good accuracy but low computational demand and it is a suitable choice as the model of prediction for predictive controllers.

This chapter begins with a brief introduction to Mixed Logical Dynamical systems in section 7.2, and then the MLD model of the hydroelectric station is discussed in section 7.3. It is followed by comparison of the MLD model with the nonlinear nonelastic model of the hydroelectric plant, section 7.4. After that the behaviour of the plant under Generalised Predictive Control with constraints (CGPC) and MLD-GPC are analysed in section 7.5. These results show the improved response provided by MLD-GPC. Section 7.6 is a brief description of how MLD can represent high-level rules in the optimisation of power plant. Finally some conclusions are drawn.

## 7.2. MLD theory

Mixed logical dynamical systems can be described by linear dynamic equations subject to linear mixed-integer inequalities [60]. These inequalities can involve continuous and binary (logical) variables. MLD is capable of representing a great variety of systems, such as hybrid systems, finite state machines, constrained linear systems and nonlinear systems using piecewise linear functions to represent the nonlinearities [61].

### 7.2.1. Hybrid systems

Hybrid systems are hierarchical systems, being composed of dynamical components at the lower level which are governed by logical/discrete components at the upper level [60, 62-64]. Hybrid systems can be used in a large number of industrial and small scale applications. Traditionally, there are two paradigms to deal with hybrid systems: aggregation and continuation. However some unified frameworks have appeared recently [60, 63]. The aggregation paradigm treats the entire system as a finite automaton or discrete-event dynamic system. It is common in this theory to partition the continuous state space and consider only the aggregate dynamics from cell to cell in the

partition. The continuous paradigm treats the whole system as a differential equation. This can be done by two techniques: Simulating the discrete actions by means of nonlinear ordinary differential equations or treating the discrete actions as disturbances of the differential equations that represent the system. The unified frameworks, such as MLD, aim to capture both discrete and continuous features to allow the designer free movement between analogue and discrete domains [60, 63].

### 7.2.2 Integer programming

Integer programming has been proved as an efficient method to translate logical problems to linear mixed-integer inequalities [65-67]. These inequalities are useful to model logical parts of processes and heuristic knowledge about plant operation; they are an important feature of MLD. Propositional logic problems are represented by inequalities of logical integer variables ($\delta_i$) as in (7.1).

$$\begin{aligned} &X_1 \vee X_2 \Rightarrow \delta_1 + \delta_2 \geq 1 \\ &X_1 \wedge X_2 \Rightarrow \delta_1 = 1, \delta_2 = 1 \\ &X_1 \oplus X_2 \Rightarrow \delta_1 + \delta_2 = 1 \end{aligned} \tag{7.1}$$

where $X_1$ and $X_2$ are logical variables (true or false) and $\delta_1$ and $\delta_2$ are integer variables (0 or 1). A complete set has been stated by Cavalier *et al* [65].

### 7.2.3 Example of a MLD system

To illustrate the characteristics of MLD, let us consider a simple linearised model of the hydraulic subsystem of Dinorwig consisting of only two units, with identical transfer function $G_j(s)$ relating changes in output ($\Delta P_{mech}$) to guide vane opening ($\Delta G$). Although the dynamic cross-coupling is not modelled, the hydraulic coupling does appear as the change in operating condition and hence $T_{wti}$.

$$G_j(s) = \frac{\Delta P_{mech}(s)}{\Delta G(s)} = \frac{A_t(1 - G_0 T_{wt1} s)}{\left(1 + \frac{G_0 T_{wt1}}{2} s\right)} \tag{7.2}$$

In (7.2), the turbine gain, $A_t$, has a nonlinear dependence on $h$ (hydraulic head).

$$A_t = \begin{cases} 1.18 & if \quad 1.00 \geq h > 0.95 \\ 1.05 & if \quad 0.95 \geq h \geq 0.90 \end{cases} \tag{7.3}$$

$T_{wti}$ is the water starting time of the main tunnel and a single penstock and it has a dependence on the number of units active ($U_o$).

$$T_{wti} = \begin{cases} 0.695 & if \quad U_o = 1 \\ 1.083 & if \quad U_o = 2 \end{cases} \tag{7.4}$$

$G_o$ is the operating point and typically varies from 0.5 to 0.95 for an active unit. In order to keep this example simple a fixed value of 0.9 will be considered. Now defining the following integer variables:

$$p_1 = \begin{cases} 0 & if \quad U_o = 1 \\ 1 & if \quad U_o = 2 \end{cases} \tag{7.5a}$$

$$p_2 = \begin{cases} 0 & if \quad 0.95 \geq h \geq 0.90 \\ 1 & if \quad 1.00 \geq h > 0.95 \end{cases}. \tag{7.5b}$$

If the following integer variables are defined:

$$\begin{aligned} \delta_1 &= 1 \quad if \quad p_1 = 0 \wedge p_2 = 0 \\ \delta_2 &= 1 \quad if \quad p_1 = 0 \wedge p_2 = 1 \\ \delta_3 &= 1 \quad if \quad p_1 = 1 \wedge p_2 = 0 \\ \delta_4 &= 1 \quad if \quad p_1 = 1 \wedge p_2 = 1 , \end{aligned} \tag{7.5c}$$

there follows the condition:

$$\bigoplus_{i=1}^{4} [\delta_i = 1].$$

By defining: $\Delta P_{mech}(s)=Y(s)$ and $\Delta G(s)=u(s)$

the system (7.2) can be described as a MLD system in discrete time with $T$=0.25, see equation (7.6).

$$y_j(k) = \sum_{i=1}^{4} z_i(k) \tag{7.6a}$$

where the auxiliary variable $z_i(k)$ is defined by:

$$\begin{aligned} z_1(k) &= 0.45y(k-1) - 2.10u(k) + 2.68u(k-1) \quad if \quad \delta_1 = 1 \\ z_2(k) &= 0.60y(k-1) - 2.10u(k) + 2.52u(k-1) \quad if \quad \delta_2 = 1 \\ z_3(k) &= 0.45y(k-1) - 2.36u(k) + 3.01u(k-1) \quad if \quad \delta_3 = 1 \\ z_4(k) &= 0.60y(k-1) - 2.36u(k) + 2.83u(k-1) \quad if \quad \delta_4 = 1 \end{aligned} \tag{7.6b}$$

under the following constraints:

$$z_i(k) \leq M\delta_i \qquad z_i(k) \geq m\delta_i \tag{7.6c}$$

where $M$=1 is the maximum value of $y(k)$ and $m$=0 is the minimum value of $y(k)$ [60].

For example, if $h$=0.94 and $U_o$=2 then $\delta_3$=1

and

$$z_1(k)=0$$
$$z_2(k)=0$$
$$z_3(k)=0.45y(k-1)-2.36u(k)+3.01u(k-1)$$
$$z_4(k)=0$$

then $y_{1,2}(k)=0.45y(k-1)-2.36u(k)+3.01u(k-1)$

where $1\geq y_{1,2}(k)\geq 0$.

On the other hand, if $h$=0.91 and $U_o$=1, then: $\delta_1$=1

and

$$z_1(k)=0.45y(k-1)-2.10u(k)+2.68u(k-1)$$
$$z_2(k)=0$$
$$z_3(k)=0$$
$$z_4(k)=0$$

then
$$y_1(k)=0.45y(k-1)-2.10u(k)+2.68u(k-1)$$
$$y_2(k)=0$$

where $1\geq y_1(k)\geq 0$.

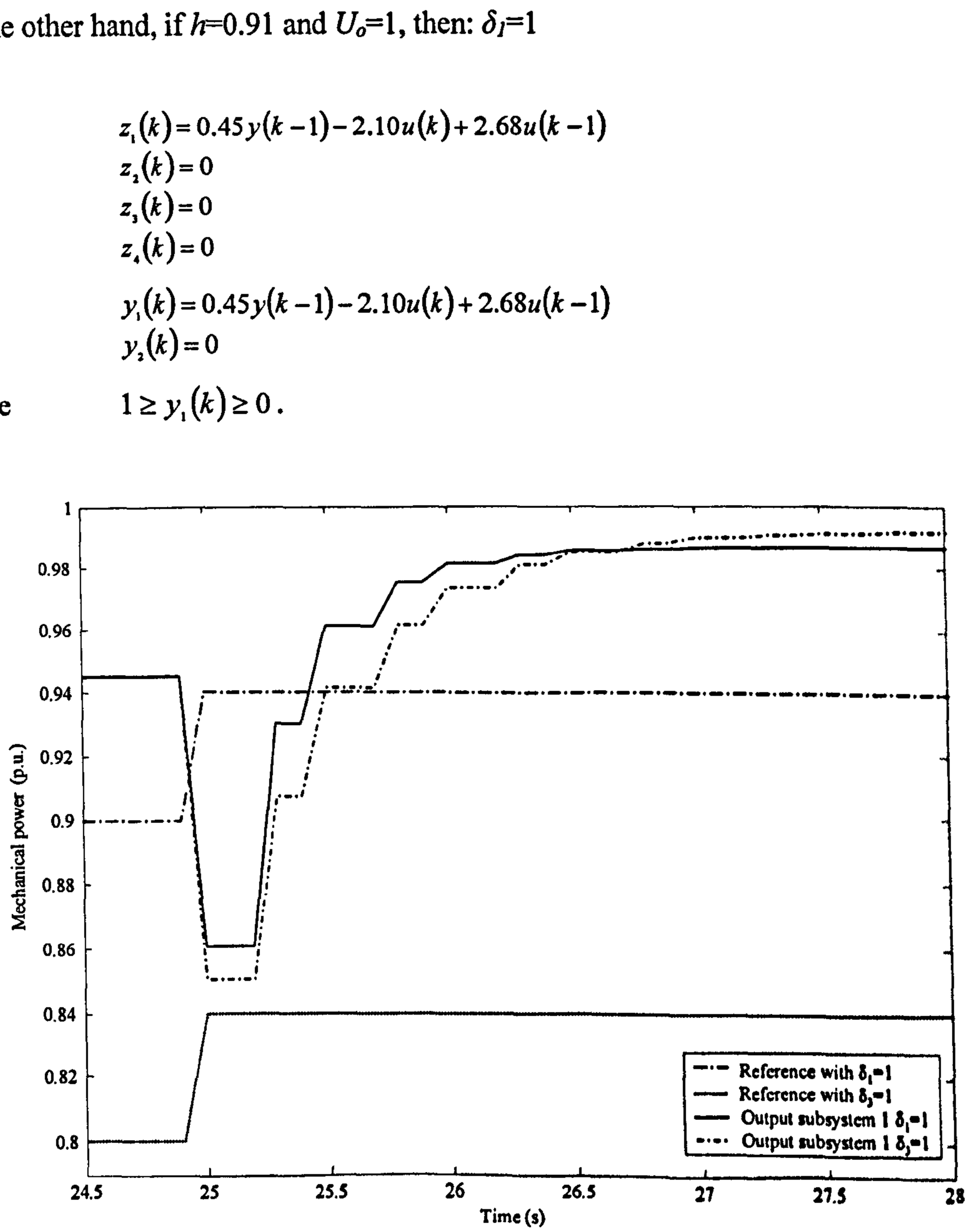


*Figure 7.2: Open loop step response of example for different operational conditions.*

The system is described differently, depending on the value of $\delta_i$. This is illustrated in Figure 7.2, where the open loop step responses of unit 1 when $\delta_1$=1 and $\delta_3$=1 are shown.

Two different values of reference were used to fix the subsystem at the same initial output power, then a small step of 0.04 p.u. was applied at t=25s. When $\delta_1$=1 there is only one unit active and the lower hydraulic head causes a lower open loop gain and hence a lower final value. When $\delta_3$=1 the hydraulic head is higher and both units are active. This increases the water starting time and the system has a longer time constant, so the response is slower. In the next section the model of the power plant including the guide vane and hydraulic subsystems will be presented and evaluated for one to six units operational.

## 7.3 MLD predictive model

### 7.3.1 Description of the MLD predictive model

In this section, a predictive model to be used in the GPC controller is set up using the MLD method. The heart of the model is the MIMO linear model discussed in section 2.2.1.2.

By defining:

$$\delta_i = 1 \leftrightarrow U_0 = i \forall i = 1,...,6 \tag{7.7}$$

where $\bigoplus_{i=1}^{6} [\delta_i = 1]$.

The first three cases of the piecewise linear model of the hydroelectric plant are:

$$Y(s) = \begin{cases} G_1(s)U(s) & if \quad \delta_1 = 1 \\ \begin{bmatrix} G_2(s) & X_2(s) \\ X_2(s) & G_2(s) \end{bmatrix} U(s) & if \quad \delta_2 = 1 \\ \begin{bmatrix} G_3(s) & X_3(s) & X_3(s) \\ X_3(s) & G_3(s) & X_3(s) \\ X_3(s) & X_3(s) & G_3(s) \end{bmatrix} U(s) & if \quad \delta_3 = 1 \end{cases} \tag{7.8}$$

where $G_i(s)$ and $X_i(s)$ are, respectively, the direct and cross-coupling transfer functions, which vary according to the operating point ($O_p$) and the number of units active ($U_o$), according to Table 2.1, section 2.2.1.2, where

$$G_i(s) = f(U_o, O_p) \text{ and } X_i(s) = f(U_o, O_p).$$

There are computational benefits in keeping the model as a piecewise representation [60, 66] because it needs fewer logical variables than the full MLD model and the logic is less complex.

### 7.3.2 Evaluation of the MLD predictive model

Several simulations were carried out in order to determine the accuracy of the predictions made by the MLD model. The nonlinear nonelastic model was taken as a basis of comparison. The output of the linear MIMO model which, it will be recalled, was fixed at the six units operational case, is also shown. The relationship between the nonlinear nonelastic model and the full nonlinear model has been discussed previously (sections 2.2 and 2.6).

Figure 7.4 shows the open loop responses of the hydraulic models, including guide vanes, when a 0.04 p.u. step is applied with the operating point fixed to 0.8 p.u. Figures 7.4-a and 7.4-b show the responses with one unit operational and six units operational, respectively. In both graphs the response of the MLD model is a good approximation to the response of the non-linear model. Note that the models have a different behaviour depending on the number of units active. With six units operational both linear model have exactly the same response, as expected. The NMP characteristic is more marked in both linear cases; this and other differences between the models are mainly because the linear models are not taking into account other factors, such as friction losses.

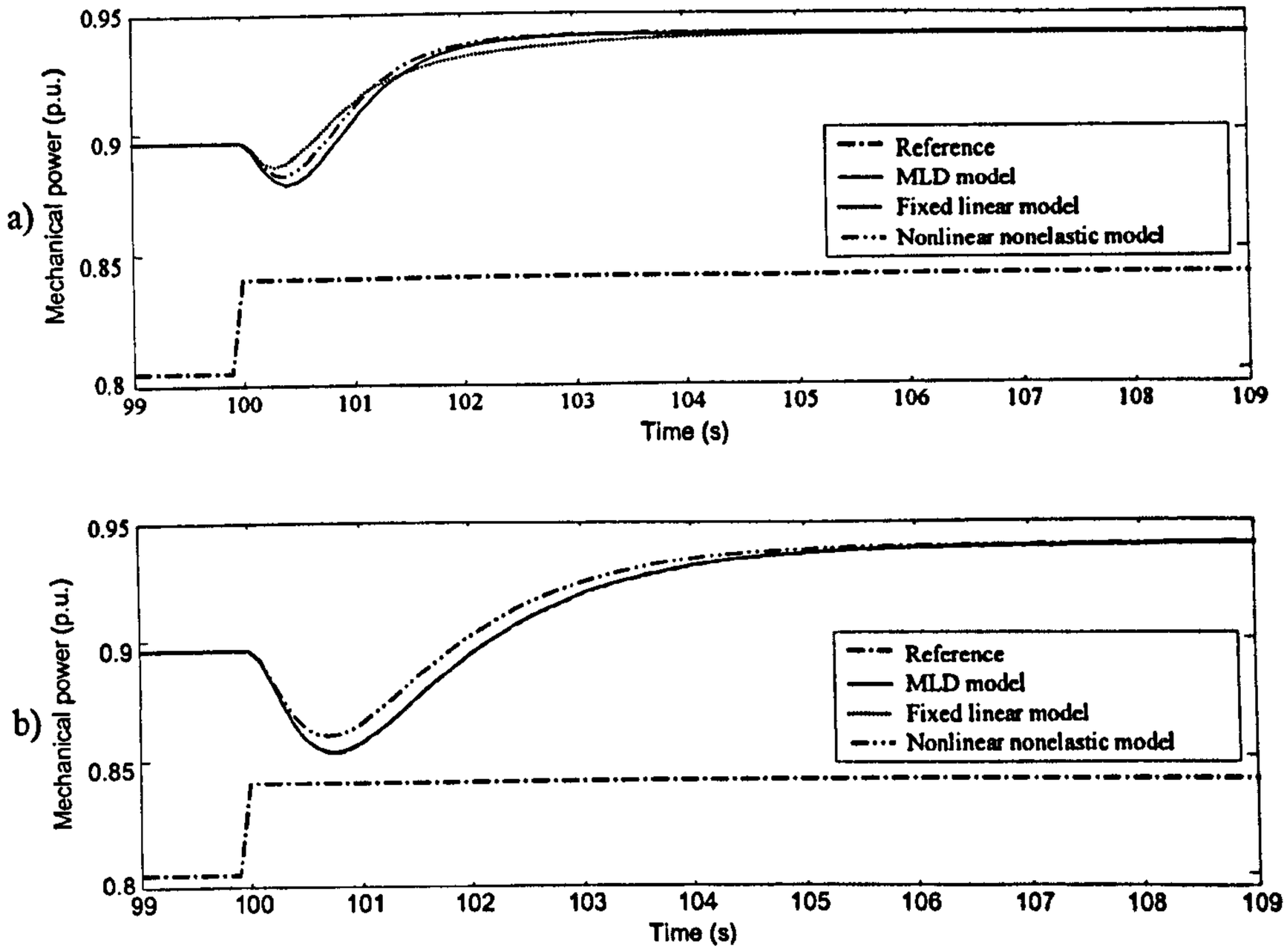


*Figure 7.4: Open loop step response of MLD and non-linear models with 0.8 as operating point: (a) one unit operational, (b) six units operational.*

Nevertheless, the MLD model has better or equal performance to the fixed linear model and it follows the non-linear model accurately, regardless of the number of units active. This adaptive characteristic is extremely important when a controller is designed to maintain the same performance under different operational conditions.

The direct and cross-coupling step responses of the MLD and non-linear models are shown in Figure 7.5. The upper graph shows the response of unit 1 and in the lower graph is shown the response of units 2-6 in synchrony. The simulation first establishes an operating point of 0.76 p.u. for all units, then a step of 0.04 is applied to unit one at 100 seconds of simulation, followed by a step of the same amplitude applied to units 2-6 at 110 seconds. As can be seen from Figure 7.5 the responses of the models are comparable with best agreement occurring, as expected, for the case of 6 units active, which was the case chosen for linearisation.

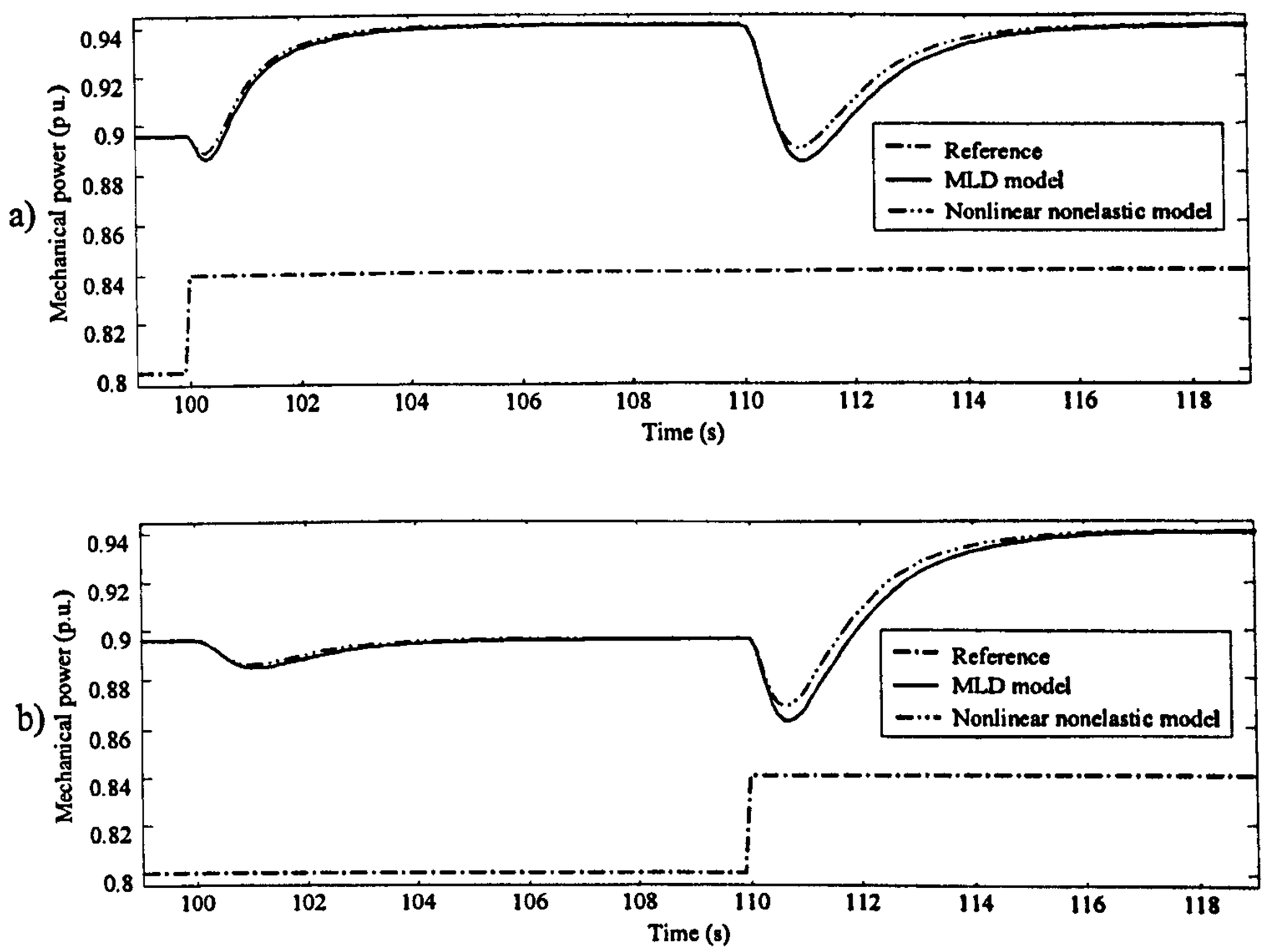


*Figure 7.5: Direct and cross-coupling step response: (a) response of unit 1, (b) response of units 2-6.*

In order to show how the MLD model adapts according to the number of units active, a simulation that involves large and small step responses was developed, Figure 7.6. Unit 1 is set to 0.8 p.u. at t=5s, units 2-6 being inactive. At t=25s a 0.1 p.u. step is applied to Unit 1. Units 2 and 3 are turned on at t=50s and at the same time Unit 1 is set back to 0.8. A 0.1 step is then applied to units 1 to 3. This pattern is repeated when units 4-6 are turned on at 100 seconds of simulation.

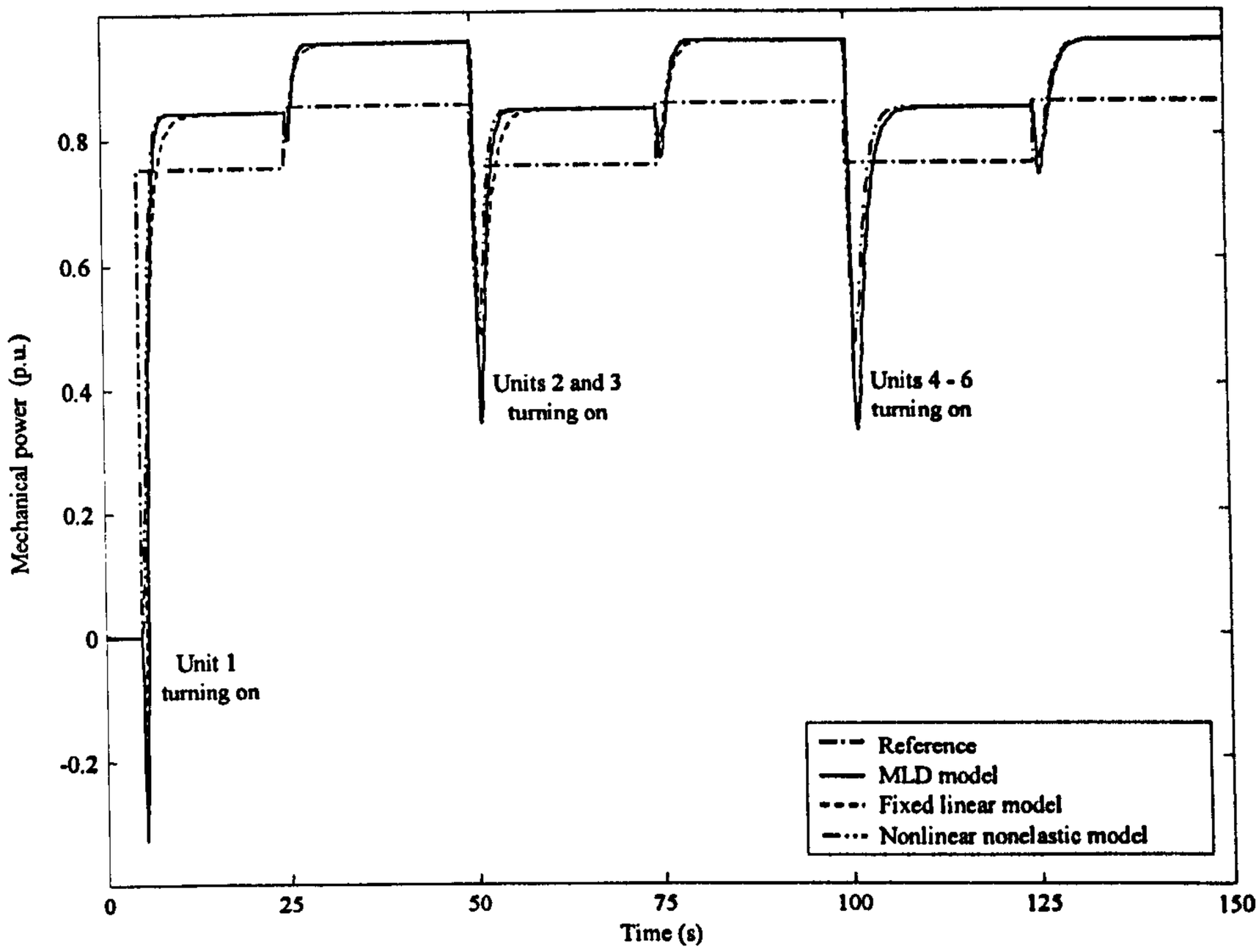


*Figure 7.6: Open loop step response of MLD and non-linear models with different units operational.*

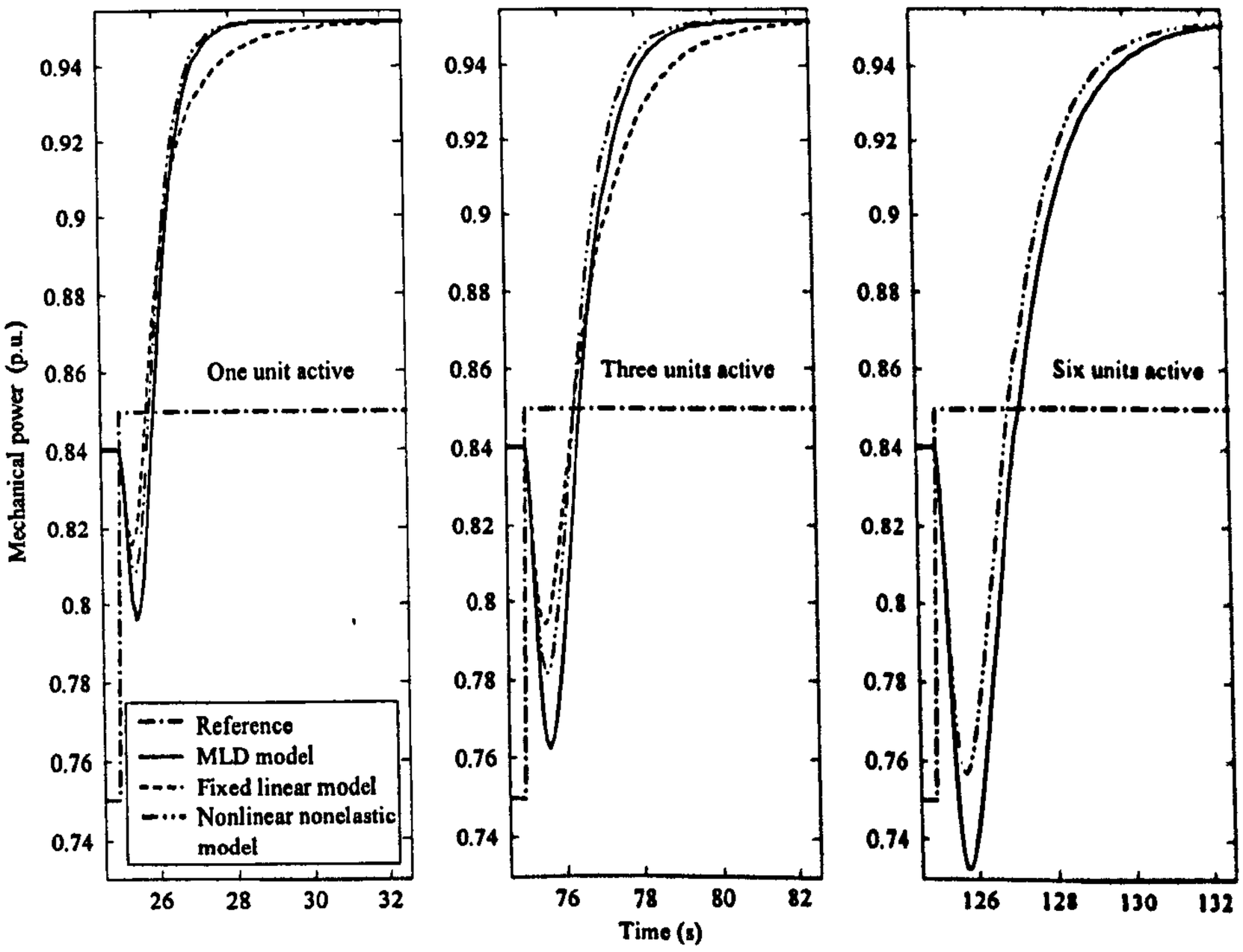


*Figure 7.7. Detail of the open loop small step response of MLD and non-linear models with different units operational.*

As can be seen from Figure 7.7 the response of the fixed linear model deviates more from the reference than does the MLD model's response. The MLD linear model has approximately the same accuracy in all cases. The MLD model could also modify its response to take into account changes to the operating point (*i.e.* the load) of a single turbine, but it was found that the improvement was negligible.

Figure 7.8 shows the detail of the cross coupling response of unit 1 when other units are starting. The undershoot of the MLD model response is bigger, but after a few seconds it moves close to the response of the nonlinear model.

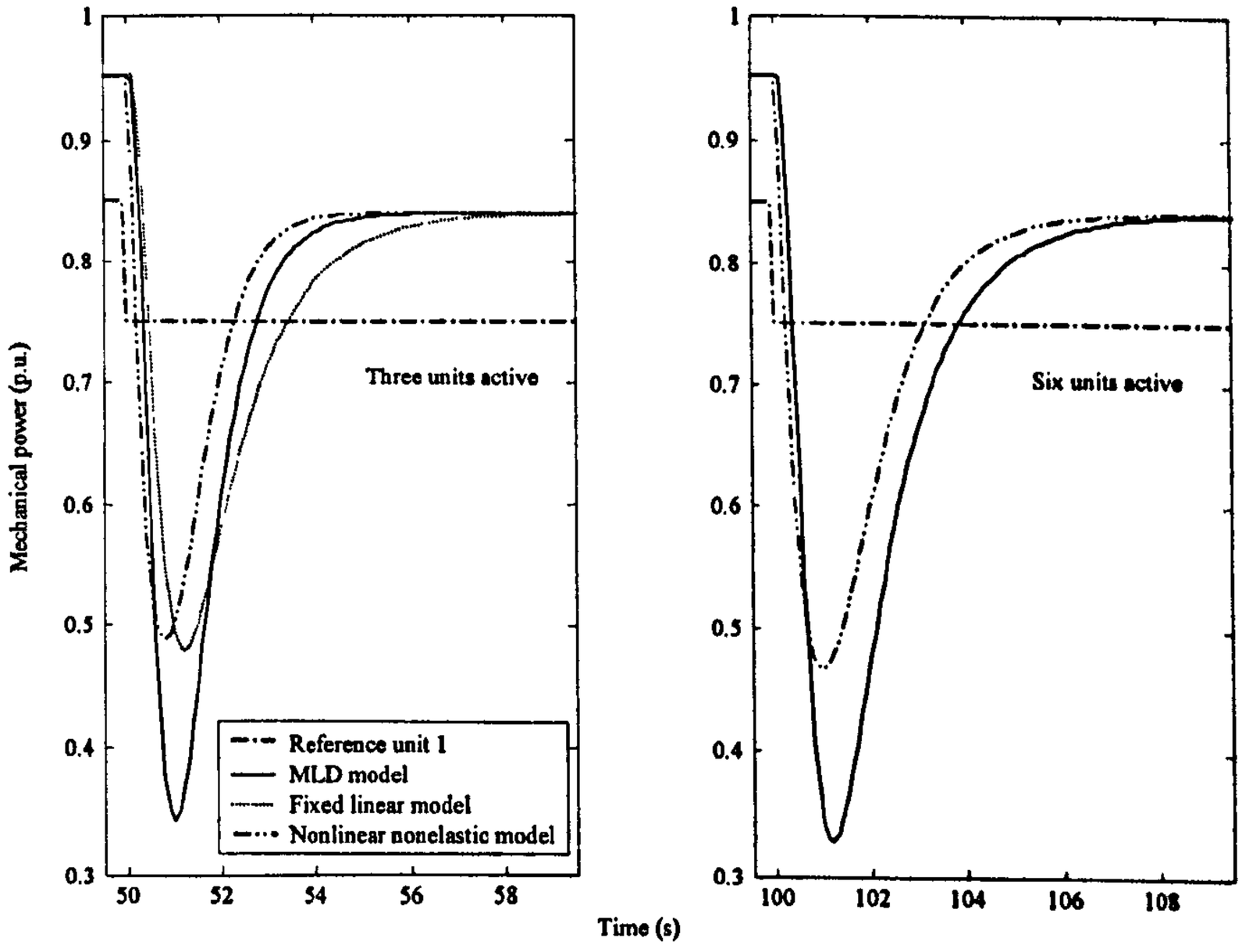


*Figure 7.8. Detail of the cross-coupling response of MLD and non-linear models with different units operational.*

# 7.4 Model Based Predictive Control using the MLD model for prediction

## 7.4.1 Predictive control of MLD systems

Model Based Predictive Control (MBPC) has to calculate the future output and control signals of the plant at every step of iteration; different MBPC approaches use different types of models of the plant to obtain these predictions. For example Generalised Predictive Control (GPC) uses a CARIMA representation of the plant and Dynamic

Matrix Control (DMC) uses the step response to model the plant [30]. Hybrid systems have been used as the model of the plant in some MBPC approaches. Branicky *et al* [63] proposed using an hybrid model to represent dynamic systems together with discrete phenomena, based on an analogy of finite automata with variable state systems. Bemporad and Morari [60] have used MLD models to represent plants and discrete (qualitative and quantitative) inputs and outputs as a part of MPC control. Applications of MLD or equivalent models to controlling or monitoring power systems have recently appeared. Lu [68] has applied hybrid control to a hydroturbine-generator set. Thomas *et al* [69] have used a MLD framework for fault detection in the sensors of a steam generator.

In this chapter a MLD model is considered as the model of prediction for GPC while the plant is now modelled using the nonlinear elastic representation of section 2.2.3. The MLD model produces a piecewise CARIMA model, whose exact structure and value depends on the number of units active. The MLD model also depends on the operating point but it was found that including this feature increased the computation significantly while providing little benefit in terms of improved accuracy.

### 7.4.2 Applying a MLD-GPC to the hydroelectric station

Because the MLD model is a better representation of the plant, it allows a lower horizon of prediction ($N$) to be used, thus decreasing the computational effort. Lower values of the weight control factor ($\lambda$) can be selected too, which accelerates the response of the system. The MLD-GPC was tuned with $N$=10 (horizon of prediction), $N_u$=10 (horizon of control) and $\alpha$=0 (weight factor on the reference trajectory).

The $\lambda$ value was tuned by gain scheduling. A value of $\lambda$=40 was selected for one unit operational, linearly incrementing by 3, per unit active, up to $\lambda$=55 for six units operational. The same constraint limits were employed for CGPC as in Chapters 5 and 6.

The MLD-GPC was compared with the constrained GPC (CGPC) as previously described in Chapter 6. Recall that this has the fixed linear model for prediction and was tuned with $N$=40, $N_u$=10, $\lambda$=250 and $\alpha$=0. Figure 7.9 shows the response of the full nonlinear model of Dinorwig [3] to a large step (0.3 p.u.) under both controllers. The

upper graph shows the six units operational and the lower shows the one unit operational case; in both cases MLD-GPC is faster. The better prediction of the MLD model allows the controller to be tuned with lower values of $\lambda$. As a result the controller can use more gain in the control loop thus increasing the speed of the response. CGPC was tuned for the case of six units operational and, as can be seen from Figures 7.9 and 7.10, it is in this case that CGPC performs best.

Figure 7.9 shows the response of the plant to a small step (0.04 p.u.). Here, the MLD-GPC is faster than CGPC in the one unit operational (lower graphic) case. The responses for six units operational are similar. The primary response of the system using MLD-GPC was 5.4 s, while the system using CGPC has a primary response of 8.45 s, a substantial improvement.

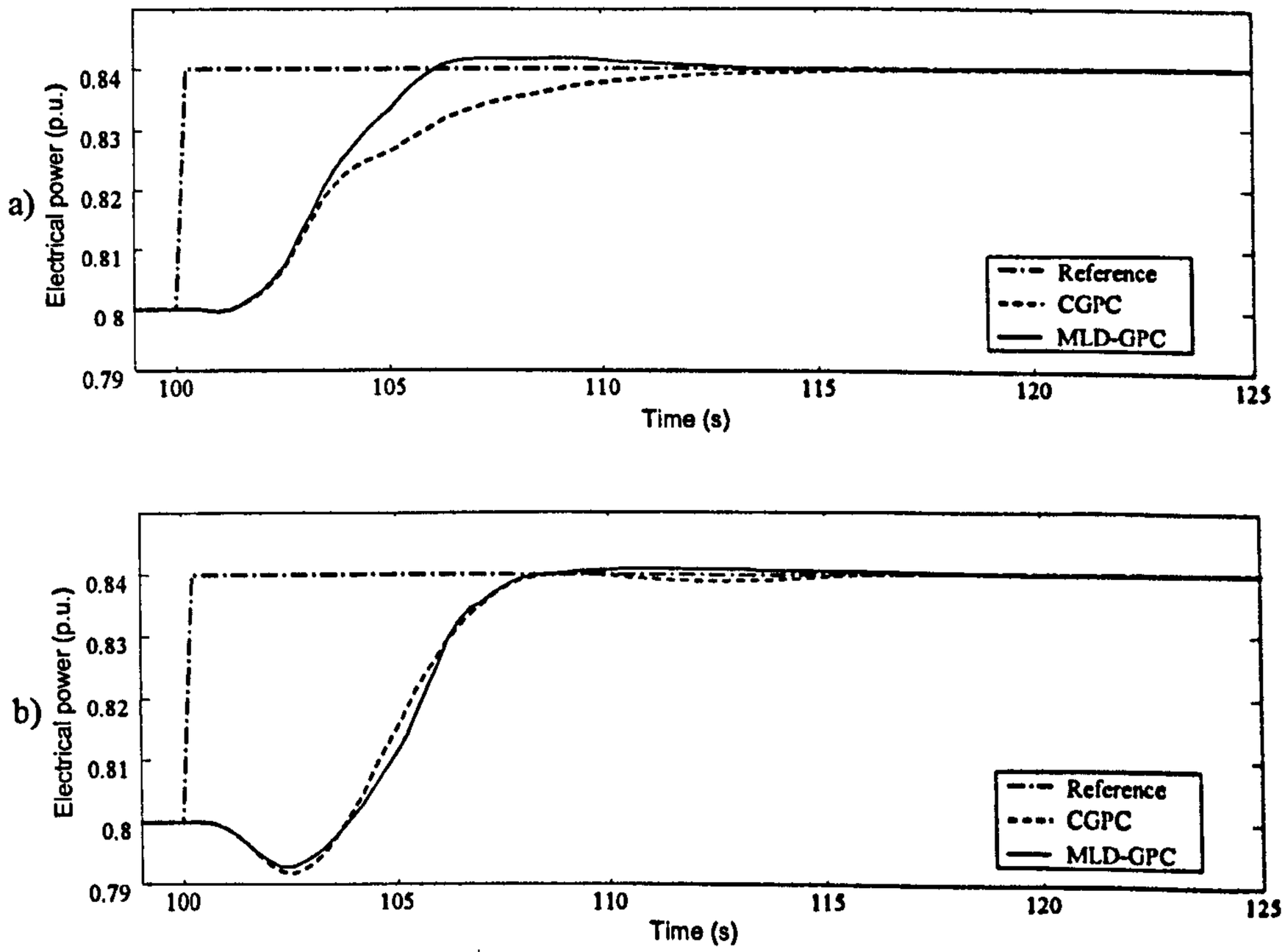


*Figure 7.9: Small step response for six and one unit operational: (a) one unit operational, (b) six units operational.*

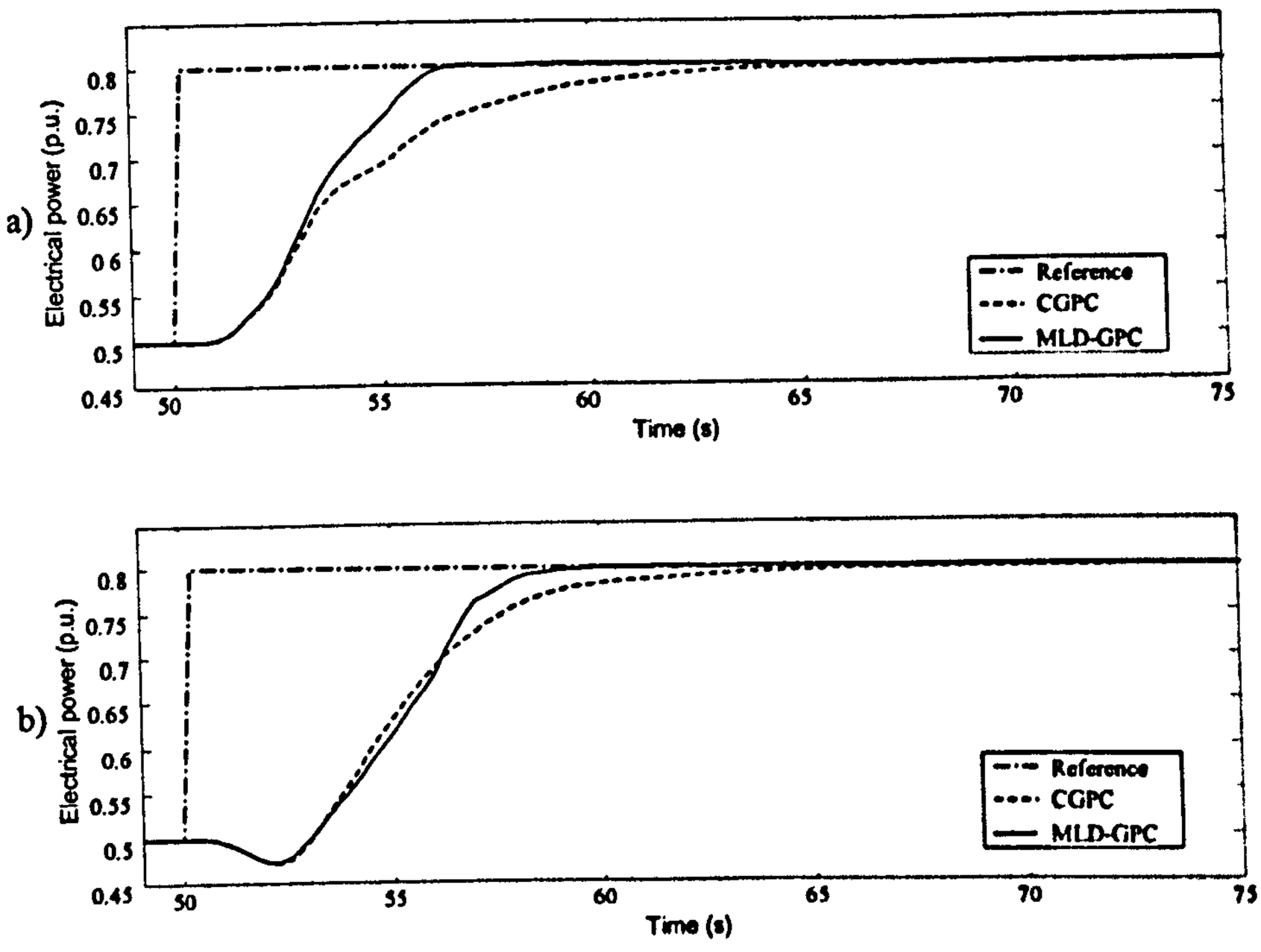


*Figure 7.10: Large step response for six and one unit operational: (a) one unit operational, (b) six units operational.*

Figure 7.11 shows the responses of the system when a large ramp signal is applied; once more the MLD-GPC is faster than the CGPC controller.

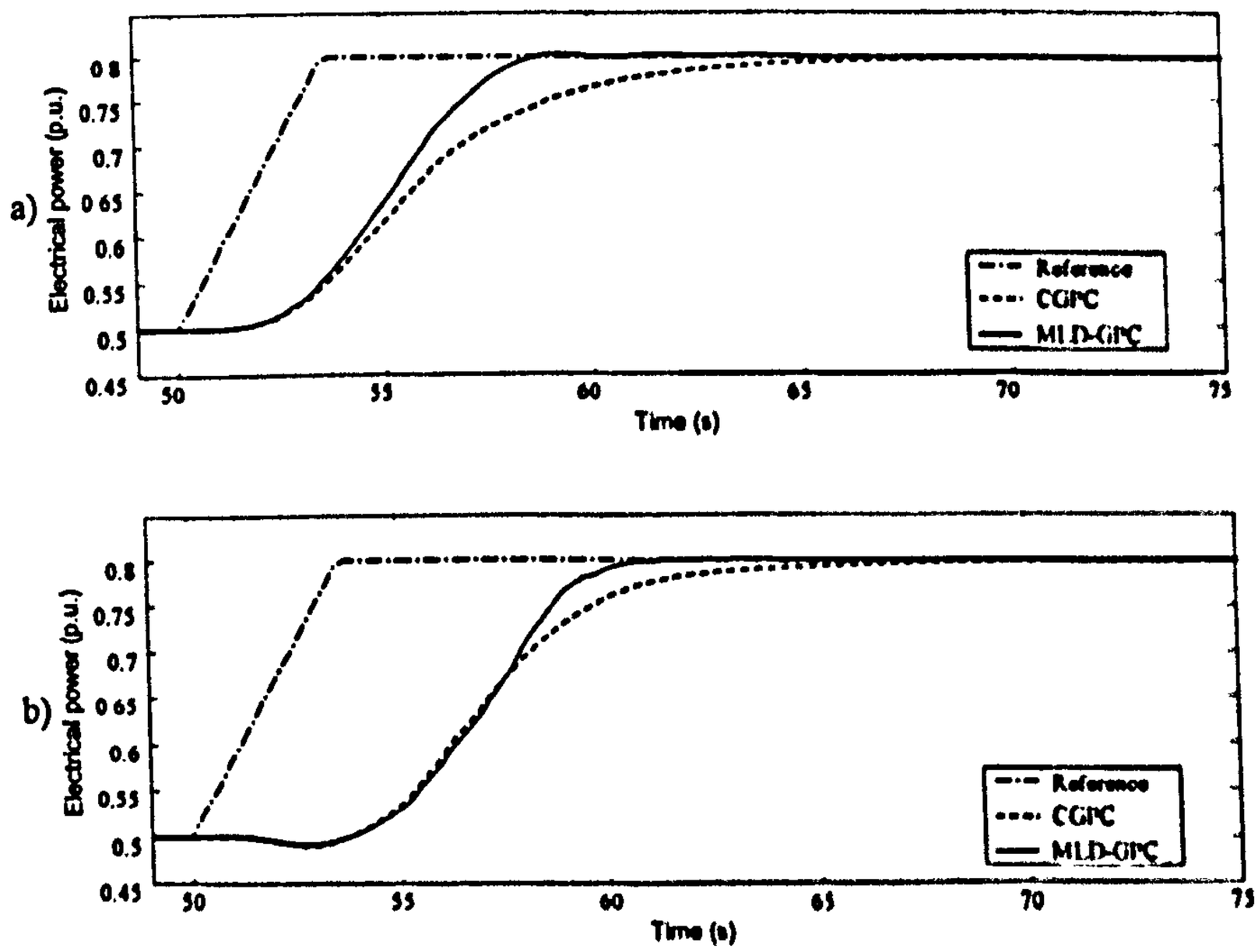


*Figure 7.11: Large ramp response for six and one unit operational: (a) one unit operational, (b) six units operational.*

If CGPC is re-tuned to reach the same performance as the MLD-GPC when one unit is operational, then a poorly damped response is produced when six units are operational. The damping can be restored by increasing or relaxing the constraints but this leads to a gain scheduled approach similar to the MLD-GPC. Figure 7.13 illustrates this behaviour. A re-tuned CGPC controller, which has a reduced value of lambda and its other tuning parameters at their original values, is compared with the original CGPC and the MLD-GPC controllers. A small step of 0.04 p.u. was applied to the system at 0.8 initial operating point. As can be seen from Figure 7.13 a, the re-tuned CGPC produces a decaying oscillatory response. Figure 7.13 c and b show the corresponding control signals. The control signals produced by CGPC when $\lambda$ =175 produces rapid changes that could cause premature fatigue to the guide vane.

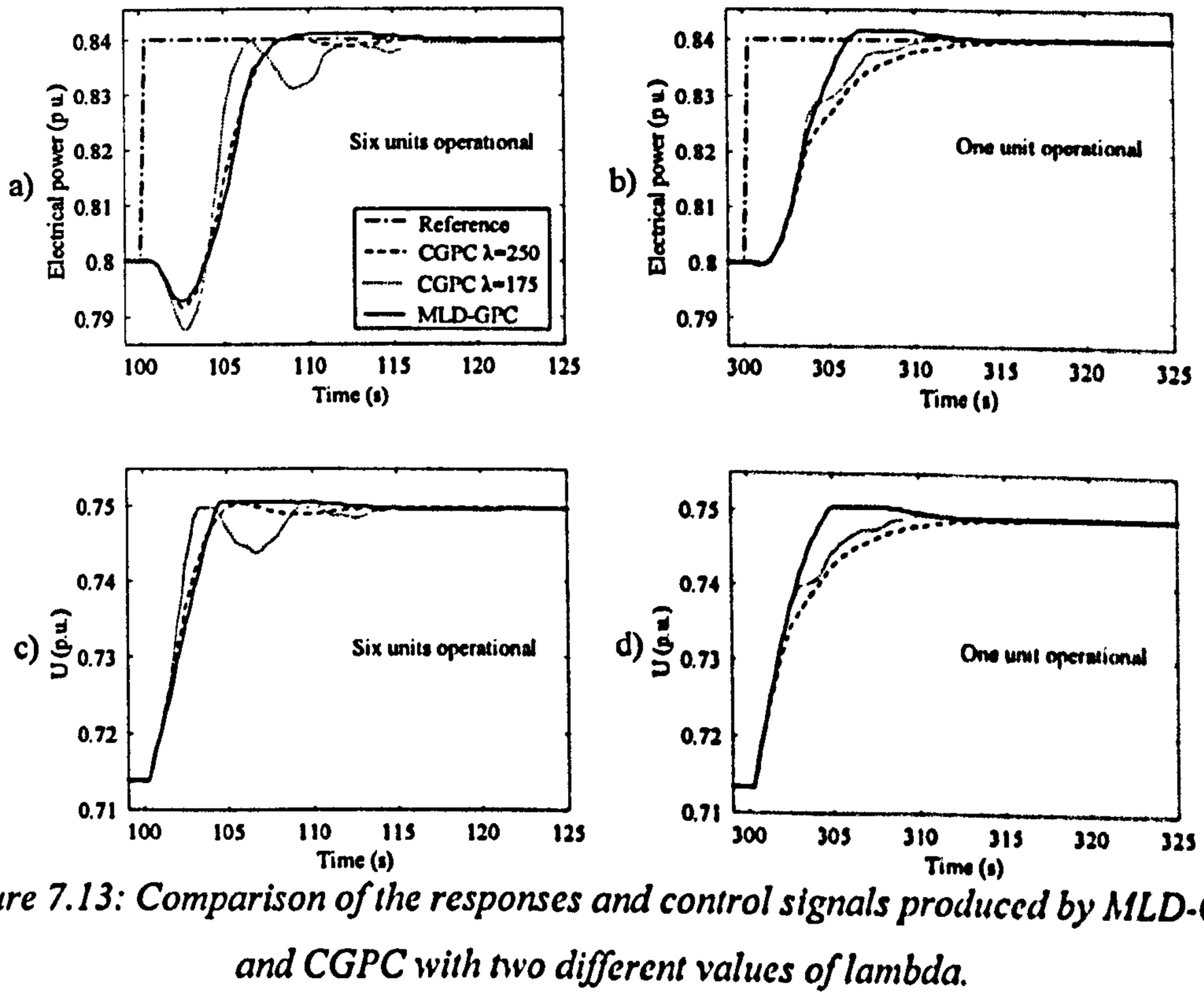


*Figure 7.13: Comparison of the responses and control signals produced by MLD-GPC and CGPC with two different values of lambda.*

As in Chapter 6, the frequency-control response of the hydroelectric plant under MLD-GPC and CGPC controllers with six units operational and a power grid model was evaluated [11]. The GPC controllers were retuned to fit this sample time of the grid model (1/3s). Again, the parameters were chosen to match the step and ramp responses as discussed previously. The responses of the system under both controllers are very similar, Figures 7.14 and 7.15. This performance was expected because the small step

and ramp responses are similar with six units operational, which was the case evaluated in this simulation. Also they are using the same droop gain (0.01), the parameter that defines the rate at which the unit picks up or sheds load relative to other units.

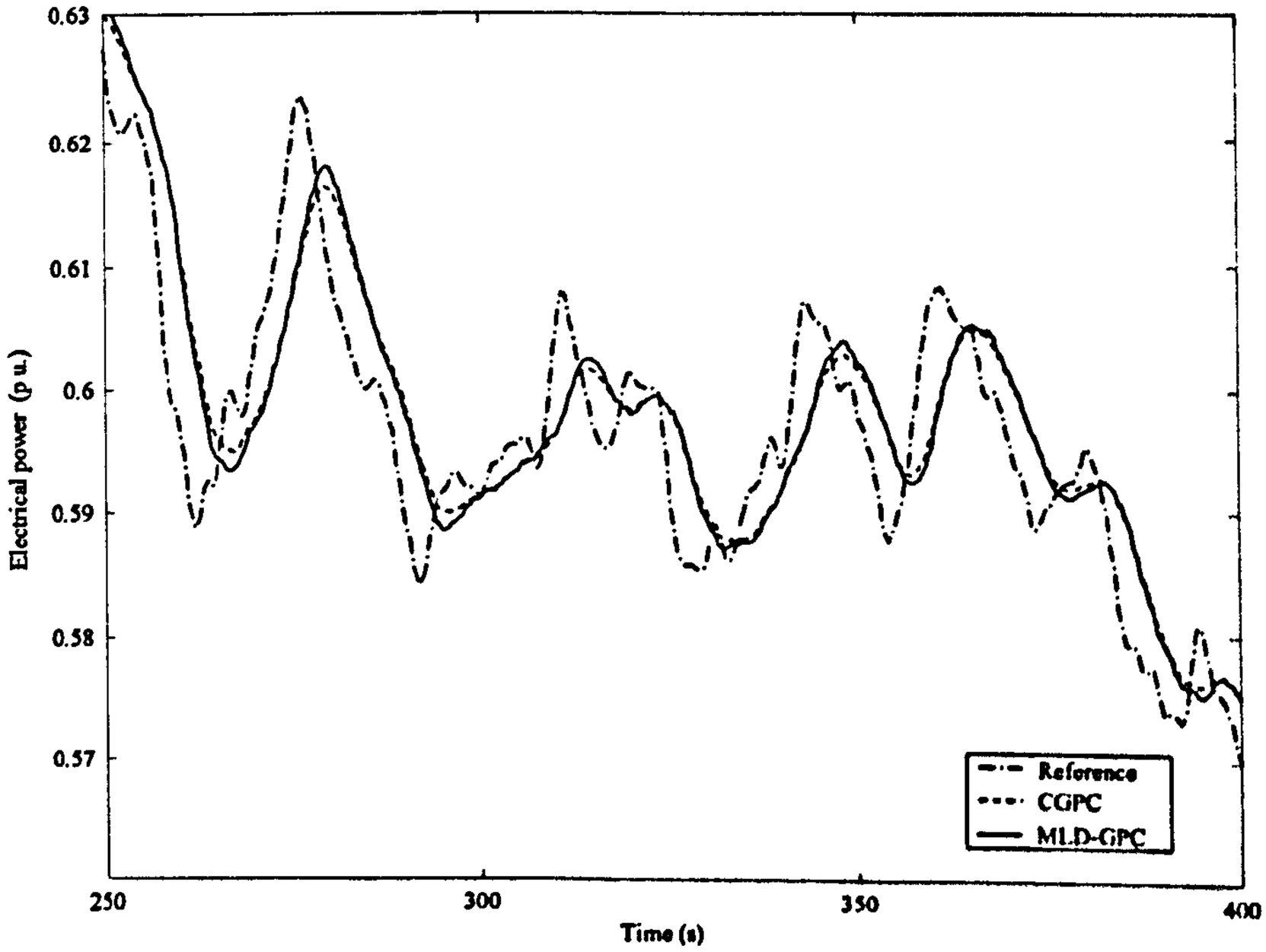


*Figure 7.14: Comparison of the responses produced by MLD-GPC and CGPC controllers in automatic frequency control mode with six units operational.*

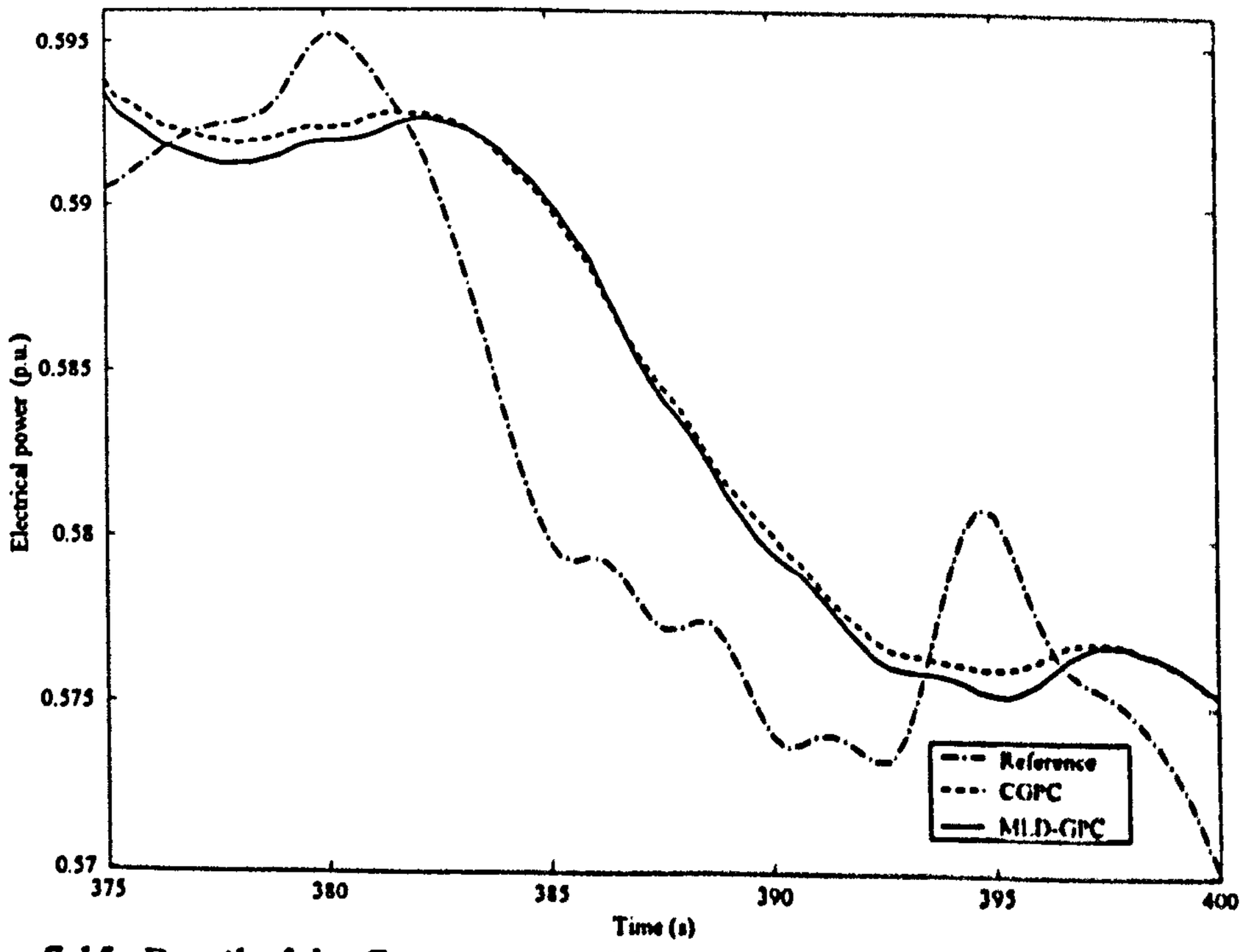


*Figure 7.15: Detail of the Comparison of the responses produced by MLD-GPC and CGPC controllers in automatic frequency control mode with six units operational.*

# 7.5. Modelling high-level control rules with MLD

## 7.5.1 Hierarchical control

For many years financial and operational aspects have been taken into account for the optimal control of plant, in any type of industry. Hierarchical control is often used to integrate these aspects at all levels of control [60,70].

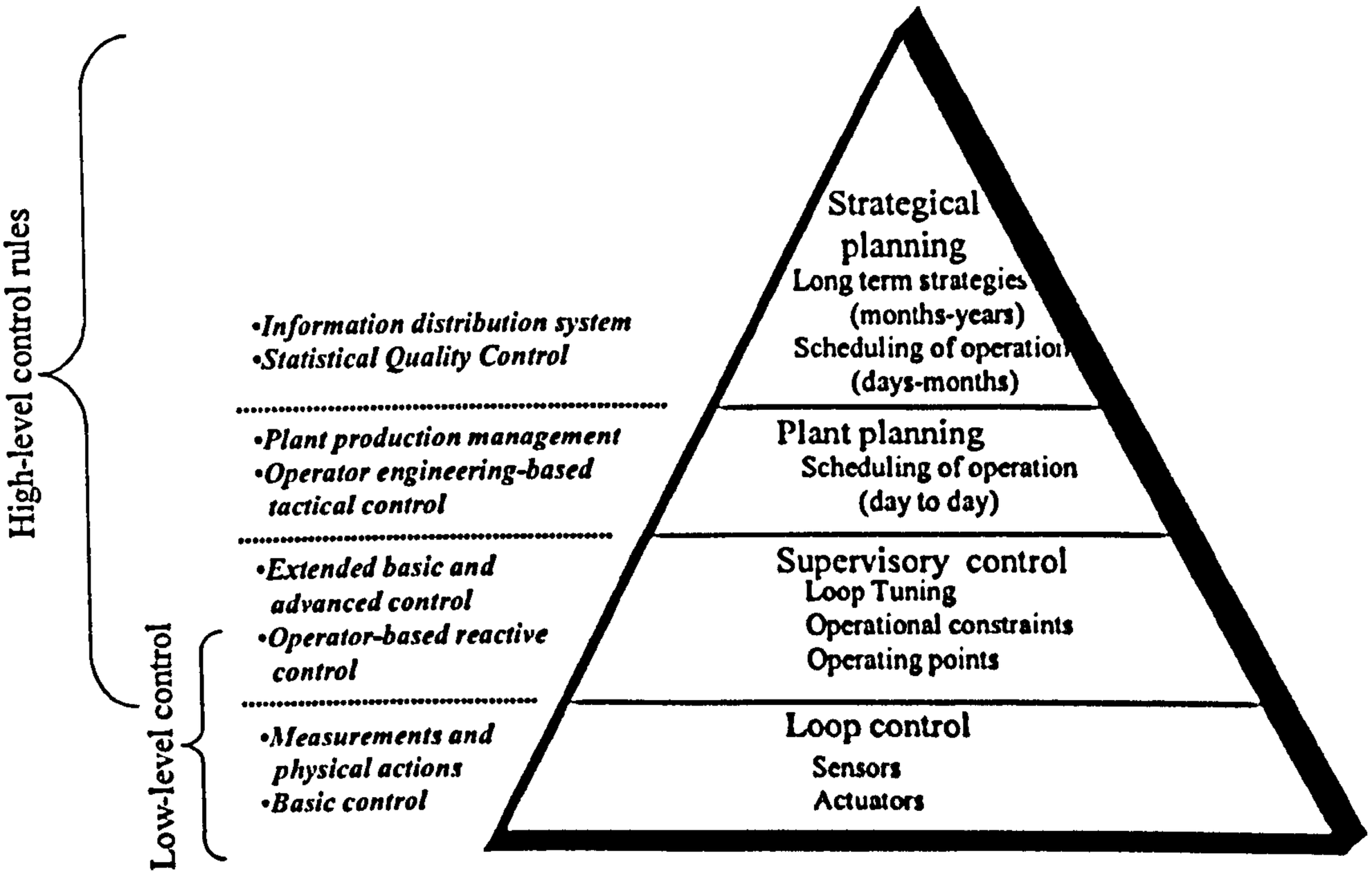


*Figure 7.16: Hierarchical Control.*

In Hierarchical control, Figure 7.16, the lowest or execution level handles the sequence of actions necessary to manipulate the system. The medium levels constitute a supervisory system with the capacity of alarm monitoring, automatic protection, fault diagnosis, and reconfiguration. The top level is able to plan and make decisions about the strategic operating planning. MLD systems, and hybrid systems in general, can be used to develop a platform to integrate all levels of control [60].

A hierarchical structure is not the only paradigm to deal with higher levels of control; other approaches exist, such as a horizontal architecture. However, all of them

distinguish between higher and lower levels of control. Logic rules and optimal functions are commonly used to represent the high control levels; therefore MLD is also suited to these paradigms.

In the electrical sector, studies have appeared where the financial aspects are the main component at all levels of day-to-day operational decisions [71,72]. Different approaches, such as fuzzy logic, have been proposed to optimise the operation of power systems [73]. Fuzzy logic control has been evaluated in Dinorwig by King *et al* [74], who have described a study where a Fuzzy inference system is assessed as the basis of a governor. MLD systems can be applied to represent control logic that involves the characteristics of both high (economics, lifetime) and low (dynamic response, accuracy) levels of control.

Recently, some studies on hydroelectric power plants have explicitly used hybrid systems techniques to integrate different levels of control. Gallestey *et al* [32] have applied MPC and MLD to optimise the operation of a power plant taking into account not only immediate profits but also lifetime consumption. Chang *et al* [75] have shown how mixed integer linear programming can be applied to short-term scheduling of a hydro system, while Lu *et al* [71] have analysed how the market clearing price can be taken into account to establish an operational strategy. In this work some examples of using MLD to integrate the high level control are presented. The models to generate high-level parameters and reference signals are not discussed here because these details are not within the scope of the study. Nevertheless, they could be assessed in future research.

### 7.5.2 Lifetime consumption

Lifetime consumption models can determine the aging process, providing information about direct relationship between plant load and plant aging, and registering the operating history of the components [32]. The aging model can be used to modify constraint limits or to alter the objective function, equation 4.1 (section 4.3), for example to include more emphasis on the reduction of control effort than on the speed of the plant response. Predictive control can deal with this situation. For example, when

Rossiter *et al* [39] applied predictive control to a fossil-fired power station, they were able to reduce the effort of control without detriment to the plant performance.

The problem of operational optimisation is an objective function subject to several constraints. The generic form of this equation is:

$$J(u)=\int_{t}^{t+N_T} e(\tau,r_u(\tau))+c(\tau,r_u(\tau))-q(\tau,r_u(\tau))d\tau \tag{7.9}$$

where: $N_T$ is the time-optimisation horizon (few days).

$r_u$ set of power plant references and constraints.

$e$ aging rate cost of plant components.

$c$ cost rates.

$q$ revenue rates.

The control constraints and references are then calculated by equation (7.9). The process could be seen as a double loop of control, where a fast internal loop, with a sample period of seconds or lower, calculates the control signal and a slow external loop, with a sample period of minutes or higher, updates the constraint limits and fixes the references taking into account not only the performance of the loop of control but also other criteria, such as the lifetime consumption. For example, if a reduction in the effort of control is required then a constraint that is based on equation (7.9) can be applied.

Figure 7.18 shows the comparison of the effects of this constraint in the output and control signals of a nonlinear model under a MLD-GPC, which was tuned as in the previous section. As can be seen from the figure, the response with constraints is not only faster but also requires less control effort.

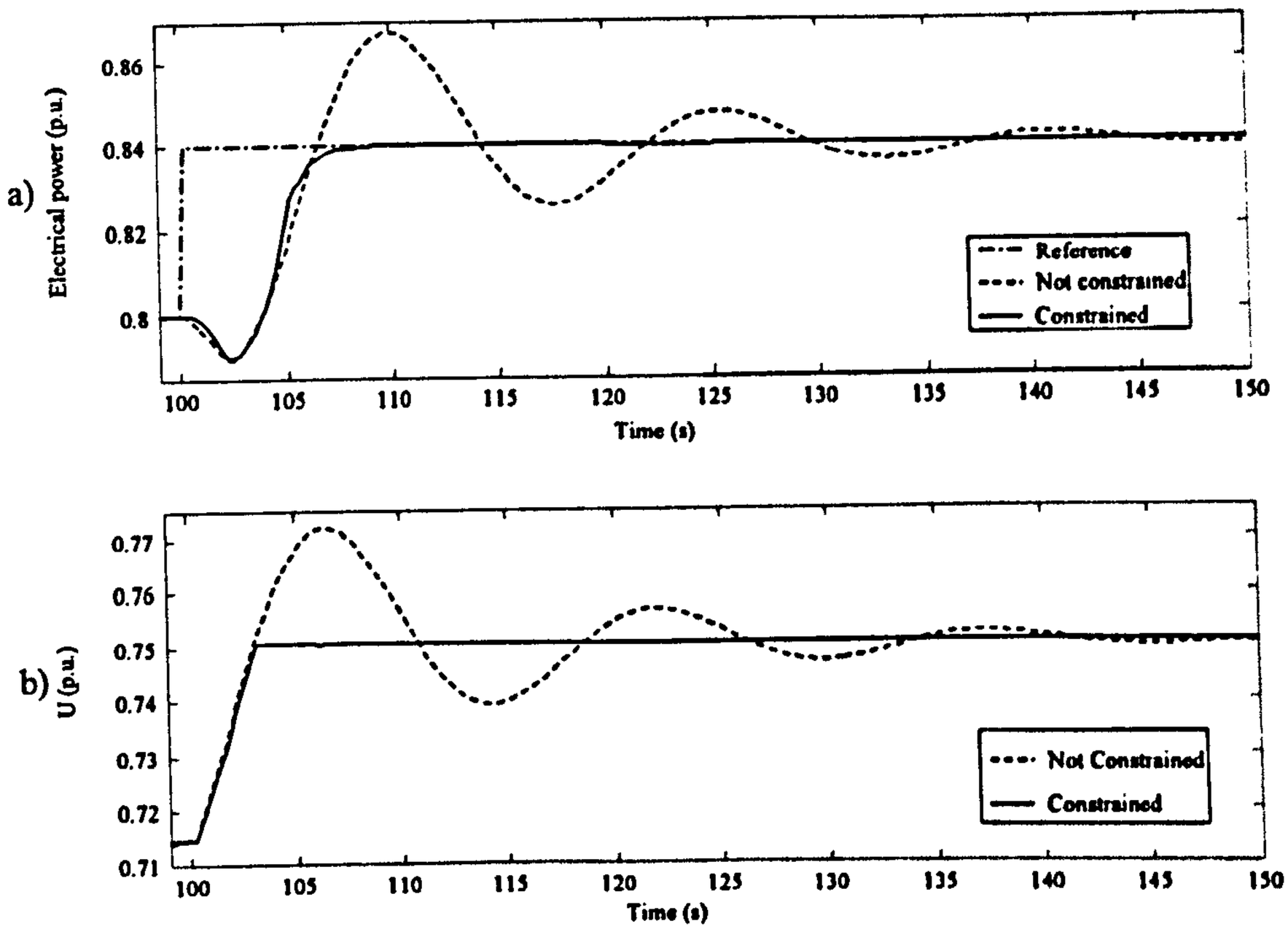


*Figure 7.18: Output and control signals of the response with and without constraints: (a) output signals, (b) control signals.*

## 7.6. Conclusions

The results have shown how MLD-GPC can be applied to a hydroelectric pumped-storage station to improve its fast-response characteristics. The direct transient responses are improved compared with CGPC, when the multivariable nature of the plant is taken explicitly into account. In particular selecting different values of $\lambda$ and different predictive models, depending on the number of units active, allows MLD-GPC to produce a fast response across the operational range. Inclusion of rate and saturation constraints in both GPC controllers yields a fast, well-damped response in the common case when only a single unit is in operation, without compromising stability when multiple units are on-line.

The brief discussion of the integration of high-level control rules into MLD-GPC and the simple example presented are intended to help in the elucidation of future research rather than form a comprehensive study. Nevertheless the versatility of this approach has been described and its potential for application to pumped storage stations has been discussed.

# Chapter 8

# Conclusions

## 8.1 Review of the Thesis

This thesis has described the application of Generalised Predictive Control to Dinorwig Power Station. It was found that this type of control is able to maintain its performance in all operational conditions of the plant. The study has also demonstrated that GPC can manage the nonlinearities of Dinorwig without losing control accuracy. The inclusion of constraints not only keeps the operation of the plant inside the accepted limits but also increases the speed of the plant response.

Chapter 2 describes methods of modelling hydroelectric power plants by means of linear and nonlinear models. They contain the principal features of the plant's dynamics and were applied to the Dinorwig power plant. The representation includes the hydraulic, guide vane and electrical subsystems. The models were developed in Simulink and an open modular software platform was constructed based on them.

Chapter 3 gives a brief review of the turbine-generator control developments and presents the Dinorwig Governor configuration. It is illustrated that the current governor cannot satisfy the entire operational specifications, enunciated in that Chapter. The

closed loop analysis offers guidance on selecting the parameters of a classic PI controller. This analysis also shows the dependence between the performance of the controller and the dynamic parameters of the system.

Chapter 4 constitutes a review of the basic theory of Model Based Predictive Controls (MBPC), with special emphasis on Generalised Predictive Control (GPC), and in the applications of this control approach to electric power generation. GPC tuning guidelines are also presented. The GPC algorithms have been programmed using Matlab. The software platform permits the analysis of models of the hydroelectric station and control methods. The modular and open characteristics of this software tool have been important to increasing rapidly and incrementally the complexity of the control algorithm and the plant itself.

A general guide for optimum adjustment of the parameters of the GPC controller, when the Power Plant is modelled as a SISO linear system, is provided in Chapter 5. The appropriate selection of values of the control parameters yields an improved response of the linear SISO model of the hydroelectric plant. Comparisons between the results from the GPC controller and from the classic PI Governor show an improvement in the performance of the power plant when GPC controllers are used. The primary advantage of the GPC over conventional PI and PI anti-windup controllers, is the smooth treatment of the non-minimum phase response, resulting in minimisation of undershoot. The inclusion of constraints on the control within the GPC algorithm yields a response which is closer to the 'hydraulic limit' than achieved by optimised retuned PI control.

In Chapter 6 the multivariable nature of the plant, is taken explicitly into account, which considers both the direct and cross-coupled transient responses. When a rate constraint is included in the GPC controller, the response of the system is fast and well-damped despite the number of units active. GPC controllers also improve power delivery when the plant is operated in frequency control mode. The frequency change predictor yields a faster response that gives more accurate tracking of the power target. The robustness of the system to changes in the number of units active and variations in the hydraulic head is improved when GPC controllers are used. This improvement is very valuable, due to the diversity of operational conditions that the plant encounters during an operational day.

The versatility of a Mixed Logical Dynamical (MLD) controller and its potential application to pumped storage stations are discussed in Chapter 7. That chapter presented a brief introduction to MLD systems, a MLD model of the hydroelectric station and the inclusion of this model within a GPC controller of Dinorwig. The MLD model has been shown to agree well with the MIMO nonlinear nonelastic model of the power plant. When this MLD model is used as the model of prediction in the GPC controller for Dinorwig, the behaviour of the plant is further improved. The possibility of automatically selecting different values of $\lambda$ depending on the number of units active and the inclusion of constraints permits MLD-GPC to produce a fast response in all operational cases. Consequently the system with one unit operational has a rapid response without compromising the performance when multiple units are on-line. There is also the possibility of integrating high-level control rules into MLD-GPC, expanding the scope of the controller. Economic and operational aspects could then be integrated directly into the formulation of the optimisation problem.

## 8.2 Conclusions

The purpose of this work was to evaluate the application of MPC to Dinorwig power station, in order to offer to the company an alternative controller that improves the response of the Power Plant and maintains its performance over all operational conditions.

Other approaches were considered for this purpose. For instance, a Neural Network approach was considered but rejected because, although the plant has a MIMO nonlinear behaviour, a deterministic pre-calculated model, as used in MPC, has been shown to be sufficiently accurate to represent the plant. This type of model is less computationally demanding. Fuzzy logic was another control method considered. However, improved plant performance was not really evident. This approach could possibly be useful when high level control is considered.

The controller developed in this work has improved the speed of response of the system, with a slight improvement in NMP response. Nonetheless, the GPC controllers, in

particular CGPC and MLD-CGPC have the characteristic of robustness that allows the system to run near its optimal performance in all cases evaluated in this work. Therefore, it can be said that the main objectives of this study were accomplished. The controller now deals with the MIMO characteristic of the plant in a natural way, the performance of the extreme cases (one and six unit operational) are not so different from those with the classic controller currently installed, and the nonlinearities of the system have a lower effect in the performance of the plant; as a summary the major benefits from this study can be stated as follows:

- The speed of response of the Power station was improved when tracking the demanded power. GPC controllers reduce the *primary response* compared with the classic PI Governor, when the response to a small step is evaluated. This criterion is also improved using GPC controllers when ramp input signals are considered.

- The Power plant under GPC control has a better balance in its performance over all operational conditions. The plant reaches the 90% of the reference change, with less difference between the two extreme operational cases (one and six units active) when these controllers are used as the Dinorwig Governor, instead of the classic PI.

- A modest reduction of the cross-coupling interaction has been achieved. When one unit is operating on a fixed reference and the references of the others five units are changed, the GPC controllers have overshoots that are lower than those produced by the PI Governor. The ISA and IAE indexes are also reduced.

- Constraints not only for safety reasons but also as a method to improve the performance of the plant were evaluated in this study. The possibility of increasing the control loop gain allows the system to run near the limit while maintaining a good performance in all operational conditions. This approach was included in the GPC controllers, increasing the speed response of the plant from one to six units operational.

To date, implementation of GPC control on the plant is considered premature. There are practical and technical restrictions, such as the need to install synchronised communication between the individual unit governors. The financial penalty, which accompanies any loss of operational capability, is the greater factor. As a result, any radical change in the control software should be co-ordinated with the next major revision of governor hardware, possibly some years hence. Nonetheless, this work has provided Dinorwig and similar hydroelectric stations with an assessment of the potential of GPC and valuable tuning guidelines for the contractor responsible for the implementation.

## 8.3 Directions for future work

The thesis has offered an extensive study that shows the advantages of the application of GPC to Dinorwig. Throughout the development of this thesis, some lines for additional research have been noted. These will be stated here and new ideas will be included.

- The objective function, as currently implemented, can be changed to a multi-objective equation, expanding the capabilities for managing constraints in the control of the plant.

- For frequency control, a better predictor could increase the accuracy of the plant response. Although, there are studies that explore the characteristics of the national Grid, until now, these studies have been not able to offer a reliable method for predicting several seconds in advance the variation of the grid frequency.

- Real time simulation should be examined in order to assess the computational requirements that involve the solution of the control problem. In particular, the Quadratic Programming solution, used in the constrained cases, needs to be reviewed.

- Additional work is required to integrate high-level control into the control process. The few examples shown in this study illustrate the great potential that this fusion has in the improvement of plant response. Furthermore, the "good understanding" of the plant operation and the possibility of integrating heuristic knowledge makes the use of the MLD technique for fault detection a relevant line of research to explore.

3rd party copyright material excluded from digitised thesis.

Please refer to the original text to see this material.

# Bibliography


1. Working group on prime mover energy supply, "Hydraulic turbine and turbine control model for system dynamic studies", IEEE Transactions on Power Systems, vol. 7, p.p. 167-179, 1992

2. Kundur, P., "Power System Stability and Control", Mc Graw Hill, New York, USA, 1994

3. Mansoor, S. P., "Behaviour and Operation of Pumped Storage Hydro Plants", PhD. Thesis, University of Wales, Bangor, U.K., Bangor, U.K., 2000

4. Jones, D. I., "Multivariable control analysis of a hydraulic turbine", Transactions of the Institute of measurement and control, vol. 2-3, p.p. 122-136, 1999

5. El-Wakil, M. M., "Powerplant technology", McGraw-Hill, USA, 1984

6. Brown, D. and Hamilton III, E. P., "Electromechanical energy conversion", Macmillan, USA, 1984

7. Elgerd, O. I., "Basic electric power engineering", Addison-Wesley, USA, 1977

8. Mansoor, S. P., Jones, D. I., Bradley, D. A., Aris, F. C. and Jones, G., "Stability of a pumped storage hydropower station connected to a power system", IEEE Power Eng. Soc. Winter Meeting, p.p. 646-650, New York, 1999

9. Hannett, L. N., Feltes, J. W., Fardanesh, B. and Crean, W., "Modeling and Control Tuning of a Hydro Station with Units Sharing a Common Penstock Section", IEEE Transactions on Power Systems, vol. 14, p.p. 1407-1414, 1999

10. Anderson, P. M. and Mirheydar, M., "A Low-Order system frequency response model", IEEE Transactions on Power Systems, vol. 5, p.p. 720-729, 1990

11. Jones, D. I., "Estimation of power system parameters", IEEE Transactions on Power Systems, vol. 19, p.p. 1980-1989, 2004

12. MathWorks, "Using Matlab, Version 6", MathWorks, Natick, USA, 2000

13. Fasol, K. H., "A short history of hydropower control", IEEE Control Systems Magazine, vol. 22, p.p. 68-76, 2002

14. Wright, R. M., "Understanding modern generator control", IEEE Transactions on Energy Conversion, vol. 4, p.p. 453-458, 1989

15. Leum, M., "The development and filed experience of a transistor electric governor for Hydro Turbines", IEEE Transactions on Power Apparatus and Systems, vol. 85, p.p. 393-400, 1966

16. Ham, P. A. L. and Green, N. J., "Developments and experience in digital turbine control", IEEE Transactions on Energy Conversion, vol. 3, p.p. 568-574, 1988

17. Thorne, D. H. and Hill, E. F., "Extensions of stability boundaries of a hydraulic turbine generating unit", IEEE Transactions on Power Apparatus and Systems, vol. PAS-94, p.p. 1401-1409, 1975

18. Dhaliwal, N. S. and Wichert, H. E., "Analysis of P.I.D. governors in multimachine system", IEEE Transactions on Power Apparatus and Systems, vol. PAS-97, p.p. 456-463, 1978

19. Hagihara, S., Yaokota, H., Goda, K. and Isobe, K., "Stability of a hydraulic turbine generating unit controlled by PID Governor", IEEE Transactions on Power Apparatus and Systems, vol. PAS-98, p.p. 2294-2298, 1979

20. Orelind, G., Wozniak, L., Medanic, J. and Whitemore, T., "Optimal PID gain schedule for Hydrogenerators-Design and application", IEEE Transactions on Energy Conversion, vol. 4, p.p. 300-307, 1989

21. Ye, L., Wei, S., Xu, H., Malik, O. P. and Hope, G. S., "Variable structure and time-varying parameter control for hydroelectric generating unit", IEEE Transactions on Energy Conversion, vol. 4, p.p. 293-299, 1989

22. Mansoor, S. P., Jones, D. I., King, D. J., Bradley, D. A., Aris, F. C. and Jones, G. R., "Investigation into a new governor scheme for the Dinorwig pumped-storage plant." Proceedings International Conference in Hydropower & Dams, p.p. 29-38, Kiris, Turkey, 2002

23. Lansberry, J. E. and Wozniak, L., "Adaptive hydrogenerator governor tuning with a genetic algorithm", IEEE Transactions on Energy Conversion, vol. 9, p.p. 179-183, 1994

24. Eker, I. and Tumay, M., "Robust multivariable-cascade governors for hydroturbine controls", Electrical Engineering, vol. 84, p.p. 229-237, 2002

25. Mansoor, S. P., Jones, D. I., Bradley, D. A., Aris, F. C. and Jones, G. R., "Reproducing oscillatory behaviour of a hydroelectric power station by computer simulation", Control Engineering practice, vol. 8, p.p. 1261-1272, 2000

26. Jones, D. I., Mansoor, S. P., Aris, F. C., Jones, G. R., Bradley, D. A. and King, D. J., "A standard method for specifying the response of hydroelectric plant in frequency-control mode", Electric Power Systems Research, vol. 68, p.p. 19-32, 2004

27. IEEE Power generation committee, "IEEE Recommended practice for preparation of equipment specifications for speed-governing of hydraulic turbines intended to drive electric generators"

28. Munoz-Hernandez, G. A. and Jones, D. I., "Applying Generalized Predictive Control to a pumped-storage hydroelectric power station", IASTED MIC, p.p. 380-385, Grindelwald, Switzerland, 2004

29. Alpigini, J. and Piovoso, M. J., "Visual tuning of controllers", IEE Computing and Control Engineering, vol. June/July, p.p. 34-39, 2004

30. Camacho, E. F. and Bordons, C., "Model Predictive Control", Springer-Verlag, UK, 1999

31. Maciejowski, J., "Predictive Control with constraints", Prentice Hall, Essex U.K., 2001

32. Gallestey, E., Stothert, A., Antoine, M. and Morton, S., "Model predictive control and the optimization of power plant load while considering lifetime consumption", IEEE Transactions on Power Systems, vol. 17, p.p. 186-191, 2002

33. Rossiter, J. A., "Model-Based Predictive Control", CRC Press, Florida, U.S., 2003

34. Richalet, J., Rault, A., Testud, J. L. and Papon, J., "Model Predictive Heuristic Control: Applications to Industrial Processes", Automatica, vol. 14, p.p. 413-428, 1978

35. Peterka, V., "Predictor-based Self-tuning Control", Automatica, vol. 20, p.p. 39-50, 1984

36. De Keyser, R. M. C., Van de Velde, G. A. and Dumortier, F. A. G., "A comparative Study of Self-adaptive Long-range Control Methods", Automatica, vol. 24, p.p. 149-163, 1988

37. Clarke, D. W., Mohtadi, C. and Tuffs, P. S., "Generalized Predictive Control (Part I The basic algorithm)", Automatica, vol. 23, p.p. 137-148, 1987

38. Prasad, G., Irwin, G. W., Swidenbank, E. and Hogg, B. W., "A hierarchical physical model-based approach to predictive control of a thermal power plant for efficient plant-wide disturbance rejection", Transactions of the Institute of measurement and control, vol. 24, 2, p.p. 107-128, 2002

39. Rossiter, J. A., Neal, P. W. and Yao, L., "Applying predictive control to a fossil-fired power station", Transactions of the Institute of measurement and control, vol. 24, 3, p.p. 177-194, 2002

40. Ramond, G., Dumur, D., Libaux, A. and Boucher, P., "Direct Adaptive Predictive Control of an hydro-electric plant", IEEE Int. Conf. on Control Applications, p.p. 606-611, Mexico D.F., 2001

41. Sansevero, G. and Pascoli Botura, C., "Model Predictive Control Algorithm for Francis Hydro Turbo-Generators", Waterpower XIII, p.p. Art. 157, Buffalo, New York USA, 2003

42. Richalet, J., "Industrial Applications of Model Based Predictive Control", Automatica, vol. 29, p.p. 1251-1274, 1993

43. Clarke, D. W., "Application of Generalized Predictive Control to industrial processes", IEEE Control Systems Magazine, vol. 8, p.p. 49-55, 1988

44. Lu, S. and Hogg, B. W., "Predictive co-ordinated control for power-plant steam pressure and power output", Control Eng. practice, vol. 5, p.p. 79-84, 1997

45. Bordons, C. and Camacho, E. F., "A Generalized Predictive Controller for a wide class of industrial processes", IEEE Transactions on Control Systems Technology, vol. 6, p.p. 372-387, 1998

46. Chow, C., Kuznetsov, A. and Clarke, D. W., "Application of generalised predictive control to the paper machine benchmark", Control Engincering Practice, vol. 3, p.p. 1483-1486, 1995

47. Clarke, D. W., Mohtadi, C. and Tuffs, P. S., "Generalized Predictive Control (Part II Extensions and interpretations)", Automatica, vol. 23, p.p. 149-160, 1987

48. Clarke, D. W. and Mohtadi, C., "Properties of Generalized Predictive Control", Automatica, vol. 25, p.p. 859-875, 1989

49. Clarke, D. W., "Advances in Model-Based Predictive Control", Oxford Science Publications, Midsomer Norton, Avon U.K., 1994

50. Tsang, T. T. C. and Clarke, D. W., "Generalised predictive control with input constraints", IEE Proceedings Pt. D., vol. 135, p.p. 451-460, 1988

51. Rossiter, J. A. and Kouvaritakis, B., "Constrained stable generalised predictive control", IEE Proceedings Pt. D, vol. 140, p.p. 243-254, 1993

52. Banerjee, P. and Shah, S. L., "Tuning guidelines for Robust Generalized Predictive Control", Conference on Decision and Control, p.p. 3233-3234, Tucson, USA, 1992

53. Hannett, L. N., Feltes, J. W. and Fardanesh, B., "Field tests to validate Hydro Turbine-Governor model structure and parameters", IEEE Transactions on Power Systems, vol. 9, p.p. 1744-1751, 1994

54. De Jaeger, E., Janssens, N., Malfliet, B. and Van de Meulebroeke, F., "Hydro turbine model for system dynamic studies", IEEE transactions on Power Systems, vol. 9, p.p. 1709-1715, 1994

55. Peng, Y., Vrancic, D. and Hanus, R., "Anti-windup, bumpless, and conditioned transfer techniques for PID controllers", IEEE Control Systems Magazine, vol. 16, p.p. 48-57, 1996

56. Bohn, C. and Atherton, D. P., "An analysis package comparing PID anti-windup strategies", IEEE Control Systems Magazine, vol. 15, p.p. 34-40, 1995

57. Goodwin, G. C., Graebe, S. F. and Salgado, M. E., "Control system design", Prentice Hall, USA, 2001

58. Skogestad, S. and Postlethwaite, I., "Multivariable Feedback Control", John Wiley, 1996

59. Jones, D. I. and Mansoor, S. P., "Predictive feedforward control for a hydroelectric plant", IEEE Transactions on Control Systems Technology, vol. 12, p.p. 956-965, 2004

60. Bemporad, A. and Morari, M. H., "Control of systems integrating logic, dynamics, and constraints." Automatica, vol. 35, p.p. 407-427, 1999

61. Bemporad, A., Torrisi, F. D. and Morari, M., "Performance Analysis of Piecewise Linear Systems and Model Predictive Control Systems", Conference on Decision and Control, p.p. 4957-4962, Sydney, Australia, 2000

62. Witsenhausen, H. S., "A Class of Hybrid-State Continuous-Time dynamic systems", IEEE Transactions on Automatic Control, vol. 11, p.p. 161-167, 1966

63. Branicky, M. S., Borkar, V. S. and Mitter, S. K., "A unified framework for Hybrid Control: Model and Optimal control theory", IEEE Transactions on Automatic Control, vol. 43, p.p. 31-45, 1998

64. Gollu, A. and Varaiya, P., "Hybrid Dynamical Systems", 28th Conference on Decision and Control, p.p. 2708-2712, Tampa, Florida, 1989

65. Cavalier, T. M., Pardalos, P. M. and Soyster, A. L., "Modelling and integer programming techniques applied to propositional calculus", Computers and Operations Research, vol. 17, p.p. 561-570, 1990

66. Williams, H. P., "Logic applied to integer programming and integer programming applied to logic", European Journal of Operational Research, vol. 81, p.p. 605-616, 1995

67. Tyler, M. L. and Morari, M., "Propositional logic in control and monitoring problems", Automatica, vol. 35, p.p. 565-582, 1999

68. Lu, Q., "SDM hybrid control approach for nonlinear systems and application to power systems", International Conference on Power Control, p.p. 19-23, China, 2002

69. Thomas, J., Dumur, D., Buisson, D., Falinower, C. M. and Bendotti, P., "Moving horizon state estimation of hybrid systems. Application to fault detection of sensors of a steam generator", IEEE Int. Conf. on Control Applications, p.p. 1375-1380, 2003

70. Ulieru, M., "Approaching intelligent control systems design", International Conference on intelligent systems for the 21st Century, p.p. 563-568, 1995

71. Lu, N., Chow, J. H. and Desrochers, A. A., "Pumped-Storage hydro-turbine bidding strategies in a competitive electricity market", IEEE Transactions on Power Systems, vol. 19, p.p. 834-841, 2004

72. Pereira, M. V. F., McCoy, M. F. and Merrill, H. M., "Managing risk in the new power business", IEEE Computer Applications in Power, vol. p.p. 18-24, 2000

73. Song, Y. and Johns, A. T., "Applications of fuzzy logic in power systems", Power Engineering Journal, vol. 13, p.p. 97-103, 1999

74. King, D. J., Bradley, D. A., Mansoor, S. P., Jones, D. I., Aris, F. C. and Jones, G. R., "Using a fuzzy inference system to control a pumped storage hydro plant", IEEE International Fuzzy Systems, p.p. 1008-1011, 2001

75. Chang, G. W., Aganagic, M., Waight, J. G., Medina, J., Burton, T., Reeves, S. and Christoforidis, M., "Experiences with mixed integer linear programming based approaches on short-term hydro scheduling", IEEE Transactions on Power Systems, vol. 16, p.p. 743-749, 2001